Rho GTPase Signaling in Excitatory Synapse Development and Intellectual Disability

Wei Ba

DONDERS
SERIES

Rho GTPase signaling in excitatory synapse development and intellectual disability

Wei Ba

Cover design: Ying Zhang

Printed by: PROEFSCHRIFTMAKENM

ISBN: 978-94-6284-095-9

Rho GTPase signaling in excitatory synapse development and intellectual disability

PROEFSCHRIFT

ter verkrijging van de graad van doctor

aan de Radboud Universiteit Nijmegen

op gezag van de rector magnificus prof. dr. J.H.J.M. van Krieken,

volgens besluit van het college van decanen

in het openbaar te verdedigen op maandag 20 maart 2017

om 16.30 uur precies

door

Wei Ba

geboren op 30 juni 1984

te Wuhan city (China)

Promotor

Prof. dr. ir. J.H.L.M. van Bokhoven

Copromotor

Dr. N. Nadif Kasri

Manuscriptcommissie

Prof. dr. Gerard J.M. Martens

Prof. dr. José A. Esteban (Universidad Autónoma de Madrid, Madrid, Spain)

Dr. Wim J.J.M. Scheenen

Table of contents

Chapter 1

General introduction

Part of this chapter has been published as a review:
Rho GTPase signaling at the synapse: implications for intellectual disability.
Experimental Cell Research. 2013 319:2368-74.

The human brain is one of the most complex and fascinating organs, which governs fundamental processes including learning and memory. The brain is not a passive recording machine of existing facts. Instead, it can dynamically encode, retain, edit and retrieve information based on experiences. Human memories are associated with emotion, episodes of experiences and acquired knowledge/skills in lives, allowing us to comprehend, define and adapt to the world with our personal tags. Unraveling the mechanisms underlying learning and memory has become a central issue in neuroscience in the last decades. It is now widely believed that synaptic plasticity, the ability of the brain to modify the efficacy of neuronal communication in response to experience, is the cellular basis of learning and memory [1,2]. The dynamic modification of neuronal communication can be achieved by the structural regulation of spines, small actin enriched protrusions on dendrites, as well as the functional regulation via remodeling neurotransmitter receptors such as glutamate ionotropic alpha-amino-3-hydroxy-5-methyl-4-isoxazole propionic acid receptors (AMPArs). The number of AMPArs and the geometry of dendritic spines have been found to be tightly correlated [3–5]. Rho subfamily of GTP-binding proteins, key regulators of actin cytoskeleton dynamics, play critical roles in synapse formation, maturation and maintenance, directly affecting both synapse structure and function [6–8]. It is therefore not surprising that genetic mutations involving Rho GTPase signaling have been implicated in several neurodevelopmental disorders such as autism spectrum disorders (ASD) and intellectual disability (ID).

The aim of the research described in this thesis is to elucidate the role of Rho GTPase signaling pathways in regulating synaptic structure and function in normal brain, and therefore to enrich our understanding of cellular and molecular mechanisms underlying learning and memory, and to shed light on novel and effective therapies for neurological disorders including ID.

1. The Synapse

Neurons communicate with each other through specialized sites called synapses, which were first documented by Ramón y Cajal more than 100 years ago and which is derived from the Greek word *συνάπσις* (Synapsis), meaning “to clasp”. Most synapses in the central nervous system (CNS) are chemical synapses, which utilize neurotransmitters to convey signals. Synapses consist of a presynaptic axonal terminal (or bouton) and a postsynaptic compartment, which are separated by a synaptic cleft (Figure 1). Synaptic vesicles containing

neurotransmitters are docked and primed for release in the active zone, a specialized region on the presynaptic membrane. After crossing the narrow cleft (~20 nm), released neurotransmitters act on their corresponding receptors on the postsynaptic side. Two major categories of synapses have been identified based on their appearance under electron microscopy (EM): type I (asymmetric, shown to be excitatory), and type II (symmetric, shown to be inhibitory) [9,10]. The most prominent postsynaptic component of excitatory synapses is the postsynaptic density (PSD), an electron-dense structure with a thickness of 35-50 nm on the postsynaptic membrane. The PSD contains a variety of scaffolding proteins, receptors and signaling complexes involved in synaptic transmission and plasticity, such as PSD95, Shank and Homer family proteins, glutamate receptors, CaMKII, and small GTPases [11]. Intensive studies have established that the strength of a synapse is fundamentally dependent on two main factors: presynaptic factors such as the number, content and release probability of synaptic vesicles, and postsynaptic factors including the amount and properties of receptors [12,13].

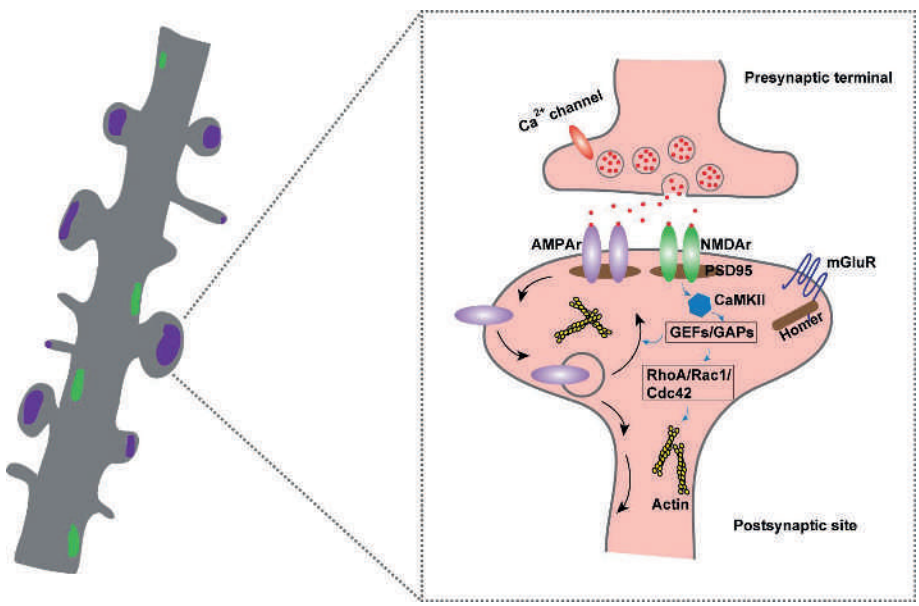

Figure 1 Schematic diagram of the basic structure of synapses.
Left, a piece of dendrite containing spines with diverse shapes. Purple and green highlight the excitatory and inhibitory synaptic sites, respectively. Right, a zoomed in picture showing the basic composition of pre- and post- synaptic compartments.

In the mammalian brain, most excitatory synapses are formed on dendritic spines, small protrusions on the dendrite. Spines come in a wide range of sizes and shapes and they are typically categorized into three groups based on the anatomical studies: thin spines (long neck and small heads, <0.6 μm in diameter); mushroom spines (constricted neck and large bulbous head, >0.6 μm in diameter) and stubby spines (similar head and neck widths). The shapes of the spines represent their maturation status. Mushroom and stubby spines are mature and relative stable while thin spines, which are extremely motile, are considered as the precursors of mature spine [14]. One remarkable feature of synapses is their structural variability. Dynamic alterations in the shape and density of spines are occurring in response to activity and/or during development, which largely rely on the primary cytoskeletal element within the spine, actin. The actin cytoskeleton undergoes dynamic turnover with a total protein replacement every 2-3 min [15]. Both monomers of globular actin (G-actin) and polymers of filamentous actin (F-actin) are present in the spines and they dynamically cycle through a process known as treadmilling. The amount of actin assembly is determined by the available pool of G-actin since F-actin is formed by the polymerization of ATP-bound G-actin. A large group of actin-binding proteins (ABPs) that cooperate actin-mediated cellular events have been found enriched in the spines, such as the Arp2/3 complex, which orchestrates *de novo* actin polymerization, and its activators cortactin, Abp1, N-WASP and WAVE-1, as well as ADF/cofilin and gelsolin which participate in F-actin severing. Deficiencies of these ABPs have been shown to lead to abnormal dendritic spines [16–18]. By transmitting and integrating signals to ABPs, Rho GTPases are able to regulate actin dynamics, and therefore control spine morphology and stability [19].

In rat hippocampus, nascent synapses appear as early as postnatal day 1 [20]. The density of synapses doubles from postnatal day 7 to day 15 and then gradually increases until adulthood [21]. In general terms, excitatory synapse development directly relates with spinogenesis. The balance between spine formation and elimination determines spine density. In the early development, abundant highly motile, thin spines are detected. Upon an adhesive contact with the presynaptic axon, these thin spines gradually transform into more stable mushroom spines. In accordance, rapid conversion from immature “silent synapses” which are characterized by the presence of postsynaptic N-methyl-D-aspartic acid receptor (NMDArs) but not AMPArs [22] into mature AMPArs containing synapses happens during the first two weeks of postnatal development. In adult animals, spine formation and elimination reach a plateau and the overall spine density remains roughly constant [23–25]. In spite of this relative

stability throughout adulthood, dynamic remodeling of synaptic structure and transmission in the brain is still continuously occurring. This plastic nature of synapses is termed synaptic plasticity.

2. Synaptic plasticity

Synaptic plasticity refers to the capacity of synapses to strengthen or weaken in response to activity and/or experience and it is considered to underlie the ability of the brain to encode and store information. The hypothesis of learning resulting from changes in synaptic strength was first proposed by Ramón y Cajal in 1904, based on his anatomical studies: “the future will prove the great physiological role played by the dendritic spines". This idea was later refined by Donald Hebb in the 1940s, stating as “neurons that fire together wire together”. This axiom reminds us that our experience, feelings and thoughts are embedded in thousands of neurons that form a network. The long-lasting increase and decrease in synaptic strength, known as long-term potentiation (LTP) and long-term depression (LTD), respectively, are two most well-studied forms of Hebbian synaptic plasticity. LTP and LTD occur in an input-/synapse-specific manner and have been observed in many brain regions [26–28]. To date, they are well accepted as the cellular mechanisms of learning and memory and are considered essential for normal cognitive function [29,30]. Experimentally, LTP and LTD can be induced by electrophysiological/pharmacological paradigms or by introducing several learning tasks in animal models [30–33]. Diverse molecules and signaling pathways have been reported to be involved in distinct forms of LTP/LTD, depending on the brain region, induction paradigm as well as synapse type. Most studies have focused on hippocampal Schaffer collateral synapses on CA1 pyramidal neurons (CA3-CA1) where high frequency stimulation (HFS, typically 100 Hz) induces classical NMDAr-dependent LTP [34,35]. The same stimulus paradigm, however at the dentate gyrus (DG) mossy fiber synapse (DG-CA3) induces LTP by increasing presynaptic release probability, independently of postsynaptic NMDAr [36], indicating that the cellular mechanisms of Hebbian plasticity are synapse specific.

Interestingly, intimate association between LTP/LTD and enlargement/shrinkage of dendritic spines have been observed [37,38], which leads to the concepts of functional plasticity and structural plasticity. At the single synapse level, NMDArs activation increases spine Ca^{2+} concentrations and activates Ca^{2+}-calmodulin-dependent kinase (CaMKII), which further phosphorylates and activates several critical proteins including Ras and Rho GTPases. By acting

on their downstream effectors, activated Rho GTPases trigger remodeling of actin cytoskeleton and eventually enlarge spine size. In the meanwhile, AMPARs exocytosis occurs upon Ras GTPases activation and results in elevated synaptic efficacy. Previous studies have shown that inhibition of spine enlargement by blocking actin polymerization prevents normal LTP expression [39,40]. Of note, increasing spine size alone, through actin polymerization, is not sufficient to express LTP [41–43].

Although many mechanisms can regulate the onset or magnitude of synaptic plasticity, one common mechanism has appeared to control long-lasting changes of synaptic strength: insertion or removal of AMPARs at synapses [44–48].

2.1 AMPAr trafficking in synaptic plasticity

Glutamate receptors mediate most excitatory transmission in the CNS. In particular, AMPARs play a key role in synaptic transmission and plasticity. AMPARs consist of four subunits, GluA1-GluA4. The extracellular and transmembrane regions of AMPARs subunits are very similar, but their intracellular regions which contain regulatory domains involved in multiple signaling pathways are variable. GluA1, GluA4 and GluA2L (a long splice form of GluA2) have long cytoplasmic carboxy-terminal tail (C-tail) while GluA2, GluA3 and GluA4c (a short splice form of GluA4) contain short C-tails. AMPARs are usually assembled as heteromers and the composition of subunits varies depending on the age and the brain region. In mature hippocampal excitatory synapses, GluA1/GluA2 and GluA2/GluA3 are the two major heterodimers of AMPARs [49]. GluA2 subunit is also subject to RNA editing, the glutamine codon is replaced by an arginine codon (Q/R editing) [50,51]. This editing largely regulates the property of AMPARs, such as the calcium permeability, channel conductance and kinetics [52,53]. Intracellular polyamines strongly interact with GluA2 lacking AMPARs and result in a voltage-dependent block, namely rectification, in these receptors [54,55].

Compared to NMDARs, AMPARs are highly mobile proteins, which are subject to controlled exo-/endocytosis, recycling and/or degradation. It is still controversial how AMPARs are targeted to the synapse after being generated in endoplasmic reticulum (ER) and Golgi apparatus in the soma. Most evidence suggests that AMPARs are first transported by motor proteins such as kinesin, dynein, as well as myosins in dendrites and then directly inserted at synaptic sites [56–60], although some other studies showed that most AMPARs are first inserted into the plasma membrane at the soma at extrasynaptic sites, and then travel to synapses via

lateral diffusion[61–63]. In addition, several studies reported that AMPARs can also be synthesized in dendrites and then directly inserted into synapse [64,65]. It is likely that a combination of these three processes mediates AMPAr insertion in the synapse.

AMPAr endocytosis is regulated by conserved clathrin-mediated endocytic machinery, which also plays a role in presynaptic vesicle recycling [66,67]. Previous studies have shown that clathrin-mediated AMPAr endocytosis mainly occurs at endocytic zones (EZs), stably positioned sites adjacent to the PSD [68]. Methods that block clathrin-dependent endocytosis including high concentrations of sucrose or dominant-negative forms of key components of clathrin complex have been found to block AMPArs endocytosis [69]. After endocytosis, AMPArs are sorted to early endosomes for recycling or to late endosomes and lysosomes that allow degradation [70,71]. The amount of AMPArs at synapses is determined by the relative rate of exocytosis and endocytosis [13].

AMPAr subunits undergo constitutive (the constitutive pathway) or activity-dependent (the regulated pathway) exchanges at synapses [72,73]. Under basal conditions, short C-tailed subunits like GluA2 continuously cycles in and out of synapses, whereas the trafficking of long C-tailed subunits GluA1 and GluA4 is activity and NMDAr activation dependent [72,74,75]. When GluA1/2 heteromeric channels are expressed, the activity-dependent trafficking of GluA1 dominates, whereas GluA2/3 heteromeric channels behave more like GluA2 homomeric channels and traffic constitutively in and out of synapses [67]. The different trafficking preferences are mainly due to various interacting proteins via the C-terminus of AMPAr subunits. For example, GluA2 interactors such as N-ethylmaleimide-sensitive fusion protein (NSF), protein interacting with C kinases 1 (PICK1) and glutamate receptor interacting protein (GRIP) are largely involved in controlling GluA2/3 subunit trafficking. The interaction of GluA2/3 and GRIP promotes synaptic targeting while NSF binding dissociates the GluA2-PICK1 complex and allows insertion. It is believed that the constitutive pathway maintains the basal synaptic strength and the regulated pathway acts upon the induction of synaptic plasticity [67]. Enhanced AMPAr exocytosis and recycling have been observed during LTP, regardless of the exact sites of AMPAr delivered into synapses, enhanced AMPAr exocytosis and recycling have been observed during LTP. Conversely, increased endocytosis rate occurs during LTD [48,67].

2.2 Rho GTPase signaling in synaptic plasticity

The pivotal role of actin in the regulation of synaptic structure and function pointed to Rho GTPase family members as key contributors, since they directly regulate the actin dynamics and organization[76]. Rho GTPases belong to the Ras superfamily of small (~21 kDa) GTPases, which function as molecular switches cycling between an active GTP-bound form and an inactive GDP-bound form. So far, 22 human members of the Rho family have been identified and they can be divided in eight different subgroups: Rho (RhoA-RhoC); Rac (Rac1-Rac3, RhoG) Cdc42 (Cdc42, TC10, and TCL, Chp, Wrch-1); RhoD (RhoD and Rif); Rnd (Rnd1, Rnd2, RhoE/Rnd3); RhoH/TTF; RhoBTB (RhoBTB1 and RhoBTB2); and Miro (Miro-1 and Miro-2) [77]. The activity of Rho GTPases is mainly regulated by guanine nucleotide exchange factors (GEFs), which are positive regulators, by GTPases activating proteins (GAPs) and guanine nucleotide dissociated inhibitors (GDIs), which are negative regulators [76].

2.2.1 Synaptic function of RhoA, Rac1 and Cdc42

The best-characterized Rho family members are RhoA, Rac1 and Cdc42. In the first study addressing the role of Rho GTPase signaling in spine morphogenesis, Luo et al. found a decrease in spine size and an increase in spine density, as well as a corresponding increase in number of synapses in cerebellar Purkinje cells of transgenic mice expressing a constitutive active form of Rac1 (CA Rac1) [78]. Subsequent studies in neuronal cultures and brain slices expressing CA and dominant-negative (DN) mutant forms of Rac1 confirmed the importance of proper Rac1 signaling in dendritic spine morphology. Expression of CA Rac1 in hippocampal brain slices resulted in the formation of multiple small spines[79–81]. Conversely, expression of a DN Rac1 mutant in mouse and rat hippocampal slices caused a reduction in spine density and a corresponding reduction in synapse formation[80,82]. Notably, the spines of DN Rac transfected neurons were in general significantly longer than control spines, and detailed analysis revealed that blocking Rac1 transforms a subset of existing spines into long, thin filopodia-like protrusions. Furthermore, inhibition of Rac1 reduces spine head growth (particularly in mature neurons), morphological changes, and spine stability [82]. Beside the critical role of Rac1 in controlling spine morphology and motility, Rac1 is also directly implicated in controlling synaptic function. Overexpression of wild type (WT) Rac1 or CA Rac1 induces clustering of AMPARs, resulting in an enhancement of excitatory synaptic transmission [83]. All of these studies overwhelmingly show that Rac1 is a significant modulator of spine morphology and

synaptic function. The role for Cdc42 in spine morphogenesis was initially less well defined. In hippocampal pyramidal neurons in organotypic slices, expression of a CA- or DN-Cdc42 mutant did not have a significant effect on spine density or length [80]. However, Cdc42 has been demonstrated to affect spine formation in other systems. Loss of function of Cdc42 in vertical system neurons in the *Drosophila* visual system leads to a reduction in the density of spine-like structures [84]. Another study identified two different variants of Cdc42, an isoprenylated and a palmitoylated variant in the brain. Both are present in dendrites, but only the palmitoylated variant was found in dendritic spines. Using elegant experiments in which they selectively down regulated one of the two variants, they found a specific role for the palmitoylated form in spine formation [85]. Furthermore they showed that changes in palmitoylation of Cdc42 could quickly decrease in response to glutamate, a condition that causes rapid spine contraction and removal. Thus regulated palmitoylation of Cdc42 potentially underlies the changes in spine morphology in response to synaptic activity.

Effects of Rac1 and Cdc42 on spine number and morphology were shown to be mediated by the well-characterized downstream pathway, PAK/LIM kinase/actin depolymerization factor (ADF)/cofilin. Activation of Rac/p21-activated kinase (PAK) leads to phosphorylation of LIMK and subsequently to the inhibition of ADF/cofilin mediated actin-filament disassembly. This leads to an increase in the number of actin filaments. In addition PAK has been shown to also directly phosphorylate myosin IIB, which is present in the postsynaptic density, where it regulates spine morphology [86]. Furthermore, the PAK signaling pathway regulates spine morphogenesis in both intact animals and cultured neurons [87]. Rac1 has also been reported to affect the actin cytoskeleton in spines by the activation of the Arp2/3 complex through WAVE complex, which is localized to dendritic spines in hippocampal neurons. Similarly, Cdc42 has been shown to promote actin polymerization via the neural Wiskott-Aldrich syndrome protein (N-WASP) and the Arp2/3 complex. Upon activation by Cdc42 in dissociated hippocampal neurons, N-WASP regulates actin polymerization by stimulating the actin-nucleating activity of the Arp2/3 complex. Activation of the Arp2/3 complex results in the assembly of branched actin networks, leading to the cytoskeletal reorganization of spines. Besides N-Wasp, also the insulin receptor substrate 53 (IRSp53) and PAK3 have been shown to mediate the effects of Cdc42 on spine morphogenesis. Of note, whereas IRSp53 seems to bind equally to Cdc42 and Rac1, Pak3 preferentially binds to Cdc42 [88].

In contrast to Rac1, RhoA appears to inhibit the growth and/or stability of dendritic spines [82]. In general, increased RhoA activity has been coupled to reduced spine length, size, and density [80,89,90], whereas, low levels of RhoA have been associated with the maintenance of dendritic spine structures [79,91,92]. Interestingly, a few groups reported a decrease in endogenous RhoA activity upon ionotropic and metabotropic glutamate receptor activation [91,93], suggesting a link between synaptic input and regulation of endogenous RhoA activity. Rho-kinase (also called ROK or ROCK) has been well documented to play a key role in RhoA-induced actin reorganization and to mediate at least in part RhoA's effects on spine morphogenesis [82,94]. Rho-kinases appear to influence the actin cytoskeleton by acting on LIM Kinase (LIMK), myosin light chain (MLC) and/or MLC phosphatase. Rho-kinase phosphorylates and activates LIMK, which in turn phosphorylates and inactivates the actin depolymerization factor ADF/cofilin [95–97]. Phosphorylation of MLC by Rho-kinase results in the stimulation of myosin-actin interactions [98]. Rho-kinase can also regulate the amount of phosphorylated MLC by phosphorylating and inactivating MLC phosphatase [99]. Finally, ROCK has been shown to directly phosphorylate myosin IIB and it was shown that myosin IIB, which binds and contracts actin filaments, is essential for spine morphology and dynamics, as well as synaptic function [86].

Importantly, emerging evidence has shown that the formation of both stable LTP and LTD at glutamatergic synapses are accompanied with enduring structural changes in spine heads that are dependent on actin dynamics. Inhibition of actin polymerization attenuates LTP maintenance, whereas LTD is associated with actin filament disassembly [42]. Therefore, it is not surprising that Rho GTPases have been found to play important roles in synaptic plasticity [100–102]. Rapid activation of Cdc42 and RhoA has been observed in a single spine where LTP is induced by local glutamate uncaging. Inhibition of Cdc42-PAK and RhoA-ROCK pathways block initiation and maintenance, respectively, of spine growth during LTP [103]. It has demonstrated that postnatal disruption of Cdc42 leads to impairments of transient and sustained spine enlargement induced by glutamate uncaging, as well as a pronounced deficit of remote memory [104]. Moreover, ADF/cofilin has been shown as a pivotal downstream Rho GTPase effector protein involved in spine shrinkage (LTD) and enlargement (LTP). ADF/cofilin, whose activity depends on its phosphorylation state, can be regulated by various Ca^{2+}-dependent kinases (CamKII), phosphatases (calcineurin and PP1) and Rho GTPase activity (LIMK). When ADF/cofilin is phosphorylated on Ser-3, and thus inactivated, it facilitates actin polymerization.

Dephosphorylation of ADF/cofilin has been associated with spine shrinkage upon low-frequency induced LTD in hippocampal brain slices that was dependent on NMDAr activation [37]. Conversely, ADF/cofilin was found to be phosphorylated, upon LTP signaling synapses [105]. Since ADF/cofilin can be phosphorylated by either the RhoA/ROCK/LIMK or Rac/PAK/LIMK pathway the question arises as to which GTPase signaling pathway might be involved in LTP. One study addressed this question by investigating the role of RhoA and Rac signaling cascade in LTP. They found that NMDAr-dependent LTP sets in motion two distinct signaling cascades: a RhoA/Rock/LIMK/cofilin pathway, which is required for the initial induction of LTP, and a Rac/PAK pathway that is required for the later LTP consolidation phase [106]. The distinct functional roles of the RhoA and Rac cascade in LTP therefore suggest the sequential activity dependent remodeling of actin involving first RhoA and then Rac1 signaling. One possibility is that RhoA and Rac1 target a distinct pool of actin in dendritic spines and as such contribute to different aspects of LTP-induced actin remodeling [15]. In addition, Brain-derived neurotrophic factor (BDNF) also induces LTP in hippocampus, which is associated with cofilin phosphorylation. Up-regulation of RhoA was observed upon BDNF stimulation, suggesting that RhoA could also be implicated in BDNF-induced LTP [107].

2.2.2 Synaptic function of GEFs and GAPs

Although the precise roles of all Rho GTPase regulatory proteins in CNS are far from complete, the synaptic functions of a number of important GEFs and GAPs have been well described. Accumulating evidence indicates that an individual Rho GTPase regulator displays unique structure, expression pattern and synaptic function. Here I describe two key Rho regulators, Kalirin7 and Tiam1.

The extensively studied Rho GEF Kalirin7 (Kal7) has been found to be highly expressed in the mature hippocampus and cortex. It is exclusively localized to the postsynaptic compartment of excitatory synapses in hippocampus. Kal7 contains two GEF domains, and GEF1 targets Rac1/RhoG while GEF2 activates RhoA. It has been shown that elevated Kal7 levels increase spine density and size, whereas downregulation of endogenous Kal7 leads to a decrease in spine and synapse density both *in vitro* and *in vivo* [108,109]. Kal7 interacts with multiple proteins at synapse including NR2B subunit of NMDArs [110]. Loss of Kal7 results in a decrease of NR2B containing NMDAr in PSDs and specifically impairs NMDAr-dependent LTP and LTD [111]. A recent study suggests that a loss of Kal7 in spinal neurons impairs the induction

of synaptic potentiation without affecting basal transmission, due to a direct disruption of Kal7 interacting with proteins in PSD [112]. Additionally, Kal7 has been reported to mediate cocaine induced plasticity in the nucleus accumbens (NAc) via its downstream effectors Rac1 and PAK [113,114]. In contrast, another GEF Tiam1 is highly expressed in the cortex and hippocampus early in development, with an established role in axon extension and neuronal migration both *in vitro* and *in vivo* [115–117]. Inhibition of neuronal migration and axon formation have been observed in the condition of decreased Tiam1. Also, knocking down Tiam1 significantly reduces dendritic arborization and spine density, as well as frequency of miniature excitatory postsynaptic current (mEPSC) in cultured hippocampal neurons [118–120]. Tiam1 overexpression induces multiple axon-like neurites [116,117] and increases spine density [119], implying its importance in axon formation. Unlike Kalirin7, Tiam1 directly interacts to the NR1 subunit of NMDAr and is phosphorylated by CaMKII upon NMDAr stimuli. Phosphorylation of Tiam1 enhances its GEF activity, resulting in activation of Rac1. Selectively blocking Tiam1 function with either RNAi knockdown or dominant negative Tiam1 mutants reduces spine density and inhibits NMDA receptor-dependent spine formation as well as dendritic arbor growth [119]. Furthermore Tiam1 is required for NMDAr phosphorylation of AKT and EIF4E factor suggesting that Tiam1 plays a role in regulating NMDAr-dependent mRNA translation. Recently, Um et al. have demonstrated that Tiam1 forms a GEF/GAP complex with Rac GAP Bcr which is essential for Rac1 signaling and synaptogenesis, controlling excitatory synapse formation and loss in an optimal range [121].

These studies suggest that Rho regulators, through controlling specific Rho GTPase signaling in time and space, are potent manipulators of synaptic efficacy via regulating actin cytoskeleton dynamics and/or via interacting with molecular partners to control postsynaptic receptors, particularly AMPArs and NMDArs.

3. Rho GTPase signaling in ID

ID is defined by an intelligence quotient (IQ) lower than 70, associated with deficits in conceptual, social and adaptive skills [122]. The severity of ID can be divided into mild (IQ between 50 and 69), moderate (IQ between 35 and 49), severe (IQ between 20 and 34) and profound ID (IQ lower than 20) [122]. Clinically, ID has been grouped into non-syndromic ID, which is characterized by impaired cognitive function without any other clinical features, and syndromic ID in which patients additionally present multiple biological or metabolic defects.

The causes of ID are highly heterogeneous and include environmental factors that influence the development of nervous system, and/or genetic factors, such as chromosomal aneuploidies and single gene mutations [123]. Over the past two decades, great efforts have been made to identify ID genes, resulting in a list of approximately 700 ID causing genes [122]. Several of these genes are associated with severe brain abnormalities, such as neuronal heterotopia, lissencephaly, and microcephaly. A vast number of other genes however have been associated with ID disorders with no apparent gross abnormalities in brain structure and architecture. Because learning deficits are a constant feature of ID patients, it is tempting to attribute some of ID traits to alterations in synaptic function. Several lines of evidences point into this direction. First, many of the ID-related proteins are enriched at pre- and/or post-synaptic compartments [124]. Second, alterations in dendritic spines, actin-rich structures on which most excitatory synapses in the brain are located, are observed in patients with ID. Such alterations are recapitulated in mouse models of ID, including Fragile X, which is the most common form of ID. Third, recent studies have provided functional evidence for alterations in synaptic strength in models of ID. These observations support the notion that many forms of ID, may share a common synaptic component [125].

For most of the ID genes identified, little information is available as to how mutations in these genes result in cognitive impairment. The functions of these genes vary largely including regulating cell adhesion, Rho and Ras signaling, gene transcription and chromatin remodeling. Given the actin-rich nature of dendritic spines, the Rho GTPase family, as key regulator of actin dynamics and organization, has recently received much attention in ID research [8,126] (Figure 2) Indeed, mutations in regulators and effectors of the Rho GTPases have been found to underlie various forms of ID. Here, we describe some of the Rho GTPase signaling pathways involved in ID.

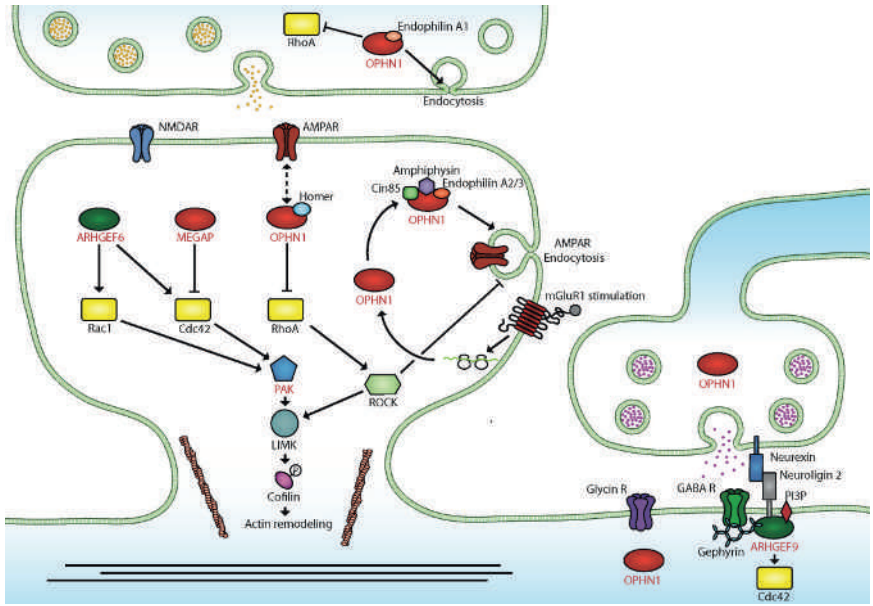

Figure 2 Overview of the ID genes discussed in this chapter and their functions in Rho-GTPase signaling at the synapse.
On the left an excitatory synapse and on the right an inhibitory synapse. Rho-GTPases are depicted as yellow squares, GAP proteins as red ovals, GEF proteins as green ovals and ID gene names are highlighted in red. When activated, Rac1, Cdc42 and RhoA interact with downstream effector proteins, which eventually results in actin remodeling. At the postsynaptic compartment of excitatory synapses, ARHGEF6 positively regulates Rac1 and Cdc42 activity, MEGAP negatively regulates Cdc42 activity and OPHN1 negatively regulates RhoA activity. PAK is a downstream effector of Rac1 and Cdc42. OPHN1 is furthermore involved in AMPAr-mediated synaptic transmission, which is dependent of the interaction with Homer, and OPHN1 expression increases upon mGluR1 stimulation. The Cin85, Amphiphysin, Endophilin A2/3, OPHN1 complex mediates AMPAr endocytosis. At the presynaptic compartment of excitatory synapses, OPHN1 regulates RhoA activity and the Endophilin A1 OPHN1 complex is involved in endocytosis. At the postsynaptic compartment of inhibitory synapses, OPHN1 is present and ARHGEF9 regulates Cdc42 activity. ARHGEF9 furthermore binds to Gephyrin, Neuroligin2 and PI3P. OPHN1 is also present at the presynaptic compartment of inhibitory synapses.

Oligophrenin-1

Oligophrenin-1 (OPHN1), the first identified Rho-linked ID gene, encodes a Rho-GAP protein that negatively regulates RhoA in neurons [127]. Besides RhoA, OPHN1 also interacts with Homer 1b/c [127], endophilin A1 and A2/3 (EndoA1, A2/3) [128], amphiphysins, and CIN85 [129]. The protein is abundantly expressed in the brain, where it is found in neurons of all major regions, including hippocampus and cortex, and is present in axons, dendrites and spines [127]. Families with mutations in the *OPHN1* gene have syndromic ID with cerebellar abnormalities, of which cerebellar hypoplasia is the most recurring phenotype [130–133].

All *OPHN1* mutations identified to date appear to result in a loss of protein function.

Several studies have provided insight as to how mutations in *OPHN1* may impact neuronal function. Knockdown of *Ophn1* in CA1 pyramidal neurons in hippocampal slices resulted in a significant decrease in dendritic spine length. This phenotype was mimicked by using a constitutive active RhoA mutant and was rescued by inhibiting a key effector of RhoA, Rho-kinase (ROCK) [127]. In accordance, Nadif Kasri and colleagues demonstrated that knocking down *Ophn1* in hippocampal neurons inhibited AMPAr- and NMDAr-mediated currents and impeded synaptic maturation and both structural and functional LTP [89]. These defects were dependent on Rho-GAP activity, and the interaction of OPHN1 with Homer 1b/c [89,134]. Conversely, overexpressing OPHN1 selectively enhanced AMPAr-mediated synaptic transmission and increased spine density [89]. Using a peptide derived from the C-terminus of the AMPAr GluA2 subunit that blocks AMPAr endocytosis [135], they have further demonstrated that OPHN1 can regulate synaptic function and structure by stabilizing synaptic AMPArs. A model was therefore proposed in which OPHN1 during early development contributes to excitatory synapse maturation at the CA3-CA1 synapse by stabilizing AMPArs. OPHN1 was also found to play an important role in metabotropic glutamate receptor-induced LTD (mGluR-LTD). OPHN1 expression was rapidly increased at the synapse upon mGluR1 stimulation, an increase in OPHN1 that was required for the proper expression of mGluR-LTD. Interestingly, the role of OPHN1 in mediating mGluR-LTD could molecularly be dissociated from its role in basal AMPAr-mediated synaptic transmission [134]. Whereas the former required OPHN1's interaction with EndoA2/3, the latter requires OPHN1's Rho-GAP activity and interaction with the Homer 1b/c proteins. Studies in *Ophn1* KO mice provided further evidence for the importance of OPHN1 in spine morphology and the regulation of AMPAr trafficking [129,136]. Disruption of OPHN1 in mice was shown to increase the number of filopodia-like spines and impaired NMDA receptor-dependent LTD. Interestingly, the deficits in AMPAr endocytosis and LTD could be reversed completely using a Rho kinase inhibitor. A recent study unveiled that the interaction of OPHN1 and Homer is critical for the positioning of endocytic zones (EZs) near the PSD and disruption of the OPHN1-Homer interaction results in impaired receptor recycling/exocytosis along with a decrease in synaptic AMPAr expression [137]. At the pre-synaptic compartment, a reduction in endocytosis of synaptic vesicles was observed in cortical neurons of *Ophn1* KO mice. Additionally, Nakano-Kobayashi and colleagues demonstrated that OPHN1 controls pre-synaptic vesicle cycling in CA3 neurons by forming a complex with EndoA1 [128]. Besides controlling excitatory synaptic transmission, OPHN1 is also important for inhibitory synaptic

transmission [138]. Impairments in presynaptic vesicle recycling and a reduction in the readily releasable pool were recently observed in inhibitory synapses in the dentate gyrus of *Ophn1* KO mice [138]. Interestingly, pharmacologic treatment with Rho kinase inhibitors rescued these deficits [139]. Finally, OPHN1 has been implicated in circadian clock regulation through its interaction with the nuclear receptor Rev-erbα in the hippocampus [140]. Accordingly, they observed circadian rhythm deficits in *Ophn1* KO mice. This is particularly interesting since sleep disturbances are common in children and adults with ID [140]. Together, these studies clearly illustrate the multifaceted function of OPHN1 in spine morphology, synaptic plasticity and vesicle recycling at the pre- and post-synaptic terminals.

ARHGEF6

Mutations in *ARHGEF6*, also known as *alphaPIX* or *Cool-2*, have been found in patients with non-syndromic ID. The first mutation was identified in a male ID patient carrying a reciprocal X;21 translocation breakpoint located between exons 10 and 11 of the *ARHGEF6* gene. Additionally, mutations were detected in the first intron of this gene [141]. *ARHGEF6* codes for a Cdc42/Rac1 exchange factor, which was initially isolated as a PAK-interacting protein. Previous studies have unraveled the complex nature of its GEF activity towards Rac1 and Cdc42. In its dimeric form, ARHGEF6 functions as a Rac1-specific GEF, whereas in its monomeric form, ARHGEF6 can act as a GEF for Rac1 and Cdc42, but only upon binding of PAK to its SH3 domain [142]. In the brain, ARHGEF6 is highly expressed in hippocampus compared to cortex and cerebellum. Previous studies showed that, in cultured neurons, overexpressed ARHGEF6 localizes specifically at the post-synaptic compartment of excitatory synapses, suggesting an important synaptic function of ARHGEF6 [143]. Subsequently, several lines of evidence have demonstrated a crucial role of ARHGEF6 in regulating spine morphology, synaptogenesis and synaptic plasticity. Knocking down *Arhgef6* by RNAi in cultured neurons resulted in a decrease of large mushroom spines as well as an increase of elongated spines and filopodia–like protrusions. This phenotype could be rescued by a constitutively active form of PAK3 [143]. Moreover, *Arhgef6* KO mice showed longer and more branched dendrites and an increase in the density of spines in CA1 pyramidal neurons. Surprisingly, the increase in dendritic spines on apical dendrites was accompanied by a reduction in excitatory synapses. In addition, *Arhgef6* KO mice showed a significant impairment in early-phase LTP (E-LTP) and an increase in NMDAr-dependent LTD. These changes in synaptic plasticity were attributed to a dramatic

reduction in the levels of the active form of Rac1 and Cdc42 in the hippocampus, in accordance with the Rho-GEF function of ARHGEF6. Furthermore, behavioral characterization showed impairments in complex spatial learning, associated with deficits in coping with altered learning tasks or sensory stimuli [144]. These deficits caused by the loss of *ARHGEF6* may mimic, at least in part, the human ID phenotype.

PAK3

PAK3 encodes p21-activated kinase 3, a member of the PAK family of serine/threonine protein kinases which are downstream effectors for Rac/Cdc42 Rho GTPases. Different mutations of PAK3 have been found in non-syndromic X-linked ID patients [145–147]. PAK3 is prominently expressed in different regions of the brain [148]. Activation of PAK by Rac1 or Cdc42 leads to the phosphorylation of LIM Kinase (LIMK). In turn, activated LIMK phosphorylates and inactivates cofilin, resulting in actin depolymerization [149,150].

Several studies, using knockdown and overexpression approaches in neuronal cell cultures and transgenic animal models, have elucidated the role of PAK3 in spine morphogenesis and synaptic plasticity *in vitro* and *in vivo*. In rat hippocampal organotypic slice cultures, antisense- and RNAi-mediated suppression of PAK3 levels, or expression of a dominant negative PAK3 (dnPAK3) mutant carrying the human (MRX30) mutation, decreased the number of mature spines and promoted thin, immature spines. These changes in dendritic spines were accompanied by impaired AMPAr transmission and LTP [151]. These spine phenotypes were largely recapitulated in transgenic mice expressing dnPAK3 (*dnPAK)*. At the functional level, these mice also displayed enhanced LTP and reduced LTD in the cortex. Furthermore, behavioral tests showed impaired memory consolidation [87]. Mice lacking the PAK3 gene, showed no obvious deficits in neuronal structures. Functionally however, these mice were selectively impaired in late-phase hippocampal LTP (L-LTP) and showed a dramatic decrease in the levels of the active form of cAMP-responsive element-binding protein (CREB) in the hippocampus [152]. The reduction of active CREB, which is required for activity-dependent transcription, may therefore contribute to the L-LTP phenotype. A more recent investigation indicated a dual role of PAK3 in regulating activity-dependent and learning-associated structural plasticity. Dubos et al. found that PAK3 negatively regulated spine growth, as loss of PAK3 function caused uncontrolled and excessive growth of new spines. This suggests that PAK3 may be involved in homeostatic regulation of spine morphology upon synaptic activity.

On the other hand, they showed that PAK3 was activated in spines during LTP induction and was specifically recruited to dendritic spines by synaptic activity. PAK3 inhibition prevented stimulated spines to maintain in a stable state. This indicates that PAK3 is involved in regulating activity-mediated rearrangement of synaptic connectivity [153].

Interestingly, in *Fmr1* KO mice, a model for Fragile X syndrome, inhibition of PAK3 activity by dnPak or PAK inhibitor could reverse the abnormalities in dendritic spines, synaptic plasticity and behavior [154,155]. This indicates that Rac/Cdc42-PAK pathway may have therapeutic potential for ID. In addition, PAK signaling has also been found to play an important role in Alzheimer disease (AD) and Huntington disease (HD), which has recently been reviewed in detail [156].

As mentioned above, PAK and Rho-kinases both stimulate LIMK. It is therefore interesting that *LIMK1* is one of the genes heterozygously deleted in Williams-syndrome, a rare (1 in 25,000) genetic disorder [157]. Patients with this syndrome suffer from a variety of abnormalities, including mild ID. Of particular interest is the fact that *Limk1* knockout mice show abnormal spine morphology, abnormal synaptic plasticity, and impaired spatial learning. Together these studies indicate that regulation of the actin cytoskeleton by Rho GTPases through ARHGEF6/Rac-Cdc42/PAK3/LIMK1 pathway plays a crucial role in controlling local spine growth and stability, which subsequently contribute to learning and memory processes.

MEGAP

The *MEGAP* gene was identified as a gene that is disrupted in patients suffering from $3p^-$ syndrome. These patients exhibit microcephaly, growth failure, heart and renal defects, hypotonia, facial abnormalities and ID [158]. Due to the finding of heterozygous *MEGAP*-truncating mutations in three healthy families, the implication of *MEGAP* in ID is currently under debate [159].

The MEGAP (mental-disorder-associated GAP) gene product was initially identified as a WAVE-associated protein (WRP) and as a SLIT-ROBO interacting protein (srGAP3) [160,161]. The MEGAP mRNA transcript is predominantly expressed in fetal and adult brain, and is enriched in the neurons of the hippocampus, cortex and amygdala [158]. The RhoGAP domain of MEGAP strongly enhances intrinsic Rac1 GTPase activity and to a lower extent Cdc42 [158]. Besides the RhoGAP domain, MEGAP contains two other conserved domains, a WAVE1 binding SH3 domain and a lipid membrane binding IF-BAR domain. MEGAP was also shown to regulate key

aspects of synapse development and function [162]. Using a MEGAP conditional KO mouse they showed that, in hippocampal cultured neurons, only removing MEGAP in early development decreases filopodia and spine formation. This phenotype could be rescued by overexpressing either the IF-BAR truncation or full-length MEGAP. Knockout of *Megap* at later stages did not result in any spine phenotype. These results were confirmed *in vivo,* strongly supporting the idea that MEGAP is required during the early (filopodial) stages of spine development and that the IF-BAR domain is important in this function. In addition, loss of *Megap* led to significant impairments in long-term memory as measured in multiple behavioral tests such as novel object recognition, water maze, and passive avoidance [162]. Interestingly, mice expressing a WRP binding impaired mutant form of WAVE-1, were also deficient in long-term memory [19]. Together these findings suggest that signaling through MEGAP and WAVE-1 to the actin cytoskeleton is important for normal neuronal function.

ARHGEF9/Collybistin

Although much of the ID research has been directed towards the formation of excitatory synapses, Rho GTPase regulatory proteins also function in the formation inhibitory synapses. ARHGEF9 is the best-characterized Rho-family GEF involved in the formation of inhibitory synapses.

ARHGEF9 is located on the X chromosome and the first mutation, located in exon2, was detected in a patient with severe ID and clinical symptoms of hyperekplexia and epilepsy [163]. Subsequent studies have shown that loss of function mutations in the *ARHGEF9* gene cause ID associated epilepsy [164–167]. *ARHGEF9* encodes a Cdc42 GEF protein collybistin (Cb), which is highly expressed throughout the adult brain and is specifically enriched in neuronal dendrites [168,169]. In rodents, four distinct splice variants (Cb1-Cb3) have been described. Three of them differ in their C-termini (Cb1-3). Cb2 exists with ($Cb2_{SH3+}$) and without a SH3 domain ($Cb2_{SH3-}$). In the human brain, only a single isoform (hPEM2, human homolog of Posterior End Mark-2) corresponding to Cb3, was found to be expressed [163,170,171]. All Cb isoforms contain a Dbl-homology (DH) domain, which is known to be responsible for the GDP/GTP exchange activity, and a pleckstrin-homology (PH) domain. Cb is required for formation and maintenance of postsynaptic gephyrin scaffolds and the synaptic localization of gephyrin-dependent $GABA_AR$ subtypes[163,172]. The PH domain of Cb was shown to selectively bind with phosphatidylinositol-3-phosphate (PI3P) and overexpressed $Cb2_{SH3-}$ mutant lacking the PH-domain interfered with

gephyrin clustering at inhibitory postsynaptic sites[165]. Interestingly, the GEF activity of Cb seems not to be essential for gephyrin clustering [163,173,174]. It has been proposed that the interaction of the Cb PH domain and the plasma membrane may be sufficient for establishing and maintaining gephyrin clustering-dependent GABAergic synapses, since any of the Cb isoforms can rescue the impairment in GABAergic neurotransmission induced by Cb knockdown [175]. Studies comparing Cb isoforms with or without SH3 domain further revealed that the SH3 domain exerts an autoinhibitory function, as $Cb2_{SH3-}$ was constitutively active and promoted the clustering of gephyrin while Cb_{SH3+} isoforms did not. Interestingly, SH3 domain containing Cb isoforms were found to be activated by neuroligin 2 (NL2), as the binding of NL2 and $GABA_AR\alpha2$ released the autoinhibition of Cb by its SH3 domain [176,177]. A recent study further demonstrated that Cb can adopt open/active and closed/inactive conformations and act as a switchable adaptor that links gephyrin to plasma membrane phosphoinositides. This function is regulated by binding of NL-2 [178]. *Arhgef9* KO mice displayed deficits in spatial learning and increased anxiety-like behavior. These mice showed a reduced density of both synaptic gephyrin clusters and $GABA_AR$ in hippocampus, amygdala and cerebellum. Consequently, GABAergic transmission in the hippocampus was significantly impaired, as both the frequency and the amplitude of GABAergic miniature inhibitory post synaptic currents (mIPSC) from CA1 pyramidal neurons were dramatically reduced in *Arhgef9* KO mice. In addition, in *Arhgef9* knockout mice, theta-burst induced LTP was increased. Blocking GABAR by applying picrotoxin eliminated the difference between *Arhgef9* KO and control mice, indicating that the reduction of GABAergic inhibition contributed to the changes in LTP [179].

Conclusion

Spine abnormalities are associated with numerous neurodevelopmental, neuropsychiatric, and neurodegenerative disorders [180–182]. It is therefore not surprising that Rho GTPase signaling, as a critical controller of the actin cytoskeleton pathway, has emerged as a major signaling pathway affected in these disorders. More specifically, Rho GTPase signaling plays an important role as a key signaling integrator regulating both synaptic structure and function through the control of AMPAr trafficking.

The knowledge gained from the identification and characterization of Rho-linked genes associated with different forms of ID has now opened new avenues for the development of therapeutic strategies for cognitive disorders. Indeed, in some cases targeting Rho GTPase

signaling has recently proven to be successful to rescue cellular and behavioral phenotypes [139].

Finally, these are exciting times for ID research because many more genes in ID will be discovered. Since many more GEFs and GAPs, with unknown function, are expressed in the brain, it is to be anticipated that more Rho regulators will be identified that play critical roles in spine morphology and synaptic function.

Scope and outline of this thesis

Functional analysis of uncharacterized genes that are vital for neuronal function during development will largely enhance our understanding of how the healthy brain governs cognitive processes and will further provide insight into the mechanisms underlying neurological diseases such as ID and ASD. The aim of the research described in this thesis is to enrich our knowledge of the cellular and molecular mechanisms of learning and memory in health and disease, by elucidating the roles of novel genes implicated in ID and ASD in modulating synaptic function and neuronal development. I particularly focus on the role of Rho GTPase signaling in regulating synaptic structure and function.

In order to achieve these goals, I initiated my research by screening 22 genes encoding Rho GTPases and their regulators for their spatial and temporal expression patterns, as is described in **chapter 2**. Based on the developmental expression profile in the hippocampus, a well-studied brain region responsible for spatial memory and navigation, as well as the implication in neurological disorders of these genes, I selected several genes that are potentially important for hippocampal synaptic function and development for subsequent in-depth studies. **Chapters 3, 4 and 5** of this thesis describe in detail the functions of three genes encoding Rho regulators at the synaptic level. A previously unstudied gene, *Arhgap12*, has drawn particular attention due to its highly specific expression in the hippocampal CA1 region during early development. The novel function of ARHGAP12 in maintaining proper spine formation, synaptic transmission and plasticity is described in **chapter 3**. We identified ARHGAP12 as a "structure-function coordinator" during hippocampal development. The underlying mechanism is attributed to its ability of regulating both Rac1 GTPase signaling mediated modification of spine structure via its GAP activity, and clathrin-mediated AMPArs trafficking via its interaction with CIP4. **Chapter 4** reports on an intragenic *de novo* deletion and three truncating mutations of *TRIO*, a gene encoding a Rho GEF, in patients with ID and

the neurophysiological basis of mild to borderline ID caused by mutations of this gene. **Chapter 5** reports on the functional characterization of *Ocrl1*, a gene associated with Lowe Syndrome and Dent Disease. I showed that OCRL1 bidirectionally controls dendritic spine density, miniature excitatory synaptic transmission and LTP. In addition, OCRL1 regulates AMPAr endocytosis and the homeostasis of cellular AMPAr amount in primary hippocampal neurons. In **chapter 6**, we report on a disruptive mutation in the X-linked *KIF4A* and a *de novo* missense mutation in *KIF5C* in patients with ID and epilepsy. I further describe emerging roles of KIF4A and KIF5C in maintaining the balance between excitation and inhibition. In **chapter 7,** a discussion of all the collected data is provided, and prospects for future work and the potential therapeutic implications for neurological disorders are discussed.

References

1. Bliss, T. V. P. & Lomo, T. Long-Lasting Potentiation of Synaptic Transmission in the Dentate Area of the Anaesthetized Rabbit Following Stimulation of the Perforant Path. 331–356 (1973). doi:10.1113/jphysiol.1973.sp010273
2. Bliss, T. V & Collingridge, G. L. A synaptic model of memory: long-term potentiation in the hippocampus. *Nature* **361,** 31–39 (1993).
3. Engert, F. & Bonhoeffer, T. Dendritic spine changes associated with hippocampal long-term synaptic plasticity. *Nature* **399,** 66–70 (1999).
4. Kopec, C. & Malinow, R. Matters of Size. **314,** 8–10 (2006).
5. Matsuzaki, M., Honkura, N., Ellis-Davies, G. C. R. & Kasai, H. Structural basis of long-trm potentiation in single dendritic spines. *Nature* **429,** 761–766 (2004).
6. Tolias, K. F., Duman, J. G. & Um, K. Control of synapse development and plasticity by Rho GTPase regulatory proteins. *Prog. Neurobiol.* **94,** 133–148 (2011).
7. Ba, W., van der Raadt, J. & Nadif Kasri, N. Rho GTPase signaling at the synapse: Implications for intellectual disability. *Exp. Cell Res.* **319,** 2368–2374 (2013).
8. Nadif Kasri, N. & Van Aelst, L. Rho-linked genes and neurological disorders. *Pflugers Arch.* **455,** 787–97 (2008).
9. Gray, E. G. Axo-somatic and axo-dendritic synapses of the cerebral cortex. *J. Anat.* **93,** 420–433 (1959).
10. Siekevitz, P. The postsynaptic density: a possible role in long-lasting effects in the central nervous system. *Proc. Natl. Acad. Sci. U. S. A.* **82,** 3494–3498 (1985).
11. Sheng, M. & Kim, E. The postsynaptic organization of synapses. *Cold Spring Harb. Perspect. Biol.* **3,** a005678 (2011).
12. Michel, K., Müller, J. A., Oprişoreanu, A. M. & Schoch, S. The presynaptic active zone: A dynamic scaffold that regulates synaptic efficacy. *Exp. Cell Res.* **335,** 157–164 (2015).
13. Anggono, V. & Huganir, R. L. Regulation of AMPA receptor trafficking and synaptic plasticity. *Curr. Opin. Neurobiol.* **22,** 461–9 (2012).
14. Hotulainen, P. & Hoogenraad, C. C. Actin in dendritic spines: connecting dynamics to function. *J. Cell Biol.* **189,** 619–29 (2010).
15. Honkura, N., Matsuzaki, M., Noguchi, J., Ellis-Davies, G. C. R. & Kasai, H. The subspine organization of actin fibers regulates the structure and plasticity of dendritic spines. *Neuron* **57,** 719–29 (2008).
16. Gu, J. *et al.* ADF/cofilin-mediated actin dynamics regulate AMPA receptor trafficking during synaptic plasticity. *Nat. Neurosci.* **13,** 1208–15 (2010).
17. Grove, M. *et al.* Abi2-De cient Mice Exhibit Defective Cell Migration, Aberrant Dendritic Spine Morphogenesis, and De cits in Learning and Memory. *Society* **24,** 10905–10922 (2004).
18. Wegner, A. M. *et al.* N-WASP and the Arp2/3 complex are critical regulators of actin in the development of dendritic spines and synapses. *J. Biol. Chem.* **283,** 15912–15920 (2008).
19. Soderling, S. H. *et al.* A WAVE-1 and WRP signaling complex regulates spine density, synaptic plasticity, and memory. *J. Neurosci.* **27,** 355–65 (2007).
20. Fiala, J. C., Feinberg, M., Popov, V. & Harris, K. M. Synaptogenesis via dendritic filopodia in developing hippocampal area CA1. *J. Neurosci.* **18,** 8900–8911 (1998).
21. Harris, K. M., Jensen, F. E. & Tsao, B. Three-dimensional structure of dendritic spines and synapses in rat hippocampus (CA1) at postnatal day 15 and adult ages: implications for the maturation of synaptic physiology and long-term potentiation. *J. Neurosci.* **12,** 2685–2705 (1992).
22. Hanse, E., Seth, H. & Riebe, I. AMPA-silent synapses in brain development and pathology. *Nat. Rev. Neurosci.* **14,** 839–50 (2013).
23. Zuo, Y., Lin, A., Chang, P. & Gan, W. B. Development of long-term dendritic spine stability in diverse regions of cerebral cortex. *Neuron* **46,** 181–189 (2005).
24. Mostany, R. & Portera-Cailliau, C. Absence of large-scale dendritic plasticity of layer 5 pyramidal

neurons in peri-infarct cortex. *J. Neurosci.* **31,** 1734–1738 (2011).
25. Chen, C.-C., Lu, J. & Zuo, Y. Spatiotemporal dynamics of dendritic spines in the living brain. *Front. Neuroanat.* **8,** 28 (2014).
26. Recanzone, G. H., Schreiner, C. E. & Merzenich, M. M. Plasticity in the frequency representation of primary auditory cortex following discrimination training in adult owl monkeys. *J. Neurosci.* **13,** 87–103 (1993).
27. Koekkoek, S. K. E. *et al.* Cerebellar LTD and Learning-Dependent Timing of Conditioned Eyelid Responses. *Science (80-.).* **301,** 1736–1739 (2003).
28. Calabresi, P., Maj, R., Pisani, A., Mercuri, N. & Bernardi, G. Long-term synaptic depression in the striatum: physiological and pharmacological characterization. *J.Neurosci.* **12,** 4224–4233 (1992).
29. Nabavi, S. *et al.* Engineering a memory with LTD and LTP. *Nature* **511,** 348–352 (2014).
30. Whitlock, J. R., Heynen, A. J., Shuler, M. G. & Bear, M. F. Learning Induces Long Term Potentiation in the Hippocampus. *Science (80-.).* **313,** 1093–1097 (2006).
31. Fujii, S., Ji, Z., Morita, N. & Sumikawa, K. Acute and chronic nicotine exposure differentially facilitate the induction of LTP. *Brain Res.* **846,** 137–143 (1999).
32. Liu, Q., Pu, L. & Poo, M. Repeated cocaine exposure in vivo facilitates LTP induction in midbrain dopamine neurons. *Nature* **437,** 1027–1031 (2005).
33. Schroeder, B. W. & Shinnick-Gallagher, P. Fear learning induces persistent facilitation of amygdala synaptic transmission. *Eur. J. Neurosci.* **22,** 1775–1783 (2005).
34. Staubli, U. & Lynch, G. Stable hippocampal long-term potentiation elicited by 'theta' pattern stimulation. *Brain Res.* **435,** 227–234 (1987).
35. Lüscher, C. & Malenka, R. C. NMDA receptor-dependent long-term potentiation and long-term depression (LTP/LTD). *Cold Spring Harb. Perspect. Biol.* **4,** 1–16 (2012).
36. Harris, E. W. & Cotman, C. W. Long-term potentiation of guinea pig mossy fiber responses is not blocked by N-methyl D-aspartate antagonists. *Neurosci. Lett.* **70,** 132–137 (1986).
37. Zhou, Q., Homma, K. J. & Poo, M. Shrinkage of dendritic spines associated with long-term depression of hippocampal synapses. *Neuron* **44,** 749–57 (2004).
38. Matsuzaki, M. *et al.* Dendritic spine geometry is critical for AMPA receptor expression in hippocampal CA1 pyramidal neurons. *Nat. Neurosci.* **4,** 1086–1092 (2001).
39. Fukazawa, Y. *et al.* Hippocampal LTP is accompanied by enhanced F-actin content within the dendritic spine that is essential for late LTP maintenance in vivo. *Neuron* **38,** 447–460 (2003).
40. Ramachandran, B. & Frey, J. U. Interfering with the actin network and its effect on long-term potentiation and synaptic tagging in hippocampal CA1 neurons in slices in vitro. *J. Neurosci.* **29,** 12167–12173 (2009).
41. Cingolani, L. a & Goda, Y. Actin in action: the interplay between the actin cytoskeleton and synaptic efficacy. *Nat. Rev. Neurosci.* **9,** 344–56 (2008).
42. Okamoto, K.-I., Nagai, T., Miyawaki, A. & Hayashi, Y. Rapid and persistent modulation of actin dynamics regulates postsynaptic reorganization underlying bidirectional plasticity. *Nat. Neurosci.* **7,** 1104–12 (2004).
43. Wang, X., Yang, Y. & Zhou, Q. Independent expression of synaptic and morphological plasticity associated with long-term depression. *J. Neurosci.* **27,** 12419–12429 (2007).
44. Barry, M. F. & Ziff, E. B. Receptor trafficking and the plasticity of excitatory synapses. *Curr. Opin. Neurobiol.* **12,** 279–286 (2002).
45. Bredt, D. & Nicholl, R. a. AMPA Receptor Trafficking at Excitatory Synapses. *Neuron* **40,** 361–379 (2003).
46. Scannevin, R. H. & Huganir, R. L. Postsynaptic organization and regulation of excitatory synapses. *Nat. Rev. Neurosci.* **1,** 133–141 (2000).
47. Malinow, R. & Malenka, R. C. AMPA receptor trafficking and synaptic plasticity. *Annu. Rev. Neurosci.* **25,** 103–126 (2002).
48. Kessels, H. W. & Malinow, R. Synaptic AMPA receptor plasticity and behavior. *Neuron* **61,** 340–50 (2009).
49. Wenthold, R. J., Petralia, R. S., Blahos J, I. I. & Niedzielski, a S. Evidence for multiple AMPA

receptor complexes in hippocampal CA1/CA2 neurons. *J. Neurosci.* **16,** 1982–1989 (1996).
50. Jonas, P. & Burnashev, N. Molecular mechanisms controlling calcium entry through AMPA-type glutamate receptor channels. *Neuron* **15,** 987–990 (1995).
51. Kask, K. *et al.* The AMPA receptor subunit GluR-B in its Q/R site-unedited form is not essential for brain development and function. *Proc. Natl. Acad. Sci. U. S. A.* **95,** 13777–13782 (1998).
52. Geiger, J. R. *et al.* Relative abundance of subunit mRNAs determines gating and Ca2+ permeability of AMPA receptors in principal neurons and interneurons in rat CNS. *Neuron* **15,** 193–204 (1995).
53. Swanson, G. T., Kamboj, S. K. & Cull-Candy, S. G. Single-channel properties of recombinant AMPA receptors depend on RNA editing, splice variation, and subunit composition. *J. Neurosci.* **17,** 58–69 (1997).
54. Donevan, S. D. & Rogawski, M. a. Intracellular polyamines mediate inward rectification of Ca(2+)-permeable alpha-amino-3-hydroxy-5-methyl-4-isoxazolepropionic acid receptors. *Proc. Natl. Acad. Sci. U. S. A.* **92,** 9298–9302 (1995).
55. Bowie, D. & Mayer, M. L. Inward Rectification of Both AMPA and Kainate Subtype Glutamate Receptors Generated by Polyamine-Mediated Ion Channel Block. **15,** 453–462 (1995).
56. Perestenko, P. V & Henley, J. M. Characterization of the intracellular transport of GluR1 and GluR2 alpha-amino-3-hydroxy-5-methyl-4-isoxazole propionic acid receptor subunits in hippocampal neurons. *J. Biol. Chem.* **278,** 43525–43532 (2003).
57. Setou, M. *et al.* Glutamate-receptor-interacting protein GRIP1 directly steers kinesin to dendrites. *Nature* **417,** 83–87 (2002).
58. Shin, H. *et al.* Association of the kinesin motor KIF1A with the multimodular protein liprin-α. *J. Biol. Chem.* **278,** 11393–11401 (2003).
59. Ko, J. *et al.* Interaction between liprin-alpha and GIT1 is required for AMPA receptor targeting. *J. Neurosci.* **23,** 1667–1677 (2003).
60. Lisé, M. F. *et al.* Involvement of myosin Vb in glutamate receptor trafficking. *J. Biol. Chem.* **281,** 3669–3678 (2006).
61. Adesnik, H., Nicoll, R. a. & England, P. M. Photoinactivation of native AMPA receptors reveals their real-time trafficking. *Neuron* **48,** 977–985 (2005).
62. Tardin, C., Cognet, L., Bats, C., Lounis, B. & Choquet, D. Direct imaging of lateral movements of AMPA receptors inside synapses. *EMBO J.* **22,** 4656–4665 (2003).
63. Borgdorff, A. J. & Choquet, D. Regulation of AMPA receptor lateral movements. *Nature* **417,** 649–653 (2002).
64. Ju, W. *et al.* Activity-dependent regulation of dendritic synthesis and trafficking of AMPA receptors. *Nat. Neurosci.* **7,** 244–253 (2004).
65. Sekine-Aizawa, Y. & Huganir, R. L. Imaging of receptor trafficking by using α-bungarotoxin-binding-site-tagged receptors. *Proc. Natl. Acad. Sci. U. S. A.* **101,** 17114–17119 (2004).
66. Man, H. Y. *et al.* Regulation of AMPA receptor-mediated synaptic transmission by clathrin-dependent receptor internalization. *Neuron* **25,** 649–662 (2000).
67. Shepherd, J. D. & Huganir, R. L. The cell biology of synaptic plasticity: AMPA receptor trafficking. *Annu. Rev. Cell Dev. Biol.* **23,** 613–43 (2007).
68. Lu, J. *et al.* Postsynaptic positioning of endocytic zones and AMPA receptor cycling by physical coupling of dynamin-3 to Homer. *Neuron* **55,** 874–89 (2007).
69. Heuser, J. E. & Anderson, R. G. W. Hypertonic media inhibit receptor-mediated endocytosis by blocking clathrin-coated pit formation. *J. Cell Biol.* **108,** 389–400 (1989).
70. Ehlers, M. D. Reinsertion or degradation of AMPA receptors determined by activity-dependent endocytic sorting. *Neuron* **28,** 511–525 (2000).
71. Lee, S. H., Simonetta, A. & Sheng, M. Subunit rules governing the sorting of internalized AMPA receptors in hippocampal neurons. *Neuron* **43,** 221–236 (2004).
72. Shi, S.-H., Hayashi, Y., Esteban, J. a. & Malinow, R. Subunit-Specific Rules Governing AMPA Receptor Trafficking to Synapses in Hippocampal Pyramidal Neurons. *Cell* **105,** 331–343 (2001).
73. Kakegawa, W., Tsuzuki, K., Yoshida, Y., Kameyama, K. & Ozawa, S. Input- and subunit-specific

AMPA receptor trafficking underlying long-term potentiation at hippocampal CA3 synapses. *Eur. J. Neurosci.* **20,** 101–110 (2004).
74. Passafaro, M., Piëch, V. & Sheng, M. Subunit-specific temporal and spatial patterns of AMPA receptor exocytosis in hippocampal neurons. *Nat. Neurosci.* **4,** 917–926 (2001).
75. Malinow, R., Mainen, Z. F. & Hayashi, Y. LTP mechanisms: From silence to four-lane traffic. *Curr. Opin. Neurobiol.* **10,** 352–357 (2000).
76. Van Aelst, L. & D'Souza-Schorey, C. Rho GTPases and signaling networks. *Genes Dev.* **11,** 2295–2322 (1997).
77. Aspenström, P., Fransson, A. & Saras, J. Rho GTPases have diverse effects on the organization of the actin filament system. *Biochem. J.* **377,** 327–37 (2004).
78. Luo, L. *et al.* Differential effects of the Rac GTPase on Purkinje cell axons and dendritic trunks and spines. *Nature* **379,** 837–840 (1996).
79. Nakayama, A. Y., Harms, M. B. & Luo, L. Small GTPases Rac and Rho in the maintenance of dendritic spines and branches in hippocampal pyramidal neurons. *J. Neurosci.* **20,** 5329–5338 (2000).
80. Tashiro, A., Minden, A. & Yuste, R. Regulation of dendritic spine morphology by the Rho family of small GTPases: antagonistic roles of Rac and Rho. *Cereb. Cortex* **10,** 927–938 (2000).
81. Pilpel, Y. & Segal, M. Activation of PKC induces rapid morphological plasticity in dendrites of hippocampal neurons via Rac and Rho-dependent mechanisms. *Eur. J. Neurosci.* **19,** 3151–3164 (2004).
82. Tashiro, A. & Yuste, R. Regulation of dendritic spine motility and stability by Rac1 and Rho kinase: Evidence for two forms of spine motility. *Mol. Cell. Neurosci.* **26,** 429–440 (2004).
83. Wiens, K. M. Rac1 Induces the Clustering of AMPA Receptors during Spinogenesis. *J. Neurosci.* **25,** 10627–10636 (2005).
84. Scott, E. K., Reuter, J. E. & Luo, L. Small GTPase Cdc42 is required for multiple aspects of dendritic morphogenesis. *J. Neurosci.* **23,** 3118–3123 (2003).
85. Kang, R. *et al.* Neural palmitoyl-proteomics reveals dynamic synaptic palmitoylation. *Nature* **456,** 904–9 (2008).
86. Ryu, J. *et al.* A critical role for myosin IIB in dendritic spine morphology and synaptic function. *Neuron* **49,** 175–182 (2006).
87. Hayashi, M. L. *et al.* Altered cortical synaptic morphology and impaired memory consolidation in forebrain- specific dominant-negative PAK transgenic mice. *Neuron* **42,** 773–87 (2004).
88. Kreis, P. *et al.* The p21-activated kinase 3 implicated in mental retardation regulates spine morphogenesis through a Cdc42-dependent pathway. *J. Biol. Chem.* **282,** 21497–21506 (2007).
89. Nadif Kasri, N., Nakano-Kobayashi, A., Malinow, R., Li, B. & Van Aelst, L. The Rho-linked mental retardation protein oligophrenin-1 controls synapse maturation and plasticity by stabilizing AMPA receptors. *Genes Dev.* **23,** 1289–302 (2009).
90. Zhang, H. & Macara, I. G. The PAR-6 Polarity Protein Regulates Dendritic Spine Morphogenesis through p190 RhoGAP and the Rho GTPase. *Dev. Cell* **14,** 216–226 (2008).
91. Van Aelst, L. & Cline, H. T. Rho GTPases and activity-dependent dendrite development. *Curr. Opin. Neurobiol.* **14,** 297–304 (2004).
92. Sfakianos, M. K. *et al.* Inhibition of Rho via Arg and p190RhoGAP in the postnatal mouse hippocampus regulates dendritic spine maturation, synapse and dendrite stability, and behavior. *J. Neurosci.* **27,** 10982–10992 (2007).
93. Schubert, V., Da Silva, J. S. & Dotti, C. G. Localized recruitment and activation of RhoA underlies dendritic spine morphology in a glutamate receptor-dependent manner. *J. Cell Biol.* **172,** 453–467 (2006).
94. Riento, K. & Ridley, A. J. Rocks: multifunctional kinases in cell behaviour. *Nat. Rev. Mol. Cell Biol.* **4,** 446–56 (2003).
95. Maekawa, M. Signaling from Rho to the Actin Cytoskeleton Through Protein Kinases ROCK and LIM-kinase. *Science (80-.).* **285,** 895–898 (1999).
96. Sumi, T., Matsumoto, K., Takai, Y. & Nakamura, T. Cofilin phosphorylation and actin cytoskeletal

dynamics regulated by Rho- and Cdc42-activated LIM-kinase 2. *J. Cell Biol.* **147,** 1519–1532 (1999).
97. Amano, T., Tanabe, K., Eto, T., Narumiya, S. & Mizuno, K. LIM-kinase 2 induces formation of stress fibres, focal adhesions and membrane blebs, dependent on its activation by Rho-associated kinase-catalysed phosphorylation at threonine-505. *Biochem. J.* **354,** 149–159 (2001).
98. Amano, M. *et al.* Phosphorylation and Activation of Myosin by Rho-associated. *J. Biol. Chem.* **271,** 20246–20249 (1996).
99. Kimura, K. *et al.* Regulation of Myosin Phosphatase bu Rho and Rho-Associated Kinase (Rho-Kinase). 245 (1996).
100. Fortin, D. a *et al.* Long-term potentiation-dependent spine enlargement requires synaptic Ca2+-permeable AMPA receptors recruited by CaM-kinase I. *J. Neurosci.* **30,** 11565–11575 (2010).
101. Rex, C. S. *et al.* Different Rho GTPase-dependent signaling pathways initiate sequential steps in the consolidation of long-term potentiation. *J. Cell Biol.* **186,** 85–97 (2009).
102. Asrar, S. *et al.* Regulation of hippocampal long-term potentiation by p21-activated protein kinase 1 (PAK1). *Neuropharmacology* **56,** 73–80 (2009).
103. Murakoshi, H., Wang, H. & Yasuda, R. Local, persistent activation of Rho GTPases during plasticity of single dendritic spines. *Nature* **472,** 100–4 (2011).
104. Kim, I. H., Wang, H., Soderling, S. H. & Yasuda, R. Loss of Cdc42 leads to defects in synaptic plasticity and remote memory recall. *Elife* e02839 (2014). doi:10.7554/eLife.02839
105. Chen, L. Y., Rex, C. S., Casale, M. S., Gall, C. M. & Lynch, G. Changes in synaptic morphology accompany actin signaling during LTP. *J. Neurosci.* **27,** 5363–5372 (2007).
106. Rex, C. S. *et al.* Different Rho GTPase-dependent signaling pathways initiate sequential steps in the consolidation of long-term potentiation. *J. Cell Biol.* **186,** 85–97 (2009).
107. Troca-Marin, J. A., Alves-Sampaio, A., Tejedor, F. J. & Montesinos, M. L. Local translation of dendritic RhoA revealed by an improved synaptoneurosome preparation. *Mol. Cell. Neurosci.* **43,** 308–314 (2010).
108. Ma, X.-M. *et al.* Kalirin-7 is required for synaptic structure and function. *J. Neurosci.* **28,** 12368–82 (2008).
109. Ma, X. M. *et al.* Kalirin-7, an important component of excitatory synapses, is regulated by estradiol in hippocampal neurons. *Hippocampus* **21,** 661–677 (2011).
110. Kiraly, D. D., Lemtiri-Chlieh, F., Levine, E. S., Mains, R. E. & Eipper, B. a. Kalirin Binds the NR2B Subunit of the NMDA Receptor, Altering Its Synaptic Localization and Function. *J. Neurosci.* **31,** 12554–12565 (2011).
111. Lemtiri-Chlieh, F. *et al.* Kalirin-7 is necessary for normal NMDA receptor-dependent synaptic plasticity. *BMC Neurosci.* **12,** 126 (2011).
112. Lu, J. *et al.* A role for Kalirin-7 in nociceptive sensitization via activity-dependent modulation of spinal synapses. *Nat. Commun.* **6,** 6820 (2015).
113. Kiraly, D. D. *et al.* Behavioral and morphological responses to cocaine require Kalirin7. *Biol. Psychiatry* **68,** 249–255 (2010).
114. Wang, X. *et al.* Kalirin-7 Mediates Cocaine-Induced AMPA Receptor and Spine Plasticity, Enabling Incentive Sensitization. *J. Neurosci.* **33,** 11012–11022 (2013).
115. Kawauchi, T., Chihama, K., Nabeshima, Y. & Hoshino, M. The in vivo roles of STEF / Tiam1 , Rac1 and JNK in cortical neuronal migration. *EMBO J.* **22,** 4190–4201 (2003).
116. Matsuo, N., Terao, M., Nabeshima, Y. I. & Hoshino, M. Roles of STEF/Tiam1, guanine nucleotide exchange factors for Rac1, in regulation of growth cone morphology. *Mol. Cell. Neurosci.* **24,** 69–81 (2003).
117. Patricia, K., Gabriela, P. & Caceres, A. Evidence for the Involvement of Tiam1 in Axon Formation. *Mol. Biol. Cell* **21,** 2261–72 (2001).
118. Zhang, H. & Macara, I. G. The polarity protein PAR-3 and TIAM1 cooperate in dendritic spine morphogenesis. *Nat. Cell Biol.* **8,** 227–237 (2006).
119. Tolias, K. F. *et al.* The Rac1-GEF Tiam1 couples the NMDA receptor to the activity-dependent

development of dendritic arbors and spines. *Neuron* **45,** 525–538 (2005).
120. Duman, J. G. *et al.* The adhesion-GPCR BAI1 regulates synaptogenesis by controlling the recruitment of the Par3/Tiam1 polarity complex to synaptic sites. *J. Neurosci.* **33,** 6964–78 (2013).
121. Um, K. *et al.* Dynamic Control of Excitatory Synapse Development by a Rac1 GEF/GAP Regulatory Complex. *Dev. Cell* **29,** 701–715 (2014).
122. van Bokhoven, H. Genetic and epigenetic networks in intellectual disabilities. *Annu. Rev. Genet.* **45,** 81–104 (2011).
123. Chelly, J., Khelfaoui, M., Francis, F., Chérif, B. & Bienvenu, T. Genetics and pathophysiology of mental retardation. *Eur. J. Hum. Genet.* **14,** 701–13 (2006).
124. Humeau, Y., Gambino, F., Chelly, J. & Vitale, N. X-linked mental retardation: focus on synaptic function and plasticity. *J. Neurochem.* **109,** 1–14 (2009).
125. Pavlowsky, a, Chelly, J. & Billuart, P. Major synaptic signaling pathways involved in intellectual disability. *Mol. Psychiatry* **17,** 663 (2012).
126. Valnegri, P., Sala, C. & Passafaro, M. Synaptic Dysfunction and Intellectual Disability. *Adv Exp Med Biol* 433–449 (2012).
127. Govek, E.-E. *et al.* The X-linked mental retardation protein oligophrenin-1 is required for dendritic spine morphogenesis. *Nat. Neurosci.* **7,** 364–72 (2004).
128. Nakano-Kobayashi, A., Nadif Kasri, N., Newey, S. E. & Van Aelst, L. The Rho-linked mental retardation protein OPHN1 controls synaptic vesicle endocytosis via endophilin A1. *Curr. Biol.* **19,** 1133–9 (2009).
129. Khelfaoui, M. *et al.* Inhibition of RhoA pathway rescues the endocytosis defects in Oligophrenin1 mouse model of mental retardation. *Hum. Mol. Genet.* **18,** 2575–83 (2009).
130. Bergmann, C. *et al.* Oligophrenin 1 (OPHN1) gene mutation causes syndromic X-linked mental retardation with epilepsy, rostral ventricular enlargement and cerebellar hypoplasia. *Brain* **126,** 1537–44 (2003).
131. Philip, N. *et al.* Mutations in the oligophrenin-1 gene (OPHN1) cause X linked congenital cerebellar hypoplasia. *J. Med. Genet.* 441–446 (2003).
132. des Portes, V. *et al.* Specific clinical and brain MRI features in mentally retarded patients with mutations in the Oligophrenin-1 gene. *Am. J. Med. Genet. A* **124A,** 364–71 (2004).
133. Zanni, G. *et al.* Oligophrenin 1 mutations frequently cause X-linked mental retardation with cerebellar hypoplasia. *Neurology* 1364–1369 (2005).
134. Nadif Kasri, N., Nakano-Kobayashi, A. & Van Aelst, L. Rapid synthesis of the X-linked mental retardation protein OPHN1 mediates mGluR-dependent LTD through interaction with the endocytic machinery. *Neuron* **72,** 300–15 (2011).
135. Ahmadian, G. *et al.* Tyrosine phosphorylation of GluR2 is required for insulin-stimulated AMPA receptor endocytosis and LTD. *EMBO J.* **23,** 1040–50 (2004).
136. Khelfaoui, M. *et al.* Loss of X-linked mental retardation gene oligophrenin1 in mice impairs spatial memory and leads to ventricular enlargement and dendritic spine immaturity. *J. Neurosci.* **27,** 9439–50 (2007).
137. Nakano-Kobayashi, a., Tai, Y., Nadif Kasri, N. & Van Aelst, L. The X-linked Mental Retardation Protein OPHN1 Interacts with Homer1b/c to Control Spine Endocytic Zone Positioning and Expression of Synaptic Potentiation. *J. Neurosci.* **34,** 8665–8671 (2014).
138. Powell, A. D. *et al.* Rapid reversal of impaired inhibitory and excitatory transmission but not spine dysgenesis in a mouse model of mental retardation. *J. Physiol.* **590,** 763–76 (2012).
139. Meziane, H. *et al.* Fasudil treatment in adult reverses behavioural changes and brain ventricular enlargement in Oligophrenin-1 mouse model of intellectual disability. *Hum. Mol. Genet.* **0,** ddw102 (2016).
140. Valnegri, P. *et al.* A circadian clock in hippocampus is regulated by interaction between oligophrenin-1 and Rev-erbα. *Nat. Neurosci.* **14,** 1293–301 (2011).
141. Kutsche, K. *et al.* Mutations in ARHGEF6, encoding a guanine nucleotide exchange factor for Rho GTPases, in patients with X-linked mental retardation. *Nat. Genet.* **26,** 247–50 (2000).

142. Feng, Q., Baird, D. & Cerione, R. a. Novel regulatory mechanisms for the Dbl family guanine nucleotide exchange factor Cool-2/alpha-Pix. *EMBO J.* **23,** 3492–504 (2004).
143. Nodé-Langlois, R., Muller, D. & Boda, B. Sequential implication of the mental retardation proteins ARHGEF6 and PAK3 in spine morphogenesis. *J. Cell Sci.* **119,** 4986–93 (2006).
144. Ramakers, G. J. a *et al.* Dysregulation of Rho GTPases in the αPix/Arhgef6 mouse model of X-linked intellectual disability is paralleled by impaired structural and synaptic plasticity and cognitive deficits. *Hum. Mol. Genet.* **21,** 268–86 (2012).
145. Allen, K. M. *et al.* PAK3 mutation in nonsyndromic X-linked mental retardation. *Nat. Genet.* **20,** 25–30 (1998).
146. Bienvenu, T. *et al.* Missense mutation in PAK3, R67C, causes X-linked nonspecific mental retardation. *Am. J. Med. Genet.* **93,** 294–8 (2000).
147. Gedeon, A. K., Nelson, J., Gécz, J. & Mulley, J. C. X-linked mild non-syndromic mental retardation with neuropsychiatric problems and the missense mutation A365E in PAK3. *Am. J. Med. Genet. A* **120A,** 509–17 (2003).
148. Rousseau, V., Goupille, O., Morin, N. & Barnier, J.-V. A new constitutively active brain PAK3 isoform displays modified specificities toward Rac and Cdc42 GTPases. *J. Biol. Chem.* **278,** 3912–20 (2003).
149. Edwards, D. C., Sanders, L. C., Bokoch, G. M. & Gill, G. N. Activation of LIM-kinase by Pak1 couples Rac/Cdc42 GTPase signaling to actin cytoskeletal dynamics. *Nat. Cell Biol.* **1,** 253–9 (1999).
150. Meng, Y. *et al.* and Enhanced LTP in LIMK-1 Knockout Mice. **35,** 121–133 (2002).
151. Boda, B. *et al.* The mental retardation protein PAK3 contributes to synapse formation and plasticity in hippocampus. *J. Neurosci.* **24,** 10816–25 (2004).
152. Meng, J., Meng, Y., Hanna, A., Janus, C. & Jia, Z. Abnormal long-lasting synaptic plasticity and cognition in mice lacking the mental retardation gene Pak3. *J. Neurosci.* **25,** 6641–50 (2005).
153. Dubos, A. *et al.* Alteration of synaptic network dynamics by the intellectual disability protein PAK3. *J. Neurosci.* **32,** 519–27 (2012).
154. Hayashi, M. L. *et al.* Inhibition of p21-activated kinase rescues symptoms of fragile X syndrome in mice. *Proc. Natl. Acad. Sci. U. S. A.* **104,** 11489–94 (2007).
155. Dolan, B. M. *et al.* Rescue of fragile X syndrome phenotypes in Fmr1 KO mice by the small-molecule PAK inhibitor FRAX486. *Proc. Natl. Acad. Sci. U. S. A.* **110,** 5671–5676 (2013).
156. Ma, Q.-L., Yang, F., Frautschy, S. a & Cole, G. M. PAK in Alzheimer disease, Huntington disease and X-linked mental retardation. *Cell. Logist.* **2,** 117–125 (2012).
157. Hoogenraad, C. C., Akhmanova, A., Galjart, N. & De Zeeuw, C. I. LIMK1 and CLIP-115: linking cytoskeletal defects to Williams syndrome. *Bioessays* **26,** 141–50 (2004).
158. Endris, V. *et al.* The novel Rho-GTPase activating gene MEGAP/ srGAP3 has a putative role in severe mental retardation. *Proc. Natl. Acad. Sci. U. S. A.* **99,** 11754–9 (2002).
159. Hamdan, F. F. *et al.* Srgap3/megap,. *Arch Neurol* 675–677 (2009).
160. Soderling, S. H. *et al.* The WRP component of the WAVE-1 complex attenuates Rac-mediated signaling. *Nat. Cell Biol.* **4,** 970–5 (2002).
161. Wong, K. *et al.* Signal transduction in neuronal migration: roles of GTPase activating proteins and the small GTPase Cdc42 in the Slit-Robo pathway. *Cell* **107,** 209–21 (2001).
162. Carlson, B. R. *et al.* WRP/srGAP3 facilitates the initiation of spine development by an inverse F-BAR domain, and its loss impairs long-term memory. *J. Neurosci.* **31,** 2447–60 (2011).
163. Harvey, K. *et al.* The GDP-GTP exchange factor collybistin: an essential determinant of neuronal gephyrin clustering. *J. Neurosci.* **24,** 5816–26 (2004).
164. Marco, E. J. *et al.* ARHGEF9 disruption in a female patient is associated with X linked mental retardation and sensory hyperarousal. *J. Med. Genet.* **45,** 100–5 (2008).
165. Kalscheuer, V. M. *et al.* A balanced chromosomal translocation disrupting ARHGEF9 is associated with epilepsy, anxiety, aggression, and mental retardation. *Hum. Mutat.* **30,** 61–8 (2009).
166. Lesca, G. *et al.* De novo Xq11.11 microdeletion including ARHGEF9 in a boy with mental

retardation, epilepsy, macrosomia, and dysmorphic features. *Am. J. Med. Genet. A* **155A,** 1706–11 (2011).
167. Shimojima, K. *et al.* Loss-of-function mutation of collybistin is responsible for X-linked mental retardation associated with epilepsy. *J. Hum. Genet.* **56,** 561–5 (2011).
168. Tyagarajan, S. K., Ghosh, H., Harvey, K. & Fritschy, J.-M. Collybistin splice variants differentially interact with gephyrin and Cdc42 to regulate gephyrin clustering at GABAergic synapses. *J. Cell Sci.* **124,** 2786–96 (2011).
169. Kneussel, M., Engelkamp, D. & Betz, H. Distribution of transcripts for the brain-specific GDP/GTP exchange factor collybistin in the developing mouse brain. *Eur. J. Neurosci.* **13,** 487–92 (2001).
170. Kins, S., Betz, H. & Kirsch, J. Collybistin, a newly identified brain-specific GEF, induces submembrane clustering of gephyrin. *Nat. Neurosci.* **3,** 22–9 (2000).
171. Reid, T., Bathoorn, a, Ahmadian, M. R. & Collard, J. G. Identification and characterization of hPEM-2, a guanine nucleotide exchange factor specific for Cdc42. *J. Biol. Chem.* **274,** 33587–93 (1999).
172. Chiou, T.-T. *et al.* Differential regulation of the postsynaptic clustering of γ-aminobutyric acid type A (GABAA) receptors by collybistin isoforms. *J. Biol. Chem.* **286,** 22456–68 (2011).
173. Patrizi, A. *et al.* Selective localization of collybistin at a subset of inhibitory synapses in brain circuits. *J. Comp. Neurol.* **520,** 130–41 (2012).
174. Reddy-Alla, S. *et al.* PH-domain-driven targeting of collybistin but not Cdc42 activation is required for synaptic gephyrin clustering. *Eur. J. Neurosci.* **31,** 1173–84 (2010).
175. Körber, C. *et al.* Effects of distinct collybistin isoforms on the formation of GABAergic synapses in hippocampal neurons. *Mol. Cell. Neurosci.* **50,** 250–9 (2012).
176. Poulopoulos, A. *et al.* Neuroligin 2 drives postsynaptic assembly at perisomatic inhibitory synapses through gephyrin and collybistin. *Neuron* **63,** 628–42 (2009).
177. Saiepour, L. *et al.* Complex role of collybistin and gephyrin in GABAA receptor clustering. *J. Biol. Chem.* **285,** 29623–31 (2010).
178. Soykan, T. *et al.* A conformational switch in collybistin determines the differentiation of inhibitory postsynapses. *EMBO J.* **33,** 1–21 (2014).
179. Papadopoulos, T. *et al.* Impaired GABAergic transmission and altered hippocampal synaptic plasticity in collybistin-deficient mice. *EMBO J.* **26,** 3888–99 (2007).
180. Newey, S. E., Velamoor, V., Govek, E.-E. & Van Aelst, L. Rho GTPases, dendritic structure, and mental retardation. *J. Neurobiol.* **64,** 58–74 (2005).
181. Fiala, J. C., Spacek, J. & Harris, K. M. Dendritic spine pathology: cause or consequence of neurological disorders? *Brain Res. Brain Res. Rev.* **39,** 29–54 (2002).
182. Kaufmann, W. E. & Moser, H. W. Dendritic anomalies in disorders associated with mental retardation. *Cereb. Cortex* **10,** 981–91 (2000).

Chapter 2

Developmental mRNA expression profiles of Rho GAPs and GEFs in the rat brain

Wei Ba, Yorick Bleijenberg, Astrid R. Oudakker and Nael Nadif Kasri

Abstract

As key regulators of cytoskeletal dynamics, Rho GTPases contribute to a wide variety of actin-based cellular processes. The ability of Rho GTPases to control diverse cellular events largely relies on the tight spatial-temporal regulation mediated by their regulators, namely GEFs, GAPs and GDIs. It has been proposed that the developmental-specific expression of Rho regulatory proteins is one of the critical features that enable them to control Rho GTPase signaling in time and space. However, the expression patterns, as well as the function of most Rho regulators in the brain are unknown. In this study, we analysed mRNA levels of 22 genes encoding Rho GTPases and their regulators during rat hippocampal and cortical development by performing qPCR experiments. Our results reveal unique developmental expression patterns of previously unstudied Rho proteins and provide an important indication for the direction of future investigation regarding the novel roles of Rho GTPase signaling pathways in controlling neuronal function.

Introduction

Rho GTPases are key regulators of cytoskeletal dynamics in a wide variety of actin-based cellular events, such as spine morphogenesis, cell migration, axonal guidance and cytokinesis [1–4]. Rho GTPases cycle between an active GTP-loaded and an inactive GDP-loaded state, which is highly regulated by their interaction with several regulators. Guanine nucleotide exchange factors (GEFs) are positive regulators which turn on signaling by promoting the replacement of GDP by GTP, and GTPase-activating proteins (GAPs) are negative regulators that terminate signaling by providing an essential catalytic group for GTP hydrolysis. A third class of regulator, the GDP dissociated inhibitors (GDIs), have also been found to be involved in regulating the activity of Rho GTPase by inhibiting the dissociation of bound GDP from their partner GTPases [5]. In the active form, they are able to bind to numerous effector proteins and activate downstream signaling pathways.

The ability of Rho GTPases to control diverse cellular processes largely relies on the tight spatial-temporal regulation mediated by their regulators. So far, 22 human members of the Rho family have been identified [6]. Surprisingly, approximately 80 Rho GEFs and 70 GAPs have been found in the human genome, leading to a ratio of GEFs/GAPs to Rho proteins roughly 4:1. In addition, Rho GAPs and GEFs exhibit a wide variety of subcellular distribution and their expression is developmentally regulated. Importantly, most Rho GAPs and GEFs possess multiple conserved domains, which enable them to receive diverse upstream cues as well as interact with their targeting Rho proteins and multiple downstream effectors [7]. Despite the fact that the biological function of most Rho GEFs/GAPs remains elusive, all the features of Rho GTPases regulators indicate their ability of controlling specific Rho GTPases signaling in time and space.

In order to identify and characterize critical Rho GTPase regulators involved in synaptic function and development, we performed expression profiling of several candidate genes encoding Rho GTPase regulators at various stages of hippocampal and cortical development by using quantitative polymerase chain reaction (qPCR). Our data showed that most Rho proteins we analyzed display unique developmental-specific expression patterns in both hippocampus and cortex, which provides novel indications of directions for future investigations on potentially critical Rho GTPase proteins in neuronal development.

Results

We selected candidate genes based on four criteria: 1) previously reported to be enriched in PSD in both human and mouse brains [8]; 2) present in hippocampus and cortex, two important brain regions for learning and memory (©2014 Allen Institute for Brain Science; Allen Mouse Brain Atlas from: http://mouse.brain-map.org/); 3) associated with neurological disorders, particularly reported targets of Fragile X mental retardation protein (FMRP), whose loss of function leads to Fragile X syndrome [9]; 4) functions in the brain are unknown.

In total, 22 genes including 10 GAPs, 1 GDI, 10 GEFs and 1 Rho GTPase were selected (Table 1). We then collected rat hippocampi and cortices at embryonic day 17 (E17), postnatal day (P) 3, P10, P17, P24 and P90 (adult), corresponding to different critical stages of neuronal development. We subsequently performed qPCR experiments on mRNAs isolated from these tissue and analyzed expression patterns of all the genes. Our results showed that most genes exhibit developmental expression patterns in both hippocampus and cortex (Table 2 and Table 3). The levels of most Rho GEFs genes increase during development. Among these genes, *Dock2* and *Dock10* display remarkable steep increasing curves, reaching peaks at P24, indicating their importance in both developing and mature brains. Conversely, we found that the expression of most genes encoding Rho GAPs are constant or decreasing with age. Of note, some genes showed opposite expression patterns in hippocampus and cortex. For example, the level of *Arhgap6* significantly decreases after birth in the hippocampus whereas its expression increases during cortical development, suggesting that *Arhgap6* might contribute to different developmental events in hippocampus and in cortex.

GEFs	GAPs	GDI	Rho GTPase
Arhgef2	*Arhgap1*	*Arhgdia*	*Rho B*
Arhgef7	*Arhgap6*		
Dock1	*Arhgap11*		
Dock2	*Arhgap12*		
Dock3	*Arhgap15*		
Dock4	*Arhgap21*		
Dock5	*Arhgap23*		
Dock9	*Arhgap26*		
Dock10	*Bcr*		
Trio	*Ocrl1*		

Table 1 Summary of selected genes of Rho protein and regulators
22 genes encoding 10 GAPs, 1 GDI, 10 GEFs and 1 Rho GTPase were selected for qPCR experiments.

Genes	E17	P3	P10	P17	P24	Adult
Arhgef2	1.00	0.75	1.02	1.26	1.29	1.55
Arhgef7	1.00	1.98	2.34	1.63	1.49	1.04
Dock1	1.00	1.10	1.40	1.40	1.65	2.39
Dock2	1.00	2.86	6.35	7.39	25.41	12.02
Dock3	1.00	1.99	2.87	2.18	1.78	3.36
Dock4	1.00	2.07	3.58	6.82	7.61	3.82
Dock5	1.00	1.10	0.99	1.72	3.41	20.85
Dock9	1.00	6.23	7.59	7.30	7.03	4.28
Dock10	1.00	3.04	7.34	21.78	41.93	21.28
Trio	1.00	0.31	0.16	0.17	0.13	0.20
Arhgap1	1.00	1.61	1.50	1.35	1.06	1.00
Arhgap6	1.00	0.33	0.35	0.39	0.48	0.50
Arhgap11	1.00	0.25	0.16	0.13	0.13	0.25
Arhgap12	1.00	0.93	0.82	0.51	0.50	0.32
Arhgap15	1.00	6.03	8.45	6.21	6.04	10.95
Arhgap21	1.00	1.13	1.09	1.20	1.44	1.53
Arhgap23	1.00	1.61	1.69	1.56	1.93	2.91
Arhgap26	1.00	3.86	7.48	8.57	8.88	12.97
Bcr	1.00	0.88	0.90	0.65	0.58	1.14
Ocrl1	1.00	1.20	1.14	1.00	1.29	1.16
Arhgdia	1.00	1.34	2.20	1.87	1.63	1.67
Rho B	1.00	1.92	2.68	2.21	2.46	2.01

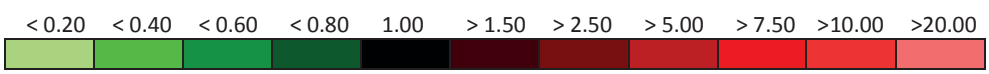

Table 2 Expression of Rho protein and regulators during hippocampal development
Relative expression levels of selected genes at different hippocampal developmental stages. Expression of individual genes at each time point are normalized to the expression of E17. The expression changes of each gene are colour-coded by a green to red colour gradient, corresponding to decreased (green) or increased (red) expression.

Genes	E17	P3	P10	P17	P24	ADULT
Arhgef2	1.00	1.67	0.96	1.14	1.70	1.12
Arhgef7	1.00	2.58	2.51	1.76	2.00	1.07
Dock1	1.00	0.78	0.75	0.82	1.31	1.18
Dock2	1.00	2.39	6.50	5.78	10.68	9.35
Dock3	1.00	4.26	4.81	2.27	2.07	2.79
Dock4	1.00	1.80	1.92	2.34	3.14	4.26
Dock5	1.00	1.27	4.45	2.70	6.93	7.82
Dock9	1.00	6.40	7.90	4.62	4.53	4.39
Dock10	1.00	2.27	2.84	7.26	11.60	13.06
Arhgap1	1.00	1.38	1.10	0.78	0.95	0.93
Arhgap6	1.00	2.93	4.84	8.73	9.38	24.70
Arhgap11	1.00	0.22	0.08	0.03	0.03	0.04
Arhgap12	1.00	0.934	0.821	0.511	0.503	0.840
Arhgap15	1.00	3.32	5.87	6.65	10.13	10.67
Arhgap21	1.00	0.99	0.72	0.62	1.00	1.22
Arhgap23	1.00	4.99	2.18	1.09	2.04	1.79
Arhgap26	1.00	2.58	6.67	10.49	11.47	12.70
Bcr	1.00	0.91	0.78	0.51	0.54	0.73
Ocrl1	1.00	2.01	1.69	1.47	1.72	1.35
Arhgdia	1.00	1.38	1.45	1.48	1.45	1.31
Rho B	1.00	1.86	1.87	1.71	1.65	2.14

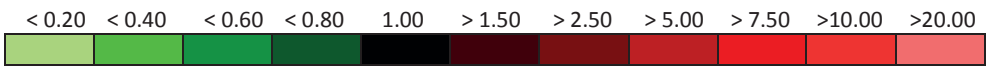

Table 3 Expression of Rho protein and regulators during cortical development
Relative expression levels of selected genes at different cortical developmental stages. Expression of individual genes at each time point are normalized to the expression of E17. The expression changes of each gene are colour-coded by a green to red colour gradient, corresponding to decreased (green) or increased (red) expression.

Discussion

It has been proposed that the developmental-specific expression of Rho regulatory proteins is one of the critical features that enable them to control Rho GTPase signaling pathways in time and space [10]. By performing transcriptional expression profiling, one could gain better insights on when and where the genes that encode Rho proteins play a role in modulating neuronal function, since the physical distribution of Rho GTPases and their regulators is instructive for their function [11].

In order to identify and characterize critical Rho GTPase proteins that are involved in synaptic function and development, in the present study, we generated a transcriptional map of 22 genes encoding Rho GTPases and their regulators. We observed diverse expression patterns of individual Rho proteins during hippocampal and cortical development. For instance, *Arhgap12* and *Arhgap15*, two closely related members of RhoGAP subfamily [12], exhibit complimentary expression pattern. *Arhgap12* is highly expressed in early development whereas the level of *Arhgap15* rapidly increases after birth and reaches a peak level in adulthood. So far, detailed functional analysis of *Arhgap12* and *Arhgap15* in neurons have not been reported, although *Arhgap15* has been implicated in ASD [13]. Our results indicate that it is likely that these two homologous proteins play roles at different stages of hippocampal and cortical development. Of note, the mRNA of *Arhgap12* has been shown to be prominently expressed in hippocampal CA1 region in mice (©2014 Allen Institute for Brain Science; Allen Mouse Brain Atlas from: http://mouse.brain-map.org/), suggesting that *Arhgap12* plays vital roles in sculpting specific hippocampal circuits and function.

Ocrl1, a gene mutated in patients with Lowe syndrome and type 2 Dent Disease, displays relative constant expression in both hippocampal and cortical development. Most studies have focused on non-neuronal cells whereas the function of *Ocrl1* in the brain remains elusive. Experiments illustrating the role of *Ocrl1* in normal neuronal function are needed to reveal how mutations in this gene lead to ID.

Our data also showed that the mRNA level of *Trio* is the highest at embryonic stage and gradually decreases with age in the hippocampus, which is consistent with the previous report of the expression pattern of *Trio* [14]. Compared to its homolog Kalirin, the neuronal function of TRIO is much less understood, partially due to the lethality of global *Trio*$^{-/-}$ knockout in rodents [15]. Analysis of *Drosophila Trio* (*dTrio*) mutants highlighted its role in axon formation and path finding [16–18]. Importantly, we recently identified mutations in *TRIO* in patients with ID

(described in **chapter 4**). Therefore functional analysis of *Trio* will significantly advance our understanding of pathogenesis of ID.

Furthermore, our data showed that the mRNA levels of most members of DOCK-family RhoGEFs increase during development and sustain high in adulthood, implying their contribution in both juvenile and mature hippocampus and cortex. Interestingly, a recent study has reported distinct patterns of the DOCK-family members in cerebellum Purkinje cells [19]. The mRNAs of *Dock1, Dock2* and *Dock3,* could not be detected due to extremely low expression levels. *Dock4* is stably expressed in the first two postnatal weeks followed by a significant drop at the third week, while *Dock9* and *Dock10* levels significantly increase during the second and third postnatal weeks. The different expression patterns between cerebellum and hippocampus/cortex further support the hypothesis that distinct spatial-temporal expressions of Rho regulators enhance the specificity of Rho GTPase signaling-mediated cellular events. Future experiments will reveal the roles and differences of individual RhoGEFs in neuronal function and brain development.

Collectively, our data reveal developmental-specific expression patterns of novel Rho proteins and shed light on directions of future investigations. We further selected *Arhgap12, Ocrl1* and *Trio* for detailed functional analysis, as described in **chapters 3, 4 and 5**.

Material and Methods

Animals

Wistar rats were housed per 2 or 3 animals on a 12-h light cycle in a temperature-controlled (21 ± 1°C) environment with ad libitum access to food and water. Rats were sacrificed at E17, P3, P10, P17, P24 and P90 (adult). The hippocampus and cortex were dissected out and snap-frozen in liquid nitrogen. All samples were stored at -80°C for further analysis. All experiments involving animals were evaluated and approved by the Committee for Animal Experiments of the Radboud university medical center, Nijmegen, the Netherlands.

RNA isolation, reverse transcription and qPCR

Total RNA from the tissue was isolated using *RNeasy Lipid Tissue mini kit* (Qiagen). cDNA was synthesized from 0.5–1 mg RNA using iScript™ cDNA Synthesis Kit. QPCR experiments were subsequently performed in 7900HT Fast Real-Time PCR System using GoTaq qPCR Master mix (Promega).

Primers used for qPCR

DOCK1_RTqPCR_rat_F	ttaccttccgccatagatcc
DOCK1_RTqPCR_rat_R	gggtggtcccatcatatctc
DOCK10_RTqPCR_rat_F	aagacttaccgggatgatgc
DOCK10_RTqPCR_rat_R	ctgtgctctgcttcttctgg
DOCK2_RTqPCR_rat_F	gaggacaggaggctctcaag
DOCK2_RTqPCR_rat_R	cctgtattcgaaccacatcg
DOCK3_RTqPCR_rat_F	gggaaatgatgttgctgttg
DOCK3_RTqPCR_rat_R	agggtcactgcagggtttac
DOCK4_RTqPCR_rat_F	caaaatcatggaccaacagc
DOCK4_RTqPCR_rat_R	catgccctcgacatacaaac
DOCK5_RTqPCR_rat_F	tcaggtcatctccaaagcag
DOCK5_RTqPCR_rat_R	aaccggtttgtccttgtagc
DOCK9_RTqPCR_rat_F	caagagcaccagagaagcag
DOCK9_RTqPCR_rat_R	tggcttcacttctggttcag
ARHGAP1_RTqPCR_rat_F	atgataagtacgggcggaag
ARHGAP1_RTqPCR_rat_R	ggtgcaggtacaggagtgtg
ARHGAP21_RTqPCR_rat_F	ccacacattggactggtctg
ARHGAP21_RTqPCR_rat_R	tcaccctgttccctttccatc
ARHGAP23_RTqPCR_rat_F	tccagcattctgactggttc
ARHGAP23_RTqPCR_rat_R	caggggttctctctcctttg
ARHGAP26_RTqPCR_rat_F	aacccccttgaacacaagac
ARHGAP26_RTqPCR_rat_R	gaaccatggtgatttgcttg
ARHGDIA_RTqPCR_rat_F	atctctttccgggtgaacag
ARHGDIA_RTqPCR_rat_R	tcccgaccatgtagtcagtc
ARHGEF2_RTqPCR_rat_F	tgatgacagatgtgctggtg
ARHGEF2_RTqPCR_rat_R	ataccactgagggcttgtcc
ARHGEF7_RTqPCR_rat_F	cctcagacctctcggaagac
ARHGEF7_RTqPCR_rat_R	aagcaacacttgtggagcag
ARHGAP6_RTqPCR_rat_F	cagcatctggaaaaacatgg
ARHGAP6_RTqPCR_rat_R	tgtgctcctcttccagacag

ARHGAP11a_RTqPCR_rat_F	agctgttgccaagtcatctc
ARHGAP11a_RTqPCR_rat_R	tcgccttaggtctgtactgg
ARHGAP15_RTqPCR_rat_F	aagtctccctccaccaaatc
ARHGAP15_RTqPCR_rat_R	agaagggtgggtccaaatac
ARHGAP12_RTqPCR_rat_F	agcagttgtttcagccagtc
ARHGAP12_RTqPCR_rat_R	acatgcttgagccacttttc
OCRL1_RTqPCR_rat_F	agtccccaatcagactctcc
OCRL1_RTqPCR_rat_R	cttttcacctcattggcatc
BCR_RTqPCR_rat_F	cactacccaacatccctctg
BCR_RTqPCR_rat_R	agcttcttcctcagcctctc
RhoB_RTqPCR_rat_F	ttgaggttgagaggaagcag
RhoB_RTqPCR_rat_R	aggcacaaagttcgcttatg
TRIO_RTqPCR_rat_F1	gtcacggaacatgttgaagg
TRIO_RTqPCR_rat_R1	cctgtatcacctcacggatg
TRIO_RTqPCR_rat_F2	tcgaggaagttgcacagaac
TRIO_RTqPCR_rat_R2	actcttcggggtcacattc
TRIO_RTqPCR_rat_F3	agttggagaacgggtacagg
TRIO_RTqPCR_rat_R3	acctcgctcaatgggataac
Hprt1_RTqPCR_rat_F	tgctgaagatttggaaaagg
Hprt1_RTqPCR_rat_R	cccatctccttcatgacatc
Tbp_RTqPCR_rat_F	ctgggattgtaccacagctc
Tbp_RTqPCR_rat_R	cgcttgggattatattcagc

Reference genes

Two housekeeping genes were used: TBP, TATA-binding protein; PPIA, Peptidylprolyl isomerase A [20].

Data processing and analysis

Raw data was processed by SDS QR Manager 2.3. The relative levels of individual genes were normalized to the expression of E17 and calculated using $2^{-\Delta\Delta Ct}$ ($\Delta Ct = Ct_{\text{candidate genes}} - Ct_{\text{corresponding reference genes}}$; $\Delta\Delta Ct$ (different ages) = ΔCt (different ages) – ΔCt (E17)). The heat map

was generated to present relative expressions of individual genes during hippocampal and cortical development.

References

1. Govek, E.-E. *et al.* The X-linked mental retardation protein oligophrenin-1 is required for dendritic spine morphogenesis. *Nat. Neurosci.* **7,** 364–72 (2004).
2. Ip, J. P. K. *et al.* α2-chimaerin controls neuronal migration and functioning of the cerebral cortex through CRMP-2. *Nat. Neurosci.* **15,** 39–47 (2011).
3. Yan, Y., Eipper, B. A. & Mains, R. E. Kalirin-9 and kalirin-12 play essential roles in dendritic outgrowth and branching. *Cereb. Cortex* **25,** 3487–3501 (2015).
4. Zhu, C. & Jiang, W. Cell cycle-dependent translocation of PRC1 on the spindle by Kif4 is essential for midzone formation and cytokinesis. *Pro. Natl. Aca. Sci., USA* **102,** 343–348 (2005).
5. Van Aelst, L. & D'Souza-Schorey, C. Rho GTPases and signaling networks. *Genes Dev.* **11,** 2295–2322 (1997).
6. Aspenström, P., Fransson, A. & Saras, J. Rho GTPases have diverse effects on the organization of the actin filament system. *Biochem. J.* **377,** 327–37 (2004).
7. Duman, J. G., Mulherkar, S., Tu, Y.-K., Cheng, J. & Tolias, K. F. Mechanisms for spatiotemporal regulation of Rho-GTPase signaling at synapses. *Neurosci. Lett.* **601,** 4–10 (2015).
8. Bayés, À. *et al.* Comparative Study of Human and Mouse Postsynaptic Proteomes Finds High Compositional Conservation and Abundance Differences for Key Synaptic Proteins. *PLoS One* **7,** (2012).
9. Ascano, M. *et al.* FMRP targets distinct mRNA sequence elements to regulate protein expression. *Nature* **492,** 382–6 (2012).
10. Tolias, K. F., Duman, J. G. & Um, K. Control of synapse development and plasticity by Rho GTPase regulatory proteins. *Prog. Neurobiol.* **94,** 133–148 (2011).
11. Govek, E.-E., Hatten, M. E. & Van Aelst, L. The role of Rho GTPase proteins in CNS neuronal migration. *Dev. Neurobiol.* **71,** 528–53 (2011).
12. Seoh, M. L., Ng, C. H., Yong, J., Lim, L. & Leung, T. ArhGAP15, a novel human RacGAP protein with GTPase binding property. *FEBS Lett.* **539,** 131–137 (2003).
13. O'Roak, B. J. *et al.* Exome sequencing in sporadic autism spectrum disorders identifies severe de novo mutations. *Nat. Genet.* **43,** 585–589 (2011).
14. Ma, X. M., Huang, J. P., Eipper, B. a. & Mains, R. E. Expression of Trio, a member of the Dbl family of rho GEFs in the developing rat brain. *J. Comp. Neurol.* **482,** 333–348 (2005).
15. O'Brien, S. P. *et al.* Skeletal muscle deformity and neuronal disorder in Trio exchange factor-deficient mouse embryos. *Proc. Natl. Acad. Sci. U. S. A.* **97,** 12074–12078 (2000).
16. Liebl, E. C. *et al.* Dosage-sensitive, reciprocal genetic interactions between the Abl tyrosine kinase and the putative GEF trio reveal trio's role in axon pathfinding. *Neuron* **26,** 107–118 (2000).
17. Bateman, J., Shu, H. & Van Vactor, D. The guanine nucleotide exchange factor trio mediates axonal development in the Drosophila embryo. *Neuron* **26,** 93–106 (2000).
18. Awasaki, T. *et al.* The Drosophila trio plays an essential role in patterning of axons by regulating their directional extension. *Neuron* **26,** 119–131 (2000).
19. Jaudon, F. *et al.* The RhoGEF DOCK10 is essential for dendritic spine morphogenesis. *Mol. Biol. Cell* **26,** 2112–2127 (2015).
20. Pernot, F., Dorandeu, F., Beaup, C. & Peinnequin, A. Selection of reference genes for real-time quantitative reverse transcription-polymerase chain reaction in hippocampal structure in a murine model of temporal lobe epilepsy with focal seizures. *J. Neurosci. Res.* **88,** 1000–1008 (2010).

Chapter 3

ARHGAP12 functions as a developmental brake on excitatory synapse function

Wei Ba, Martijn M. Selten, Jori van der Raadt, Herman van Veen, Li-Li Li, Marco Benevento, Astrid R. Oudakker, Rizky S.E. Lasabuda, Stef J. Letteboer, Ronald Roepman, Richard J.A. van Wezel, Michael J. Courtney, Hans van Bokhoven, Nael Nadif Kasri

Published in:
Cell Reports. 2016 16:1355-68

Abstract

The molecular mechanisms that promote excitatory synapse development have been extensively studied. However, the molecular events preventing precocious excitatory synapse development so that synapses form at the correct time and place are less well understood. Here, we report the functional characterization of ARHGAP12, a previously uncharacterized Rho GTPase-activating protein (RhoGAP), in the rat brain. ARHGAP12 is specifically expressed in the CA1 region of the hippocampus where it localizes to the postsynaptic compartment of excitatory synapses. ARHGAP12 negatively controls spine size via its RhoGAP activity and promotes, by interacting with CIP4, postsynaptic AMPA receptor endocytosis. Notably, *Arhgap12* knockdown results in precocious maturation of excitatory synapses, as indicated by a reduction in the proportion of silent synapses. Collectively, our data show that ARHGAP12 is a synaptic RhoGAP that regulates excitatory synaptic structure and function during development.

Highlights

- ARHGAP12 functions at excitatory synapses of CA1 hippocampal neurons
- ARHGAP12 promotes postsynaptic AMPA receptor endocytosis
- ARHGAP12 restricts synaptic maturation by limiting silent synapse unsilencing

Graphical Abstract

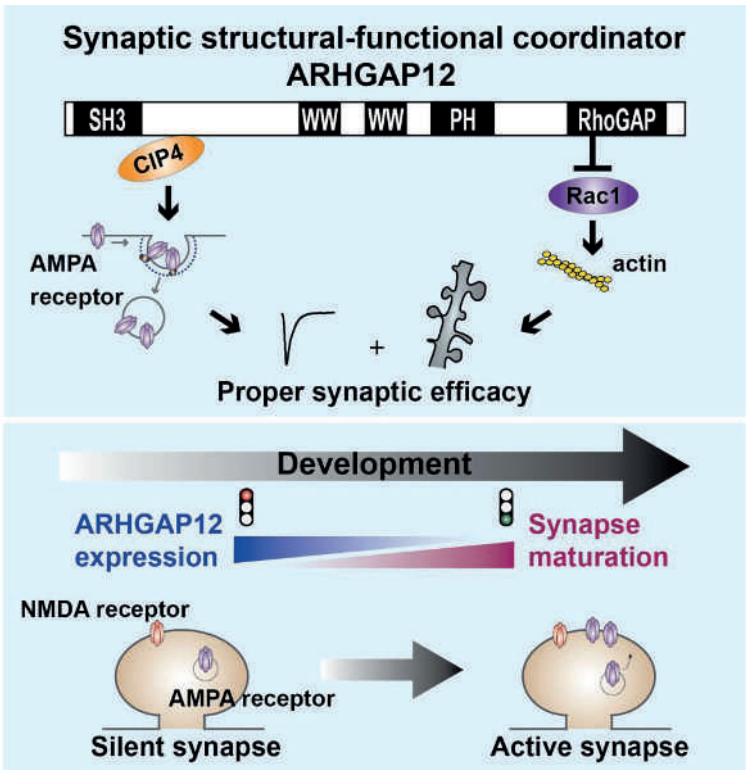

Introduction

The dynamic process of formation and fine-tuning of synaptic connections between neurons is critical for neuronal development and proper brain function [1,2]. Most excitatory synapses are located on dendritic spines, small filamentous actin (F-actin) enriched protrusions on dendrites [3]. Synaptic efficiency is rapidly modified during development or in response to changes in activity by the remodeling of spine structure and the trafficking of glutamate ionotropic alpha-amino-3-hydroxy-5-methyl-4-isoxazole propionic acid receptors (AMPArs) [4].

Several observations have shown that the number of AMPArs and the geometry of dendritic spines are tightly correlated [5–7]. Actin remodeling, which occurs in dendritic spines, drives changes in spine morphology and is required, but not sufficient, for stable long-term potentiation (LTP), one of the core mechanisms of synaptic plasticity underlying learning and memory [8,9]. Indeed, inhibition of spine enlargement by blocking actin polymerization prevents proper LTP expression [10,11], whereas increasing spine size alone, by promoting actin polymerization, is not sufficient to express LTP [8,12,13]. Importantly, evidence suggests that impairments in spine structure and synaptic strength during development contribute to numerous neurological diseases including intellectual disability (ID), autism spectrum disorder (ASD) and schizophrenia [14–17].

How modifications in spine structure and synaptic strength are coordinated, however, remains largely unknown. As key regulators of the actin cytoskeleton, the Rho subfamily members of GTP-binding proteins play a critical role in synapse formation, maturation and maintenance, directly affecting both synapse structure and function [14,18,19]. The Rho subfamily of GTP-binding proteins acts as molecular switches cycling between an active GTP-bound form and an inactive GDP-bound form. Their activity is mainly regulated by guanine nucleotide exchange factors (GEFs), which are positive regulators, and by GTPases activating proteins (GAPs) and guanine nucleotide dissociated inhibitors (GDIs), which are negative regulators [20]. GEFs and GAPs are typically multi-domain proteins and their expression levels are tightly regulated during development. Their specific spatial and temporal expression patterns enable them to regulate synaptic function through the interaction with diverse upstream molecules and downstream effectors [18]. Several Rho GEFs and GAPs have been shown to uniquely regulate synaptic development and plasticity [21–23]. In addition, a number of Rho GTPase regulators and effectors have been directly associated with ID, including Oligophrenin-1 (OPHN1) [24,25], OCRL1 [26], ARHGEF6 [27] and PAK3 [28]. However, remarkably little is known about

how individual GEFs or GAPs precisely coordinate synaptic morphology and function during development.

In this study, we focused on ARHGAP12, a RhoGAP that negatively regulates Rac1 signaling and whose function has not yet been described in the brain. We found that ARHGAP12 is almost exclusively expressed in rat hippocampal CA1 neurons during early stages of development. We investigated the postsynaptic function of ARHGAP12 by spatially and temporally manipulating the levels of ARHGAP12, specifically at hippocampal CA3-CA1 synapses. We characterized ARHGAP12 as a "structure-function coordinator" of excitatory synapses during hippocampal development. Our results uncover a dual function for ARHGAP12 in coordinating synaptic structure and AMPAr trafficking in hippocampal CA3-CA1 synapses during development.

Results

Expression and distribution of ARHGAP12 in the rat hippocampus

To identify Rho GTPase regulators that are critical for the development of cell type-specific synapses in the hippocampus, we made use of the mRNA expression data from the Allen Brain Atlas (©2014 Allen Institute for Brain Science; Allen Mouse Brain Atlas from: http://mouse.brain-map.org/). We focused on Rho GTPase regulators with a specific spatial expression pattern. We identified the Rac1 GAP protein, ARHGAP12 [29], as an interesting candidate protein based on its very specific CA1 and to a lesser extent dentate gyrus (DG) expression (Figure 1A). We initiated the characterization of ARHGAP12 by determining its spatiotemporal distribution in the rat hippocampus. Immunostaining experiments revealed that ARHGAP12 was prominently expressed in the hippocampal CA1 region and to a lesser extent in the DG, confirming the mRNA expression data. ARHGAP12 was detected in all hippocampal CA1 pyramidal cell layers, in the somata and along the dendrites (Figure 1B). We next examined the expression of ARHGAP12 during different stages of hippocampal development by Western blot. ARHGAP12 was abundantly expressed in embryonic (E18) and early postnatal hippocampus (1-2 weeks), and thereafter its expression gradually declined into adulthood. In adult hippocampus, the expression of ARHGAP12 was still detectable but remarkably decreased compared to E18 hippocampus (Figure 1C). These results show that ARHGAP12 is expressed in a distinct spatiotemporal pattern within the hippocampus.

The subcellular distribution of Rho GEFs and GAPs is instructive for their function [30]. We therefore assessed the subcellular distribution of ARHGAP12 in hippocampal CA1 pyramidal neurons. To this end, we tagged ARHGAP12 at its N-terminus with GFP and introduced GFP-*Arhgap12* together with a red fluorescent protein, dsRed, as a cellular marker, into CA1 cells in 12 DIV organotypic hippocampal slices by biolistic transfection. The partition of ARHGAP12 between spines and dendrites was calculated from the ratio of the GFP/dsRed signal in the spine head versus the adjacent dendritic shaft [24]. Interestingly, we found a strong enrichment of ARHGAP12 in the spines compared to the dendrites (Figure 1D). Consistently, we observed overlapping localization of endogenous ARHGAP12 with PSD95 in the stratum radiatum of the hippocampal CA1 region (Figure 1E). Finally, we showed that ectopically expressed GFP-ARHGAP12 colocalized with PSD95 and was found juxtaposed to the pre-synaptic marker Synapsin-1 in hippocampal primary neurons (Figure S1). Together, these data reveal that

ARHGAP12 is located postsynaptically in excitatory synapses of hippocampal CA1 pyramidal neurons.

Figure 1

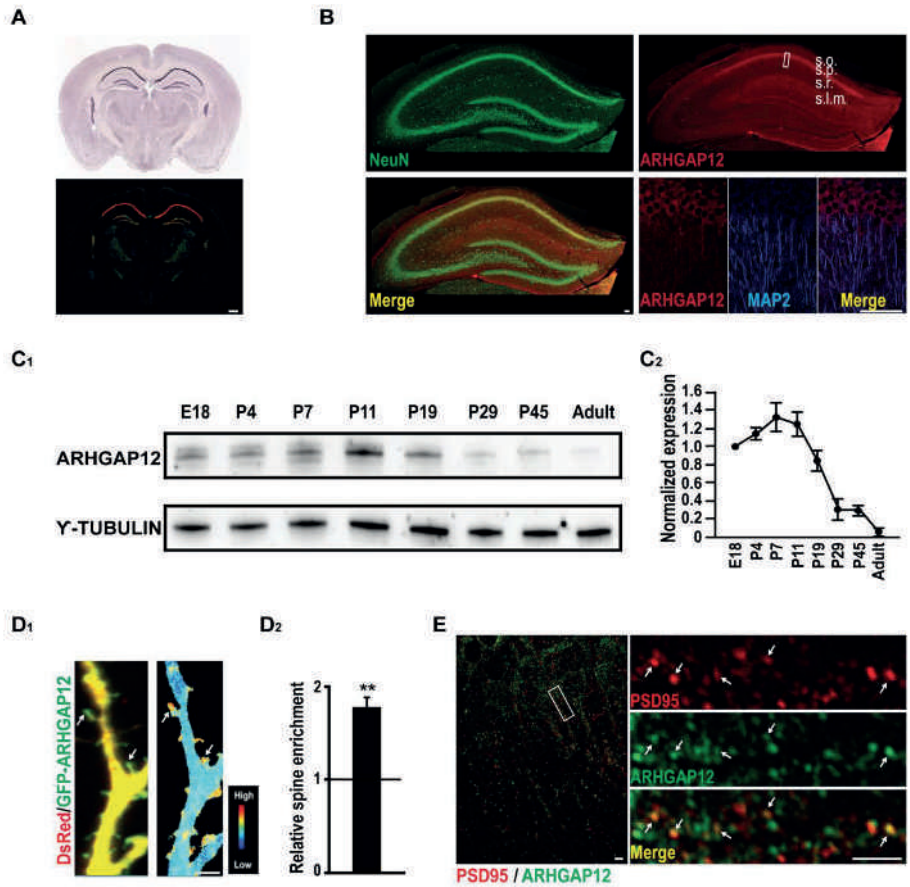

Figure 1 Expression and distribution of ARHGAP12 in the hippocampus
(A) In situ hybridization of Arhgap12 from the Allen Brain Atlas database. Scale bars, 50 µm.
(B) Hippocampi sections from a P20 rat double-immunolabled with an anti-ARHGAP12 antibody (red) and an anti-NeuN antibody (green). Scale bars, 50 µm.
(C_1) Rat hippocampi were collected at indicated ages and probed with anti-ARHGAP12 antibody. Expression of Y-TUBULIN was used as a loading control; equal amounts of protein (50 µg) were loaded.
(C_2) Quantification of ARHGAP12 proteins levels at indicated postnatal ages. ARHGAP12 expression was normalized to Y-TUBULIN in the same sample. Data are shown as mean ± SEM; n = 3.
(D_1) Left, representative images of a dendritic branch of a hippocampal CA1 pyramidal neuron co-transfected with GFP-Arhgap12 (green) and dsRed (red). Right, ratio image of the representative cell. Blue depicts low ARHGAP12 enrichment and red depicts high density. Scale bar, 5 µm.

(D_2) Quantification of GFP-ARHGAP12 enrichment in spines. Data are shown as mean ± SEM; n = 8; **P<0.01, t-test.
(E) Left, hippocampi sections from a P20 rat double-immunolabled with an anti-ARHGAP12 antibody (green) and an anti-PSD95 antibody (red). Right, higher magnification images of the area indicated in the white box on the left panel. White arrows indicate sites of co-localization of ARHGAP12 and PSD95. Scale bars, 10 μm.
See also Figure S1.

Negative regulation of spine morphology by ARHGAP12

Given the presence of ARHGAP12 in spines, and the importance of Rho GTPases in controlling actin cytoskeleton remodeling, we first examined the role of ARHGAP12 in regulating dendritic spine morphology in CA1 pyramidal neurons. We biolistically introduced a GFP-expressing construct, as a cellular marker, with or without a second construct containing *Arhgap12* into CA1 neurons in organotypic hippocampal slices. Immunostaining experiments revealed that neurons transfected with GFP alone showed similar ARHGAP12 levels compared to adjacent non-transfected neurons, whereas neurons expressing *Arhgap12* exhibited a 10-fold increase in ARHGAP12 levels (Figure S2B). Compared to neurons expressing GFP alone, *Arhgap12* overexpressing CA1 pyramidal neurons displayed a significant decrease in both spine density and volume (spine density: GFP control: 5.02 ± 0.22 spines/10 μm, *Arhgap12*: 1.87 ± 0.44 spines/10 μm; spine volume: GFP control: 270.56 ± 49.22; *Arhgap12*: 153.03 ± 52.68; Figure 2A, B, C). In addition, we found that elevated ARHGAP12 levels significantly increased the percentage of immature spines in CA1 neurons (GFP control: 6.03 ± 1.05%, *Arhgap12*: 15.90 ± 3.45%; Figure 2D). These observations are consistent with experiments in which reduced Rac1 activity has been coupled to reduced spine density and size [31].

We next examined the function of endogenous ARHGAP12 by probing the effects of reduced ARHGAP12 expression on dendritic spines. Constructs were generated to coexpress GFP and short hairpin RNA's (shRNAs) targeting either the 3'-untranslated (3'-UTR, *Arhgap12* sh#1) or the translated region (*Arhgap12* sh#2) of rat *Arhgap12* mRNA. *Arhgap12* shRNAs significantly reduced endogenous ARHGAP12 protein levels in hippocampal primary neurons (Figure S2A), as well as in organotypic hippocampal slices (Figure S2B). We found that neither shRNA (*Arhgap12* sh#1 and #2) affected spine density (GFP control: 5.02 ± 0.22 spines/10 μm, *Arhgap12* sh#1: 5.06 ± 0.62 spines/10 μm, *Arhgap12* sh#2: 5.02 ± 1.41 spines/10 μm), but both significantly increased spine volume (GFP control: 270.56 ± 49.22; *Arhgap12* sh#1: 443.69 ± 52.30; *Arhgap12* sh#2: 416.79 ± 116.03; Figure 2B, C). The percentage of immature

spines also significantly decreased in neurons expressing *Arhgap12* shRNAs (GFP control: 6.03 ± 1.05%; *Arhgap12* sh#1: 1.33 ± 1.34%; *Arhgap12* sh#2: 1.68 ± 1.42%; Figure 2D). Importantly, we were able to rescue these phenotypes by coexpressing *Arhgap12* sh#1 with an *Arhgap12* expressing vector that lacked the 3'-UTR and was therefore resistant to *Arhgap12* sh#1-mediated knockdown. This confirmed that the knockdown effects were mediated specifically by loss of ARHGAP12 (spine density: GFP control: 5.02 ± 0.22 spines/10 µm, *Arhgap12* sh#1 + *Arhgap12*: 4.77 ± 1.02 spines/10 µm; spine volume: GFP control: 270.56 ± 49.22; *Arhgap12* sh#1 + *Arhgap12*: 226.51 ± 103.55; Fig 2B, C, D). Importantly, immunostaining experiments on biolistically transfected organotypic hippocampal slices confirmed that the levels of ARHGAP12 were restored to normal levels (Figure S2B).

Next, we examined whether the regulation of ARHGAP12 on spine morphology was dependent on activity. To this end, we treated organotypic slices with high concentration of $MgCl_2$ or the NMDAr antagonist 2-amino-5-phosphonovaleric acid (APV, 100 µM) on the same day of biolistic transfection. Both manipulations however did not prevent the enlargement of spine volume induced by *Arhgap12* downregulation (Figure S3A), indicating that knocking down *Arhgap12* is sufficient to increase spine size. Since the expression of ARHGAP12 declines during normal development, we wondered whether blocking NMDAr activity would affect this process. Interestingly, we found that the gradual decrease of ARHGAP12 levels did not occur in the presence of APV (Figure S3C), suggesting that the developmental elimination of ARHGAP12 is dependent on NMDAr activity.

Together, our results support a model in which NMDAr activity during development drives the repression of ARHGAP12, resulting in the enlargement of spines.

Figure 2

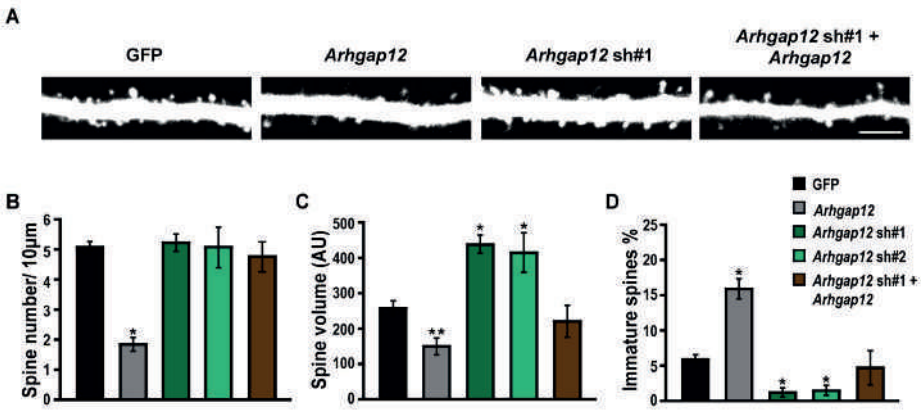

Figure 2 ARHGAP12 negatively regulates spine morphology
(A) Representative images of secondary apical dendrites from CA1 neurons transfected with indicated constructs. Scale bars, 10 µm.
(B, C, D) Quantification of spine density (B), spine volume (C) and percentage of immature spines (D) for indicated experimental conditions. Data are shown as mean ± SEM; GFP: n = 15, *Arhgap12*: n = 9, *Arhgap12* sh#1: n = 8, *Arhgap12* sh#2: n = 7, *Arhgap12* sh#1+ *Arhgap12*: n = 9 from three to four independent experiments. A minimum of 500 spines were analyzed per condition; **P*<0.05, ***P*<0.01, one-way ANOVA.
See also Figure S2 and S3.

Selective modulation of synaptic AMPA receptor mediated transmission by ARHGAP12

Due to the importance of dendritic spine structure for synaptic function and the effects of ARHGAP12 on spine morphology, we next assessed the role of ARHGAP12 in modulating excitatory synaptic function. We first examined the effects of ARHGAP12 overexpression on synaptic transmission. Simultaneous whole-cell recordings of evoked excitatory post-synaptic currents (EPSCs) were recorded at 7 DIV from CA1 pyramidal neurons expressing GFP-*Arhgap12* and from adjacent non-transfected neurons. Overexpression of *Arhgap12* significantly depressed AMPAr- and NMDAr-mediated synaptic transmission (AMPAr-EPSC: uninfected: 197.61 ± 21.15 pA, infected: 45.33 ± 4.67 pA; NMDAr-EPSC: uninfected: 193.71 ± 19.13 pA, infected: 157.84 ± 18.71 pA, Figure 3A, D), suggesting that ectopically expressed *Arhgap12* is sufficient to depress AMPAr- and NMDAr-mediated transmission. Importantly, overexpression of GFP alone did not alter AMPAr or NMDAr-mediated synaptic transmission (Figure S4A). These observations complement our finding that ectopic expression of *Arhgap12*

significantly reduced the number of mature spines and therefore could explain the changes in NMDAr-EPSCs, in addition to the changes in AMPAr-EPSCs.

Next we examined the effects of ARHGAP12 downregulation in regulating synaptic transmission. We found that downregulation of ARHGAP12 levels resulted in potentiation of AMPAr-mediated transmission, but not NMDAr-mediated transmission (*Arhgap12* sh#1: AMPAr-EPSC: uninfected: 40.03 ± 8.98 pA, infected: 60.57 ± 7.85 pA; NMDAr-EPSC: uninfected: 67.28 ± 7.40 pA, infected: 72.82 ± 9.94 pA; *Arhgap12* sh#2: AMPAr-EPSC: uninfected: 51.32 ± 8.03 pA, infected: 70.91 ± 5.43 pA; NMDAr-EPSC: uninfected: 62.13 ± 8.85 pA, infected: 67.88 ± 10.62 pA; Figure 3B, C, D), indicating that downregulation of ARHGAP12 is sufficient to enhance AMPAr-mediated transmission. These results are consistent with our observation that reducing endogenous ARHGAP12 results in larger dendritic spines without affecting the spine density. Thus, bidirectional manipulation of ARHGAP12 levels is associated with opposing effects towards AMPAr-mediated synaptic transmission.

To test whether the effect of ARHGAP12 on AMPArs is restricted to synaptic AMPArs, we recorded extrasynaptic responses evoked by bath application of AMPA (1 μM), which initiated inward currents in all neurons [32]. Interestingly, no differences in AMPA-induced inward currents were observed between control uninfected neurons and *Arhgap12* sh#1 infected neurons (Figure 3E), indicating that the modulation of glutamatergic receptors by ARHGAP12 is specific for synaptic AMPArs. Since altered AMPAr-mediated EPSC may also result from an altered proportion of GluA2-lacking AMPArs, whose currents show unique inward rectification, we further measured the rectification index of AMPAr-EPSCs by measuring AMPAr-mediated EPSCs at -60 mV and at +40 mV holding potential, in the presence of intracellular spermine [33]. We did not, however, observe a significant difference between uninfected neurons and *Arhgap12* sh#1 infected neurons (Figure 3F), indicating that enhanced AMPAr-EPSCs were not a result of changes in AMPAr subunit composition.

The changes in AMPAr-mediated transmission could result from either a change of synaptic AMPArs at individual synapses, a change in the number of functional synapses, or both. In order to determine the precise mechanism, we measured the effect of ARHGAP12 on the amplitudes and frequencies of miniature excitatory postsynaptic currents (mEPSCs). *Arhgap12* sh#1 largely increased both frequency and amplitude of mEPSCs in CA1 pyramidal neurons (Figure 3G). The change in amplitude supports our previous findings showing that ARHGAP12 affects synaptic AMPAr function. A change in frequency usually reflects a change

in the number of active synapses or in presynaptic release probability. We further examined presynaptic release by measuring the paired-pulse ratio. We did not observe significant differences between uninfected and *Arhgap12* sh#1 expressing neurons (Figure 3H), indicating that no retrograde signaling was involved to alter presynaptic release probability and the changes in frequency reflect a change in the amount of active synapses.

Finally, we evaluated the impact of ARHGAP12 on inhibitory (GABAergic) synaptic function in CA1 pyramidal neurons. Evoked inhibitory postsynaptic currents (IPSCs) were measured on neurons expressing *Arhgap12* sh#1 and adjacent control uninfected neurons on hippocampal slices at 7 DIV. We found that *Arhgap12* knockdown did not affect evoked IPSCs (Figure S4B). Together, our findings indicate that ARHGAP12 is critical for modulating excitatory, but not inhibitory, synaptic transmission at the postsynaptic terminal in a cell autonomous way.

Figure 3

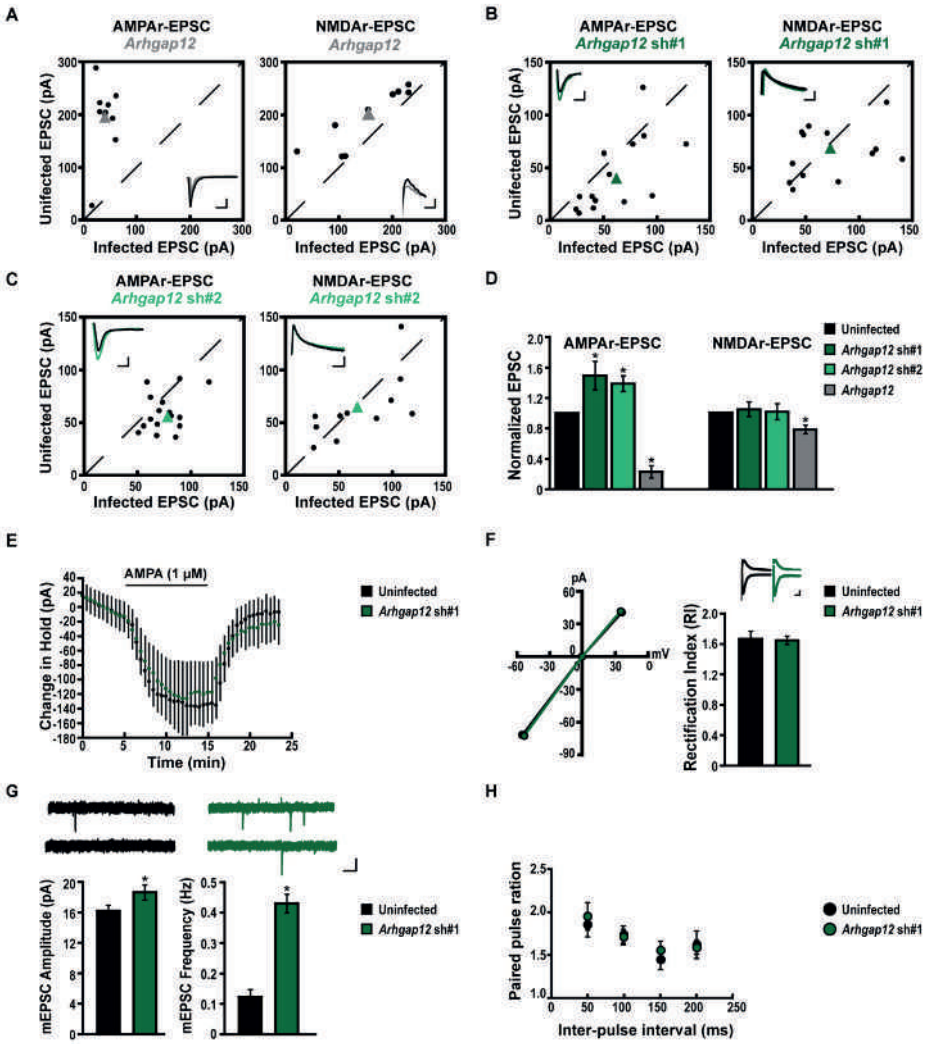

Figure 3 Post-synaptic ARHGAP12 modulates AMPA receptor mediated transmission

(A-C) Amplitudes of AMPAr (left panel) and NMDAr (right panel) EPSCs of uninfected neurons are plotted against simultaneously recorded neighboring neurons expressing *Arhgap12* (A), *Arhgap12* sh#1 (B), *Arhgap12* sh#2 (C). Recordings were performed at 7 DIV. Black symbols represent single pairs of recordings; green or grey symbols show mean values. Inserts in each panel show sample average traces; black traces, uninfected neurons; grey traces, *Arhgap12* overexpressed neurons; green traces, *Arhgap12* shRNAs expressing neurons. Scale bars, 10 ms and 25 pA.

(D) Summary of effects of *Arhgap12* overexpression or knockdown. Data are shown as mean ± SEM; n = 9-15 from three independent experiments; **P*<0.05, paired t-test.

(E) Time course of whole-cell currents recorded from CA1 pyramidal neurons infected with *Arhgap12* sh#1 or control uninfected neurons during the application of 1 μM AMPA. Uninfected: n = 9, *Arhgap12* sh#1: n = 8 from two independent experiments.
(F) Synaptic responses were recorded at -60 mV and +40 mV from CA1 pyramidal neurons infected with *Arhgap12* sh#1 or uninfected neurons in the presence of intracellular spermine. Rectification Index was calculated by dividing the amplitude at -60 mV by the amplitude at +40 mV. n = 8 for both conditions from two independent experiments.
(G) Representative traces and quantifications of excitatory miniature events recorded from uninfected neurons and neurons expressing *Arhgap12* sh#1 at 7 DIV. Scale bars, 1 s and 25 pA. Data are shown as mean ± SEM; n = 13-15 from three independent experiments; **P*<0.05, t-test.
(H) Paired-pulse facilitation ($EPSC_2/EPSC_1$) recorded from uninfected and *Arhgap12* sh#1 expressing neurons at indicated inter-stimulus intervals. Data are shown as mean ± SEM; n = 7 for both groups from three independent experiments.
See also Figure S4.

Arhgap12 knockdown promotes hippocampal synaptic development by accelerating silent synapse unsilencing

We next sought to further delineate the mechanism by which ARHGAP12 restricts synaptic function. We reasoned that a plausible mechanism could involve the regulation of silent synapse activation. Silent synapses refer to those synapses with NMDArs but no functional AMPArs [34], and they can convert to active synapses by AMPAr insertion (also termed "unsilencing") during development and/or in response to neuronal activity [35,36]. In the hippocampus, the proportion of these silent synapses rapidly decreases during the first two weeks of postnatal development [35]. To detect silent synapses, we performed whole-cell patch-clamp recordings on CA1 pyramidal neurons using minimum stimulation. In control uninfected 4 DIV CA1 neurons, the failure rate was much larger at -60 mV than at +40 mV (Figure 4A, B), indicating that a substantial fraction of the synapses are still silent at this stage of development (Figure 4C). As expected, the proportion of silent synapses gradually decreased during development, with almost all synapses unsilenced at 14 DIV (Figure 4C). Interestingly, when the same experiments were performed on *Arhgap12* sh#1 expressing hippocampal CA1 neurons, we found that the proportion of silent synapses was significantly decreased at the earlier developmental time points (4 DIV and 7-8 DIV) but was comparable to control at 13-14 DIV (Figure 4C), suggesting that *Arhgap12* downregulation promotes synaptic maturation by accelerating synapse unsilencing.

Robust synaptogenesis occurs during the first two weeks of postnatal development and a major mechanism underlying these critical events is synapse unsilencing. Since the developmental gradient of ARHGAP12 expression is inversely correlated to the trend of

synaptic maturation in hippocampus, we speculated that ARHGAP12 might act as an endogenous “brake” during development. Namely, decreasing levels of ARHGAP12 would release the repression and accelerate synaptogenesis and functional synapse maturation. If this is the case, the potentiation of CA3-CA1 synapses would be stronger when *Arhgap12* is downregulated in the early developmental stages compared to that at the later stages. Conversely, keeping ARHGAP12 expression at a high level throughout the development would severely limit excitatory synapse development. We first tested this hypothesis by knocking down *Arhgap12* in organotypic hippocampal slices and compared evoked AMPAr-EPSC on a CA1 pyramidal neuron expressing *Arhgap12* sh#1 and an adjacent uninfected neuron at different stages of the development *in vitro* (4 DIV, 7-8 DIV and 13-14 DIV). Whole-cell patch-clamp recordings revealed that neurons expressing *Arhgap12* sh#1 indeed displayed the most profound potentiation of AMPAr-EPSC at 4 DIV and this effect gradually decreased when recording at later stages, with no changes observed at 13-14 DIV (Figure 4D). Conversely, when keeping elevated levels of ARHGAP12 throughout the development of hippocampal neurons, we observed significantly decreased AMPAr-mediated synaptic transmission, measured as a reduction in amplitude and frequency of mEPSCs (Figure S5A, B). The decreased AMPAr-mediated transmission was also accompanied with a reduction in PSD95 density, further suggesting that ARHGAP12 can prevent excitatory synapse formation (Figure S5C).

Together, our results indicate that endogenous ARHGAP12 dampens synaptic development by limiting the unsilencing of silent synapses and suggest that endogenous ARHGAP12 acts as a synaptic "brake" during hippocampal development.

Figure 4

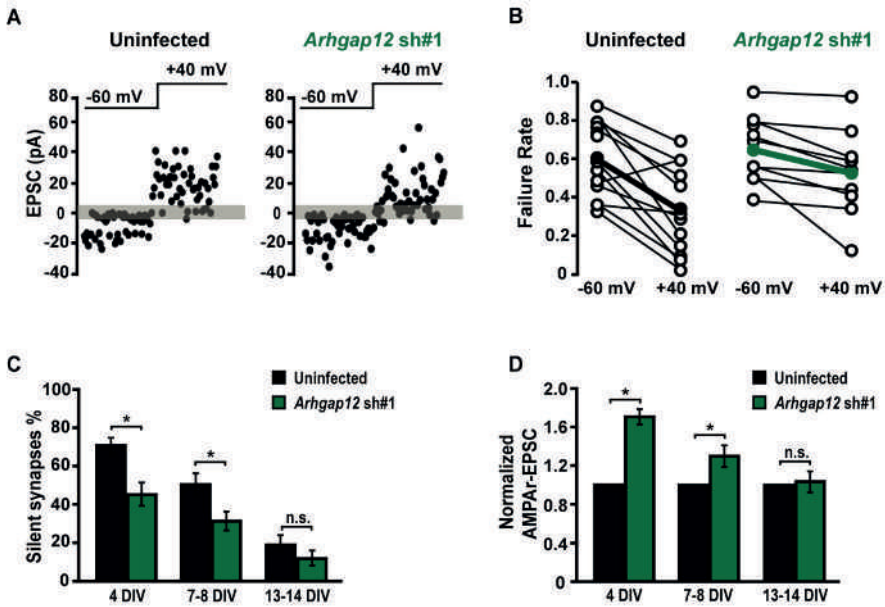

Figure 4 *Arhgap12* knockdown promotes hippocampal synaptic development by accelerating silent synapse unsilencing

(A) Minimal stimulation assay. Representative plot of individual response at -60 mV and +40 mV with minimal stimulations in indicated conditions.

(B) Failures of responses using minimal stimulation at -60 mV and +40 mV from uninfected neurons and Arhgap12 sh#1 infected neurons.

(C) Percentage of silent synapses at different developmental stages of uninfected neurons and Arhgap12 sh#1 infected neurons. Data are shown as mean ± SEM; n = 11-14 from three independent experiments; *P<0.05, paired t-test.

(D) Evoked AMPAr-mediated transmission recorded from CA1 pyramidal neurons infected with Arhgap12 sh#1 and uninfected neurons at different developmental stages. Data are shown as mean ± SEM; n = 11-15 for both groups at all time points, from three to four independent experiments; *P<0.05, paired t-test.

See also Figure S5.

Identification of Cdc42-interacting protein 4 (CIP4) as an ARHGAP12 interactor

Next, to gain insights into the mechanisms by which ARHGAP12 modulates synapses, we sought to identify direct interactors of ARHGAP12 by performing a GAL4-based interaction trap screen in yeast (yeast two-hybrid system).

ARHGAP12 contains several protein motifs: a Src homology-3 (SH3) domain at its N-terminus, two WW domains, and a Pleckstrin-homology (PH) domain, followed by a GAP domain shown to negatively regulate Rac1 GTPase [29]. Full-length human ARHGAP12 and fragments containing different conserved domains were used as baits in the yeast two-hybrid screening (Figure 5A). Interestingly, four independent cDNAs matched the sequence of Cdc42-interacting protein 4 (CIP4, also named thyroid hormone receptor 10 variant, TRIP10; Figure S7A) that harbors a highly conserved F-BAR (Fes-CIP4 homology-Bin/Amphyphysin/Rvsp) domain at the N-terminus and which has recently been implicated in neurite outgrowth [37], clathrin-mediated endocytosis, endosomal trafficking [38–40] and synaptic growth at the neuromuscular junction (NMJ) in *Drosophila* [41]. We subsequently performed co-immunopricipitation (co-IP) experiments to validate the interaction between ARHGAP12 and CIP4. Since none of the antibodies for CIP4 that we have tested to date were suitable for Western blot analysis and IP *in vivo* (data not shown, and [37]), we coexpressed GFP-*Arhgap12* WT and Myc-*Cip4* in HEK293T cells and carried out reciprocal co-IP experiments using an anti-Myc and an anti-ARHGAP12 antibody. Indeed, ARHGAP12 specifically co-immunoprecipitated with CIP4 and *vice versa* (Figure 5B, C).

Next, we set out to identify the CIP4 binding region in ARHGAP12. Given that the positive clones from the yeast two-hybrid screening encompassed the first 156 amino acids (aa) of ARHGAP12 (Figure 5A), we reasoned that ARHGAP12 is likely to bind to CIP4 via its N-terminal domain. To test this hypothesis, we generated an ARHGAP12 deletion mutant lacking aa 1-156 (Δ1-156aa) and repeated the co-IP experiment. We found that the Δ1-156aa mutant failed to bind CIP4. Since the first 156 aa of ARHGAP12 include an SH3 domain and this domain is known to be critical for protein-protein interactions, we reasoned that ARHGAP12 is likely to bind CIP4 via its SH3 domain. A deletion of the SH3 domain (ΔSH3) of ARHGAP12 was generated and tested for its ability to interact with full-length CIP4 in HEK293T cells using co-IP. Surprisingly, the SH3 domain deletion mutant (ΔSH3) of ARHGAP12 was still able to bind CIP4, indicating that the SH3 domain of ARHGAP12 is not required for interacting with CIP4. Likewise, a point mutation leading to an inactivation of the GAP function of ARHGAP12 (R695Q) (Figure S6A; Nadif Kasri et al., 2009) did not affect the ARHGAP12-CIP4 interaction *in vitro*. Overall, these data indicate that ARHGAP12 can interact with CIP4 via its N-terminal domain (aa 1-156).

Figure 5

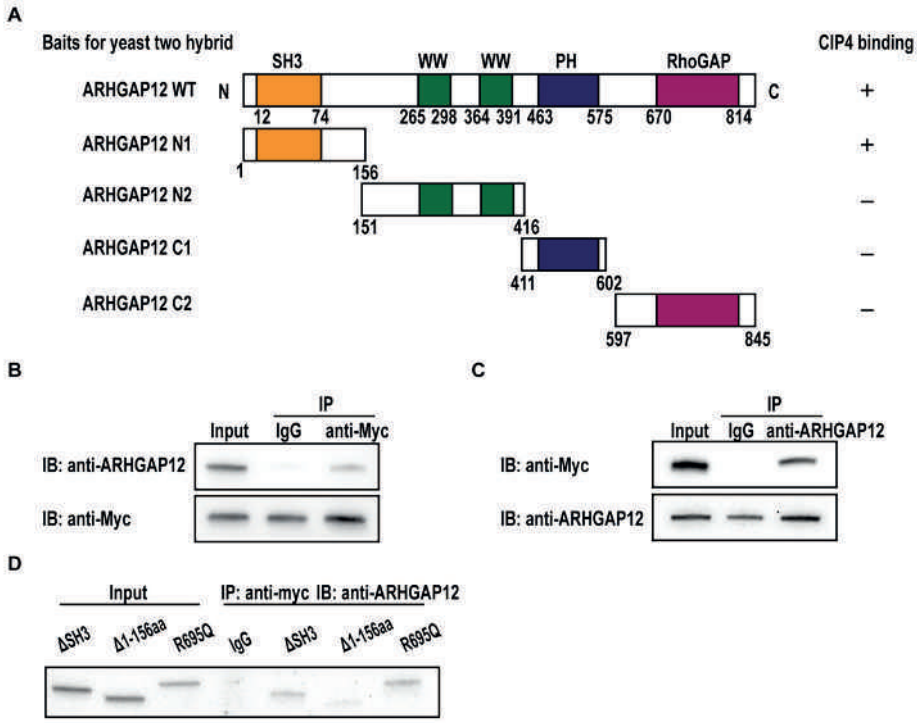

Figure 5 Interaction of ARHGAP12 with CIP4

(A) Domain structure of ARHGAP12 and fragments used as "baits" in yeast two-hybrid screening. Presence of positive colonies using distinct baits was indicated with "+" or "-".

(B-C) Co-immunoprecipitation of ARHGAP12 and CIP4 *in vitro*. Protein extract from HEK293T cells co-transfected with GFP-*Arhgap12* and myc-*Cip4* constructs for 24 hours was incubated with mouse IgG or an anti-Myc antibody (B) or an anti-ARHGAP12 antibody (C). The immunoprecipitates were analyzed by immunoblotting using indicated antibodies. n = 6.

(D) Co-immunoprecipitation of ARHGAP12 mutants and CIP4 *in vitro*. Extract from HEK293T cells co-transfected with myc-*Cip4* and indicated mutants of *Arhgap12* for 24 hours was incubated with an anti-CIP4 antibody. Immune complexes were immunoblotted with an anti-ARHGAP12 antibody. n = 3.

Functional dissection of ARHGAP12 controlling synaptic structure and strength

Previously ARHGAP12 has been shown to contain a GAP domain that negatively regulates the activity of Rac1 GTPase in non-neuronal cells [29]. We confirmed that this is also the case in hippocampal neurons by performing Rac1 activity assay (Figure S6A).

Since ARHGAP12 also interacts with CIP4 via its N-terminal domain, which has been shown to play a role in clathrin-mediated endocytosis [38–40], we wondered whether these two distinct domains play separate roles affecting synaptic structure and function, respectively. As a first step toward addressing this question, we compared the effects of regulating dendritic spine morphology between ARHGAP12 WT and two mutants, *Arhgap12*_R596Q and *Arhgap12*_Δ1-156aa. Spine structure analysis revealed that expression of the *Arhgap12*_R596Q mutant in CA1 pyramidal neurons failed to mimic the phenotype observed by expressing *Arhgap12* WT, namely decreased spine density and volume compared to GFP control (spine density: GFP control: 4.62 ± 0.51 spines/10 µm, *Arhgap12* WT: 2.21 ± 0.82 spines/10 µm, *Arhgap12*_R596Q: 4.17 ± 0.36 spines/10 µm; spine volume: GFP control: 273.72 ± 57.27, *Arhgap12* WT: 150.11 ± 52.73, *Arhgap12*_R596Q: 307.61 ± 35.2, Figure 6A, B). Conversely, *Arhgap12*_Δ1-156aa expressing CA1 neurons displayed spine morphology similar to *Arhgap12* WT expressing neurons (spine density: GFP control: 4.62 ± 0.51 spines/10 µm, *Arhgap12* WT: 2.21 ± 0.82 spines/10 µm, *Arhgap12*_ Δ1-156aa: 2.41 ± 0.78 spines/10 µm; spine volume: GFP control: 273.72 ± 57.27, *Arhgap12* WT: 150.11 ± 52.73, *Arhgap12*_Δ1-156aa: 175.45 ± 53.01; Figure 6A, B). These data indicate that the GAP activity of ARHGAP12, but not its interaction with CIP4, is required to regulate dendritic spine morphology. To corroborate our data showing ARHGAP12 affects dendritic spine structure by acting on the Rac1 signaling pathway, we examined whether inhibiting Rac1 signaling could rescue the increased spine volume resulting from *Arhgap12* knockdown by making use of the competitive inhibitor of Rac1 activation NSC23766 [42]. We found that NSC23766 (0.1 mM) treatment of *Arhgap12* shRNA transfected hippocampal slices largely rescued the spine volume defects in *Arhgap12* knockdown neurons. The mean spine volume did not significantly increase compared to control GFP expressed neurons (spine density: GFP control: 4.62 ± 0.51 spines/10 µm, *Arhgap12* sh#1: 5.06 ± 0.62 spines/10 µm, *Arhgap12* sh#1 + Rac1 inhibitor: 4.34 ± 0.75 spines/10 µm; spine volume: GFP control: 273.72 ± 57.27, *Arhgap12* sh#1: 443.69 ± 52.30, *Arhgap12* sh#1 + Rac1 inhibitor: 251.54 ± 73.82; Figure 6A, B). Moreover, we found that, as expected, treating neurons with NSC23766 resulted in decreased spine density and volume, and this treatment on *Arhgap12* overexpressed neurons did not cause additional effects on spine morphology (Figure S6B, C). Overall, these findings imply that the GAP activity of ARHGAP12, but not ARHGAP12-CIP4

interaction, is responsible for controlling dendritic spine morphology in CA1 pyramidal neurons via Rac1 GTPase signaling pathway.

Given that CIP4 is involved in clathrin-dependent endocytosis, a mechanism that mediates internalization of most plasma membrane proteins including AMPARs [43], we speculated that the inhibitory effect of ARHGAP12 on AMPAr function could be due to involvement of the ARHGAP12-CIP4 complex in AMPAr endocytosis process. To directly evaluate the AMPAr endocytotic process, live-cell antibody feeding experiments were performed in 14 DIV primary hippocampal neurons transfected with GFP, *Arhgap12* sh#1, *Arhgap12* WT, *Arhgap12*_R695Q or *Arhgap12*_Δ1-156aa. We observed impaired GluA1 endocytosis in neurons expressing *Arhgap12* sh#1. Both *Arhgap12* WT and *Arhgap12*_R659Q significantly enhanced endocytosis of GluA1 compared to the GFP control condition, whereas *Arhgap12*_Δ1-156aa mutant, did not alter GluA1 endocytosis (Figure 6C). Functionally, overexpression of *Arhgap12* WT decreased both mEPSC amplitude and frequency. *Arhgap12*_R695Q overexpression led to reduced mEPSC amplitude without affecting frequency, whereas *Arhgap12*_Δ1-156aa resulted in unaltered amplitude but reduced frequency (Figure 6D, E).

Figure 6

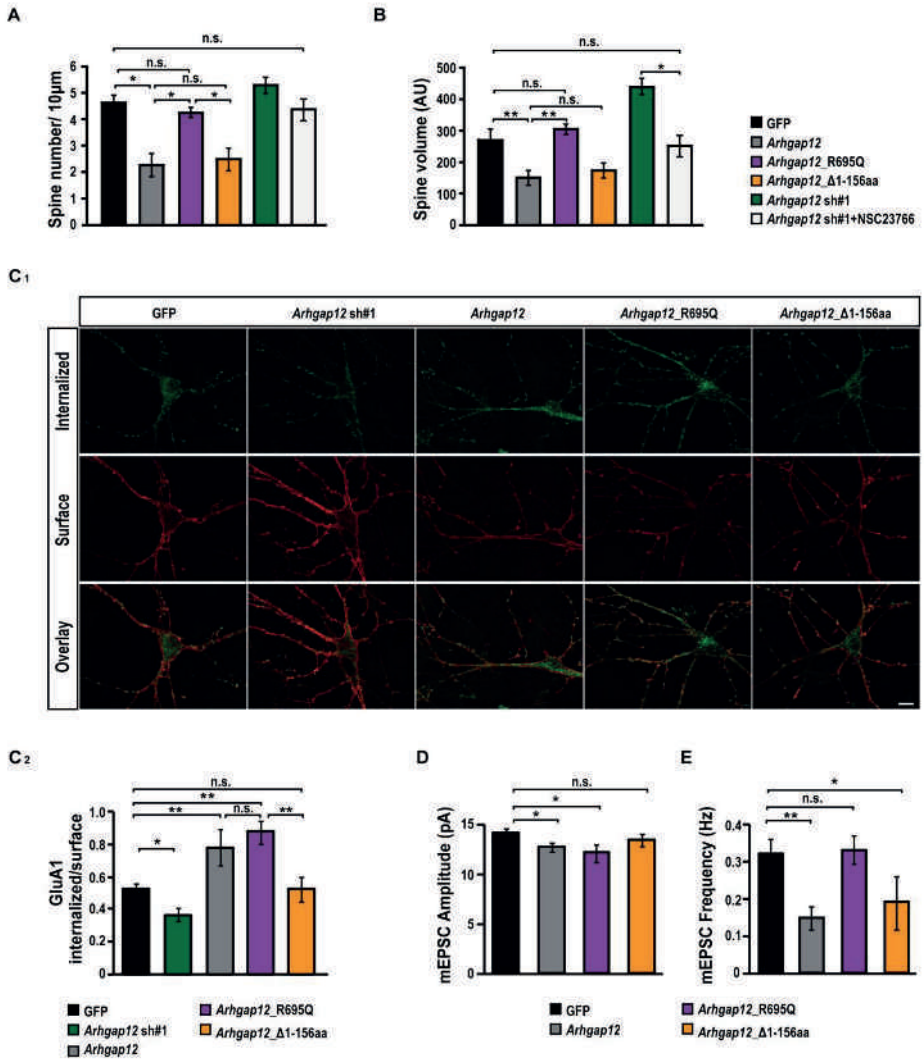

Figure 6 ARHGAP12 regulates synaptic structure and function via distinct domains
(A-B) Morphological analysis of dendritic spine density (A) and volume (B) of CA1 pyramidal neurons in indicated conditions. Data are shown as mean ± SEM; GFP: n = 15, *Arhgap12*: n = 9, *Arhgap12*_R695Q: n = 9, *Arhgap12*_Δ1-156aa: n = 8, *Arhgap12* sh#1+NSC23766: n = 6, data pooled from three to four independent experiments; **P*<0.05, ***P*<0.01, one-way ANOVA.
(C) AMPA receptor endocytosis assay. (C_1) Representative double-label images of internalized (green) and surface (red) AMPA receptor GluA1 subunit in low density 14 DIV hippocampal neurons in indicated experimental groups. (C_2) Ratiometric analysis of the intensity of internalized GluA1 to surface GluA1 in indicated conditions. Data are shown as mean ± SEM; control: n = 34, *Arhgap12* sh#1:

n = 20, *Arhgap12*: n = 15, *Arhgap12*_R695Q: n = 15, *Arhgap12*_Δ1-156aa: n = 15; data pooled from three independent cultures; **P*<0.05, t-test. Scale bars, 10 µm.
(D, E) Excitatory miniature events recorded from neurons biolistically transfected at 12 DIV with indicated constructs. Data are shown as mean ± SEM; GFP: n = 12, *Arhgap12*: n = 16, *Arhgap12*_R695Q: n = 11, *Arhgap12*_Δ1-156aa: n = 11; data pooled from three independent experiments; **P*<0.05, *P<0.01, one-way ANOVA.
See also Figure S6.

Furthermore, based on the minimal interacting sequence (414-428 aa) in CIP4 that we obtained from our yeast two-hybrid screening (Figure S7A), we designed a small interfering peptide ($Pep^{A12\text{-}CIP4}$) to disrupt the ARHGAP12-CIP4 complex. A corresponding scrambled peptide was used as a control (Pep^{ctrl}). The peptides were conjugated to the cell-membrane transduction domain of the HIV-1 TAT protein (TAT), which allowed the peptide to cross the membrane of neurons. In HEK293T cells, we found that $Pep^{A12\text{-}CIP4}$ disrupted the ARHGAP12-CIP4 interaction, whereas Pep^{ctrl} did not (Figure 7A). Additionally, we observed no effect of both Pep^{ctrl} and $Pep^{A12\text{-}CIP4}$ on surface NMDAr expression and Cdc42-CIP4 interaction (Figure S7B, C). Next we examined whether disrupting the ARHGAP12-CIP4 interaction influences GluA1 endocytosis. Live-cell antibody feeding experiments were performed in 14 DIV primary hippocampal neurons treated with Pep^{ctrl} or $Pep^{A12\text{-}CIP4}$ for 24 hours. Our results showed that $Pep^{A12\text{-}CIP4}$ significantly impaired AMPAr GluA1 subunit endocytosis compared to Pep^{ctrl} treated neurons (Figure 7B). Electrophysiologically, CA1 pyramidal neurons treated with $Pep^{A12\text{-}CIP4}$ exhibited a significantly increased amplitude compared to Pep^{ctrl} treated neurons (Figure 7C), indicating that disrupting the interaction of ARHGAP12-CIP4 was sufficient to increase the amount of AMPArs accumulating at synapses, mimicking the effect of ARHGAP12 knockdown on AMPAr mediated transmission. Finally, to further exclude the possibility that the ARHGAP12-CIP4 interaction can regulate spine morphology, we imaged dendritic spine morphology of neurons treated with Pep^{ctrl} or $Pep^{A12\text{-}CIP4}$. No significant differences between two conditions were observed (Figure 7D). These results suggest that the ARHGAP12-CIP4 interaction is responsible for controlling AMPA receptor endocytosis, but not for regulating spine morphology.

Figure 7

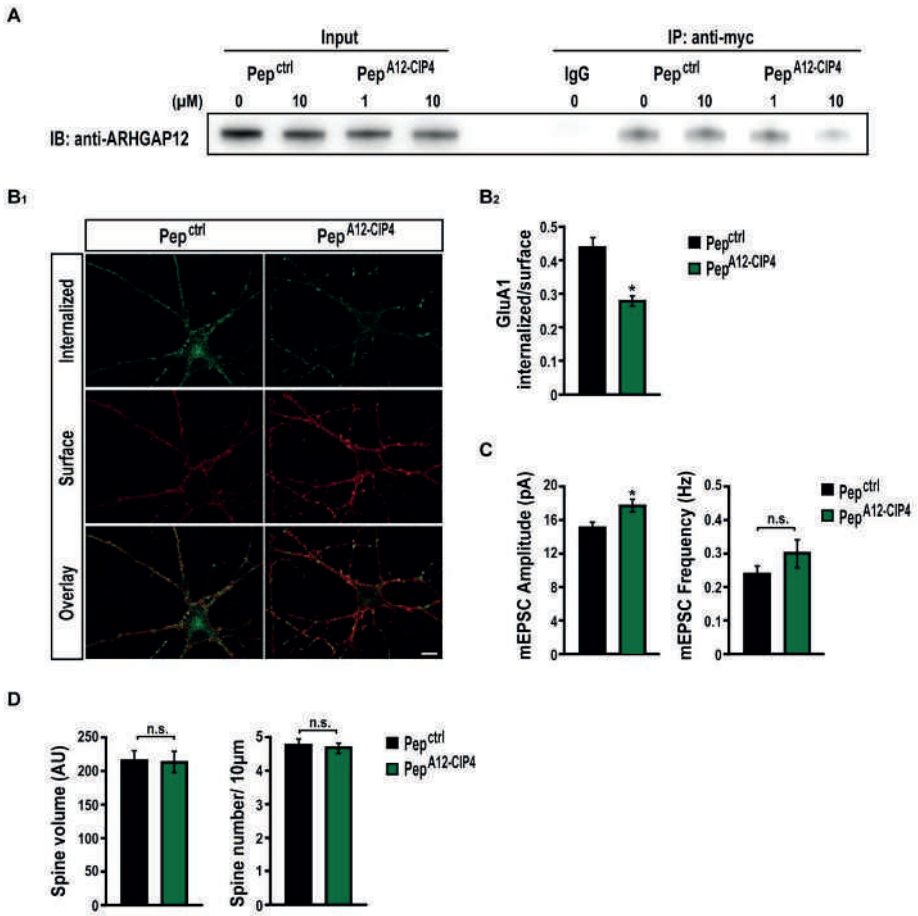

Figure 7 Disrupting ARHGAP12-CIP4 interaction impairs AMPAr endocytosis

(A) HEK293T cells co-transfected with GFP-*Arhgap12* and myc-*Cip4* constructs were incubated with Pep^{ctrl} and $Pep^{ARHGAP12\text{-}CIP4}$ with indicated concentrations for 24 hours. Interaction between ARHGAP12 and CIP4 were examined using immunoblotting with an anti-ARHGAP12 antibody. n = 3.

(B) AMPA receptor endocytosis assay. (B_1) Representative double-label images of internalized (green) and surface (red) AMPA receptor GluA1 subunit in low density 14 DIV hippocampal neurons; (B_2) Ratiometric analysis of the intensity of internalized GluA1 to surface GluA1 in Pep^{ctrl} and $Pep^{ARHGAP12\text{-}CIP4}$ conditions. Data are shown as mean ± SEM; Pep^{ctrl}: n = 18, $Pep^{ARHGAP12\text{-}CIP4}$: n = 19; data pooled from three independent cultures; **P*<0.05, t-test. Scale bar, 10 μm.

(C) Excitatory miniature events recorded at 14 DIV from organotypic hippocampal slices treated with Pep^{ctrl} or $Pep^{ARHGAP12\text{-}CIP4}$ for 24 hours. Data are shown as mean ± SEM; Pep^{ctrl}: n = 13, $Pep^{ARHGAP12\text{-}CIP4}$: n = 12; data pooled from three independent experiments; **P*<0.05, t-test.

(D) Morphological analysis of dendritic spine density and volume of CA1 pyramidal neurons treated with 10 µM pep^{ctrl} or 10 µM $pep^{ARHGAP12\text{-}CIP4}$ for 24 hours. Data shown as mean ± SEM; pep^{ctrl}: n = 7, $pep^{ARHGAP12\text{-}CIP4}$: n = 7 from three independent experiments; t-test.
See also Figure S7.

Together, our findings indicate that ARHGAP12 regulates spine morphology via its GAP activity and synaptic strength via its interaction with the F-BAR protein CIP4.

Discussion

The molecular mechanisms that promote excitatory synapse formation and maturation have been extensively studied. However, the molecular events preventing precocious excitatory synapse development so that synapses form at the correct time and place are less well understood. Here we identified ARHGAP12, a previously uncharacterized Rac1-GAP in the brain, as a critical coordinator of synaptic structure and function in the developing rat hippocampus.

ARHGAP12-Rac1 signaling in regulating spine morphology

In the present study, we focused on hippocampal CA3-CA1 synapses, based on the prominent expression of ARHGAP12 in CA1 during early development. We found that overexpressing WT *Arhgap12* resulted in reduced spine density and volume, and an increased percentage of immature spines in CA1 pyramidal neurons, whereas overexpressing the *Arhgap12* GAP mutant failed to generate a similar phenotype. In addition, we showed that downregulation of *Arhgap12* led to enlarged spine volume and this enlargement was successfully rescued by pharmacologically inhibiting overactive Rac1 signaling. These results strongly suggest that negatively regulating Rac1 signaling via ARHGAP12's GAP activity is essential for maintaining normal dendritic spine structure at the CA3-CA1 synapse. These data agree with several other reports in which downregulation or overexpression of Rac1-GAPs increased or decreased spine size and density, respectively [18]. For instance, overexpression of the Rac1 GAP, alpha 1-chimaerin, resulted in a loss of spines by inhibiting the formation of new spines as well as promoting the pruning of existing spines [44,45]. More recently, mice lacking the Rac-GAP Bcr and its relative Abr were shown to exhibit increased spine size and density [46].

An intriguing aspect of our study is that ARHGAP12 exhibits a unique spatiotemporal profile, with an almost exclusive expression in CA1 and DG. Specific spatiotemporal profiles have been observed for numerous GEFs and GAPs and are believed to contribute to the specificity of Rho signaling in the brain [18]. Our study thus unveils a vital role of ARHGAP12 in regulating spine structure via Rac1 signaling in CA1 and supports the hypothesis that Rho GEFs and GAPs cooperate in complimentary signaling pathways, so to spatially and temporally regulate Rho GTPase signaling during synapse remodeling [23]

ARHGAP12-CIP4 interaction in regulating synaptic strength

In this study, we found that knocking down *Arhgap12* potentiated hippocampal CA3-CA1 synapses, whereas *Arhgap12* up-regulation led to a significant synaptic depression. Specifically, *Arhgap12* knockdown increased AMPAr-mediated EPSCs and the frequency and amplitude of mEPSCs, indicating that reducing ARHGAP12 levels promoted synaptic expression of AMPArs. Due to the tight correlation between synaptic strength and spine size, the increase in synaptic strength could occur as a consequence of the changes in spine size [47,48]. Alternatively, ARHGAP12 could regulate synapse function independently of spine size. We found that the F-BAR containing protein CIP4 interacts with ARHGAP12. Similar to ARHGAP12, CIP4 is highly expressed during early cortical development, and CIP4 inhibits neurite formation by promoting lamellipodial protrusions [37] and restrains synaptic growth at the NMJ [41]. We demonstrated that the interaction between ARHGAP12 and CIP4 involves the N-terminus of ARHGAP12 and is independent of its GAP activity. Importantly, CIP4 is recruited in clathrin-coated pits during clathrin-mediated endocytosis [38], implying a function for CIP4 in this process. We showed that interrupting the ARHGAP12-CIP4 interaction, using a peptide mimicking the ARHGAP12 binding site on CIP4, resulted in elevated AMPAr-mediated transmission. In addition, interfering with the ARHGAP12-CIP4 interaction decreased the endocytosis of GluA1 AMPAr subunits, leading to more synaptic AMPArs. Interestingly, we found that the interaction between ARHGAP12 and CIP4 was not required for regulating spine morphology. This is somewhat different from the function of CIP4 at the NMJ in Drosophila, where dCIP4 acts downstream of Cdc42 to activate the postsynaptic Wsp–Arp2/3 pathway to restrain synaptic growth [41]. Together these data suggest that by binding to CIP4, ARHGAP12 increases AMPAr endocytosis and thereby reduces synaptic strength. Several studies have shown that events triggering changes spine morphology and insertion/removal of AMPAr subunits are distinct. How these two events are kept in check so that changes in spine morphology correlate with synaptic strength is still unclear. The GluA1 C-tail has been proposed to play a critical role herein by linking both events [49]. Our data unveil an interesting model in which ARHGAP12 via its GAP activity, regulates spine structure, while by interacting with CIP4, is able to modulate AMPAr-mediated synaptic transmission in the hippocampus. Thus neurons might use an elegant mechanism to keep changes in spine morphology and synaptic strength balanced, where ARHGAP12 signaling controls both actin polymerization and AMPAr trafficking. Exactly how ARHGAP12 and CIP4 cooperate to increase AMPAr

endocytosis still remains to be elucidated. It is possible that CIP4, similar to FBP17, affects AMPAr endocytosis by recruiting WASP and dynamin for vesicle initiation and scission [38].

Synaptic maturation is restricted by ARHGAP12 during hippocampal development

A characteristic hallmark of the developing brain is the presence of silent synapses, which contain NMDArs but lack AMPArs. Premature or delayed synapse unsilencing has been implicated in neurodevelopmental disorders, including ASD [50–52]. Since ARHGAP12 is highly expressed during early postnatal stages and followed by a gradual decline in CA1, which mirrors the trend of robust synaptogenesis, it raises the possibility that the presence of ARHGAP12 might impede synaptic development. Our data showed that the potentiation of synaptic transmission, as a result of *Arhgap12* downregulation, was the strongest at 4 DIV and gradually decreased with age. Conversely, when ARHGAP12 was maintained at a high level, synaptic development was impeded. We here thus unveil a potentially interesting positive feedback mechanism between synaptic activity and ARHGAP12 signaling, in the sense that synaptic activity is required for ARHGAP12 repression, and in turn, ARHGAP12 downregulation enhances the synaptic efficacy. Such a positive feedback relationship could play a key role during critical periods of synapse development, with too little activity preventing synapse development. Our data thus support the notion that ARHGAP12 is an intrinsic factor in the developmental program of synapses and functions as a synaptic "brake" during hippocampal development. Releasing the braking effect of ARHGAP12 at an inappropriate time might result in mistimed maturation of glutamatergic synapses and in a disrupted balance between excitation and inhibition in the hippocampus.

Also noteworthy, several genes associated with ASD have now been identified to function like synaptic brakes to prevent precocious maturation of excitatory synapses. In particular, accelerated maturation of excitatory synapses in an early period of hippocampal development has been observed in a mouse model of human *SYNGAP1* haploinsuffciency, leading to learning deficits [52]. Similarly, accelerated maturation of glutamatergic synapse has been seen in a KO mouse model for MET receptor tyrosine kinase. HGF signaling through MET receptor activation prevents the maturation of silent synapses [53]. This is of particular interest since ARHGAP12 was initially characterized as a transcriptional target of HGF in epithelial cells [29]. In addition, MET is highly expressed in CA1 pyramidal neurons during late prenatal and early postnatal development [54–56], similar to the expression pattern of ARHGAP12. This raises the

intriguing possibility that ARHGAP12 might function downstream of MET signaling, in the developing hippocampus. Future experiments will have to determine if and how ARHGAP12 participates in MET signaling during development.

Experimental Procedures

Virus production, Western blot, immunofluorescence, yeast two-hybrid and images analysis are described in Supplemental Experimental Procedures.

Animals

Wistar rats were housed per 2 or 3 animals on a 12-h light cycle in a temperature-controlled (21 ± 1°C) environment with ad libitum access to food and water. Rats were used at E18 or P6 for primary neuronal cultures or organotypic hippocampal slices, respectively. All experiments involving animals were evaluated and approved by the Committee for Animal Experiments of the Radboud University Nijmegen Medical Centre, Nijmegen, the Netherlands.

Electrophysiology

Whole-cell recordings in cultured slices were obtained with Multiclamp 700B amplifiers (Axon Instruments). To study the effects of ARHGAP12 on synaptic transmission, organotypic hippocampal slices were infected with lentiviruses expressing shRNAs on the same day of plating and recorded at indicated times after infection (4 DIV, 7 DIV, 13-14 DIV). To overexpress ARHGAP12, organotypic hippocampal slices were biolistically transfected at 5 DIV (for evoked EPSCs) or 12 DIV (for miniature EPSCs) using a Helios Gene Gun (Bio-Rad) and analyzed two days post-transfection. Whole-cell recordings were obtained simultaneously from an infected and an adjacent uninfected neuron in the CA1 region under visual guidance, using epifluorescence and transmitted light illumination. See Supplemental Experimental Procedures for details.

Two-photon laser scanning microscopy

Imaging was essentially performed as described previously [24].

Author Contributions

Conceptualization, W.B. and N.N.K.; Methodology, W.B., M.M.S., M.B. and S. L.; Investigation, W.B., N.N.K., J.v.d.R., H.v.V., L-L.L., M.J.C. and R.S.E.L.; Resources, A.R.O; R.R. and R.J. v. W.; Writing-Original Draft, W.B. and N.N.K.; Writing-Review and Editing, W.B. and N.N.K.; Supervision, H.v.B and N.N.K.; Funding Acquisition, N.N.K.

Acknowledgements

We thank Dr. M. Furuse, Dr. E. Dent and A. Craig for providing ARHGAP12 and CIP4 plasmids; J.M. Keller for proofreading the manuscript. The research of the authors is supported by grants from the “Hypatia fellowship award of the Radboudumc” [to N.N.K.]; the “FP7-Marie Curie International Reintegration Grant” [to N.N.K. grant number 277091]; the Jerome Lejeune Foundation [to N.N.K]; the Netherlands Organization for Scientific Research (NWO Vici-865.12.005 to R.R and open ALW ALW2PJ/13082 to HvB/NNK) and GENCODYS, an EU FP7 large-scale integrating project grant [Grant number 241995] [to HvB].

Conflict of Interest

The authors declare that there is no conflict of interest.

References

1. McAllister, a K. Dynamic aspects of CNS synapse formation. *Annu. Rev. Neurosci.* **30,** 425–450 (2007).
2. Li, Z. & Sheng, M. Some assembly required: the development of neuronal synapses. *Nat. Rev. Mol. Cell Biol.* **4,** 833–841 (2003).
3. Hotulainen, P. & Hoogenraad, C. C. Actin in dendritic spines: connecting dynamics to function. *J. Cell Biol.* **189,** 619–29 (2010).
4. Chater, T. E. & Goda, Y. The role of AMPA receptors in postsynaptic mechanisms of synaptic plasticity. **8,** 1–14 (2014).
5. Engert, F. & Bonhoeffer, T. Dendritic spine changes associated with hippocampal long-term synaptic plasticity. *Nature* **399,** 66–70 (1999).
6. Kopec, C. & Malinow, R. Matters of Size. **314,** 8–10 (2006).
7. Matsuzaki, M., Honkura, N., Ellis-Davies, G. C. R. & Kasai, H. Structural basis of long-trm potentiation in single dendritic spines. *Nature* **429,** 761–766 (2004).
8. Cingolani, L. a & Goda, Y. Actin in action: the interplay between the actin cytoskeleton and synaptic efficacy. *Nat. Rev. Neurosci.* **9,** 344–56 (2008).
9. Malinow, R. & Malenka, R. C. AMPA receptor trafficking and synaptic plasticity. *Annu. Rev. Neurosci.* **25,** 103–126 (2002).
10. Fukazawa, Y. *et al.* Hippocampal LTP is accompanied by enhanced F-actin content within the dendritic spine that is essential for late LTP maintenance in vivo. *Neuron* **38,** 447–460 (2003).
11. Ramachandran, B. & Frey, J. U. Interfering with the actin network and its effect on long-term potentiation and synaptic tagging in hippocampal CA1 neurons in slices in vitro. *J. Neurosci.* **29,** 12167–12173 (2009).
12. Okamoto, K.-I., Nagai, T., Miyawaki, A. & Hayashi, Y. Rapid and persistent modulation of actin dynamics regulates postsynaptic reorganization underlying bidirectional plasticity. *Nat. Neurosci.* **7,** 1104–12 (2004).
13. Wang, X., Yang, Y. & Zhou, Q. Independent expression of synaptic and morphological plasticity associated with long-term depression. *J. Neurosci.* **27,** 12419–12429 (2007).
14. Nadif Kasri, N. & Van Aelst, L. Rho-linked genes and neurological disorders. *Pflugers Arch.* **455,** 787–97 (2008).
15. Penzes, P., Cahill, M. E., Jones, K. a, VanLeeuwen, J.-E. & Woolfrey, K. M. Dendritic spine pathology in neuropsychiatric disorders. *Nat. Neurosci.* **14,** 285–293 (2011).
16. Phillips, M. & Pozzo-Miller, L. Dendritic spine dysgenesis in autism related disorders. *Neurosci. Lett.* 1–11 (2015). doi:10.1016/j.neulet.2015.01.011
17. Xu, X., Miller, E. C. & Pozzo-Miller, L. Dendritic spine dysgenesis in Rett syndrome. *Front. Neuroanat.* **8,** 1–8 (2014).
18. Tolias, K. F., Duman, J. G. & Um, K. Control of synapse development and plasticity by Rho GTPase regulatory proteins. *Prog. Neurobiol.* **94,** 133–148 (2011).
19. Ba, W., van der Raadt, J. & Nadif Kasri, N. Rho GTPase signaling at the synapse: Implications for intellectual disability. *Exp. Cell Res.* **319,** 2368–2374 (2013).
20. Van Aelst, L. & D'Souza-Schorey, C. Rho GTPases and signaling networks. *Genes Dev.* **11,** 2295–2322 (1997).
21. Guerrier, S. *et al.* The F-BAR Domain of srGAP2 Induces Membrane Protrusions Required for Neuronal Migration and Morphogenesis. *Cell* **138,** 990–1004 (2009).
22. Ip, J. P. K. *et al.* α2-chimaerin controls neuronal migration and functioning of the cerebral cortex through CRMP-2. *Nat. Neurosci.* **15,** 39–47 (2011).
23. Duman, J. G., Mulherkar, S., Tu, Y.-K., Cheng, J. & Tolias, K. F. Mechanisms for spatiotemporal regulation of Rho-GTPase signaling at synapses. *Neurosci. Lett.* **601,** 4–10 (2015).
24. Nadif Kasri, N., Nakano-Kobayashi, A., Malinow, R., Li, B. & Van Aelst, L. The Rho-linked mental retardation protein oligophrenin-1 controls synapse maturation and plasticity by stabilizing AMPA receptors. *Genes Dev.* **23,** 1289–302 (2009).

25. Nadif Kasri, N., Nakano-Kobayashi, A. & Van Aelst, L. Rapid synthesis of the X-linked mental retardation protein OPHN1 mediates mGluR-dependent LTD through interaction with the endocytic machinery. *Neuron* **72,** 300–15 (2011).
26. Hichri, H. *et al.* From lowe syndrome to Dent disease: Correlations between mutations of the OCRL1 gene and clinical and biochemical phenotypes. *Hum. Mutat.* **32,** 379–388 (2011).
27. Kutsche, K. *et al.* Mutations in ARHGEF6, encoding a guanine nucleotide exchange factor for Rho GTPases, in patients with X-linked mental retardation. *Nat. Genet.* **26,** 247–50 (2000).
28. Allen, K. M. *et al.* PAK3 mutation in nonsyndromic X-linked mental retardation. *Nat. Genet.* **20,** 25–30 (1998).
29. Gentile, a *et al.* Met-driven invasive growth involves transcriptional regulation of Arhgap12. *Oncogene* **27,** 5590–8 (2008).
30. Govek, E.-E., Hatten, M. E. & Van Aelst, L. The role of Rho GTPase proteins in CNS neuronal migration. *Dev. Neurobiol.* **71,** 528–53 (2011).
31. Haditsch, U. *et al.* A central role for the small GTPase Rac1 in hippocampal plasticity and spatial learning and memory. *Mol. Cell. Neurosci.* **41,** 409–19 (2009).
32. Arendt, K. L. *et al.* PIP3 controls synaptic function by maintaining AMPA receptor clustering at the postsynaptic membrane. *Nat. Neurosci.* **13,** 36–44 (2010).
33. Bowie, D. & Mayer, M. L. Inward Rectification of Both AMPA and Kainate Subtype Glutamate Receptors Generated by Polyamine-Mediated Ion Channel Block. **15,** 453–462 (1995).
34. Hanse, E., Seth, H. & Riebe, I. AMPA-silent synapses in brain development and pathology. *Nat. Rev. Neurosci.* **14,** 839–50 (2013).
35. Kerchner, G. a & Nicoll, R. a. Silent synapses and the emergence of a postsynaptic mechanism for LTP. *Nat. Rev. Neurosci.* **9,** 813–825 (2008).
36. Isaac, J. T. R., Nicoll, R. a. & Malenka, R. C. Evidence for silent synapses: Implications for the expression of LTP. *Neuron* **15,** 427–434 (1995).
37. Saengsawang, W. *et al.* The F-BAR protein CIP4 inhibits neurite formation by producing lamellipodial protrusions. *Curr. Biol.* **22,** 494–501 (2012).
38. Shimada, A. *et al.* Curved EFC/F-BAR-Domain Dimers Are Joined End to End into a Filament for Membrane Invagination in Endocytosis. *Cell* **129,** 761–772 (2007).
39. Tsujita, K. *et al.* Coordination between the actin cytoskeleton and membrane deformation by a novel membrane tubulation domain of PCH proteins is involved in endocytosis. *J. Cell Biol.* **172,** 269–279 (2006).
40. Itoh, T. & De Camilli, P. BAR, F-BAR (EFC) and ENTH/ANTH domains in the regulation of membrane-cytosol interfaces and membrane curvature. *Biochim. Biophys. Acta - Mol. Cell Biol. Lipids* **1761,** 897–912 (2006).
41. Nahm, M. *et al.* dCIP4 (Drosophila Cdc42-interacting protein 4) restrains synaptic growth by inhibiting the secretion of the retrograde Glass bottom boat signal. *J. Neurosci.* **30,** 8138–8150 (2010).
42. Gao, Y., Dickerson, J. B., Guo, F., Zheng, J. & Zheng, Y. Rational design and characterization of a Rac GTPase-specific small molecule inhibitor. *Proc. Natl. Acad. Sci. U. S. A.* **101,** 7618–7623 (2004).
43. Man, H. Y. *et al.* Regulation of AMPA receptor-mediated synaptic transmission by clathrin-dependent receptor internalization. *Neuron* **25,** 649–662 (2000).
44. Van de Ven, T. J., VanDongen, H. M. a & VanDongen, A. M. J. The nonkinase phorbol ester receptor alpha 1-chimerin binds the NMDA receptor NR2A subunit and regulates dendritic spine density. *J. Neurosci.* **25,** 9488–9496 (2005).
45. Buttery, P. *et al.* The diacylglycerol-binding protein alpha1-chimaerin regulates dendritic morphology. *Proc. Natl. Acad. Sci. U. S. A.* **103,** 1924–1929 (2006).
46. Um, K. *et al.* Dynamic Control of Excitatory Synapse Development by a Rac1 GEF/GAP Regulatory Complex. *Dev. Cell* **29,** 701–715 (2014).
47. Matsuzaki, M. *et al.* Dendritic spine geometry is critical for AMPA receptor expression in hippocampal CA1 pyramidal neurons. *Nat. Neurosci.* **4,** 1086–1092 (2001).

48. Nimchinsky, E. a, Sabatini, B. L. & Svoboda, K. Structure and function of dendritic spines. *Annu. Rev. Physiol.* **64,** 313–353 (2002).
49. Kopec, C., Li, B., Wei, W., Boehm, J. & Malinow, R. Glutamate receptor exocytosis and spine enlargement during chemically induced long-term potentiation. *J. Neurosci.* **26,** 2000–2009 (2006).
50. Clement, J. P., Ozkan, E. D., Aceti, M., Miller, C. a. & Rumbaugh, G. SYNGAP1 Links the Maturation Rate of Excitatory Synapses to the Duration of Critical-Period Synaptic Plasticity. *J. Neurosci.* **33,** 10447–10452 (2013).
51. Sasaki, J. *et al.* The PtdIns(3,4)P(2) phosphatase INPP4A is a suppressor of excitotoxic neuronal death. *Nature* **465,** 497–501 (2010).
52. Clement *et al.* Pathogenic SYNGAP1 mutations impair cognitive development by disrupting maturation of dendritic spine synapses. *Cell* **151,** 709–23 (2012).
53. Qiu, S., Lu, Z. & Levitt, P. MET Receptor Tyrosine Kinase Controls Dendritic Complexity, Spine Morphogenesis, and Glutamatergic Synapse Maturation in the Hippocampus. *J. Neurosci.* **34,** 16166–16179 (2014).
54. Achim, C. L. *et al.* Expression of HGF and cMET in the developing and adult brain. *Dev. Brain Res.* **102,** 299–303 (1997).
55. Thewke, D. P. & Seeds, N. W. The expression of mRNAs for hepatocyte growth factor/scatter factor, its receptor c-met, and one of its activators tissue-type plasminogen activator show a systematic relationship in the developing and adult cerebral cortex and hippocampus. *Brain Res.* **821,** 356–367 (1999).
56. Judson, M. C., Bergman, M. Y., Campbell, D. B., Eagleson, K. L. & Levitt, P. Dynamic gene and protein expression patterns of the autism-associated met receptor tyrosine kinase in the developing mouse forebrain. *J. Comp. Neurol.* **513,** 511–531 (2009).

Supplemental Data

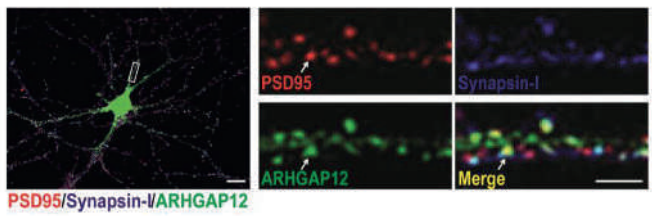

Figure S1 Localization of ectopic ARHGAP12 in hippocampal neurons (related to Figure 1). Left, representative confocal microscopy image of hippocampal neurons (21 DIV) expressing GFP-*Arhgap12* double-stained with synaptic markers Synapsin-I and PSD95. Right, high magnification images of the area indicated in the white box on the left panel. White arrows show sites of co-localization of ARHGAP12 and PSD95. Scale bars, 10 µm.

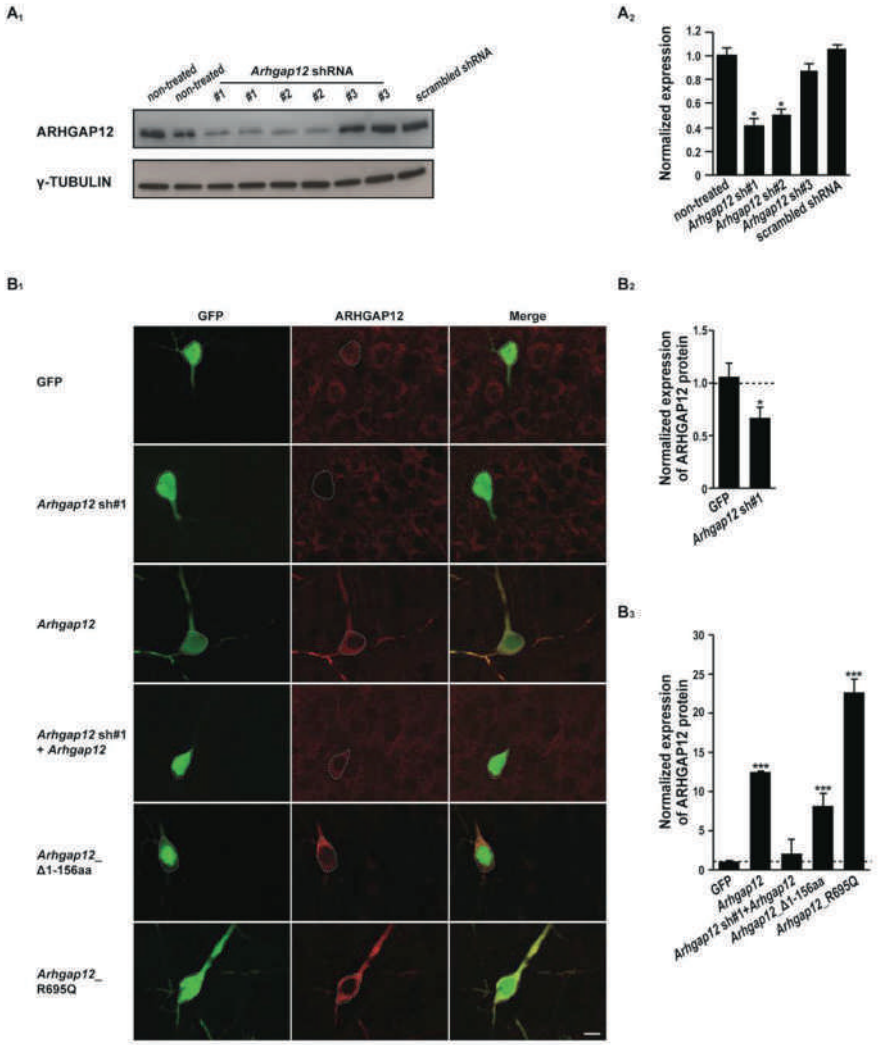

Figure S2 Evaluation of ARHGAP12 protein levels (related to Figure 2). (A_1) Verification of *Arhgap12* shRNAs. Dissociated hippocampal neurons were either non-treated or infected at 1 DIV with pTRIP lentiviral vector coexpressing GFP and scrambled shRNA, *Arhgap12* sh#1, #2 or #3. Eight days post-transfection, cell extracts were prepared and analyzed by Western blot with an anti-ARHGAP12 antibody. Expression of γ-TUBULIN was used as a loading control. (A_2) Quantification of ARHGAP12 expression. Data are shown as mean ± SEM, n = 3, **P*<0.05, t-test). (B_1) Immunofluorescence of ARHGAP12 in organotypic hippocampal slices biolistically transfected at 12 DIV with indicated constructs. Immunostaining experiments were performed two days post-transfection. (B_2-B_3) Quantification of immunofluorescence intensity in transfected neurons compared to adjacent non-transfected neurons. Dashed lines indicate endogenous ARHGAP12. Data are shown as mean ± SEM; n = 9 for each group from three independent experiments; **P*<0.05, ** *P*<0.01, *** *P*<0.001, t-test. Scale bar, 10 µm.

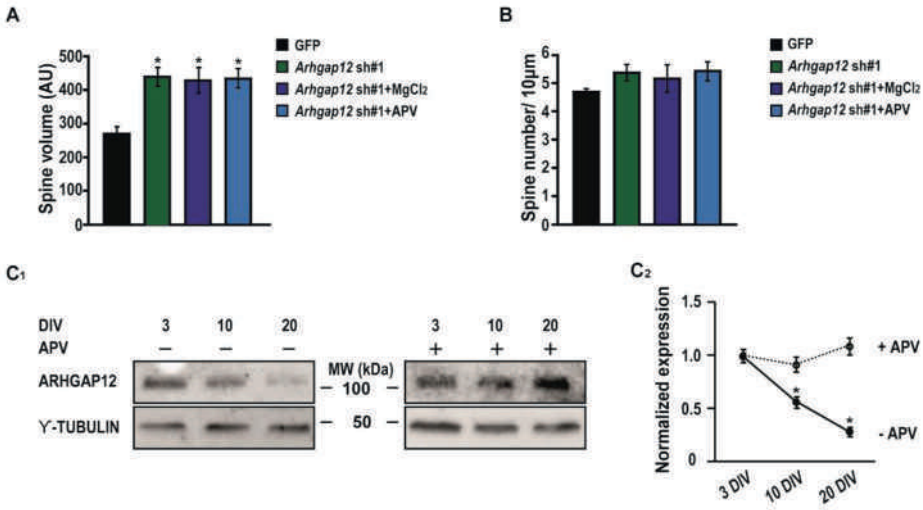

Figure S3 Effect of neuronal activity on ARHGAP12 expression and function (related to Figure 2). (A-B) Quantification of spine volume (A) and density (B) for each experimental condition as indicated. Data are shown as mean ± SEM; GFP: n = 12, *Arhgap12* sh#1: n = 8, $MgCl_2$: n = 6, APV: n = 7; data pooled from three independent experiments; **P*<0.05, one-way ANOVA. (C_1) Developmental expression of ARHGAP12 with or without the presence of 100 µM APV. (C_2) Quantification of ARHGAP12 expression. Data are shown as mean ± SEM; **P*<0.05, two-way ANOVA.

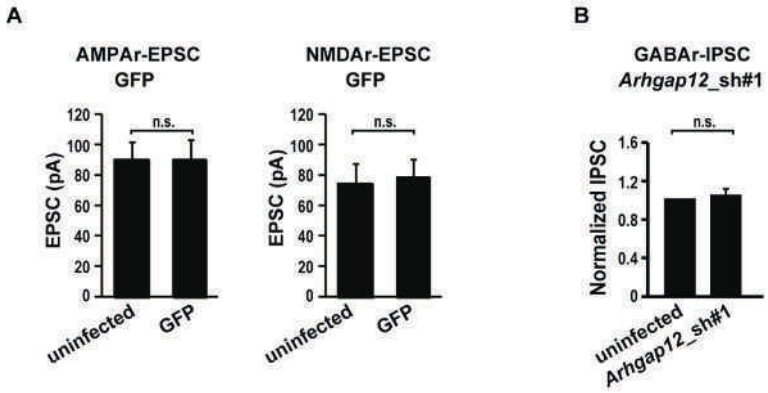

Figure S4 GFP does not affect excitatory synaptic transmission and *Arhgap12* knockdown does not alter inhibitory synaptic transmission (related to Figure 3). (A) Average AMPAr- and NMDAr-mediated EPSCs recorded simultaneously at 7 DIV from a CA1 pyramidal neuron infected with GFP and an adjacent uninfected neuron. Data are shown as mean ± SEM; n = 9 pairs from three independent experiments; paired t-test. (B) Normalized GABAr-mediated IPSCs simultaneously recorded from neighboring uninfected neurons and *Arhgap12* sh#1 infected neurons. Data are shown as mean ± SEM; n = 9 pairs from three independent experiments; paired t-test.

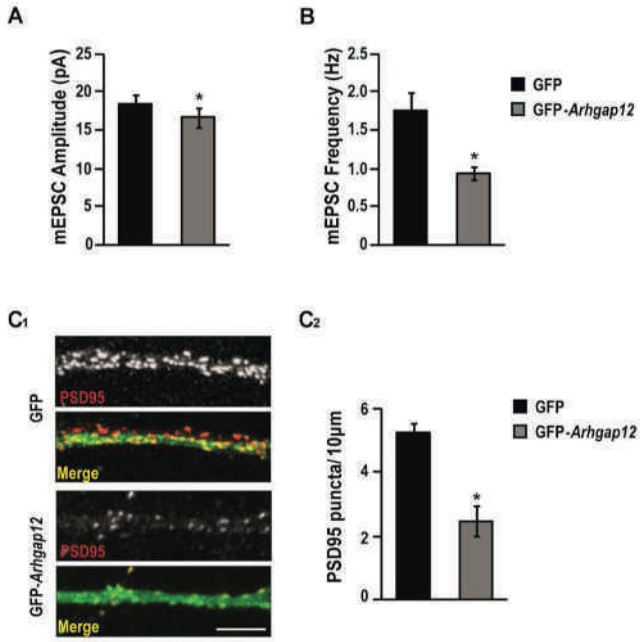

Figure S5. Elevated *Arhgap12* levels throughout hippocampal development depresses CA3-CA1 excitatory synapses (related to Figure 4). (A-B) Primary hippocampal neurons were electroporated with GFP or GFP-*Arhgap12* at 0 DIV. Miniature excitatory events (mEPSC) were recorded from 13 DIV control GFP and GFP-*Arhgap12* transfected neurons (GFP: n = 22, GFP-*Arhgap12*: n = 25, from 4 independent experiments; **P*<0.05, t-test). (C_1-C_2) Immunostaining of PSD95 on GFP and GFP-*Arhgap12* transfected neurons. (C_1) Representative images of PSD95 staining. Scale bar, 10 µm. (C_2) Quantification of PSD95 density. Data are shown as mean ± SEM; n = 16-18 from three independent experiments; **P*<0.05, t-test.

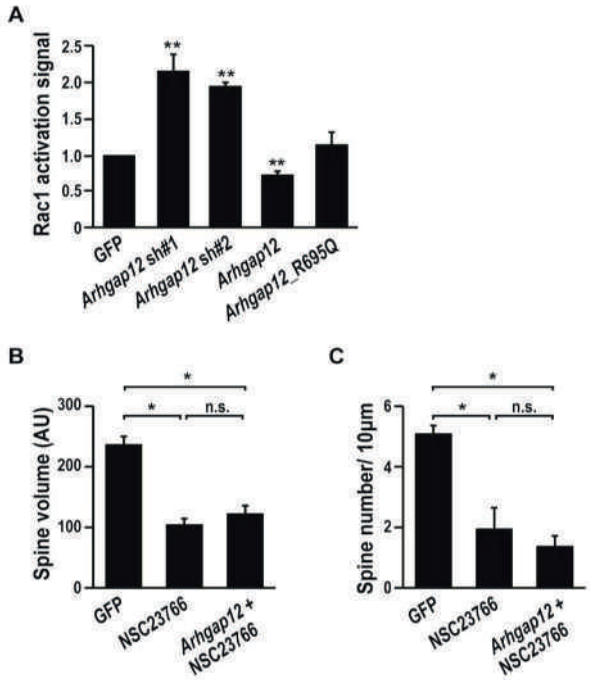

Figure S6 Regulation of ARHGAP12 on Rac1 activity and effect of inactivation of Rac1 signaling on GFP and *Arhgap12* overexpressing neurons (related to Figure 6). (A) Normalized Rac1 activation signal for indicated experimental groups. Data are shown as mean ± SEM; n = 3; ***P*<0.01, t-test. (B-C) Quantification of spine volume (B) and density (C) for each experimental condition as indicated. Data are shown as mean ± SEM; GFP: n = 12, NSC23766: n = 9, *Arhgap12*+NSC23766: n = 8 from two independent experiments; **P*<0.05, one-way ANOVA.

A

Colony	Prey	AA in gene CDS	Appeared on day	α-gal	β-gal
1	CIP4 (TRIP10)	354-467	5	1	3
2	CIP4 (TRIP10)	354-545	5	1	3
3	CIP4 (TRIP10)	374-428	11	1	2
4	CIP4 (TRIP10)	414-489	14	0	0

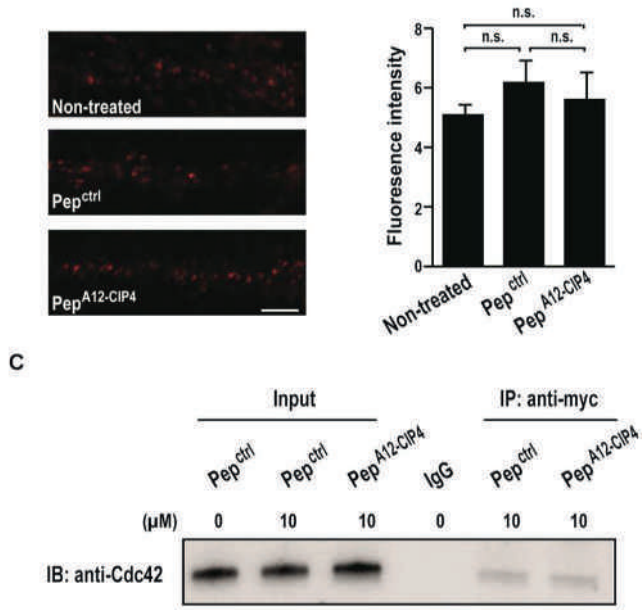

Figure S7 Overview of positive colonies matching CIP4 sequence in yeast two hybrid screening and effect of ARHGAP12-CIP4 interfering peptide on surface NMDAr expression and Cdc42-CIP4 interaction (related to Figure 7). (A) "AA in gene CDS" indicates the amino acids sequence of CIP4 interacting with ARHGAP12 in each colony; "appeared on day" indicates the days that colonies appeared in culture; "α-gal" and "β-gal" indicate the scores of each colony in galactosidase assays. (B_1-B_2) Surface labeling of NR1 subunit in 15 DIV non-treated, 10 μM Pep^{ctrl} or 10 μM Pep^{A12_CIP4} treated hippocampal neurons (B_1) and quantification of average fluorescence intensity for indicated groups (B_2). Data are shown as mean ± SEM, n = 16-18 from three independent experiments; one-way ANOVA. (C) Co-immunoprecipitation of Cdc42 and CIP4 *in vitro*. HEK293T cells co-transfected with GFP-*Cdc42* and myc-*Cip4* constructs were treated with 10 μM Pep^{ctrl} or 10 μM Pep^{A12_CIP4} for 24 hours. Protein extracts were incubated with mouse IgG or an anti-Myc antibody. The immunoprecipitates were analyzed by immunoblotting using an anti-Cdc42 antibody.

Supplemental Experimental Procedures

Primary neuronal cultures and organotypic hippocampal slice cultures

All media and reagents were purchased from Life Technologies. Dissociated hippocampal cultures were prepared form gestational day 18 fetal rats (Wistar). Pregnant rats were anaesthetized with isoflurane and sacrificed by cervical dislocation. Embryonic brains were dissected in ice-cold Hank's buffer (HBSS without Ca^{2+} and Mg^{2+}, 100 U/ml penicillin, 100 µg/ml streptomycin, 1x glutamax). The hippocampi were separated from the cortices and incubated with 0.025% trypsin for 15 min at 37°C. Neurons were mechanically dissociated in NeuroBasal medium containing 10% FCS and B27 supplement (Invitrogen) using fire-polished Pasteur pipettes. The cell suspension was filtered through a 70 µm cell strainer (BD Falcon) and plated on poly-D-lysine (Invitrogen) pre-coated glass coverslips in 12-wells plates at a density of 50.000 neurons per well. Medium was replaced after 4 hours with Neurobasal medium containing B27 supplement, and 1x GlutaMax. Neurons were maintained in a 5% CO_2 humidified 37°C incubator. Half of the medium was refreshed every three to four days. Organotypic hippocampal slices were prepared from P6 rats as described previously [1] and maintained in a 5 % CO_2 humidified 35°C incubator on slice culture medium (pH 7.3, osmolarity 317-325) consisting of MEM, 20 % horse serum, 1 mM L-Glutamine, 1 mM $CaCl_2$, 2 mM $MgSO_4$, 0.25 mg Insulin, 1.25 mM Ascorbic acid, 12.87 mM D-Glucose, 5.25 mM $NaHCO_3$ and 30 mM Hepes. Medium was refreshed every two days. For knockdown condition, slices were infected with *Arhgap12* shRNAs at 0 DIV and used for electrophysiology experiments on indicated days. To infect hippocampal slice cultures, concentrated viral solution was injected into the CA1 pyramidal cell layer using a pico-liter injector (Warner instruments). To perform functional analysis in *Arhgap12* overexpression condition, slices were biolistically transfected at 5 DIV (for evoked EPSCs) or 12 DIV (for miniature EPSCs) and recorded two days post-transfection. For morphological studies, slices were biolistically transfected at 12 DIV with indicated constructs using a Helios Gene Gun (Bio-Rad) and imaged two days post-transfection lively with two-photon microscopy (Leica TCS SP5).

DNA constructs, cloning and virus production

The GFP-*Arhgap12* wild type construct was described previously [2] and was a generous gift of Dr. M. Furuse. The *Arhgap12*_R596Q mutant was generated by introducing a point mutation (R695Q) into the catalytic domain of ARHGAP12 using the Quick Change system (Stratagene).

*Arhgap12*_ΔSH3 and *Arhgap12*_Δ1-156aa mutants were generated by PCR-based methods from the GFP-*Arhgap12* wild type construct. For RNAi knockdown experiments, the pSuper system (Oligoengine) was applied to target rat *Arhgap12* mRNA using expression of short hairpin RNAs (shRNAs) (*Arhgap12* sh#1: Forward primer, 5'-GATCCCCGGACCAGAAGGAGCTTAAATTCAAGAGATTTAAGCTCCTTCTGGTCCTTTTTA-3'; reverse primer, 5'-AGCTTAAAAAGGACCAGAAGGAGCTTAAATCTCTTGAATTTAAGCTCCTTCTGGTCCGGG-3'; *Arhgap12* sh#2: Forward primer, 5'-GATCCCCCCAGTCATATACACTGGATAATTCAAGAGATTATCCAGTGTATATGACTGGTTTTTA-3'; reverse primer, 5'-AGCTTAAAAACCAGTCATATACACTGGATAATCTCTTGAATTATCCAGTGTATATGACTGGGGG-3'). Myc-CIP4 construct was a kind gift of Dr. (E. Dent). Lentiviruses were generated by cotransfecting HEK-293T cells with FUGW plasmids containing shRNAs, the HIV-1 packaging vector Δ8.9, and the VSVG envelope glycoprotein vector, using calcium phosphate co-precipitation method. HEK293T cells were maintained in a 5% CO_2 humidified 37°C incubator and the media was replaced 5 hours after cotransfection. Supernatants of culture media were collected 48h after transfection and centrifuged at 21.000 RPM to concentrate the virus. Viruses were resuspended in HBSS without Ca^{2+} and Mg^{2+} (Life technologies). Viral stocks were aliquoted and stored at -80°C until use.

Immunofluorenscence

Immunofluorescence staining of hippocampal slices was conducted according to a previously described procedure with modifications [3,4]. For staining organotypic slices, indicated constructs were biolistically delivered at 12 DIV and fixed at 14 DIV with ice-cold 4% paraformaldehyde/ 4% sucrose in PBS. For hippocampal slices from postnatal days 20 rats, brains were fixed, embedded in low melting agarose (3%) and then being sectioned into 60 µm sections using a microtome (Leica VT-1000S). Free-floating sections or fixed organotypic slices were incubated overnight with blocking buffer containing 5% normal goat serum (Invitrogen), 5% normal donkey serum (Sigma), 5% horse serum (Sigma), 1% glycine (Sigma), 1% lysine (Sigma) and 0.4% Triton X-100, permeabilized, and incubated overnight with anti-ARHGAP12 (NBP1-91678, Novus Biologicals), anti-NeuN (ABN91, Millipore) and anti-MAP2 (188004, Synaptic system) primary antibodies, followed by incubation with Alexa-488, Alexa-

568 or Alexa-647 conjugated secondary antibody (Invitrogen) in blocking buffer. Sections were mounted onto slides with fluorescence mounting medium containing 406-diamidion-2-phenylindole (Dako, Carpinteria, California, USA). Dissociated hippocampal neurons electroporated with GFP or GFP-*Arhgap12* at DIV 0 were fixed in 4% paraformaldehyde solution at DIV 21, permeabilized with 0.2% Triton X-100 in PBS, and stained with the following primary antibodies: anti-PSD95 (MA1-045, Thermo Scientific) and anti-Synapsin-1 (AB1543P, Bio-Connect). Following secondary antibodies were used: Alexa-568 and 647 (Invitrogen). Cells were imaged using an LSM 510 confocal laser-scanning microscope (Zeiss) with a 63x/1.40 Plan-Apochromat objective or imaged with Axio Imager Z1 (Zeiss, Basel, Switzerland) equipped with a camera (AxioCam MRm; Zeiss). Images were processed using Axiovision Rel (V.4.6) and analysed using ImageJ (NIH, Bethesda, Maryland, USA). For surface labeling NR1 receptors in peptides treated hippocampal neurons, an anti-NR1 antibody (Biolegend) recognizing the extracellular region of NR1 subunit was used to feed 15 DIV neurons at 37°C for 1h, followed with fixation, blocking and incubating with an secondary antibody without permeabilization.

Western blotting

Rat hippocampal tissue or cell culture were collected and homogenized in ice-cold RIPA buffer. Lysates were then heated at 95°C for 10 min. Equal amounts of protein samples (50 µg) were fractionated on 4%-15% precast SDS-PAGE gels (Bio-Rad) then blotted to nitrocellulose membrane (Bio-Rad). Membranes were subsequently incubated for 1h at room temperature in 5% milk in PBS-Tween to prevent non-specific binding. Primary antibodies used were: anti-ARHGAP12 (Abvona), anti-PSD95 (Thermo Scientific), or anti- Y-TUBULIN (Sigma) as loading control. Secondary antibodies used were: goat anti-mouse HRP (Jackson Immuno Research Laboratories) and goat anti-rabbit (Invitrogen). Images were acquired with ChemiDoc™ imaging system (Bio-Rad).

Peptides

The sequences of $pep^{ARHGAP12\text{-}CIP4}$ and pep^{ctrl} are: NH2-GRKKRRQRRR-ahx-DSLGRTEEARNSLV-OH and NH2-GRKKRRQRRR-ahx-EAETRVLSNRGDSL-OH. The human immunodeficiency virus-type 1 Tat sequence [5] was fused to the peptides to aid delivery into the cell. Purified peptides (>90%) were obtained from Chinapeptides.

Electrophysiology

Whole-cell recordings in organotypic slices and primary hippocampal neurons were obtained with Multiclamp 700B amplifiers (Axon Instruments). The recording chamber was perfused with artificial cerebrospinal fluid (ACSF) containing 119 mM NaCl, 2.5 mM KCl, 4 mM $CaCl_2$, 4 mM $MgCl_2$, 26 mM $NaHCO_3$, 1 mM NaH_2PO_4, 11 mM glucose, 0.1 mM picrotoxin, 4 µM 2-chloroadenosine (pH 7.4), and gassed with 5% CO_2/95% O_2. Recordings were made at 30°C. Patch recording pipettes (4–7 MΩ) were filled with intracellular solution containing 115 mM cesium methanesulfonate, 20 mM CsCl, 10 mM HEPES, 2.5 mM $MgCl_2$, 4 mM Na_2ATP, 0.4 mM Na_3GTP, 10 mM sodium phosphocreatine, and 0.6 mM EGTA (pH 7.25, Osm 285-295). Evoked responses were induced using bipolar electrodes (FHC) placed on Schaffer collateral pathway (0.1 Hz). Responses were recorded at both -60 mV (for AMPAr-mediated responses) and +40 mV (for NMDAr-mediated responses). NMDAr-mediated responses were quantified as the mean between 60 and 65 ms after stimulation. Evoked IPSCs were recorded in the presence of 6-Cyano-7-nitroquinoxaline-2, 3-dione (CNQX, 5 µM) and D-(-)-2-Amino-5-phosphonopentanoic acid (D-APV, 100µM). Cells were excluded if the access resistance exceeded 25 MΩ. All data are reported as mean ± SEM. Statistical significance was determined by the paired Student's t-test (for paired recordings).

Miniature post-synaptic excitatory currents (mEPSCs) on primary hippocampal neurons and organotypic slices were recorded at -60 mV in ACSF containing 2 mM $CaCl_2$ and 1 mM $MgCl_2$ at 32°C in the presence of 1 µM TTX and 0.1 mM picrotoxin. 10 min of recordings from each cell were acquired at 5 kHz, filtered at 2 kHz and analyzed using Mini Analysis Program (Synaptosoft).

Paired pulse ratio was recorded in the presence of 0.1 mM picrotoxin and calculated as Peak2/peak1 after correcting for any residual current at the second pulse. All recordings were performed by stimulating two independent synaptic inputs. Results from each pathway were averaged and counted as n = 1.

Failure rate experiments were performed using minimum stimulation. Failure rate was calculated as a percentage of failed evoked responses over 50 sweeps at a holding potential of -60 and +40 mV. We used the peak amplitudes of individual responses as the criterion for defining success or failure. The peak amplitudes of each response were measured in Clampfit (Axon). We used a threshold (10 pA for responses at -60 mV and 20 pA for responses at +40 mV) as a cutoff criterion. Responses with a peak amplitude above the threshold were counted

as success. The success trials had a clear response above the baseline and all displayed kinetics in line with evoked responses. The percentage of silent synapses was calculated as 1-(LN failure rate -60mV)/(LN failure rate +40 mV) [6].
To record surface AMPAr responses, AMPA (1 µM, Tocris Bioscience) was applied for 10 min and holding current (V_{hold}=-60 mV) was measured every 30s. To assess the composition of GluA2-lacking AMPA receptors, rectification indexes were calculated by obtaining the ratio of mean evoked AMPAR responses at -60 mV divided by mean responses at +40 mV.

Yeast two hybrid screening

The GAL4-based yeast two-hybrid system (HybriZAP, Stratagene, La Jolla, USA) was used for identifying protein-interaction partners of ARHGAP12. Full-length human ARHGAP12 and several truncations containing different functional domains of ARHGAP12 (Figure 5), fused to a DNA-binding domain (GAL4-BD), were used as a bait for screening a human oligo-dT primed fetal brain cDNA library. The yeast strain *PJ69-4A*, which carried the *HIS3* (histidine), *ADE2* (adenine), *MEL1* (α-galactosidase) and *LacZ* (β-galactosidase) reporter genes, was used as a host. Interactions were analyzed by assessment of reporter gene activation via growth on selective media (*HIS3* and *ADE2* reporter genes), α-galactosidase colorimetric plate assays (*MEL1* reporter gene), and β-galactosidase colorimetric filter lift assays (*LacZ* reporter gene). Protein interactions were evaluated on the basis of growth on selective media and staining in α- and β-galactosidase activity assays.

Co-immunoprecipitations

Precleared HEK293T cells lysates co-transfected with Myc-*Cip4* and GFP-*Arhgap12* WT, *Arhgap12* mutants or GFP-Cdc42 for 24 hours were incubated with mouse IgG (eBioscience), anti-myc (Abcam) or anti-ARHGAP12 (Abvona) antibodies (2.5 µg/ml lysate) at 4°C for 1h. Peptides were added on the same day of transfection. Dynabeads® Protein G (50 µl per sample, Invitrogen) were then added and incubated for 1h at 4°C under gentle rotation. Samples were washed three times with lysis buffer (20 mM Tris, 150 mM NaCl, 2 mM EDTA, 1 mM DTT and protease inhibitor, pH7.4). Co-immunoprecipitated proteins were detected by Western blotting with anti-ARHGAP12 or anti-myc antibodies.

AMPA receptor endocytosis assay

Endocytosis assay was performed as previously described [7,8] with modifications. Briefly, living primary hippocampal neurons were first labeled with anti-GluA1 antibody (Millipore). Internalization of the labeled GluA1 subunits was then allowed for 2 hours at 37°C. After fixation with 4% paraformaldehyde and blocking with 5% BSA, surface-labeled GluA1 subunits were exposed to Alexa-568 secondary antibody (Invitrogen). After washing, the remaining surface GluA1 subunits were incubated with unlabeled secondary antibody at a concentration of 0.13 mg/ml overnight to saturate surface anti-GluA1 antibodies. Neurons were then permeabilized and incubated with Alexa-647 secondary antibody to label internalized GluA1 subunits. GluA1 endocytosis was calculated by dividing the intensity of internalized GluA1 by the intensity of surface GluA1 using imageJ (I_{647}/ I_{568}).

Two-photon laser scanning microscopy

Hippocampal slices were biolistically transfected at 12 DIV with indicated constructs and neurons were imaged 2 days after transfection. Experiments were performed at 30°C in physiological ACSF (119 mM NaCl, 26 mM $NaHCO_3$, 1 mM NaH_2PO_4, 11 mM D-glucose, 2.5 mM KCl, 2 mM $CaCl_2$, 1 mM $MgCl_2$, and 1.25 mM $NaHPO_4$) gassed with 5% CO_2 and 95% O_2. Before TPLSM imaging, transfected/infected CA1 pyramidal neurons were identified by epifluorescence illumination. High-resolution three-dimensional image stacks were collected on a laser-scanning microscope (Leica TCS SP5). The light source was a mode-locked Ti:sapphire laser (Coherent Chameleon, USA) running at 910 nm. We used an Olympus 20X1.0 numerical aperture objective. Each optical section was resampled three times and was captured every 0.5 µm. Images were taken from regions on apical dendrites, which were typically about 100 µm away from the soma and covered 150-200 µm in length. A minimum of 500 spines were analyzed per condition for all comparative studies, sister cultures were used.

TPLSM Image display

All images displayed in the manuscript are data from consecutive stacks displayed using a maximum value projection. At any given *x-y* coordinate, the maximum pixel value in that Z-column is displayed in the two-dimensional image. Ratio images are displayed for two-channel data (green/red; i.e., ARHGAP12/volume) and mapped in pseudocolor with red representing

a high ratio and blue a low ratio. Image analysis was conducted on raw data using full Z-stacks as discussed below.

TPLSM Quantitative image analysis

Images were analyzed as previously described [9]. Briefly, spines were analyzed using custom software written in MatLab. All analyses were conducted blind to the constructs being expressed. For each experiment, projection images of 40-60 consecutive z-series sections were generated for each cell or each time point.

For spine density and volume experiments spines were identified using green fluorescence channel and rectangular regions of interest (ROIs) were manually positioned to fully cover each spine. Spine density was calculated as the number of manually counted spines divided by dendrite segment length. Background-subtracted integrated fluorescence was taken as a measure for spine volume after normalizing to mean fluorescence at soma and large apical dendrite. No effort was made to analyze spines emerging below or above the dendrite, because the TPLSM resolution of these is compromised. It is also possible that many small structures were not detected, although point spread function limited structures were observed. Spine density and size values were compared using an unpaired two-tailed Student's t- test. Significance was set at $p < 0.05$.

For quantifications of ARHGAP12 spine enrichment, spines were identified using the dsRed channel and ARHGAP12 signal was identified using the green fluorescence channel. Spine ROIs were manually positioned to fully cover each spine, and dendrite ROIs were placed at the base of each spine centered on the dendrite with approximately the same area as the corresponding spine ROI. Enrichment of ARHGAP12 in spines is defined as (integrated spine green/integrated spine red fluorescence)/(mean dendrite green/mean dendrite red fluorescence). This approach is used as a relative means of determining enrichment. Thus, our "enrichment index" is a measurement of the relative concentration of ARHGAP12 in the spine (compared to dendritic regions), and is independent of spine size.

Rac1 activation assay

To assay Rac1 activity in cells, we used a luminescence-based G-LISA. Rac1 activation assays were executed following the manufacturer's instructions (Cytoskeleton. BK128). Briefly, primary hippocampal neurons at 0 DIV were infected with lentivirus expressing GFP control,

Arhgap1 sh#1, sh#2 or electroporated with WT *Arhgap12* or *Arhgap12*_R695Q and lysed at 7 DIV in the provided lysis buffer. Lysates were centrifuged at 13,200 rpm for 15 min at 4°C. The supernatants, each containing a total of 25-35 µg of proteins, were transferred into wells of a microtiter plate coated with Rac1 binding protein, and equal volumes of ice-cold binding buffer were added to each well. The microtiter plate was shaken on a cold orbital microtiter plate shaker (300 rpm) for 30 min at 4°C, solution was removed from wells, and the wells were incubated with diluted anti-Rac1 primary antibodies followed by secondary antibodies on a microtiter plate shaker (300 rpm) at RT for 45 min each. The plate was incubated with an HRP detection reagent for 15 min at 37°C, and after addition of an HRP stop buffer, the absorbance was immediately recorded at 490 nm.

Supplemental References

1. Zhu, Y., Xu, J. & Heinemann, S. F. Two Pathways of Synaptic Vesicle Retrieval Revealed by Single-Vesicle Imaging. *Neuron* **61,** 397–411 (2009).
2. Matsuda, M. *et al.* Identification of adherens junction-associated GTPase activating proteins by the fluorescence localization-based expression cloning. *Exp. Cell Res.* **314,** 939–49 (2008).
3. Govek, E.-E. *et al.* The X-linked mental retardation protein oligophrenin-1 is required for dendritic spine morphogenesis. *Nat. Neurosci.* **7,** 364–72 (2004).
4. Waung, M. W., Pfeiffer, B. E., Nosyreva, E. D., Ronesi, J. a. & Huber, K. M. Rapid Translation of Arc/Arg3.1 Selectively Mediates mGluR-Dependent LTD through Persistent Increases in AMPAR Endocytosis Rate. *Neuron* **59,** 84–97 (2008).
5. Kim, J. K., Palaniappan, C., Wu, W., Fay, P. J. & Bambara, R. a. Evidence for a unique mechanism of strand transfer from the transactivation response region of HIV-1. *J. Biol. Chem.* **272,** 16769–16777 (1997).
6. Marie, H., Morishita, W., Yu, X., Calakos, N. & Malenka, R. C. Generation of silent synapses by acute in vivo expression of CaMKIV and CREB. *Neuron* **45,** 741–752 (2005).
7. Carrodus, N. L., Teng, K. S.-L., Munro, K. M., Kennedy, M. J. & Gunnersen, J. M. Differential Labeling of Cell-surface and Internalized Proteins after Antibody Feeding of Live Cultured Neurons. *J. Vis. Exp.* 6–11 (2014). doi:10.3791/51139
8. Raynaud, F. *et al.* Shank3-Rich2 Interaction Regulates AMPA Receptor Recycling and Synaptic Long-Term Potentiation. *J. Neurosci.* **33,** 9699–9715 (2013).
9. Kopec, C. & Malinow, R. Matters of Size. **314,** 8–10 (2006).

Chapter 4

TRIO loss of function is associated with mild intellectual disability and affects dendritic branching and synapse function

Wei Ba*, Yan Yan*, Margot R.F. Reijnders*, Janneke H.M. Schuurs-Hoeijmakers, Ilse Feenstra, Ernie M.H.F. Bongers, Daniëlle G.M. Bosch, Nicole de Leeuw, Rolph Pfundt, Christian Gilissen, Petra F. de Vries, Joris A. Veltman, Alexander Hoischen, Heather C. Mefford, Evan E. Eichler, Betty A. Eipper, Richard E. Mains, Lisenka E.L.M. Vissers, Nael Nadif Kasri#, Bert B.A. de Vries#

* Co-first author
\# Co-last author

Published in:
Human Molecular Genetics. 2015 25:892-902

Abstract

Recently, we marked *TRIO* for the first time as a candidate gene for intellectual disability (ID). Across diverse vertebrate species, TRIO is a well-conserved Rho GTPase regulator that is highly expressed in the developing brain. However, little is known about the specific events regulated by *TRIO* during brain development and its clinical impact in humans when mutated. Routine clinical diagnostic testing identified an intragenic *de novo* deletion of *TRIO* in a boy with ID. Targeted sequencing of this gene in over 2,300 individuals with ID, identified three additional truncating mutations. All index cases had mild to borderline ID combined with behavioral problems consisting of autistic, hyperactive and/or aggressive behavior. Studies in dissociated rat hippocampal neurons demonstrated the enhancement of dendritic formation by suppressing endogenous TRIO, and similarly decreasing endogenous TRIO in organotypic hippocampal brain slices significantly increased synaptic strength by increasing functional synapses. Together, our findings provide new mechanistic insight into how genetic deficits in *TRIO* can lead to early neuronal network formation by directly affecting both neurite outgrowth and synapse development.

Introduction

Intellectual disability (ID), defined as an IQ of 70 or lower, has an estimated prevalence of 2-3% in the population [1]. The genetic etiology of ID is highly heterogeneous, with to date approximately >700 genes known to be associated with this common disorder [2], the majority of which are very rarely mutated. Novel sequencing approaches, such as massive parallel sequencing, have proven to be successful in identifying novel genes for Mendelian disorders [3]. Especially family-based whole exome sequencing (WES) in proband and parents has been instrumental to identify *de novo* pathogenic variants in sporadic cases with ID, thereby increasing the diagnostic yield in patients with severe ID (IQ<50) to up to 36% [4–10]. For mild and borderline ID, however, family-based sequencing is more complex as the distinction between a normal or a mildly affected parent can be difficult to make. This complicates the interpretation of variants from family-based WES as the phenotype can also be the result of inherited variants. To determine the role of mutations in candidate ID genes in individuals with ID, it is necessary to find additional individuals with a mutation in the same gene and a comparable phenotype. Furthermore, interpretation can be supported by functional studies to investigate the mutational effect on protein function. Recently, we marked *TRIO* [MIM 601893; NM_007118.2] for the first time as one of these candidate genes for ID, based on the identification of two potentially pathogenic *de novo* missense mutations in this gene in independent individuals with severe ID [6]. Both individuals, however, also carried a second *de novo* mutation in a known ID gene, *TCF4* and another candidate ID gene, *GFPT2*, respectively, complicating a straightforward interpretation of the contribution of the *TRIO* mutation to the patients' phenotype [6,11]. In a routine diagnostic setting using a genomic microarray, we also identified an individual with mild developmental delay carrying an 235 kb intragenic *de novo* deletion, disrupting *TRIO* [12] (chr5:14160447-14395478 (hg19)). Finally, seven *de novo* mutations were found in TRIO in the context of large scale sequencing projects focused on various neurodevelopmental conditions, including ID, epilepsy and autism [8,13,14]. Whereas these seven *de novo* mutations were not reported as conclusive cause of disease, they do support a possible role for *TRIO* in the development of ID (Fig. 1B).

TRIO is a large protein encoded by 57 coding exons (3097 amino acids) and containing several domains, including an N-terminal SEC14 domain, several spectrin repeats, two Dbl-homology-Pleckstrin-homology (DH-PH) Rho-GEF units, an Ig-like domain, and a C-terminal serine/threonine kinase domain (Fig. 1C). The serine/threonine kinase domain is presumed to

be active but quite selective; both DH-PH Rho-GEF domains are enzymatically active [15,16]. The first DH-PH domain has been shown to activate Rac1 and RhoG, whereas the second DH-DP domain activates RhoA [17,18]. Rho GTPases regulate changes in cell morphology in response to many factors including stimulation by extracellular ligands. They are activated by guanine exchange factors (GEF) catalyzing GDP dissociation and allowing the binding of GTP [19]. Interestingly, Rho GTPase signaling pathways have been identified as a major hub-signaling pathway in ID, affecting synaptic structure and function [20,21]. In *Drosophila*, *TRIO* has been shown to be involved in axon guidance and dendritic arborisation [22–24] during neuronal development. Additionally, *TRIO* is required for axonal growth in vitro and in vivo [25–27] and may contribute to the regulation of cell-cell contact [28,29]. Yet, surprisingly little is known about the function of *TRIO* in early dendrite formation and synaptic function in the mammalian system [20].

Here we report the identification of 4 cases with intragenic truncating mutations in TRIO, presenting with mild to borderline ID combined with behavioral problems consisting of autistic, hyperactive and/or aggressive behavior. Additionally, we show that during early neurodevelopment TRIO negatively regulates neurite outgrowth and synaptic strength by interfering with AMPAr endocytosis.

Results

Identification of individuals with mutations in TRIO

Based on the identification of multiple *de novo* mutations affecting *TRIO*, we decided to perform targeted sequencing for *TRIO* in >2300 patients with ID using molecular inversion probes (Materials and Methods) [30]. Filtering for putative loss-of-function mutations (initiator codon; nonsense; frameshift; canonical splice sites), we identified three additional *TRIO* truncating mutations (Fig. 1C), including one *de novo* nonsense mutation, c.4128G>A, predicted to result in p.(Trp1376*), in a 10 year old boy; a *de novo* frameshift mutation, c.3752del, predicted to result in p.(Asp1251Valfs*11) in a 35 year old woman; and a nonsense mutation, c.649A>T leading to p.(Arg217*) in a 20 year old male. The latter mutation was inherited from a similarly affected father (Supplementary Figure 1). This family also has a second child with learning difficulties and behavioral problems, who did not show the mutation upon segregation analysis, suggesting that his phenotype may have another (genetic or environmental) origin. A third, unaffected brother, did not show the variant either. DNA of

a fourth brother, the grandparents, and/or the 13 siblings from the father, was unavailable for testing. All these individuals, however, appeared to be normal.

As also *de novo* missense mutations have been implicated in ID [6], we subsequently selected for rare, possible pathogenic (CADD score $\geqslant$ 20), missense mutations in *TRIO* detected in our cohort. This analysis yielded seven missense variants (supplemental table 1), for which three could be tested for segregation in parental samples. Two of them appeared inherited from an unaffected parent, whereas the other was also identified in a father with borderline ID and behavioral problems, similar to his child. For the remaining four missense variants parental samples were not available. As from these data the impact of *(de novo)* missense mutations cannot unambiguously be assessed, we decided to further focus on the loss-of-function aspects of *TRIO*.

De novo truncating mutations have not been observed in over 2,000 healthy controls [14], but 13 different loss-of-function variants are reported in ExAC, a large databases collecting NGS variants as proxy for the general population (Supplementary Table 2)(URL: http://exac.broadinstitute.org [November 2015]). Notably, only two of 13 have been observed more than once (highest minor allele frequency 3.11E-04). These two variants represent a single base deletion- and duplication at the same genomic location, in a homopolymer stretch, potentially suggesting a sequencing and/or mapping artifact rather than the true nature of the reported variant. Comparison of the observed *de novo* mutation frequency of *TRIO* in ID to the gene specific *de novo* mutation rate [31] however indicates that we observed more *de novo* mutations in our ID cohort than expected based on chance alone (Exact Poisson Test, $p<0.005$).

In total, we identified 5 individuals from 4 families with a truncating mutation of *TRIO*, suggestive for loss of TRIO function. The clinical details for these four families are shown in Table 1. To avoid reporting inherited familial traits, the father of individual 2, who also had learning difficulties and behavior problems, was not included in this table. In summary, all of the index cases (age range 7-35 years) showed mild to borderline ID (IQ range 68-81) with autistic, hyperactive and aggressive behavioral problems. All individuals attended special education and needed special therapy to improve their language and motor development. Other observed features were recurrent infections (3/4 individuals), micrognathia (3/4), minor hand abnormalities (4/4), microcephaly (2/4), or low normal head circumference (2/4). No

congenital abnormalities were observed and only mild facial dysmorphisms were noted (Fig. 1A).

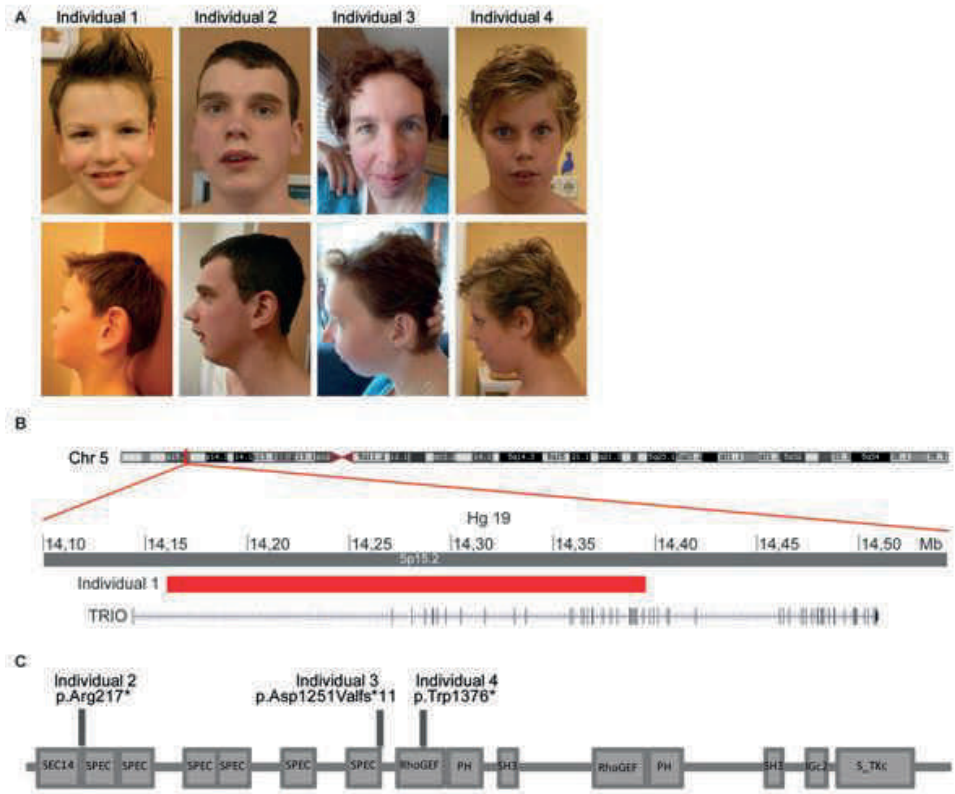

Figure 1 Individuals with loss-of-function *TRIO* mutations.
(A) Frontal and lateral photographs of individual 1 with the deletion disrupting *TRIO* and individuals 2, 3 and 4 with loss-of-function mutations in *TRIO*. Only mild facial dysmorphisms were observed.
(B) Schematic overview of the 235kb *de novo* deletion on chromosome 5, partially disrupting *TRIO* in individual 1.
(C) Schematic overview of TRIO, including the known domains (N-terminal SEC14 domain, several spectrin repeats, two Dbl-homology-Pleckstrin-homology (DH-PH) Rho-GEF units, Ig-like domain, and C-terminal putative serine/threonine kinase domain). The positions of the three identified mutations in individuals 2, 3 and 4 (p.Trp1376*, p.Asp1251Valfs*11 and p.(Arg217*) are depicted.

Developmental expression of TRIO and its role in neurite outgrowth

To find supportive evidence for TRIO as underlying cause in the phenotypes observed in our individuals, we investigated the neuronal function of TRIO in mammalian cells by examining

the expression of TRIO during rat hippocampal development. Western blot analysis of protein extracts revealed that full length TRIO is expressed during the early postnatal (P) period, but rapidly decreases after postnatal (P) day 11 (Fig. 2A, B). The rapid reduction in TRIO during postnatal development was further confirmed by measuring *Trio* mRNA expression (Fig. 2C). This decreased expression of TRIO is consistent with previous results [32] and suggests a role for TRIO in early neuronal development.

To study the function of endogenous TRIO during early neuronal development, we designed short hairpin RNAs (shRNAs) targeting the spectrin repeat region of *Trio*, a region that is present in most of the alternately spliced *Trio* transcripts [33]. The efficiency of *Trio* shRNA#1 and #2 was verified by co-expression with a vector encoding myc-TRIO (full length) in HEK293 cells (Fig. 2D). Dissociated rat hippocampal neurons were nucleofected at days *in vitro* (DIV) 0 with either a *Trio* shRNA or a scrambled shRNA control; expression of DsRed, which is encoded by the same vector, allowed identification of transfected cells and assessment of neuronal morphology. We first evaluated whether TRIO contributes to axon specification in early development by immunostaining neurons with a monoclonal antibody against Ankyrin G, which localizes to the axon initial segment [34]. A single Ankyrin G-positive process was identified in the control group and in the *Trio* knock-down groups at DIV4 and DIV7 (Fig. 2E), indicating that axon polarity is not affected by the absence of endogenous TRIO. Next, we examined dendritic arbor formation. Compared to control neurons, expression of *Trio* shRNAs significantly increased both the number of primary dendrites and branch points observed at DIV4 and at DIV7 (Fig. 2E, F). Similar results were obtained at DIV2 (data not shown). These results demonstrate that endogenous TRIO limits dendrite formation, without affecting the establishment of axon polarity. Kalirin, a TRIO orthologue with 64% identical protein structure, is emerging as a key regulator of structural and functional plasticity. Interestingly, Kalirin has been reported to exhibit the opposite effect, stimulating both dendritic outgrowth and branching at this stage of neuronal development [35].

Figure 2

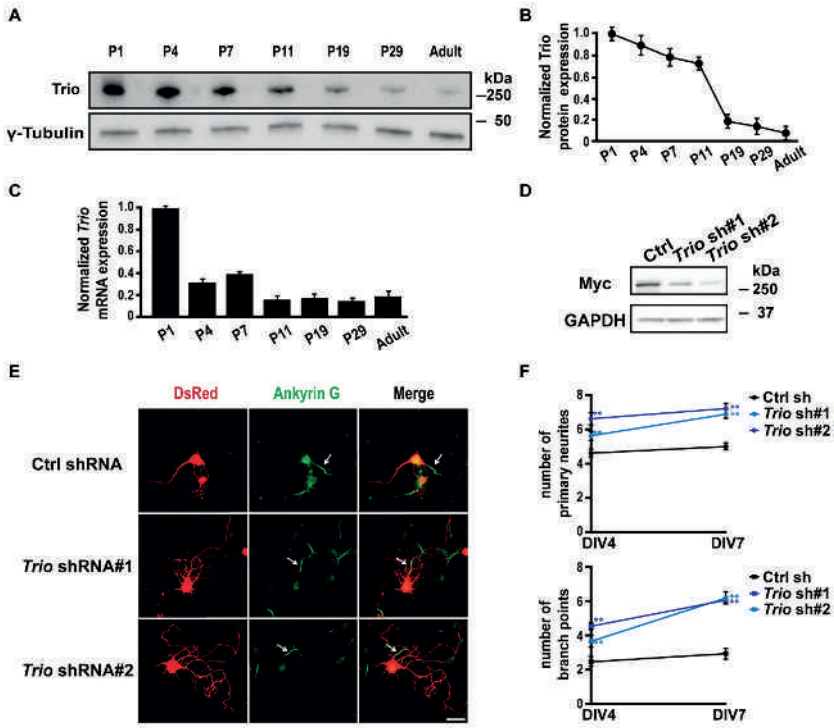

Figure 2 Developmental expression of TRIO and its role in neurite outgrowth.
(A) Rat hippocampi were collected at the indicated ages; equal amounts of protein (50 µg) were subjected to Western blot analysis and representative blots are shown.
(B) Quantification of Trio protein levels at different postnatal ages, normalized to the levels at P1 (n=3).
(C) Quantification of Trio mRNA levels using Q-PCR at different postnatal ages (n=3).
(D) 293 cells co-transfected with vectors encoding MYC-TRIO and *Trio* shRNA #1 and #2 were harvested after 24 h. Western blot analysis using a MYC antibody demonstrated that both Trio shRNA #1 and #2 efficiently reduced Trio expression.
(E) Rat hippocampal neurons nucleofected at the time of plating with a control (scrambled) shRNA or *Trio* shRNA #1 or #2 were fixed and analyzed at the indicated times. shRNA transfected neurons were identified by DsRed co-expression; axon initial segments were identified by staining for Ankyrin G; representative images at DIV7 are shown. Scale bar, 50 µm.
(F) Quantification of primary neurites and branch points at DIV4 and DIV7. Neurons expressing *Trio* shRNAs exhibited more primary neurites and more branch points than neurons expressing the control shRNA. Five separate experiments were performed; 20-30 neurons per group per experiment were counted. **p<0.01 with respect to the control (scramble) shRNA vector.

Post-synaptic TRIO regulates synaptic transmission

Previous proteomics studies of adult tissue have shown that TRIO is present at both the human and mouse post-synaptic density (PSD) [36], suggesting that TRIO functions at this site. In addition, the major isoform of Kalirin found in the adult nervous system has been shown to play a critical role in synaptic transmission, specifically through the regulation of ionotropic AMPA receptor (AMPAr) [37] and NMDA receptor (NMDAr) [38] trafficking. Modifications in the number and/or function of glutamate receptors is a core mechanism of regulating synaptic efficiency [39]. We therefore assessed whether TRIO plays a role in synaptic transmission at the hippocampal CA3–CA1 pathway.

Organotypic hippocampal brain slices were prepared from P6 pups, a time period at which dendrites have already formed, allowing us to bypass the effect of TRIO on dendritic arborization (Fig. 2). Hippocampal brain slices were biolistically transfected with *Trio* shRNAs. Four days post-transfection, simultaneous recordings of evoked excitatory post-synaptic currents (eEPSCs) from a DsRed-labeled, shRNA expressing CA1 pyramidal neuron and an adjacent non-transfected neuron were performed (Fig. 3A). We stimulated the Schaffer collaterals with two independent bipolar electrodes and measured the evoked response while holding CA1 neurons at either -60 mV to measure AMPAr-mediated responses or at +40 mV to measure NMDAr-mediated responses. Neurons transfected with either *Trio* shRNA#1 or *Trio* shRNA#2 showed significantly increased AMPAr-mediated, but not NMDAr-mediated, transmission compared to control (Fig. 3A-D). These data indicate that TRIO, at least at excitatory CA1 synapses, is specific for AMPARs versus NMDArs. Importantly, we previously showed that expressing GFP or a scrambled shRNA by means of biolistics does not affect AMPAr-mediated synaptic transmission [40,41].

The changes in AMPAr-mediated transmission could be a result of either a change of synaptic AMPArs at individual synapses, or a change in the number of functional synapses, or both. In order to determine the precise mechanism of action of the above possibilities we measured spontaneous excitatory postsynaptic currents (sEPSCs). We observed that the frequency, but not the amplitude, of the sEPSCs was significantly increased when neurons were transfected with *Trio* shRNA#1 (Fig. 3E, F). Increases in sEPSC frequency could be due to either increased intrinsic excitability of the pre-synaptic CA3 neurons, or increased active synapse between CA3 and CA1 neurons. Since biolistic transfection resulted in low transfection efficiency (a few neurons/slice), the major contribution of knocking down *Trio*

therefore comes from the recorded transfected postsynaptic cells (CA1) of the CA3-CA1 synapse. Our data thus suggest that depleting endogenous TRIO in CA1 neurons is sufficient to increase synaptic strength by increasing the amount of functional synapses.

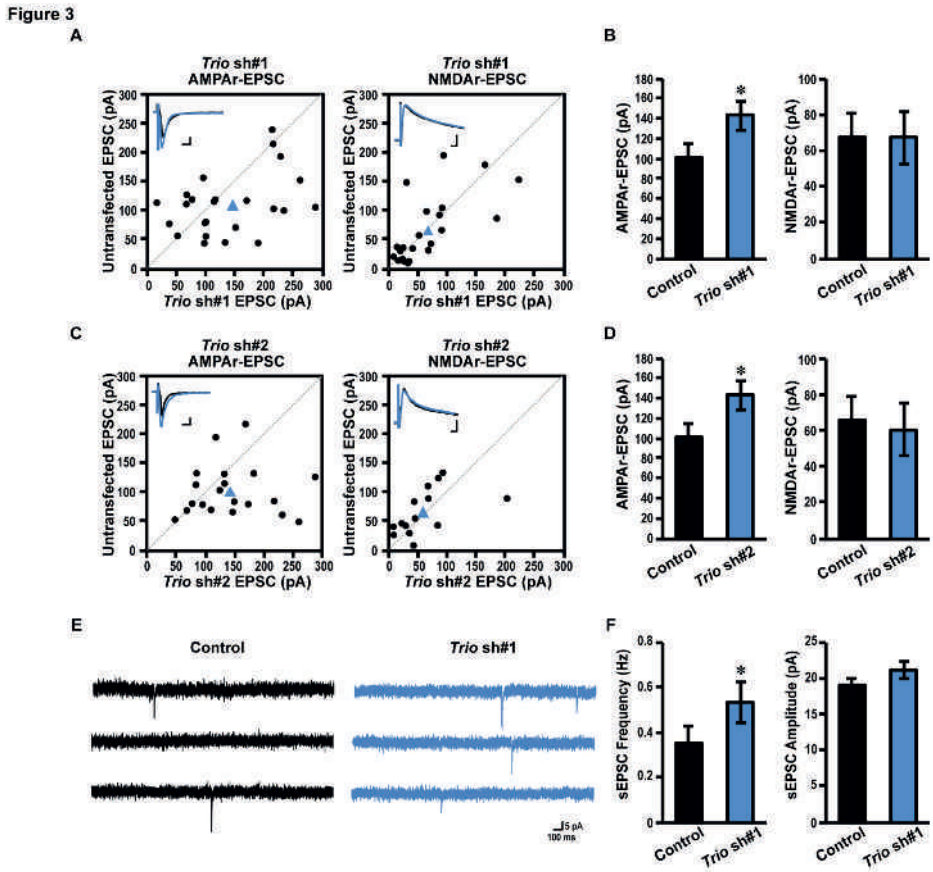

Figure 3 Post-synaptic TRIO regulates synaptic transmission.
(A, B) Amplitudes of AMPAr (left panel) and NMDAr (right panel) eEPSCs in control, non-transfected neurons are plotted against simultaneously recorded neighboring neurons expressing (A) *Trio* shRNA#1 (AMPAr n = 25; NMDAr n = 22), (B) *Trio* shRNA#2 (AMPAr n = 20; NMDAr n = 19). Black symbols represent single pairs of recordings; blue symbols show mean amplitudes. Inserts in each panel show sample averaged traces; blue traces, transfected neurons; black traces, non-transfected neighboring neurons. Scale bars represent 10 ms and 25 pA.
(C, D) Summary (mean ± SEM) of effects of expressing *Trio* shRNA#1, on AMPAr- (left) and NMDAr- (right) eEPSCs calculated as the averaged ratios obtained from pairs of infected and uninfected neighboring neurons. Data are shown as mean ± SEM. *$p < 0.05$, paired Student's t-test, *Trio* shRNA#1 (AMPAr n = 25; NMDAr n = 22), (B) *Trio* shRNA#2 (AMPAr n = 20; NMDAr n = 19).
(E) Representative traces of sEPSC recorded at −60 mV in an individual neuron from untransfected (control) or *Trio* shRNA#1 transfected group. Scale bars represent 100 ms and 5 pA.

(F) Quantification of sEPSC frequency (left) and amplitude (right) for control and *Trio* shRNA#1-expressing neurons. Data are shown as mean ± SEM. *p < 0.05, paired Student's t-test, n = 8 pairs.

Down-regulation of *Trio* reduces AMPAr endocytosis

To further understand the mechanism by which TRIO affects hippocampal glutamatergic synapses we tested whether down-regulation of *Trio* correlated with persistent changes in AMPAr internalization rate. Previously, an isoform of Trio has been shown to colocalize with Rab5 in endosomes [42] and Rab5 is required for AMPAr endocytosis at excitatory CA1 synapses [43]. We therefore assessed directly the function of Trio in AMPAr endocytosis. Primary hippocampal neurons were transfected with *Trio* shRNA#1 at DIV 3. At DIV 14 surface AMPAr GluA1 subunits were lively labeled with an antibody recognizing the extracellular epitopes of GluA1 and allowed AMPArs to internalize at 37°C for 2h. Neurons transfected with *Trio* shRNA#1 showed a marked reduction in endocystosis as assessed by the ratio between internalized and extracellular GluA1, suggesting that down-regulation of *Trio* decreases AMPAr endocytosis rate (Fig. 4A, B). Collectively, our results indicate that TRIO-mediated signaling controls synaptic function by regulating AMPAr endocytosis at CA1 excitatory synapses.

Figure 4

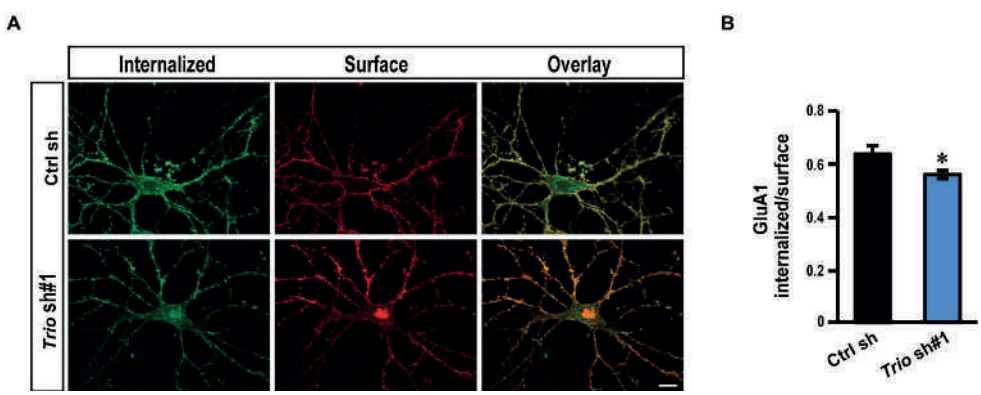

Figure 4 Down-regulation of *Trio* reduces AMPAr endocytosis.
(A) Representative double-label images of internalized (green) and surface (red) AMPAr GluA1 subunit in low-density hippocampal neurons.
(B) Ratiometric analysis of the intensity of internalized GluA1 to surface GluA1 in indicated conditions. Control shRNA: n=15; *Trio* shRNA#1: n=14; Scale bars, 10 µm; *P<0.05, t-test; Error bars represent SEM.

Discussion

Here we show that loss-of-function mutations in *TRIO* are responsible for a clinical phenotype involving mild to borderline ID with behavioral problems, and that TRIO has an important function during neurite outgrowth and basal synaptic transmission. Specifically, we demonstrated for the first time that endogenous Trio negatively regulates hippocampal synaptic strength by specifically affecting AMPAr internalization at CA1 excitatory synapses. Large scale reference data sets such as present in ExAC have now catalogued human genetic diversity at unprecedented level [44]. Whereas the LoF mutations identified in this study are not present in ExAC, 13 other truncating variants in *TRIO* (NM_007118.2) are. Four of these are located in the last exon, thereby escaping nonsense mediated mRNA decay. This leaves nine different potential loss-of-functions variants, reported to occur in 33 of >60,000 individuals represented in ExAC. Remarkably, ExAC recently reported that only 3,230 human genes (~15%) are near-completely depleted from truncating variants. This implicates that for the vast majority of genes such truncating variants are observed, and therefore likely, also include well-known disease genes causing disease by haploinsufficiency. For instance, analysis of ARID1B revealed 16 different LoF variants, identified in 29 of >60,000 individuals in ExAC (data not shown). Interestingly, however, LoF mutations in ARID1B cause autosomal dominant mental retardation type 12 [MIM 614562]. Whereas such individuals could go undiagnosed in the general population for which ExAC is a proxy, the frequency in which these ARID1B LoF mutations are observed relatively high to remain undiagnosed in the general population. In contrast, the aspecific phenotype and mild-to-borderline ID observed in patients with truncating variants in TRIO could remain undiagnosed in the population. Hence, LoF of TRIO are not unexpected to be present in ExAC.

The molecular mechanisms that promote excitatory synapse development have been extensively studied. However, the molecular events that prevent premature excitatory synapse development so that synapses form at the correct time and place are less well understood. Here we find that knockdown of *Trio*, during early development prevents both neurite outgrowth and synapse formation. Together with our observation that TRIO is highly expressed at early stages of development and that its expression decreases at the time when synapses are being formed, our data suggest that TRIO serves as an endogenous break for synaptic development. Indeed, downregulation of TRIO in hippocampal brain slices, using two

This Increased synaptic AMPAr-mediated response, was accompanied by an increase in the frequency of spontaneous excitatory currents as well as by a reduction of AMPAr internalization. Interestingly, an isoform of Trio (Trio8) has been shown to modulate early-endosome dynamics in COS-7 cells and to colocalize with Rab5 in neurons, whereas Rab5 activation drives the specific internalization of synaptic AMPArs in a clathrin-dependent manner [42,43]. It is therefore plausible that TRIO controls AMPAr endocytosis via a functional interaction with Rab5 in hippocampal neurons.

It is known that the redistribution of postsynaptic AMPARs plays a key role in controlling excitatory synaptic efficacy during early development. Early in development a majority of the synapses are silent, referring to the fact that they contain NMDArs but no functional AMPArs [45]. The proportion of these silent synapses rapidly decreases during the first two weeks of post-natal development in the hippocampus, coinciding with the maturation process of the synapses [46] and occurs as a result of AMPAr incorporation. Loss of TRIO could thus accelerate this unsilencing process. Of interest, premature maturation of excitatory synapses has been observed in several models for ASD. For example, accelerated maturation of excitatory synapses in an early period of hippocampal development contributes to the learning deficits in a mouse model of human *SYNGAP1* haploinsuffciency [47]. Similarly, accelerated maturation of glutamatergic synapses has been seen upon loss of the ID and Schizophrenia-associated microRNA, miR-137 [48].

Kalirin and TRIO belong to the dbl family of RhoGEFs and are unique within this family in that they display two GEF domains of distinct specificity. Whereas Kalirin has been extensively studied for its synaptic function, very little is known regarding the role of TRIO at the synapse. To our surprise we found that TRIO plays an opposing role compared to Kalirin both, at the level of neurite outgrowth and synaptic strength. Whereas Kalirin stimulates neurite outgrowth [35] we found that knockdown of *Trio* enhanced neurite outgrowth. Similarly, whereas Kalirin is required for activity-dependent spine enlargement and enhancement of AMPA-mediated synaptic transmission we found that TRIO negatively regulated AMPAr-mediated but did not affect NMDAr-mediated transmission [37]. The distinct effects of TRIO and Kalirin in mammals indicate that these genes contribute to different aspects of neuronal development. Their opposing roles could result in the fine balance needed to form complex dendritic arbors during development, which are critical for proper synaptogenesis and precise cognitive function. In addition, several *Trio* splicing variants have been identified [33], and the

expression of each isoform is regulated in a temporal and spatial-specific manner. These isoforms display either one or both GEF domains, suggesting that they could differentially regulate Rac1 and RhoA. Loss of TRIO in different brain structures could therefore account for different phenotypes. Functions of these isoforms are however largely unknown. Future studies will be needed to explore the function of the multiple TRIO domains in dendritic arborization and synapse formation and how the actions of the different domains are coordinated to regulate neuronal development.

In summary, our current data identified *TRIO* in patients with mild to borderline ID combined with behavioral problems and provide novel insight into how genetic deficits in *TRIO* can lead to glutamatergic dysfunction. Over the coming years, we expect many more mutations in TRIO to be identified. Therefore, we established a website (http://www.triogene.com) to collect detailed phenotypic data of individuals harboring TRIO mutations not only to gain insight into the clinical spectrum that these mutations might cause but also to obtain fundamental understanding of the pathogenic mechanisms underlying TRIO-related ID.

Materials and Methods

Identification of additional individuals with TRIO mutations

We performed targeted sequencing of the coding sequence of candidate ID genes, including *TRIO*, in a cohort of 2326 individuals with unexplained ID, using molecular inversion probes (MIPs) as described previously [30]. The individuals in this cohort were selected from the in-house collection of the Department of Human Genetics of Radboud University Medical Center (Nijmegen), containing more than 5000 samples from individuals with unexplained ID. DNA was extracted from peripheral blood. After confirmation with Sanger sequencing, *de novo* occurrence of the mutation was determined by using parental DNA. This study was approved by the institutional review board Commissie Mensgebonden Onderzoek Regio Arnhem-Nijmegen NL36191.091.11. Written informed consent was obtained from all individuals.

Cell Culture

Hippocampal neuron cultures were prepared from embryonic day 18 rats (Sprague-Dawley, Charles River) and nucleofected with various Ds-Red vectors as described previously [35]. Briefly,

hippocampal tissue was separated and meninges were removed carefully with forceps under the dissecting microscope. Tissues were digested with 0.25% trypsin (Corning) for 15 min before dissociation. Culture media contained 1 µg/ml fungizone (amphotericin B, Gibco) and 1 µM Ara-C (Sigma) until harvest. Cultures were examined at day *in vitro* (DIV) 2, 4 and 7, enumerating the numbers of primary neurites and branch points in the transfected cells, using fluorescence to identify transfected neurons [35].

Organotypic hippocampal slice cultures were prepared from postnatal day 6 rat pups as described [49]. Slices were biolistically transfected at 4 DIV using a Helios Gene Gun (Bio-Rad) [41] and recorded 4 days post-transfection.

Knockdown Experiments

To reduce expression of endogenous Trio in the cultures, shRNAs targeted the spectrin repeat region, since most of the alternately spliced Trio transcripts contain the spectrin repeats[2]; the effects of shRNAs targeting *Trio* were compared to a control shRNA (scrambled shRNA), which matches nothing in rodent genomes or transcripts. Oligonucleotides were annealed and ligated into the RNAi-Ready-pSiren-DNR-DsRed-Express vector (Clontech, Mountain View, CA). This vector utilizes the human U6 promoter to control shRNA expression and the CMV promoter to control DsRed expression[3]. The sequences targeted were: Scramble shRNA, AATGCACGCTCAGCACAAGC; *Trio* shRNA #1, TTCTGGCAGAAACAGAGGA; *Trio* shRNA #2, TTCAGACGCAGCACAATCA. All constructs were verified by sequencing. Transfection with 2 µg DNA was performed using a Nucleofector™ 2b device (Lonza) at the time of plating and $2.5x10^6$ neurons for each transfection [35]. Neurons were fixed at DIV2, 4 or 7 using 4% paraformaldehyde in phosphate buffered saline.

Immunocytochemistry and Image Acquisition

Fixed neurons were permeabilized with 0.3% Triton and stained with antisera to Ankyrin G (1: 1000; mouse, Neuromab). Images were taken using a Zeiss LSM 510 Meta confocal microscope and a 40x objective. For each neuron, numbers of primary neurites and branch points were measured from the same image. Primary neurites that are longer than one soma diameter were counted at all days *in vitro* indicated.

Western Blot Analysis

For time course studies, hippocampal tissues collected from rats at different ages were sonicated into the SDS lysis buffer, heated for 10 min at 95°C and insoluble debris was removed by centrifugation. The supernatant protein concentration was determined using the bicinchoninic acid assay (Pierce, Rockford, IL) and bovine serum albumin as the standard; 50 µg of total protein was loaded onto each lane for analysis of Trio expression. Westerns were performed with Trio antibody (UltraCruz) at 1:1000[2]. Similar expression patterns were observed in a separate set of animals.

RNA isolation, reverse transcription and Real-Time PCR

Total RNA from the tissue was isolated using Nucleospin RNA kit (Macherey-Nagel). cDNA was synthesized from 0.5–1 mg RNA using iScript™ cDNA Synthesis Kit. For detecting *Trio* expression, Real-time PCR was performed in 7900HT Fast Real-Time PCR System using GoTaq qPCR Master mix (Promega). The following primers were used: forward#1, GTCACGGAACATGTTGAAGG, reverse#1, CCTGTATCACCTCACGGATG; forward#2, TCGAGGAAGTTGCACAGAAC, reverse#2, ATCTCTTCGGGGTCACATTC; forward#3, AGTTGGAGAACGGGTACAGG; reverse#3, ACCTCGCTCAATGGGATAAC. Relative *Trio* expression compared to the control was calculated by $2^{-\Delta\Delta Ct}$.

Electrophysiology

Whole-cell recordings were obtained with Multiclamp 700B amplifiers (Axon Instruments). To monitor TRIO's effects on synaptic transmission, slices were biolistically transfected at DIV 4. Two days later, whole-cell recordings were obtained simultaneously from a transfected and an adjacent non-transfected neuron in the CA1 region under visual guidance using epifluorescence (red fluorescence) and transmitted light illumination. The recording chamber was perfused with artificial cerebrospinal fluid (ACSF) containing 119 mM NaCl, 2.5 mM KCl, 4 mM $CaCl_2$, 4 mM $MgCl_2$, 26 mM $NaHCO_3$, 1 mM NaH_2PO_4, 11 mM glucose, 0.1 mM picrotoxin, and 4 µM 2-chloroadenosine (pH 7.4), and gassed with 5% CO_2/95% O_2. Recordings were made at 30°C. Patch recording pipettes (3–5 MΩ) were filled with intracellular solution containing 115 mM cesium methanesulfonate, 20 mM CsCl, 10 mM HEPES, 2.5 mM $MgCl_2$, 4 mM Na_2ATP, 0.4 mM Na_3GTP, 10 mM sodium phosphocreatine, and 0.6 mM EGTA (pH 7.25). Evoked responses were induced using bipolar electrodes placed on Schaffer collateral pathway.

Responses were recorded at both −60 mV (for AMPAr-mediated responses) and +40 mV (for NMDAr-mediated responses). NMDAr-mediated responses were quantified as the mean between 60 and 65 msec after stimulation. All recordings were done by stimulating two independent synaptic inputs; results from each pathway were averaged and counted as n = 1. Spontaneous responses were recorded at −60 mV (sEPSC) in ACSF containing 2.5 mM $CaCl_2$ and 1.2 mM $MgCl_2$ at 30°C. sEPSCs were recorded in the presence of 0.1 mM picrotoxin. Five to 10 min of recordings were analyzed from each cell. Data were acquired at 5 kHz, filtered at 2 kHz, and analyzed using the Mini Analysis Program (Synaptosoft). All data are reported as mean ± SEM. Statistical significance was determined by the paired Student's t-test. Significance was set to $P < 0.05$.

AMPA receptor endocytosis assay

Endocytosis assay was performed as previously described (50, 51) with modifications. Briefly, living primary hippocampal neurons transfected with indicated constructs were pretreated for 30 min with 100 µg/ml leupeptin and then labeled with anti-GluA1 antibody (Millipore). Internalization of the labeled GluA1 subunits was then allowed for 2 hours at 37 °C. After fixation with 4% paraformaldehyde and blocking with 5% BSA, surface-labeled GluA1 subunits were exposed to Alexa-488 secondary antibody (Invitrogen). After washing, the remaining surface GluA1 subunits were incubated with an unlabeled secondary antibody at a concentration of 0.13 mg/ml overnight to saturate surface anti-GluA1 antibodies. Neurons were then permeabilized and incubated with Alexa-647 secondary antibody to label internalized GluA1 subunits. GluA1 endocytosis was calculated by dividing the intensity of internalized GluA1 by the intensity of surface GluA1 using imageJ (I_{488}/ I_{647}).

Acknowledgments

We are thankful to the individuals involved and their parents for their participation. This work was supported by the Netherlands Organization for Health Research and Development grant 912-12-109 (to J.A.V. and B.B.A.d.V) and 916-14-043 (to C.G.), the European research council (ERC Starting grant DENOVO 281964 to J.A.V.) and by the William Beecher Scoville (R.E.M.) and Janice and Rodney Reynolds (B.A.E.) Endowments. The research of NNK supported by grants from the “Donders Center for Neuroscience fellowship award of the Radboudumc” [to

N.N.K.]; the “FP7-Marie Curie International Reintegration Grant” [N.N.K. grant number 277091]; the Jerome Lejeune Foundation [to N.N.K]. NIH Grant Funding for this study was provided in part by the National Institutes for Mental Health (#1R01MH101221 to E.E.E.) E.E.E. is an investigator of the Howard Hughes Medical Institute.

Conflict of Interest Statement

No Conflict of Interest

References

1. Leonard, H. & Wen, X. The epidemiology of mental retardation: Challenges and opportunities in the new millennium. *Ment. Retard. Dev. Disabil. Res. Rev.* **8,** 117–134 (2002).
2. Vissers, L. E. L. M., Gilissen, C. & Veltman, J. A. Genetic studies in intellectual disability and related disorders. *Nat. Rev. Genet.* **17,** 9–18 (2015).
3. Bamshad, M. J. *et al.* Exome sequencing as a tool for Mendelian disease gene discovery. *Nat. Publ. Gr.* **12,** 745–755 (2011).
4. Yang, Y. *et al.* Clinical whole-exome sequencing for the diagnosis of mendelian disorders. *N. Engl. J. Med.* **369,** 1502–11 (2013).
5. Vissers, L. E. *et al.* A de novo paradigm for mental retardation. *Nat Genet* **42,** 1109–1112 (2010).
6. de Ligt, J. *et al.* Diagnostic exome sequencing in persons with severe intellectual disability. *N. Engl. J. Med.* **367,** 1921–9 (2012).
7. Rauch, A. *et al.* Range of genetic mutations associated with severe non-syndromic sporadic intellectual disability: An exome sequencing study. *Lancet* **380,** 1674–1682 (2012).
8. Fitzgerald, T. W. *et al.* Large-scale discovery of novel genetic causes of developmental disorders. *Nature* **519,** 223–228 (2014).
9. Wright, C. F. *et al.* Genetic diagnosis of developmental disorders in the DDD study: A scalable analysis of genome-wide research data. *Lancet* **385,** 1305–1314 (2015).
10. Yang, Y. *et al.* Molecular Findings Among Patients Referred for Clinical Whole-Exome Sequencing. *Jama* **312,** 1870–79 (2014).
11. Gilissen C Thung DT, van de Vorst M, van Bon BWM, Willemsen MH, Kwint M, Janssen IM, Hoischen A, Schenck A, Leach R, Klein R, Tearle R, Bo T, Pfundt R, Yntema HG, de Vries BBA, Kleefstra T, Brunner HG, Vissers LELM, Veltman JA., H.-K. J. Y. Genome sequencing identifies major causes of severe intellectual disability. *Nature* **000,** 344–347 (2014).
12. Vulto-van Silfhout, A. T. *et al.* Clinical Significance of De Novo and Inherited Copy-Number Variation. *Hum. Mutat.* **34,** 1679–1687 (2013).
13. Appenzeller, S. *et al.* De novo mutations in synaptic transmission genes including DNM1 cause epileptic encephalopathies. *Am. J. Hum. Genet.* **95,** 360–370 (2014).
14. Iossifov, I. *et al.* The contribution of de novo coding mutations to autism spectrum disorder. *Nature* **13,** 216–221 (2014).
15. Debant, a *et al.* The multidomain protein Trio binds the LAR transmembrane tyrosine phosphatase, contains a protein kinase domain, and has separate rac-specific and rho-specific guanine nucleotide exchange factor domains. *Proc. Natl. Acad. Sci. U. S. A.* **93,** 5466–5471 (1996).
16. Peng, Y. J. *et al.* Trio is a key guanine nucleotide exchange factor coordinating regulation of the migration and morphogenesis of granule cells in the developing cerebellum. *J. Biol. Chem.* **285,** 24834–24844 (2010).
17. Jaiswal, M., Dvorsky, R. & Ahmadian, M. R. Deciphering the Molecular and Functional Basis of Dbl Family Proteins: A NOVEL SYSTEMATIC APPROACH TOWARD CLASSIFICATION OF SELECTIVE ACTIVATION OF THE Rho FAMILY PROTEINS. *J. Biol. Chem.* **288,** 4486–4500 (2012).
18. Blangy, A. *et al.* TrioGEF1 controls Rac- and Cdc42-dependent cell structures through the direct activation of RhoG. *J. Cell Sci.* **113,** 729–39 (2000).
19. Rossman, K. L., Der, C. J. & Sondek, J. GEF means go: turning on RHO GTPases with guanine nucleotide-exchange factors. *Nat. Rev. Mol. Cell Biol.* **6,** 167–180 (2005).
20. Choi, B. J. *et al.* Miniature Neurotransmission Regulates Drosophila Synaptic Structural Maturation. *Neuron* **82,** 618–634 (2014).
21. Ba, W., van der Raadt, J. & Nadif Kasri, N. Rho GTPase signaling at the synapse: Implications for intellectual disability. *Exp. Cell Res.* **319,** 2368–2374 (2013).
22. Newsome, T. P. *et al.* Trio combines with dock to regulate Pak activity during photoreceptor axon pathfinding in Drosophila. *Cell* **101,** 283–294 (2000).
23. Iyer, S. C. *et al.* The rhogef trio functions in sculpting class specific dendrite morphogenesis in

drosophila sensory neurons. *PLoS One* **7,** (2012).
24. Shivalkar, M. & Giniger, E. Control of dendritic morphogenesis by trio in drosophila melanogaster. *PLoS One* **7,** (2012).
25. Van Haren, J. *et al.* Dynamic microtubules catalyze formation of navigator-TRIO complexes to regulate neurite extension. *Curr. Biol.* **24,** 1778–1785 (2014).
26. DeGeer, J. *et al.* Tyrosine phosphorylation of the Rho guanine nucleotide exchange factor Trio regulates netrin-1/DCC-mediated cortical axon outgrowth. *Mol. Cell. Biol.* **33,** 739–51 (2013).
27. Briançon-Marjollet, A. *et al.* Trio mediates netrin-1-induced Rac1 activation in axon outgrowth and guidance. *Mol. Cell. Biol.* **28,** 2314–23 (2008).
28. Charrasse, S. *et al.* M-cadherin activates Rac1 GTPase through the Rho-GEF trio during myoblast fusion. *Mol. Biol. Cell* **18,** 1734–43 (2007).
29. Schmidt, S. & Debant, A. Function and regulation of the Rho guanine nucleotide exchange factor Trio. *Small GTPases* **5,** (2014).
30. Roak, B. J. O. *et al.* Multiplex Targeted Sequencing Identifies Recurrently Mutated Genes in Autism Spectrum Disorders. *Science (80-.).* **338,** 1619–22 (2012).
31. Samocha, K. E. *et al.* A framework for the interpretation of de novo mutation in human disease. *Nat. Genet.* **46,** 944–50 (2014).
32. Ma, X. M., Huang, J. P., Eipper, B. a. & Mains, R. E. Expression of Trio, a member of the Dbl family of rho GEFs in the developing rat brain. *J. Comp. Neurol.* **482,** 333–348 (2005).
33. McPherson, C. E., Eipper, B. A. & Mains, R. E. Multiple novel isoforms of Trio are expressed in the developing rat brain. *Gene* **347,** 125–135 (2005).
34. Zhou, D. *et al.* Ankyrin(G) is required for clustering of voltage-gated Na channels at axon initial segments and for normal action potential firing. *J. Cell Biol.* **143,** 1295–1304 (1998).
35. Yan, Y., Eipper, B. A. & Mains, R. E. Kalirin-9 and kalirin-12 play essential roles in dendritic outgrowth and branching. *Cereb. Cortex* **25,** 3487–3501 (2015).
36. Bayés, À. *et al.* Comparative Study of Human and Mouse Postsynaptic Proteomes Finds High Compositional Conservation and Abundance Differences for Key Synaptic Proteins. *PLoS One* **7,** (2012).
37. Xie, Z. *et al.* Kalirin-7 Controls Activity-Dependent Structural and Functional Plasticity of Dendritic Spines. *Neuron* **56,** 640–656 (2007).
38. Kiraly, D. D., Lemtiri-Chlieh, F., Levine, E. S., Mains, R. E. & Eipper, B. a. Kalirin Binds the NR2B Subunit of the NMDA Receptor, Altering Its Synaptic Localization and Function. *J. Neurosci.* **31,** 12554–12565 (2011).
39. Kessels, H. W. & Malinow, R. Synaptic AMPA receptor plasticity and behavior. *Neuron* **61,** 340–50 (2009).
40. Nadif Kasri, N., Nakano-Kobayashi, A. & Van Aelst, L. Rapid synthesis of the X-linked mental retardation protein OPHN1 mediates mGluR-dependent LTD through interaction with the endocytic machinery. *Neuron* **72,** 300–15 (2011).
41. Nadif Kasri, N., Nakano-Kobayashi, A., Malinow, R., Li, B. & Van Aelst, L. The Rho-linked mental retardation protein oligophrenin-1 controls synapse maturation and plasticity by stabilizing AMPA receptors. *Genes Dev.* **23,** 1289–302 (2009).
42. Sun, Y.-J. *et al.* Solo/Trio8, a membrane-associated short isoform of Trio, modulates endosome dynamics and neurite elongation. *Mol. Cell. Biol.* **26,** 6923–35 (2006).
43. Brown, T. C., Tran, I. C., Backos, D. S. & Esteban, J. A. NMDA receptor-dependent activation of the small GTPase Rab5 drives the removal of synaptic AMPA receptors during hippocampal LTD. *Neuron* **45,** 81–94 (2005).
44. Lek, M., Konrad, K. J., V, M. E., Samocha, K. E. & MacArthur, D. G. Analysis of protein-coding genetic variation in 60,706 humans. 1–26 (2015).
45. Hanse, E., Seth, H. & Riebe, I. AMPA-silent synapses in brain development and pathology. *Nat. Rev. Neurosci.* **14,** 839–50 (2013).
46. Liao, D., Zhang, X., O'Brien, R., Ehlers, M. D. & Huganir, R. L. Regulation of morphological postsynaptic silent synapses in developing hippocampal neurons. *Nat. Neurosci.* **2,** 37–43

(1999).
47. Clement *et al.* Pathogenic SYNGAP1 mutations impair cognitive development by disrupting maturation of dendritic spine synapses. *Cell* **151,** 709–23 (2012).
48. Olde Loohuis, N. F. M. *et al.* MicroRNA-137 Controls AMPA-Receptor-Mediated Transmission and mGluR-Dependent LTD. *Cell Rep.* **11,** 1876–1884 (2015).
49. Kasri, N. N., Govek, E. E. & Aelst, L. Van. Characterization of Oligophrenin-1, a RhoGAP Lost in Patients Affected with Mental Retardation: Lentiviral Injection in Organotypic Brain Slice Cultures. *Methods Enzymol.* **439,** 255–266 (2008).

Table 1 Molecular and clinical details of individuals with *TRIO* mutations

	Individual 1	**Individual 2**	**Individual 3**	**Individual 4**
Gender	Male	Male	Female	Male
Age at last visit	7	20	35	10
Mutations				
Deletion breakpoints	Chr5:14160447-14395478	-	-	-
Deleted genes	*TRIO*	-	-	-
cDNA change	-	c.649A>T	c.3752del	c.4128G>A
Amino acid change	-	p.Arg217*	p.Asp1251Valfs*11	p.Trp1376*
Chromosome position	-	14290933	14387728	14390409
Growth				
Birth weight	0 SD	+0.25 SD	-0.75 SD	0 SD
Height	0 SD	-0.75 SD	-1.5 SD	+1.25 SD
Weight	NR	NR	+1 SD	+3 SD
Head circumference	-1 SD	-2.5 SD	-2.5 SD	-1.5 SD
Development				
Intellectual disability	Borderline (IQ81)	Borderline (IQ78)	Mild (IQ62)	Mild (IQ68)
Speech delay	+ 7 years: 5-6 words	NR NR	+ 3 years: first words	+ NR
Motor delay	+ Fine motor delay	+ 3 years: first steps	+ 2 years: first steps	+ Fine motor delay
Neurological				
Behavioral problems	+ PDD-NOS	+ ADHD	+ Autistic-like traits	+ ADHD
High reflexes	-	+	+	-
Hyperacusis	+	-	+	-
Swallow difficulties	-	NR	+	+
Facial				
Facial asymmetry	-	+	+	-

Periorbital fullness	+	-	+	-
Full lips	-	+	+	-
High palate	-	+	NR	+
Dental crowding	-	+	+	+
Micrognathia	-	+	+	+
Other facial dysmorphism	High forehead, large protruding ears, short philtrum	-	High forehead, Full eyebrows, Downslanted palperbral fissures, full nasal tip	High forehead, Long philtrum
Extremities				
Minor hand abnormalities	+ Short, broad with Simian creases and volaire pads	+ Broad proximal interphalangeal joints, camptodactyly dig V	+ Brachydactyly dig I, tapering fingers	+ Tapering fingers
Other				
Recurrent infections	+	NR	+	+
Kyphosis	-	-	+	+
Fatigue	+	-	+	-
Neonatal feeding difficulties	+	-	NR	+
Other clinical features	Anal fistula, scapula alatae, 4th palmar crease, clinodactyly digitus 5, sandal gap	Torsio testis, pectus excavatum, tremor	Constipation, hypercalcemia, hypotonia, pes planus, varices	Automutilation

NR= not reported

Supplemental Data

Supplementary Tables

Supplementary Table 1: Highly conserved missense mutations in 2,326 patients with ID

Genomic position	cDNA change (NM_007118.2)	Predicted protein change	CADD score	Mutation type	Segregation
chr5(GRCh37):g.14366984C>A	c.2770C>A	p.Arg924Ser	34	missense	paternally inherited
chr5(GRCh37):g.14387688T>C	c.3712T>C	p.Tyr1238His	27	missense	n.a.
chr5(GRCh37):g.14471427G>A	c.5764G>A	p.Ala1922Thr	20	missense	maternally inherited
chr5(GRCh37):g.14471479G>A	c.5816G>A	p.Ser1939Asn	25	missense	paternally inherited
chr5(GRCh37):g.14482826C>G	c.6601C>G	p.Leu2201Val	24	missense	n.a.
chr5(GRCh37):g.14485261G>C	c.6741G>C	p.Glu2247Asp	23	missense	n.a.
chr5(GRCh37):g.14498270G>A	c.8120G>A	p.Arg2707Gln	24	missense	n.a.

Supplementary Table 2: Overview of truncating mutations from ExAC for TRIO based on NM_007118.2 [November 2015]

dB Origin	cDNA	Predicted protein effect	Individuals tested	Allele frequencies (mut/wt)	Genotypes (hmz mut - het - hmz wt)	Minor Allele Frequency
ExAC	c.1708_1709del	p.Val570Phefs*41	57,499	1/114,998	0 - 1 - 57,498	0.0000087
ExAC	c.3358G>T	p.Glu1120*	51,398	1/102,796	0 - 1 - 51,397	0.0000097
ExAC	c.5032C>T	p.Arg1678*	60,427	1/120,854	0 - 1 - 60,426	0.0000083
ExAC	c.6657+1dup	p.?	58,349	1/116,698	0 - 1 - 58,348	0.0000086
ExAC	c.7050del	p.Val2351Cysfs*62	33,774	21/67,548	0 - 21 - 33,753	0.0003109
ExAC	c.7050dup	p.Val2351Argfs*90	33,774	5/67,548	0 - 5 - 33,769	0.0000740
ExAC	c.7448dup	p.Ser2484Leufs*41	43,966	1/87,932	0 - 1 - 43,965	0.0000114
ExAC	c.8019+1G>T	p.?	60,265	1/120,530	0 - 1 - 60,264	0.0000083
ExAC	c.8665G>T	p.Glu2889*	60,296	1/120,592	0 - 1 - 60,295	0.0000083
ExAC	c.8773G>T	p.Glu2925*	59,864	1/119,728	0 - 1 - 59,863	0.0000084
ExAC	c.9207_9210del	p.Phe3069Leufs*58	59,959	1/119,918	0 - 1 - 59,958	0.0000083
ExAC	c.9209_9210insGG	p.Ile3070Metfs*59	59,931	1/119,862	0 - 1 - 59,930	0.0000083
ExAC	c.9268C>T	p.Gln3090*	58,469	1/116,938	0 - 1 - 58,468	0.0000086

S

Supplementary Figures

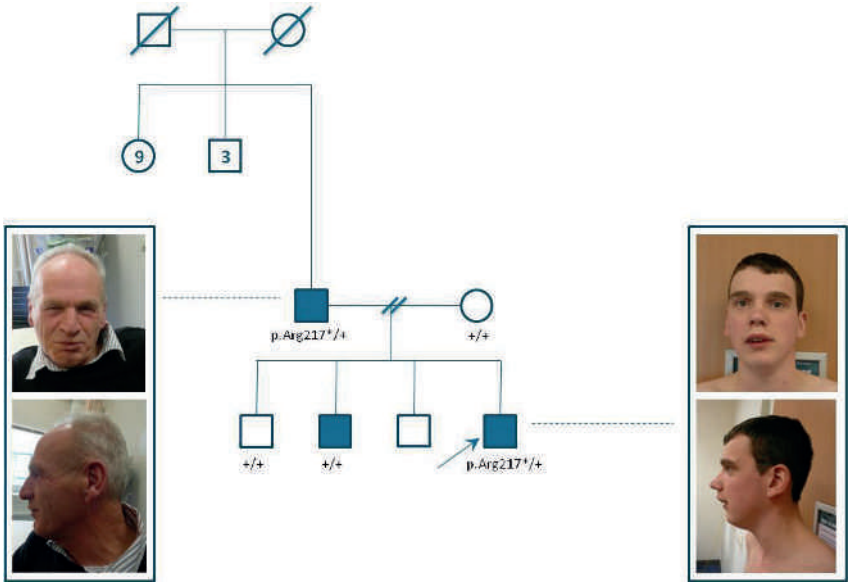

Figure 1 Pedigree of family with dominantly segregating nonsense mutation in *TRIO*

Chapter 5

Functional characterization of the Lowe Syndrome protein OCRL1 at the synapse

Wei Ba, Martijn M. Selten, Herman van Veen, Rizky S.E. Lasabuda, Inge Schreurs, Daisy van der Heijden, Astrid R. Oudakker, Hans van Bokhoven, Nael Nadif Kasri

Abstract

Lowe syndrome (LS) is a developmental disorder caused by mutations in the *OCRL1* gene. Although one of the major tissues affected in LS is the brain, surprisingly little is known about the neuronal function of OCRL1. Here, we report the functional characterization of OCRL1 in the rat hippocampus. OCRL1 is present in the hippocampus with constant developmental expression. Functionally, OCRL1 regulates both spine density and basal synaptic transmission at mature CA3-CA1 synapses. In addition, OCRL1 downregulation causes a “traffic jam” of AMPArs on the endocytic-lysosomal trafficking route, indicated by impaired AMPAr endocytosis, increased extrasynaptic accumulation of AMPArs and elevated total AMPAr levels. Of note, aberrant expression of OCRL1 leads to altered long-term potentiation (LTP). Overall, our findings for the first time provide evidence that loss of OCRL1 alters synaptic structure and function in the hippocampus, which may explain how mutations in *OCRL1* result in cognitive impairment in LS.

Introduction

Intellectual disability (ID) consists of a wide range of disorders that are characterized by cognitive impairment and reduced adaptive skills. ID affects 2% - 3% of the population and it can be resulted from genetic defects as well as environmental causes. To date, over 700 genes have been associated with ID [1] and a major challenge has been to uncover the cellular mechanisms responsible for declined cognitive function. ID has long been proposed to be "a disease of the synapse". This assumption is supported by the observation that ID genes converge to common signaling cascades that impinge on synaptic function. During normal brain development and learning and memory, synapses undergo rapid and/or long-lasting changes due to the remodeling of synaptic structure (e.g. spine size and density) and function (e.g. presynaptic neurotransmitter release, expression of postsynaptic receptors), eventually leading to changes in synaptic strength. A number of molecules and signaling pathways have been implicated in these processes, including Rho GTPase signaling [2–4], AMPA receptor trafficking signaling [5–9] and phospholipid signaling [10–14]. It is, therefore, not surprising that the vast majority of ID genes, such as *OPHN1*, *BRAG1, ARHGEF6, FMR1* and *TSPAN7,* are involved in these signaling pathways [15–19].

The gene *OCRL1* lies across 24 exons on the X-chromosome encoding the inositol 5-phosphotase OCRL1. Mutations of *OCRL1* result in oculocerebrorenal syndrome of Lowe (Lowe Syndrome, LS), a rare X-linked disorder characterized by congenital cataracts, ID and renal proximal tubulopathy. Another rare X-linked disorder, type 2 Dent disease, which shows selectively renal dysfunction has also been reported to result from *OCRL1* mutations [20,21]. OCRL1 is a multidomain protein containing an N-terminal PH domain, a central inositol 5-phosphatase domain, a C-terminal ASH and a RhoGAP-like domain, as well as two clathrin binding motifs [22] (Figure 1A). Through these domains and motifs, OCRL1 interacts with key components of membrane trafficking machineries such as clathrin, clathrin adaptors, Rab and Rho GTPases, as well as the endocytic proteins APPL1. Consistently, OCRL1 has been reported to display a broad cellular distribution including the plasma membrane, the endosomal system, the Golgi complex and clathrin-coated vesicles [23–26]. OCRL1 has two splice isoforms that differ by a single exon encoding 8 amino acids. The longer isoform a is the only form present in the brain, whereas both isoforms are expressed in all other tissues [27]. Over 120 mutations in *OCRL1* have been identified in the patients with LS, including premature stop codons, frameshift mutations, in-frame deletions, genomic or exon deletions and missense

mutations [28–31]. These mutations lead to misfolding, loss of stability and interactions, as well as loss of catalytic activity of OCRL1 protein, indicating that both structure and catalytic activity of OCRL1 are important for normal cell physiology [32].

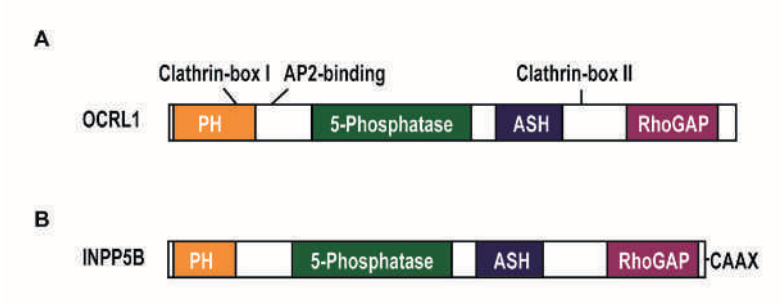

Figure 1 Domain organization of OCRL1 and INPP5B
(A) OCRL1 contains an N-terminal PH domain, followed by a 5-phosphatase domain, an ASH and a GAP domain. Besides, OCRL1 has two clathrin-binding motifs an AP2 binding motif.
(B) INPP5B has the same domain structure as OCRL1, but lacks the clathrin and AP2 binding motifs. In addition, INPP5B contains a CAAX motif at its C-terminus.

Intensive studies have been performed, in non-neuronal cells, regarding the cellular function of OCRL1 [23,26,33]. Phosphoinositides (PIs) are involved in diverse cellular events such as signal transduction, exo- and endocytosis, membrane trafficking and regulation of the actin cytoskeleton [14,34,35]. Reversible phosphorylation of the inositol ring at position 3, 4 and 5 generates seven PIs each of which has a unique subcellular distribution [36]. As one of the ten conserved 5-phosphatases, OCRL1 preferentially dephosphorylates PI(4,5)P2 and also displays activity toward PI(3,4,5)P3 to a less extent *in vitro* [37,38]. Previous studies have found that cell lines derived from LS patients show a reduced 5-phosphatase activity (less than 10% compared to unaffected individuals) and elevated PI(4,5)P2 levels [39], suggesting an essential role of OCRL1 in controlling PI homeostasis. In addition, OCRL1 has been reported to be essential for protein trafficking from endosomes to the trans-Golgi network via its 5-phosphatase activity [40]. Defects in clathrin-mediated endocytosis and recycling of several receptors including megalin have been observed in cells lacking OCRL1 [41]. Interestingly, OCRL1 has been found to regulate actin cytoskeleton dynamics by modulating PI(4,5)P2 homeostasis as well as Rac1 GTPases activity via its GAP domain, although it has been reported to possess only a weak GAP activity in some cell lines previously [33]. Cells lacking OCRL1 display elevated

PI(4,5)P2 levels and produce actin comets from the Golgi apparatus and endosomes in an N-WASP-dependent manner. Vicinanza *et al*. further confirmed that OCRL1 regulates endosomal actin polymerization via PI(4,5)P2-Arp2/3-N-WASP signaling [40]. Together, these data strongly indicate that OCRL1 regulates general membrane trafficking and actin dynamics.

So far, no ideal murine model has been available for studying the mechanisms of LS and Dent disease. One reason may lie with the functional redundancy for OCRL1 and INPP5B, an OCRL1 homolog with ~45% sequence identity and similar protein structure [42] (Figure 1B). The loss of OCRL1 in mice is fully compensated by INPP5B, therefore, no phenotype is detectable in *Ocrl1* KO mice [44]. In human, the degree of compensation is lower compared to that in mice, which might due to two reasons: the relative low levels of INPP5B and the different splicing of human *INPP5B* gene leading to a shorter version of INPP5B protein [44]. A "humanized" mouse line was generated by expressing human INPP5B in *Ocrl1/Inpp5b* double knockout mice. These mice show reduced growth and a renal tubulopathy however do not show any ocular or neurological defects [45]. In addition, several groups have made use of zebrafish models for studying OCRL1 function. A mutant zebrafish in which OCRL1 expression is attenuated by insertion of a retrovirus in the promoter has been generated and delayed brain and eye development with impaired cell proliferation as well as increased apoptosis have been observed in this mutant [46]. Other studies used depletion of OCRL1 by injecting antisense morpholinos in zebrafish and reported altered ciliogenesis [47].

Although one of the most debilitating symptoms in LS is intellectual disability, until now the function of OCRL1 in the brain remains elusive. In this study, we clarify the role of OCRL1 in the brain by examining its expression and impact on synapse structure and function in the hippocampus, a region that plays a key role in learning and memory. We show that OCRL1 is expressed in all hippocampal subregions and the mRNAs of *Ocrl1* is stably expressed throughout hippocampal development. Elevated *Ocrl1* levels significantly increase dendritic spine density and mEPSC frequency of mature CA1 pyramidal neurons while depletion of *Ocrl1* displays opposing effect. In addition, overexpression of *Ocrl1* impairs LTP, one of the major molecular mechanisms underlying learning and memory, whereas downregulation of *Ocrl1* enhances LTP magnitude. Of note, *Ocrl1* knockdown significantly increases total GluA1 protein levels and impairs AMPAr endocytosis. We therefore propose a model in which loss of OCRL1 causes a "traffic jam" of AMPArs on the endocytic-lysosomal trafficking route, which is likely to expand the mobile pool of AMPArs and subsequently facilitate LTP. Overall, our

findings for the first time provide evidence of loss of OCRL1 leading to altered spine structure and function, which may explain how mutations in OCRL1 result in cognitive impairment in LS.

Results

OCRL1 in the hippocampus

We initiated the characterization of *Ocrl1* by determining its spatiotemporal expression in hippocampus. By using quantitative polymerase chain reaction PCR (*qPCR*), we examined the transcriptional expression pattern of *Ocrl1* during hippocampal development. Our results showed that *Ocrl1* levels were constant throughout all developmental stages in the hippocampus (**chapter 2** and Figure 2A). To determine the spatial distribution of OCRL1 in hippocampus, we performed immunostaining experiments on rat brain sections. We found that OCRL1 was highly expressed in all hippocampal subregions, with relative higher levels in CA3 and dentate gyrus (DG) (Figure 2B). Together, these results reveal a significant presence of OCRL1 throughout hippocampal development, implying its contribution in both developing and mature hippocampus.

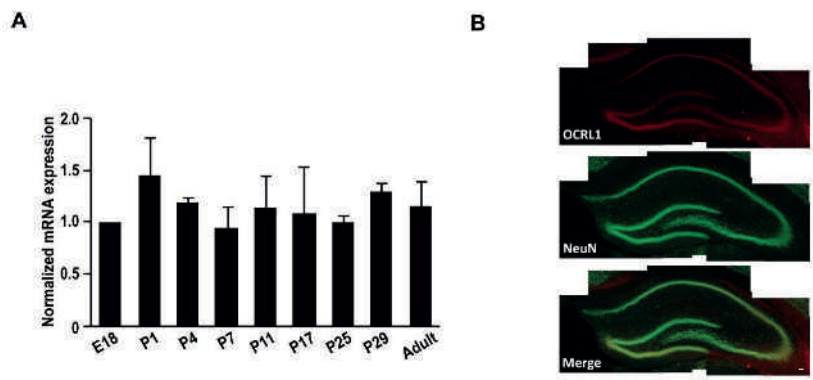

Figure 2 Expression and distribution of OCRL1 in the hippocampus
(A) Expression of *Ocrl1* mRNA during hippocampal development.
(B) Hippocampi sections from a P20 rat double-immunolabled with an anti-OCRL1 antibody (red) and an anti-NeuN antibody (green). Scale bars, 50 µm.

OCRL1 regulates dendritic spine morphology

OCRL1 contains several conserved protein domains that have been shown to regulate actin cytoskeleton dynamics via distinct signaling pathways, such as a 5-phosphatase domain and a RhoGAP-like domain. We speculated that OCRL1 might be important for neuronal structure, although whether the GAP-like domain is functional still remains controversial. We therefore examined the effects of OCRL1 in regulating dendritic spine morphology of CA1 pyramidal neurons by two-photon laser scanning microscopy (TPLSM). We biolistically introduced a GFP-expressing construct, as a cellular marker, with or without a second construct containing full-length human *Ocrl1* isoform a (*Ocrl1_a*) into organotypic hippocampal slices at 12 DIV and imaged GFP-labeled dendrites and spines from transfected CA1 neurons 48 hours post-transfection. Compared to neurons expressing GFP alone, *Ocrl1_a* overexpressing CA1 pyramidal neurons displayed a significant increase in spine density without changes in spine volume (Figure 3A, B). We next examined the function of endogenous OCRL1 by probing the effects of *Ocrl1* downregulation on dendritic spines of CA1 neurons, using RNAi. We verified the efficiencies of shRNAs by performing qPCR experiments. Both *Ocrl1* shRNA #1 (*Ocrl1* sh#1) and #2 (*Ocrl1* sh#2) significantly reduced endogenous *Ocrl1* mRNA levels with distinct efficiencies (sh#1: 51% and sh#2: 82%) in hippocampal neurons, whereas a control shRNA did not affect *Ocrl1* level (data not shown). We found that both shRNAs significantly reduced spine density (Figure 3A, B) without affecting spine volume. These results suggest that OCRL1 bidirectionally controls dendritic spine density in hippocampal CA1 pyramidal neurons.

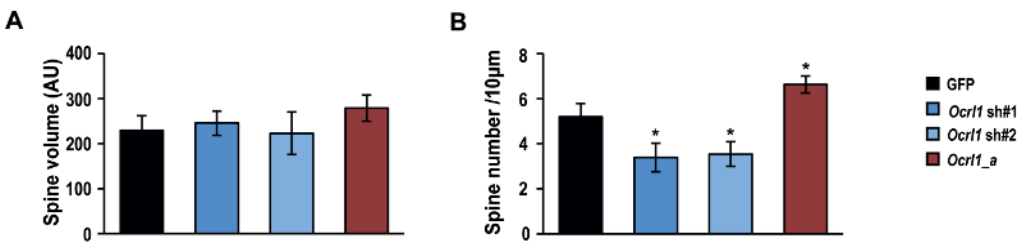

Figure 3 OCRL1 regulates spine morphology
Quantification of spine density (A), spine volume (B). A minimum of 500 spines were analyzed per condition; *P<0.05, t-test.

OCRL1 controls excitatory synaptic transmission

Due to the tight correlation of dendritic spine morphology with synaptic function, and the effects of OCRL1 in spine density, we next sought to determine whether misregulation of OCRL1 levels disrupted excitatory synaptic transmission. By recording miniature synaptic transmission (often called "minis"), which is caused by spontaneous release of single synaptic vesicle from presynaptic neurons acting on a small amount of postsynaptic receptors, we began to probe the effect of *Ocrl1* overexpression condition. Organotypic hippocampal slices were infected with *Ocrl1_a* containing lentivirus at 0 DIV. The frequency and amplitude of miniature excitatory postsynaptic current (mEPSCs) were measured at 13 DIV, a timepoint that most neurons reach mature stage. *Ocrl1_a* significantly increased mEPSC frequency in CA1 pyramidal neurons while no difference of the amplitude was detected. We next measured minis in *Ocrl1* shRNAs infected neurons. Conversely, we found that both *Ocrl1* sh#1 and sh#2 significant decreased the mEPSCs frequency without affecting the amplitude. Since altered mEPSCs frequency could be due to either changes of the presynaptic release probability or changes of the amount of functional synapses, we further examined the release probability by recording the paired-pulse ratio (PPR). We did not detect any differences of PPR between control uninfected and *Ocrl1* sh#1 infected neurons (data not shown), indicating that *Ocrl1* knocking down did not cause substantial changes of presynaptic release probability. Thus, these results support our findings of OCRL1 bidirectionally controls dendritic spine density and suggest that OCRL1 plays an important role in regulating synaptic transmission at hippocampal CA3-CA1 synapses.

To determine whether OCRL1 plays a role in controlling synaptic transmission during development, we monitored the changes of synaptic transmission at earlier stages of hippocampal development. We first recorded mEPSCs in CA1 neurons infected with *Ocrl1* sh#2 at 11 DIV. Surprisingly, we did not observe any significant changes in the frequency or the amplitude of mEPSCs in *Ocrl1* downregulated neurons compared to uninfected control neurons, suggesting that decreased level of *Ocrl1* did not influence synaptic transmission at this stage. Next, we evaluated the effects of OCRL1 in regulating synaptic function at 7 DIV. Due to extremely low amount of minis at this age, we measured evoked excitatory post-synaptic currents (eEPSCs) using whole-cell simultaneous recordings. Organotypic hippocampal slices were injected with *Ocrl1*_sh#1 containing lentivirus at 0 DIV and eEPSCs were measured simultaneously from an infected CA1 pyramidal neuron and an adjacent

control uninfected neuron at 7 DIV. Our results showed that decreased OCRL1 levels did not influence eEPSCs mediated by AMPAr (AMPAr-EPSC) or by NMDAr (NMDAr-EPSC). Together, these findings indicate that misregulating OCRL1 leads to synaptic dysfunction in mature hippocampal CA1 neurons.

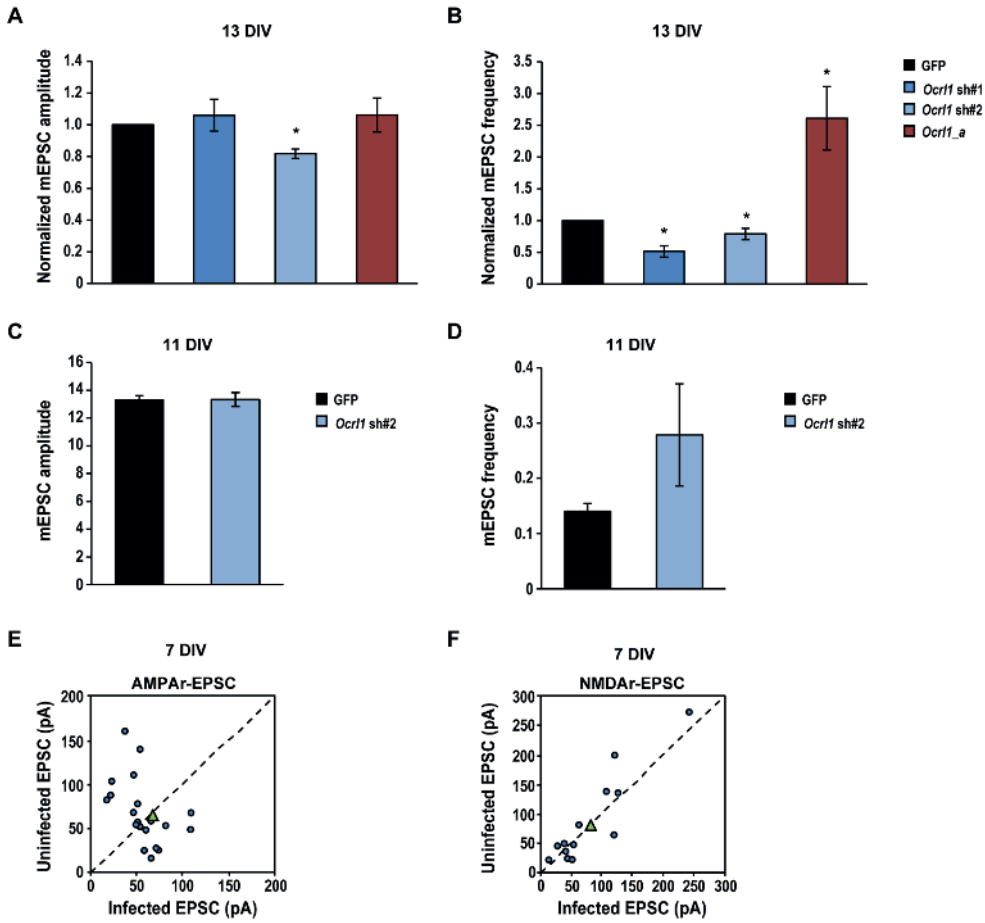

Figure 4 OCRL1 regulates synaptic transmission
(A, B) Effects of *Ocrl1* overexpression or knockdown in regulating mEPSC at 13 DIV.
(C, D) Effects of *Ocrl1* knockdown in mEPSC at 11 DIV.
(E, F) Effects of Ocrl1 knockdown in eEPSC at 7 DIV. Blue symbols represent single pairs of recordings. Green symbols show mean value.
Data are shown as mean ± SEM; **P*<0.05, t-test.

OCRL1 maintains homeostatic AMPAr expression and trafficking

Due to the presence of OCRL1 in the endocytic pathway and its role of regulating synaptic transmission, we hypothesized that OCRL1 might be critical for regulating AMPAr expression and trafficking in hippocampal CA1 neurons. To test this hypothesis, we first examined the protein levels of AMPAr GluA1 subunit in control uninfected, *Ocrl1_a* expressing and *Ocrl1* shRNAs expressing hippocampal neurons by performing Western blot analysis. We observed

a significant decrease of GluA1 levels in *Ocrl1* overexpressed neurons compared to control neurons. On the contrary, we found that reduced *Ocrl1* levels led to elevated expression of GluA1 (Figure 5). These results suggest that aberrant levels of OCRL1 disrupt homeostatic protein expression of AMPARs in the hippocampus.

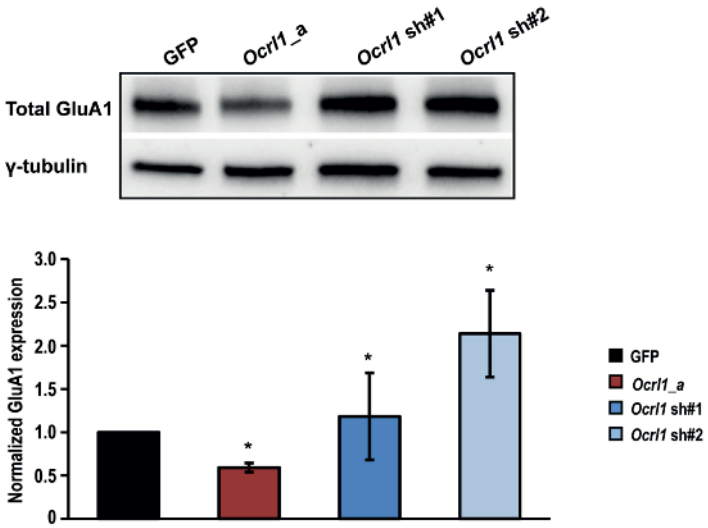

Figure 5 OCRL1 regulates cellular abundance of GluA1
Representative results and quantification of total GluA1 expression in Ocrl1 overexpression or knockdown condition. Data are shown as mean ± SEM; **P*<0.05, t-test.

To directly evaluate the endocytic process of GluA1 in *Ocrl1* knocking-down condition, we performed live-cell antibody feeding experiments on 14 DIV hippocampal neurons which were infected with *Ocrl1* shRNAs at 2 DIV. Our results showed that GluA1 endocytosis was significantly impaired in *Ocrl1* sh#2 infected neurons. *Ocrl1* sh#1 infected neurons also exhibited reduced GluA1 endocytosis, although not statistically significant (Figure 6A). Following recycling assay revealed that reduced *Ocrl1* levels did not influence AMPAr recycling (Figure 6B). In addition, we visualized surface-expressed AMPAr in *Ocrl1* downregulated neurons by using pH-sensitive GFP fused GluA1 (pHluorin-GluA1) construct [48]. Hippocampal neurons were electroporated with pHluorin-GluA1 at 0 DIV and transfected with *Ocrl1* siRNA at 18 DIV. Immunostaining of MAP2 on transfected neurons were performed at 21 DIV. We found that knocking down *Ocrl1* resulted in a significant enhancement of GFP

signal, indicating increased surface expression of GluA1 AMPAr subunit (Figure 6C). Together, these results indicate that OCRL1 plays a critical role in maintaining AMPArs homeostasis and endocytosis.

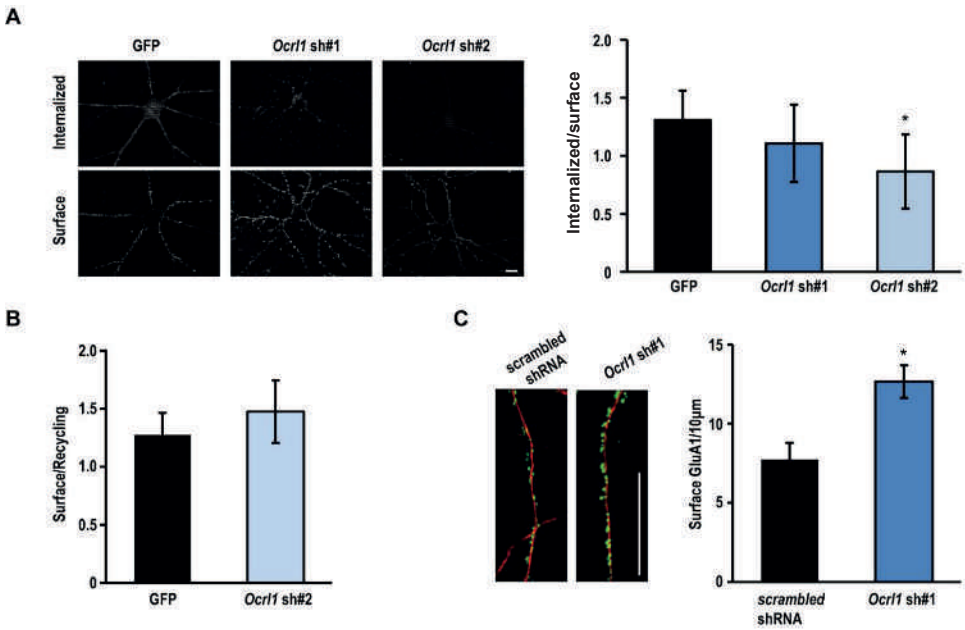

Figure 6 OCRL1 is involved in controlling AMPAr trafficking
(A) AMPA receptor endocytosis assay. Left, representative double-label images of internalized and surface AMPA receptor GluA1 subunit in low density 14 DIV hippocampal neurons in indicated experimental groups. Right, ratiometric analysis of the intensity of internalized GluA1 to surface GluA1 in indicated conditions. **P*<0.05, t-test. Scale bars, 10 µm.
(B) Ratiometric analysis of AMPAr recycling assay. The average intensity of surface GluA1 to recycled GluA1 in control and *Ocrl1* sh#2 neurons are presented.
(C) Left, representative double-label images of MAP2 (red) and surface GluA1 (green) in low density 21 DIV hippocampal neurons. Right, quantification of the amount of surface GluA1. **P*<0.05, t-test. Scale bars, 10 µm.

OCRL1 modulates synaptic plasticity in CA1

Knowing that OCRL1 loss of function results in intellectual disability, one of the symptoms of LS, and the involvement of OCRL1 in controlling synaptic structure and transmission, we reasoned that OCRL1 might also be important for synaptic plasticity. To this end, LTP was induced by using the pairing protocol in organotypic hippocampal slices infected with *Ocrl1_a* or *Ocrl1* sh#1 expressing virus at 0 DIV. Simultaneous recordings from an infected neuron and

an adjacent non-infected control neuron were performed at 6-7 DIV (Figure 7A). We first examined the effect of *Ocrl1* overexpression. Our data showed that elevated *Ocrl1* levels led to reduced magnitude of LTP (Figure 7B). We subsequently examined the effects of *Ocrl1* knocking down on both functional and structural plasticity in hippocampal CA1 neurons. Our results revealed a significant increase of LTP magnitude in *Ocrl1* downregulated neurons compared to control uninfected neurons (Figure 7C).

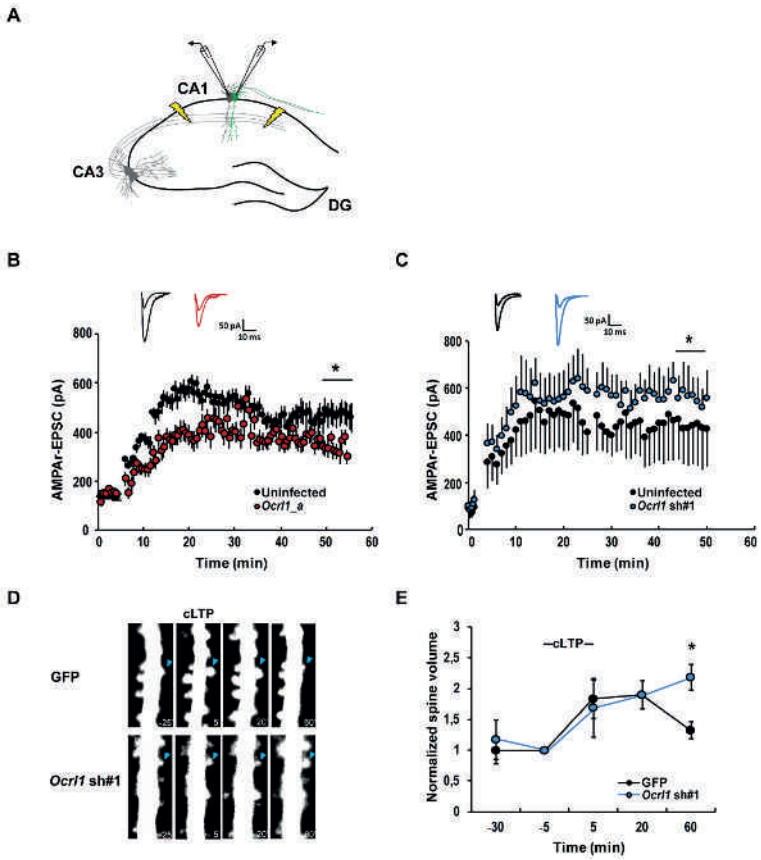

Figure 7 OCRL1 modulates synaptic plasticity

(A) Schematic figure indicating simultaneous recordings of LTP from an infected neuron and an adjacent non-infected control neuron. All experiments were performed at 6-7 DIV.

(B) Impaired LTP in neurons with elevated *Ocrl1* levels.

(C) Enhanced LTP in neurons with reduced *Ocrl1* levels.

(D, E) Sustained spine enlargement in *Ocrl1* Knocked down neurons. (D), representative images of changes in spine volume during the induction of cLTP. (E), quantification of average spine size during cLTP. **P*<0.05, t-test.

To study the effect of OCRL1 in structural plasticity, we biolistically transfected GFP or *Ocrl1* sh#1 constructs into 5 DIV hippocampal slices and used a chemical LTP (cLTP) protocol as described previously two days post-transfection [49]. Changes in spines of GFP and *Ocrl1* sh#1 transfected neurons were monitored by TPLSM. Consistent with previous studies [49], we observed a rapid and persistent spine enlargement in GFP control neurons. Also, neurons with low *Ocrl1* levels displayed similar enlarged spine size after cLTP induction. Interestingly, we observed more profound increase of spine size 60 minutes after the induction compared to GFP control neurons (Figure 7D, E).

Collectively, these data indicate that OCRL1 plays an important role in synaptic plasticity in the Schaffer collateral-CA1 pathway.

Discussion

Functional characterization of individual genes that are associated with cognitive deficits will provide valuable insights into the neuronal basis of cognition. Lots of efforts have be made to unravel the biological function of genes that are identified to be linked to ID, such as TSPAN7 and OPHN1 [19,50,51]. Lowe Syndrome, a rare monogenic disorder resulting from mutated *OCRL1* gene, affects eyes, kidney and nervous system. Despite being first described more than half a century ago, the neurological function of OCRL1 remains unclear. The ubiquitous expression pattern, the wide variety of interactors and the functional redundancy with INPP5B for OCRL1 make it challenging to unravel the molecular mechanisms underlying LS. Here, we report for the first time the role of OCRL1 in the brain at the synaptic level *in vitro*. We have provided evidence encompassing following primary points: 1) OCRL1 is present in the hippocampus and the transcript levels of *Ocrl1* are constant throughout hippocampal development; 2) elevated/reduced *Ocrl1* levels increases/decreases dendritic spine density and the frequency of mEPSCs; 3) OCRL1 modulates functional and structural LTP; 4) loss of OCRL1 impedes AMPAr endocytosis and 5) OCRL1 is essential for maintaining cellular abundance of GluA1 AMPAr subunit.

OCRL1 controls dendritic spine morphology

In the present study, we report that dendritic spine morphology is remarkably impacted by aberrant levels of OCRL1. Growing evidence suggests that changes in brain function, both normal and pathological, consistently correlate with dynamic changes in neuronal anatomy [52,53]. Focusing on dendritic spines, the highly dynamic sites where most excitatory synapses are located, we genetically manipulated *Ocrl1* levels and evaluated the effects of OCRL1 in CA1 pyramidal neurons. We observed a significant reduction in spine density when knocking down *Ocrl1* in CA1 neurons. Conversely, elevated *Ocrl1* levels led to increased spine density. These results suggest that OCRL1 is essential for maintaining normal spine density. Abnormalities in spine structure have been well documented in numerous neurological disorders including ID and ASD [54,55]. Particularly, decreased spine density in several brain regions has also been observed in patients and a mouse model of Rett Syndrome, an X-chromosomal disorder causing severe ID in females [56,57]. Therefore, impaired spinogenesis might be a primary outcome of pathogenic *OCRL1* mutations in LS patients. Subsequent lack of sufficient synaptic input on post-synaptic CA1 neurons may compromise synaptic connectivity and eventually lead to cognitive deficits in LS.

Dynamic changes and enduring stabilization of dendritic spines are intimately associated with the coordinated regulation of actin cytoskeleton [58]. Polymerization of F-actin promotes formation of dendritic spines while actin depolymerization results in spine elimination [59,60]. By interacting with a series of molecular partners, OCRL1 is involved in several signaling pathways that control the assembly and disassembly of actin cytoskeleton. Previous studies have shown that, despite a low activity, OCRL1 interacts with Rac1 and strongly inhibits Rac-dependent actin polymerization via its GAP-like domain in cell lines [33]. If this is also the case in neurons, downregulation of *Ocrl1* would promote spinogenesis instead of repressing it. It is therefore unlikely that OCRL1 controls dendritic spine density via Rac GTPase signaling. Further investigations examining whether and how OCRL1 regulates Rac signaling in neurons will test this possibility. An alternative possibility is that OCRL1 controls spine morphogenesis by manipulating synaptic lipid homeostasis via its 5-phosphatase catalytic activity. The main substrate of OCRL1, PI(4,5)P2, has been reported to facilitate actin polymerization by activating N-WASP- and Arp2/3-mediated actin branching and impairing activation of actin-severing proteins including gelsolin and cofilin/ADF [61]. Therefore, reduced spine density in *Ocrl1* downregulated neurons could be due to accumulated PIP2-induced actin

polymerization. If so, restoring PIP2 levels to physiological levels might rescue the phenotype in spine density. Inhibiting the production of PIP2 by genetically suppressing the expression of PtdIns4P 5-kinase (PIP5K), a major kinase converting PI(4)P to PI(4,5)P2, has been successfully used in *Ocrl1* depleted cells and a zebrafish model of LS [40,47]. More recently, a small molecule inhibitor of PIP5K1C, UNC3230, has been identified in a high-throughput screen. UNC3230 has been found to lower membrane PIP2 levels in dorsal root ganglia neurons and attenuate pain in animal models [62]. Thus, it would be interesting to take advantage of these genetic and pharmacological tools and examine whether the abnormal spine morphology resulting from loss of function of OCRL1 could be rescued by rebalancing PIP2 levels at the synapse. This will also provide important clue of searching for effective therapeutic targets for LS.

OCRL1 controls synaptic transmission in late hippocampal development

In line with our observations in spine morphology, we found that knocking down *Ocrl1* significantly reduced the frequencies of mEPSCs at hippocampal CA3-CA1 synapses, whereas *Ocrl1* overexpression led to the opposing effect at 13 DIV. The amplitudes of mEPSCs in both manipulations did not change. These results indicate that altered spine density in *Ocrl1* misregulated CA1 neurons leads to synaptic dysfunction.

It is worth noting that the deficient synaptic transmission was detectable only in late hippocampal development *in vitro* (13 DIV). One could speculate that a profound reduction in excitatory input caused by selective loss of OCRL1 in post-synaptic CA1 neurons might trigger a series of machineries, such as enhanced local translation of the OCRL1 homologue INPP5B, increased pre-synaptic release probability or downregulated GABAergic system, to counterbalance the excitatory dysfunction to a certain extent. These compensations, however, are not sufficient to keep correcting miswired network until late developmental stages. Future experiments are required to determine the precise mechanisms underlying these events. Alternatively, the protein levels of OCRL1 have been found to be low in embryonic and early postnatal stages and gradually increases with age (EI Demerdash and Fernandez-Monreal, personal communication), despite the constant mRNA levels of *Ocrl1* throughout development observed in our study. This raises the possibility that post-transcriptional/translational modifications might be involved to ensure precise temporal expression of OCRL1 protein in hippocampus. It could also explain our findings in the sense

that manipulating *Ocrl1* levels when endogenous OCRL1 proteins are expressed at a low level might not lead to any functional consequences. It has been unveiled that RhoGTPase signaling undergoes post-transcriptional regulations. For example, miR-124 which is enriched in developing and adult neurons suppresses Cdc42 and Rac1 expression and regulates axon growth [63]. P250GAP, a recently identified candidate gene for schizophrenia [64], has also been found to be a target of miR-132. The miR-132-p250GAP pathway is reported to be required for normal dendritic development and leptin-induced synaptogenesis [65,66]. Elucidating regulatory mechanisms for the temporal expression of OCRL1 will shed more light on the role of OCRL1 in regulating synaptic function.

OCRL1 determines the routes of AMPAr trafficking and regulates LTP

Involvement of OCRL1 in endocytic machinery has previously been proposed both in cell lines and a zebrafish model for LS [47]. Here, we specified the role of OCRL1 in controlling AMPAr amount and trafficking route in neurons. By performing AMPAr endocytosis and recycling assay, we provided direct evidence indicating that *Ocrl1* knockdown significantly impaired GluA1 endocytosis without affecting recycling process. Making use of pH-sensitive GFP fused GluA1 construct, we observed enhanced surface GluA1 signal in *Ocrl1* depleted neurons compared to control neurons. Together with unaltered amplitude of mEPSCs, these results suggest that lacking of *Ocrl1* leads to impaired AMPAr endocytosis and subsequent accumulation of excess AMPArs at extrasynaptic sites. Moreover, we detected elevated total amount of GluA1 protein in *Ocrl1* downregulated neurons and decreased GluA1 protein levels in neurons overexpressed *Ocrl1*, suggesting that OCRL1 is critical for neurons to maintain proper levels of AMPAr. It has been demonstrated that, after being internalized via clathrin-mediated endocytosis, AMPArs are either sorted into recycling pathway back to the cell surface or transported to late endosomes and retained for degradation in lysosomes [67,68]. Therefore, our initial findings reveal an interesting scenario, in which loss of OCRL1 causing a "traffic jam" on the "membrane-endosome-lysosome" highway results in disrupted dynamic equilibrium of AMPArs in neurons.

Previous studies have shown that OCRL1 directly interacts with the key components of endocytosis, clathrin and adaptor protein 2 (AP2) [26], and loss of OCRL1 causes deficits in clathrin-mediated endocytosis in fibroblasts of LS patients [41]. It is therefore not surprising that AMPAr endocytosis, which is largely dependent on clathrin, is impaired in *Ocrl1* lacking

neurons. Apart from its direct interaction with clathrin and AP2, OCRL1 might impact clathrin-mediated endocytic process via indirect manipulation of PI(4,5)P2 levels. By binding to PI(4,5)P2, AP2 is recruited to the plasma membrane and subsequently initiates formation of clathrin-coated pit (CCP). Besides, the release of AP2 from CCP in the uncoating stage of clathrin-mediated endocytosis is in a PI(4,5)P2-dependent manner. Consistently, two other 5-phosphatases, Synaptojanin and SHIP2 have also been reported to control clathrin-mediated endocytosis [69,70]. Future experiments will have to determine the precise mechanisms of how the clathrin-bind boxes and catalytic domain of OCRL1 interact and control clathrin-mediated endocytosis in neurons. In general, the ratio of synthesis and degradation eventually determines global protein expression. The late-endosomal and lysosomal localization of OCRL1 in cell lines highlight the possibility that OCRL1 plays an essential role for proper clearance of proteins, including AMPArs in lysosome and for maintenance of optimal protein concentrations required for normal cellular function. Accumulation of non-degraded molecules resulting from lysosomal dysfunction has been reported to cause lysosomal storage diseases, which lead to multisystem manifestation such as bony abnormalities, ophthalmologic signs and intellectual disability [71]. It would be interesting to examine whether general protein homeostasis is disrupted due to misregulated *Ocrl1* levels and whether this disruption partially accounts for the pathology of LS.

Another important finding in the present study is that knocking down *Ocrl1* increased the magnitude of LTP whereas *Ocrl1* overexpression exhibited the opposing effect. Although remaining controversial, both lateral movement and exocytosis of AMPArs have been shown to contribute to LTP [8,72–77]. It is likely that lateral diffusion of AMPArs from nonsynaptic sites enhances synaptic strength while exocytosis replenishes the extrasynaptic pool of AMPArs during LTP [8]. In *Ocrl1* lacking neurons, on one hand, elevated surface accumulation enlarging extrasynaptic AMPAr pool might facilitate lateral diffusion in response to LTP-induction, on the other hand, increased AMPArs levels might subsequently increase the size of intracellular reserve pool of AMPArs and indirectly promotes LTP. Future experiments will have to determine the precise mechanisms of OCRL1 in controlling synaptic plasticity.

Materials and Methods

Animals

Wistar rats were housed per 2 or 3 animals on a 12-h light cycle in a temperature-controlled (21 ± 1°C) environment with ad libitum access to food and water. Rats were sacrificed at E17, P3, P10, P17, P24 and P90 (adult). The hippocampus and cortex were dissected out and snap-frozen in liquid nitrogen. All samples were stored at -80°C for further analysis. All experiments involving animals were evaluated and approved by the Committee for Animal Experiments of the Radboud university medical center, Nijmegen, the Netherlands.

RNA isolation, reverse transcription and qPCR

Total RNA from the tissue was isolated using *RNeasy Lipid Tissue mini kit* (Qiagen). cDNA was synthesized from 0.5–1 mg RNA using iScript™ cDNA Synthesis Kit. QPCR experiments were subsequently performed in 7900HT Fast Real-Time PCR System using GoTaq qPCR Master mix (Promega).

Immunofluorenscence

For hippocampal slices from postnatal days 20 rats, brains were fixed, embedded in low melting agarose (3%) and then being sectioned into 60 µm sections using a microtome (Leica VT-1000S). Free-floating sections or fixed organotypic slices were incubated overnight with blocking buffer containing 5% normal goat serum (Invitrogen), 5% normal donkey serum (Sigma), 5% horse serum (Sigma), 1% glycine (Sigma), 1% lysine (Sigma) and 0.4% Triton X-100, permeabilized, and incubated overnight with custom anti-OCRL1 and anti-NeuN (ABN91, Millipore) primary antibodies, followed by incubation with Alexa-488 or Alexa-568 conjugated secondary antibody (Invitrogen) in blocking buffer. Sections were mounted onto slides with fluorescence mounting medium containing 406-diamidion-2-phenylindole (Dako, Carpinteria, California, USA).

Western blotting

Rat hippocampal tissue or cell culture were collected and homogenized in ice-cold RIPA buffer. Lysates were then heated at 95°C for 10 min. Equal amounts of protein samples (50 µg) were fractionated on 4%-15% precast SDS-PAGE gels (Bio-Rad) then blotted to nitrocellulose membrane (Bio-Rad). Membranes were subsequently incubated for 1h at room temperature

in 5% milk in PBS-Tween to prevent non-specific binding. Primary antibodies used were: anti-GluA1 (Millipore) or anti- Y-TUBULIN (Sigma) as loading control. Secondary antibodies used were: goat anti-mouse HRP (Jackson Immuno Research Laboratories) and goat anti-rabbit (Invitrogen). Images were acquired with ChemiDoc^{TM} imaging system (Bio-Rad).

Two-photon laser scanning microscopy

Hippocampal slices were biolistically transfected at 12 DIV with indicated constructs and neurons were imaged 2 days after transfection. Experiments were performed at 30°C in physiological ACSF (119 mM NaCl, 26 mM $NaHCO_3$, 1 mM NaH_2PO_4, 11 mM D-glucose, 2.5 mM KCl, 2 mM $CaCl_2$, 1 mM $MgCl_2$, and 1.25 mM $NaHPO_4$) gassed with 5% CO_2 and 95% O_2. Before TPLSM imaging, transfected/infected CA1 pyramidal neurons were identified by epifluorescence illumination. High-resolution three-dimensional image stacks were collected on a laser-scanning microscope (Leica TCS SP5). The light source was a mode-locked Ti:sapphire laser (Coherent Chameleon, USA) running at 910 nm. We used an Olympus 20X1.0 numerical aperture objective. Each optical section was resampled three times and was captured every 0.5 µm. Images were taken from regions on apical dendrites, which were typically about 100 µm away from the soma and covered 150-200 µm in length. A minimum of 500 spines were analyzed per condition for all comparative studies, sister cultures were used. For the chemical LTP experiments, slices were incubated with Mg^{2+} free ACSF containing forskolin and rolipram. Images were taken at indicated time points for the same regions of interest (ROIs).

TPLSM Image display

All images displayed are data from consecutive stacks displayed using a maximum value projection. At any given *x-y* coordinate, the maximum pixel value in that Z- column is displayed in the two-dimensional image. Image analysis was conducted on raw data using full Z-stacks as discussed below.

TPLSM Quantitative image analysis

Spines were analyzed using custom software written in MatLab. All analyses were conducted blind to the constructs being expressed. For each experiment, projection images of 40-60

consecutive z-series sections were generated for each cell or each time point.

For spine density and volume experiments spines were identified using green fluorescence channel and rectangular ROIs were manually positioned to fully cover each spine. Spine density was calculated as the number of manually counted spines divided by dendrite segment length. Background-subtracted integrated fluorescence was taken as a measure for spine volume after normalizing to mean fluorescence at soma and large apical dendrite. No effort was made to analyze spines emerging below or above the dendrite, because the TPLSM resolution of these is compromised. It is also possible that many small structures were not detected, although point spread function limited structures were observed. Spine density and size values were compared using an unpaired two-tailed Student's t- test. Significance was set at $p < 0.05$.

Electrophysiology

Whole-cell recordings in organotypic slices were obtained with Multiclamp 700B amplifiers (Axon Instruments). The recording chamber was perfused with artificial cerebrospinal fluid (ACSF) containing 119 mM NaCl, 2.5 mM KCl, 4 mM $CaCl_2$, 4 mM $MgCl_2$, 26 mM $NaHCO_3$, 1 mM NaH_2PO_4, 11 mM glucose, 0.1 mM picrotoxin, 4 µM 2-chloroadenosine (pH 7.4), and gassed with 5% CO_2/95% O_2. Recordings were made at 30°C. Patch recording pipettes (4–7 MΩ) were filled with intracellular solution containing 115 mM cesium methanesulfonate, 20 mM CsCl, 10 mM HEPES, 2.5 mM $MgCl_2$, 4 mM Na_2ATP, 0.4 mM Na_3GTP, 10 mM sodium phosphocreatine, and 0.6 mM EGTA (pH 7.25, Osm 285-295). Evoked responses were induced using bipolar electrodes (FHC) placed on Schaffer collateral pathway (0.1 Hz). Responses were recorded at both -60 mV (for AMPAr-mediated responses) and +40 mV (for NMDAr-mediated responses). NMDAr-mediated responses were quantified as the mean between 60 and 65 ms after stimulation. All data are reported as mean ± SEM. Statistical significance was determined by the paired Student's t-test (for paired recordings).

Miniature post-synaptic excitatory currents (mEPSCs) on organotypic slices were recorded at -60 mV in ACSF containing 2 mM $CaCl_2$ and 1 mM $MgCl_2$ at 32°C in the presence of 1 µM TTX and 0.1 mM picrotoxin. 10 min of recordings from each cell were acquired at 5 kHz, filtered at 2 kHz and analyzed using Mini Analysis Program (Synaptosoft).

LTP was induced with a pairing protocol: postsynaptic depolarization at 0mV was paired with synaptic stimulation (3 Hz for 90 s). Whole-cell recordings were obtained simultaneously from an infected and an adjacent uninfected neuron in the CA1 region under visual guidance, using epifluorescence and transmitted light illumination.

AMPA receptor trafficking assay

For AMPAr endocytosis assay, living primary hippocampal neurons were first labeled with anti-GluA1 antibody (Millipore). Internalization of the labeled GluA1 subunits was then allowed for 2 hours at 37°C. After fixation with 4% paraformaldehyde and blocking with 5% BSA, surface-labeled GluA1 subunits were exposed to Alexa-568 secondary antibody (Invitrogen). After washing, the remaining surface GluA1 subunits were incubated with unlabeled secondary antibody at a concentration of 0.13 mg/ml overnight to saturate surface anti-GluA1 antibodies. Neurons were then permeabilized and incubated with Alexa-647 secondary antibody to label internalized GluA1 subunits. GluA1 endocytosis was calculated by dividing the intensity of internalized GluA1 by the intensity of surface GluA1 using imageJ (I_{647}/I_{568}).

For AMPAr recycling assay, living primary hippocampal neurons were first incubated with Leupeptin for 30 min at 37 °C, followed by labelling with anti-GluA1 antibody (Millipore) at 10°C for 20 min. Neurons were then incubated for 30 min at 37°C to allow internalization. The remaining surface GluA1 proteins were saturated with unlabelled secondary antibody. Neurons were then incubated for additional 30 min at 37°C to allow recycling of internalized GluA1 subunits. After fixation with 4% paraformaldehyde and blocking with 5% BSA, surface-labeled GluA1 subunits were exposed to Alexa-568 secondary antibody (Invitrogen). Neurons were then permeablized and incubated with Alexa-647 secondary antibody to label internalized GluA1 subunits. GluA1 recycling was calculated by dividing the intensity of surface GluA1 by the intensity of internalized GluA1 using imageJ (I_{568}/I_{647}).

References

1. Kochinke, K. *et al.* Systematic Phenomics Analysis Deconvolutes Genes Mutated in Intellectual Disability into Biologically Coherent Modules. *Am. J. Hum. Genet.* **98,** 149–164 (2016).
2. Ba, W., van der Raadt, J. & Nadif Kasri, N. Rho GTPase signaling at the synapse: Implications for intellectual disability. *Exp. Cell Res.* **319,** 2368–2374 (2013).
3. Nadif Kasri, N. & Van Aelst, L. Rho-linked genes and neurological disorders. *Pflugers Arch.* **455,** 787–97 (2008).
4. Tolias, K. F., Duman, J. G. & Um, K. Control of synapse development and plasticity by Rho GTPase regulatory proteins. *Prog. Neurobiol.* **94,** 133–148 (2011).
5. Derkach, V. a, Oh, M. C., Guire, E. S. & Soderling, T. R. Regulatory mechanisms of AMPA receptors in synaptic plasticity. *Nat. Rev. Neurosci.* **8,** 101–13 (2007).
6. Henley, J. M., Barker, E. a & Glebov, O. O. Routes, destinations and delays: recent advances in AMPA receptor trafficking. *Trends Neurosci.* **34,** 258–68 (2011).
7. Park, M., Penick, E. C., Edwards, J. G., Kauer, J. a & Ehlers, M. D. Recycling endosomes supply AMPA receptors for LTP. *Science* **305,** 1972–5 (2004).
8. Makino, H. & Malinow, R. AMPA receptor incorporation into synapses during LTP: the role of lateral movement and exocytosis. *Neuron* **64,** 381–90 (2009).
9. Anggono, V. & Huganir, R. L. Regulation of AMPA receptor trafficking and synaptic plasticity. *Curr. Opin. Neurobiol.* **22,** 461–9 (2012).
10. Poste, G. & Allison, a C. Membrane fusion. *Biochim. Biophys. Acta* **300,** 421–465 (1973).
11. Liscovitch, M. & Cantley, L. C. Signal transduction and membrane traffic: the PITP/phosphoinositide connection. *Cell* **81,** 659–662 (1995).
12. Ueda, Y. & Hayashi, Y. PIP_3 regulates spinule formation in dendritic spines during structural long-term potentiation. *J. Neurosci.* **33,** 11040–7 (2013).
13. Sasaki, J. *et al.* The PtdIns(3,4)P(2) phosphatase INPP4A is a suppressor of excitotoxic neuronal death. *Nature* **465,** 497–501 (2010).
14. Arendt, K. L. *et al.* PIP3 controls synaptic function by maintaining AMPA receptor clustering at the postsynaptic membrane. *Nat. Neurosci.* **13,** 36–44 (2010).
15. Govek, E., Newey, S. E. & Aelst, L. Van. The role of the Rho GTPases in neuronal development The role of the Rho GTPases in neuronal development. *Genes Dev.* **19,** 1–49 (2005).
16. Scotto-Lomassese, S. *et al.* Fragile X mental retardation protein regulates new neuron differentiation in the adult olfactory bulb. *J. Neurosci.* **31,** 2205–15 (2011).
17. Myers, K. R. *et al.* Arf6-GEF BRAG1 regulates JNK-mediated synaptic removal of GluA1-containing AMPA receptors: a new mechanism for nonsyndromic X-linked mental disorder. *J. Neurosci.* **32,** 11716–26 (2012).
18. Kutsche, K. *et al.* Mutations in ARHGEF6, encoding a guanine nucleotide exchange factor for Rho GTPases, in patients with X-linked mental retardation. *Nat. Genet.* **26,** 247–50 (2000).
19. Bassani, S. *et al.* The X-linked intellectual disability protein TSPAN7 regulates excitatory synapse development and AMPAR trafficking. *Neuron* **73,** 1143–58 (2012).
20. Hoopes, R. R. *et al.* Dent Disease with mutations in OCRL1. *Am. J. Hum. Genet.* **76,** 260–267 (2005).
21. Bökenkamp, A. *et al.* Dent-2 Disease: A Mild Variant of Lowe Syndrome. *J. Pediatr.* **155,** 94–99 (2009).
22. Lowe, M. Structure and function of the Lowe syndrome protein OCRL1. *Traffic* **6,** 711–9 (2005).
23. Dressman, M. a, Olivos-Glander, I. M., Nussbaum, R. L. & Suchy, S. F. Ocrl1, a PtdIns(4,5)P(2) 5-phosphatase, is localized to the trans-Golgi network of fibroblasts and epithelial cells. *J. Histochem. Cytochem.* **48,** 179–190 (2000).
24. Noakes, C. J., Lee, G. & Lowe, M. The PH domain proteins IPIP27A and B link OCRL1 to receptor recycling in the endocytic pathway. *Mol. Biol. Cell* **22,** 606–623 (2011).
25. Erdmann, K. S. *et al.* A Role of the Lowe Syndrome Protein OCRL in Early Steps of the Endocytic

Pathway. *Dev. Cell* **13,** 377–390 (2007).
26. Choudhury, R. *et al.* Lowe Syndrome Protein OCRL1 Interacts with Clathrin and Regulates Protein Trafficking between Endosomes and the Trans-Golgi Network □. **16,** 3467–3479 (2005).
27. Johnson, J. M. *et al.* Genome-wide survey of human alternative pre-mRNA splicing with exon junction microarrays. *Science* **302,** 2141–2144 (2003).
28. Kawano, T., Indo, Y., Nakazato, H., Shimadzu, M. & Matsuda, I. Oculocerebrorenal syndrome of Lowe: Three mutations in the OCRL1 gene derived from three patients with different phenotypes. *Am. J. Med. Genet.* **77,** 348–355 (1998).
29. Utsch, B. *et al.* Novel OCRL1 Mutations in Patients With the Phenotype of Dent Disease. *Am. J. Kidney Dis.* **48,** 942–954 (2006).
30. Sethi, S. K. *et al.* Mutations in OCRL1 gene in Indian children with Lowe syndrome. *Clin. Exp. Nephrol.* **12,** 358–362 (2008).
31. Leahey, A., Charnas, L. R. & Nussbaum, R. L. Nonsense mutations in the OCRL-1 gene in patients with the oculocerebrorenal syndrome of Lowe. **2,** 461–463 (1993).
32. Hichri, H. *et al.* From lowe syndrome to Dent disease: Correlations between mutations of the OCRL1 gene and clinical and biochemical phenotypes. *Hum. Mutat.* **32,** 379–388 (2011).
33. Faucherre, A. *et al.* Lowe syndrome protein OCRL1 interacts with Rac GTPase in the trans-Golgi network. *Hum. Mol. Genet.* **12,** 2449–2456 (2003).
34. Cremona, O. & De Camilli, P. Phosphoinositides in membrane traffic at the synapse. *J. Cell Sci.* **114,** 1041–1052 (2001).
35. Takenawa, T. & Itoh, T. Phosphoinositides, key molecules for regulation of actin cytoskeletal organization and membrane traffic from the plasma membrane. *Biochim. Biophys. Acta - Mol. Cell Biol. Lipids* **1533,** 190–206 (2001).
36. Di Paolo, G. & De Camilli, P. Phosphoinositides in cell regulation and membrane dynamics. *Nature* **443,** 651–657 (2006).
37. Zhang, X., Jefferson, a B., Auethavekiat, V. & Majerus, P. W. The protein deficient in Lowe syndrome is a phosphatidylinositol-4,5-bisphosphate 5-phosphatase. *Proc. Natl. Acad. Sci. U. S. A.* **92,** 4853–4856 (1995).
38. Attree, O. *et al.* The Lowe's oculocerebrorenal syndrome gene encodes a protein highly homologous to inositol polyphosphate-5-phosphatase. *Nature* **358,** 239–242 (1992).
39. Zhang, X., Hartz, P. a., Philip, E., Racusen, L. C. & Majerus, P. W. Cell lines from kidney proximal tubules of a patient with Lowe syndrome lack OCRL inositol polyphosphate 5-phosphatase and accumulate phosphatidylinositol 4,5-bisphosphate. *J. Biol. Chem.* **273,** 1574–1582 (1998).
40. Vicinanza, M. *et al.* OCRL controls trafficking through early endosomes via PtdIns4,5P2-dependent regulation of endosomal actin. *EMBO J.* **30,** 4970–4985 (2011).
41. Nandez, R. *et al.* A role of OCRL in clathrin-coated pit dynamics and uncoating revealed by studies of Lowe syndrome cells. *Elife (Cambridge)* **3,** e02975 (2014).
42. Jefferson, a B. & Majerus, P. W. Mutation of the conserved domains of two inositol polyphosphate 5-phosphatases. *Biochemistry* **35,** 7890–7894 (1996).
43. Jefferson, A. B. & Majerus, P. W. Properties of Tpye II Inositol Polyphosphate 5-Phosphatase. (1995).
44. Jänne, P. a. *et al.* Functional overlap between murine Inpp5b and Ocrl1 may explain why deficiency of the murine ortholog for OCRL1 does not cause Lowe syndrome in mice. *J. Clin. Invest.* **101,** 2042–2053 (1998).
45. Bothwell, S. P. *et al.* Mouse model for Lowe syndrome/Dent Disease 2 renal tubulopathy. *J. Am. Soc. Nephrol.* **22,** 443–448 (2011).
46. Ramirez, I. B. R. *et al.* Impaired neural development in a zebrafish model for lowe syndrome. *Hum. Mol. Genet.* **21,** 1744–1759 (2012).
47. Oltrabella, F. *et al.* The Lowe Syndrome Protein OCRL1 Is Required for Endocytosis in the Zebrafish Pronephric Tubule. *PLOS Genet.* **11,** e1005058 (2015).
48. Ashby, M. C. Removal of AMPA Receptors (AMPARs) from Synapses Is Preceded by Transient

Endocytosis of Extrasynaptic AMPARs. *J. Neurosci.* **24,** 5172–5176 (2004).
49. Kopec, C., Li, B., Wei, W., Boehm, J. & Malinow, R. Glutamate receptor exocytosis and spine enlargement during chemically induced long-term potentiation. *J. Neurosci.* **26,** 2000–2009 (2006).
50. Nakano-Kobayashi, A., Nadif Kasri, N., Newey, S. E. & Van Aelst, L. The Rho-linked Mental Retardation Protein OPHN1 Controls Synaptic Vesicle Endocytosis Via Endophilin A1. **19,** 1133–1139 (2009).
51. Nadif Kasri, N., Nakano-Kobayashi, A. & Van Aelst, L. Rapid synthesis of the X-linked mental retardation protein OPHN1 mediates mGluR-dependent LTD through interaction with the endocytic machinery. *Neuron* **72,** 300–15 (2011).
52. Engert, F. & Bonhoeffer, T. Dendritic spine changes associated with hippocampal long-term synaptic plasticity. *Nature* **399,** 66–70 (1999).
53. Kopec, C. & Malinow, R. Matters of Size. **314,** 8–10 (2006).
54. Fiala, J. C., Spacek, J. & Harris, K. M. Dendritic spine pathology: cause or consequence of neurological disorders? *Brain Res. Brain Res. Rev.* **39,** 29–54 (2002).
55. Penzes, P., Cahill, M. E., Jones, K. a, VanLeeuwen, J.-E. & Woolfrey, K. M. Dendritic spine pathology in neuropsychiatric disorders. *Nat. Neurosci.* **14,** 285–293 (2011).
56. Chapleau, C. a. *et al.* Dendritic spine pathologies in hippocampal pyramidal neurons from Rett syndrome brain and after expression of Rett-associated MECP2 mutations. *Neurobiol. Dis.* **35,** 219–233 (2009).
57. Chapleau, C. *et al.* Hippocampal CA1 pyramidal neurons of Mecp2 mutant mice show a dendritic spine phenotype only in the presymptomatic stage. *Neural Plast.* **2012,** 976164 (2012).
58. Hoogenraad, C. C. & Akhmanova, A. Dendritic spine plasticity: new regulatory roles of dynamic microtubules. *Neuroscientist* **16,** 650–61 (2010).
59. Okamoto, K.-I., Nagai, T., Miyawaki, A. & Hayashi, Y. Rapid and persistent modulation of actin dynamics regulates postsynaptic reorganization underlying bidirectional plasticity. *Nat. Neurosci.* **7,** 1104–12 (2004).
60. Fischer, M., Kaech, S., Knutti, D. & Matus, A. Rapid actin-based plasticity in dendritic spines. *Neuron* **20,** 847–854 (1998).
61. Yin, H. L. & Janmey, P. A. PHOSPHOINOSITIDE REGULATION OF THE ACTIN CYTOSKELETON. *Annu. Rev. Neurosci.* **26,** 701–728 (2003).
62. Wright, B. D. *et al.* The lipid kinase PIP5K1C regulates pain signaling and sensitization. *Neuron* **82,** 836–47 (2014).
63. Yu, J.-Y., Chung, K.-H., Deo, M., Thompson, R. C. & Turner, D. L. MicroRNA miR-124 regulates neurite outgrowth during neuronal differentiation. *Exp. Cell Res.* **314,** 2618–2633 (2008).
64. Ohi, K. *et al.* The p250GAP gene is associated with risk for schizophrenia and schizotypal personality traits. *PLoS One* **7,** e35696 (2012).
65. Wayman, G. a *et al.* An activity-regulated microRNA controls dendritic plasticity by down-regulating p250GAP. *Proc. Natl. Acad. Sci. U. S. A.* **105,** 9093–9098 (2008).
66. Dhar, M. *et al.* Leptin Induces Hippocampal Synaptogenesis via CREB-Regulated MicroRNA-132 Suppression of p250GAP. *Mol. Endocrinol.* **28,** 1073–87 (2014).
67. Fernandez-Monreal, M., Brown, T. C., Royo, M. & Esteban, J. a. The Balance between Receptor Recycling and Trafficking toward Lysosomes Determines Synaptic Strength during Long-Term Depression. *J. Neurosci.* **32,** 13200–13205 (2012).
68. Brown, T. C., Correia, S. S., Petrok, C. N. & Esteban, J. a. Functional compartmentalization of endosomal trafficking for the synaptic delivery of AMPA receptors during long-term potentiation. *J. Neurosci.* **27,** 13311–13315 (2007).
69. Rusk, N., Le, P. U. & Symons, M. Synaptojanin 2 Functions at an Early Step of Clathrin-Mediated Endocytosis. *Curr. Biol.* **13,** 659–663 (2003).
70. Malecz, N. *et al.* Synaptojanin 2, a novel Rac1 effector that regulates clathrin-mediated endocytosis. *Curr. Biol.* **10,** 1383–1386 (2000).

71. Kaye, E. M. Lysosomal storage diseases. *Curr. Treat. Options Neurol.* **3,** 249–256 (2001).
72. Borgdorff, A. J. & Choquet, D. Regulation of AMPA receptor lateral movements. *Nature* **417,** 649–653 (2002).
73. Chen, L. *et al.* Stargazin regulates synaptic targeting of AMPA receptors by two distinct mechanisms. *Nature* **408,** 936–43 (2000).
74. Park, M. *et al.* Plasticity-Induced Growth of Dendritic Spines by Exocytic Trafficking from Recycling Endosomes. *Neuron* **52,** 817–830 (2006).
75. Oh, M. C., Derkach, V. A., Guire, E. S. & Soderling, T. R. Extrasynaptic Membrane Trafficking Regulated by GluR1 Serine 845 Phosphorylation Primes AMPA Receptors for Long-term Potentiation. *J. Biol. Chem.* **281,** 752–758 (2006).
76. Wang, Z. *et al.* Myosin Vb Mobilizes Recycling Endosomes and AMPA Receptors for Postsynaptic Plasticity. *Cell* **135,** 535–548 (2008).
77. Yang, Y., Wang, X.-B., Frerking, M. & Zhou, Q. Delivery of AMPA receptors to perisynaptic sites precedes the full expression of long-term potentiation. *Proc. Natl. Acad. Sci. U. S. A.* **105,** 11388–93 (2008).

Chapter 6

Involvement of the kinesin family members *KIF4A* and *KIF5C* in intellectual disability and synaptic function

Marjolein H. Willemsen[*], Wei Ba[*], Willemijn M. Wissink-Lindhout, Arjan P.M. de Brouwer,Stefan A. Haas, Melanie Bienek, Hao Hu, Lisenka E.L.M. Vissers, Hans van Bokhoven, Vera Kalscheuer, Nael Nadif Kasri[#], and Tjitske Kleefstra[#]

* Co-first author
\# Co-last author

Published in:
Journal of Medical Genetics. 2014 57:487-494

Abstract

Kinesin superfamily *(KIF)* genes encode motor proteins that have fundamental roles in brain functioning, development, survival and plasticity by regulating the transport of cargo along microtubules within axons, dendrites and synapses. Mouse knock out studies support these important functions in the nervous system. The role of *KIF* genes in intellectual disability (ID) has so far only received limited attention, although previous studies have suggested that many ID genes impinge on synaptic function.

By applying next generation sequencing (NGS) in ID patients, we identified likely pathogenic mutations in two members of the *KIF* gene family, *KIF4A* and *KIF5C*, suggesting that these genes may be novel players in ID.

Four males from a single family with a disruptive mutation in the X-linked *KIF4A* (c.1489-8_1490delins10; p.?- exon skipping) showed mild to moderate ID and epilepsy, whereas a female patient with a *de novo* missense mutation in *KIF5C* (c.11465A>C; p.(Glu237Lys)) presented with severe ID, epilepsy, microcephaly and cortical malformation. Of interest, very recently in a family with Malformations of Cortical Development (MCD) a missense mutation in *KIF5C* was reported, further confirming a role of this gene in brain development. We found further supporting evidence for the causality of the present mutations by showing that knock-down of *Kif4a* in rat primary hippocampal neurons altered the balance between excitatory and inhibitory synaptic transmission, whereas the mutation in *Kif5c* affected its protein function at excitatory synapses. Our results suggest that mutations in *KIF4A* and *KIF5C* cause ID by tipping the balance between excitatory and inhibitory synaptic excitability.

Introduction

Kinesin superfamily proteins (KIFs) are motor proteins involved in the movement of various cargoes along the microtubules, including vesicles, organelles, protein complexes, mRNAs and chromosomes [1–4]. KIF proteins act together with motor proteins from the dynein and myosin superfamilies. These molecular motors are expected to have fundamental roles in several processes in the brain, including neuronal functioning, development, survival and plasticity, by regulating the anterograde and retrograde transport within the axons, dendrites and synapses of neurons [1–4]. Studies in mouse models support these essential functions of *KIF* genes in the development and functioning of the nervous system. Mice with homozygous knockout mutations in *Kif1a, 1b, 2a, 3a, 3b, 4a, 5a* and *5b* show various neurological phenotypes including structural brain anomalies, decreased brain size, loss of neurons, reduced rate of neuronal apoptosis and perinatal lethality due to neurological problems [4–12]. The embryonic lethality of knockout mice for *Kif2a, Kif3a* and *3b*, and *Kif5b* suggest that these *Kif* genes have an important function in general developmental processes as well [5,7,8,13]. Overexpression of *Kif17* in mice resulted in enhanced spatial learning [14]. Conditional knockout of *KIF5A* in mice led to epileptic phenotypes [15].

Several KIF genes have previously been implicated in the pathogenesis of neurodegenerative and neurodevelopmental disorders in humans. (**Table 1**)

Table 1 *KIF* genes implicated in neurodegenerative and neurodevelopmental diseases in humans.

KIF gene	Disease	Inheritance	Reference
KIF1A (MIM 601255)	Hereditary spastic paraplegia type 30 (MIM 610358) Hereditary sensory neuropathy, type IIC (MIM 614213) Non-syndromic ID	AR AR AD	([4], [16], [17])
KIF1B (MIM 605995)	Charcot-Marie-Tooth disease , type 2A1 (MIM 118210) Multiple Sclerosis (MIM 126200)	AD Susceptibility locus	([11,18])
KIF2A (MIM 602591)	Malformations of Cortical Development (MCD)	AD	([19])
KIF5A (MIM 602821)	Hereditary spastic paraplegia type 10 (MIM 604187)	AD	([4,20])
KIF5C (MIM 604593)	Malformations of Cortical Development (MCD)	AD	([19])
KIF7 (MIM 611254)	Acrocallosal syndrome (MIM 200990) Hydrolethalus syndrome (MIM 614120) Joubert syndrome 12 (MIM 200990) Syndromic ID	AR AR AR AR	([21–23])
KIF11 (MIM 148760)	Microcephaly with or without chorioretinopathy, lymphedema, or mental retardation (MIM 152950)	AD	([24])
KIF21A (MIM 608283)	Congenital opthalmoplegia (MIM 135700)	AD	([25])

AR: autosomal recessive; AD: autosomal dominant

Only a handful of previous reports relate mutations in *KIF* genes to intellectual disability (ID). Putoux *et al.* identified homozygous mutations in *KIF7* (MIM 611254) in patients with acrocallosal syndrome (MIM 200990) and hydrolethalus syndrome (MIM 614120) [21] and homozygous mutations in the same gene were also found in patients with Joubert syndrome 12 (MIM 200990) [22]. In these ciliary disorders ID is part of the phenotype. Najmabadi *et al.* identified a homozygous missense mutation in *KIF7* by targeted sequencing of exons from homozygous linkage intervals in a consanguineous family with ID, clubfeet, cataract, hearing

loss and midface hypoplasia [23]. More recently, the first dominant *de novo* missense mutation in a *KIF* gene (*KIF1A*) was found in a patient with non-syndromic ID [17]. Very recently, Poirier *et al.* reported the identification of mutations in *KIF2A* and *KIF5C* in patients with Malformations of Cortical Development (MCD). These patients presented with ID as well [19].

Here we report the identification of mutations in *KIF4A* (MIM 300521) and *KIF5C* (MIM 604593) in an X-linked ID family, presenting with mild to moderate ID and epilepsy, and in a sporadic patient with severe ID, microcephaly, epilepsy and cortical malformation, respectively. In addition, we studied the effects on synaptic function of these *KIF* genes using a knockdown system in rat primary neurons.

Results

Clinical description patients

Family 1

We searched for the causative mutation in a family (family 1) with five affected males in different generations (Fig. 1), suggesting X-linked recessive inheritance. The patients presented with mild to moderate ID, were able to speak simple sentences and lived and worked in sheltered places. Four of the five individuals had epilepsy that manifested at later childhood or adolescent age and comprised complex partial and generalized seizures (both absences and tonic-clonic seizures). Head circumferences were small to low-normal (0.6th-10th centile). Facial dysmorphisms were mild and non-specific. A CT-scan of the brain in two of the probands (III:7 at age 53 years and IV:3 at age 7 years) had shown central atrophy of both lateral hemispheres and wide posterior horns, respectively. Previous genetic investigations in this family included conventional karyotyping, genome-wide array analysis by the 2.7M Affymetrix array platform, DNA analysis of *FMR1* (MIM 309550) and *ARX* (MIM 300382), and a metabolic screen. The results did not provide an explanation for their phenotype. Linkage analysis, based on an X-linked recessive inheritance pattern with complete penetrance, indicated two intervals with a LOD-score of 1.8 that could contain the pathogenic mutation, one of 70 cM on Xp22q13 and the other of 30 cM on Xq23q27.

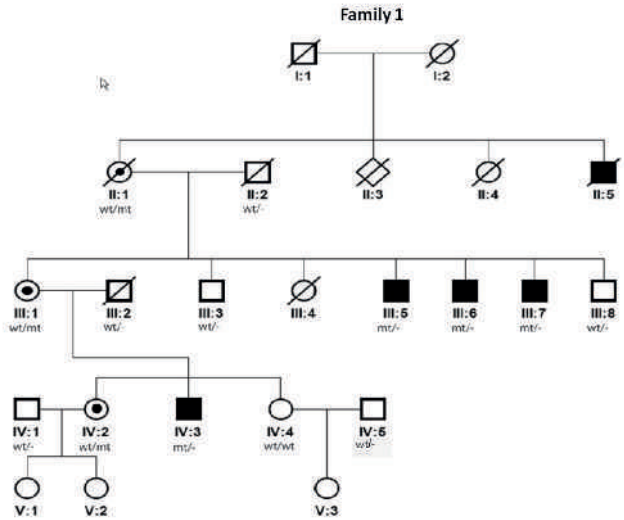

Figure 1 Pedigree of family 1
X-linked pedigree of family 1 with 5 affected males over 3 generations. The mutation in *KIF4A* was shown to co-segregate in affected males (III:5, III:6, III:7 and IV:3, a DNA sample of II:5 was not available) and was not present in two unaffected males (III:3 and III:8). Females II:1, III:1 and IV:2 were carriers.

Massive parallel sequencing of the X-chromosome specific exons revealed a likely pathogenic in-frame mutation, c.1489-8_1490delins10 (NM_012310.4), in *KIF4A*, which was predicted to affect the acceptor splice site of exon 15.(Fig. 2) *KIF4A* is located in the large Xp22q13 linkage interval. No rare deleterious mutations in known X-linked ID genes were identified. Sanger sequencing confirmed the presence of the *KIF4A* mutation and co-segregation analysis showed that the mutation segregated with the phenotype in all affected males (a DNA sample of the uncle was not available). In addition, three females from three generations were shown to be carriers of this mutation and the mutation was absent in two unaffected males.(Fig. 1) Further analysis of the mutation at RNA level and sequencing of the cDNA of the PCR product showed that exon 15 is spliced out and skipped. (Fig. 3A and B) Figure 4A shows a schematic presentation of the KIF4A protein and the relative position of the altered residue.

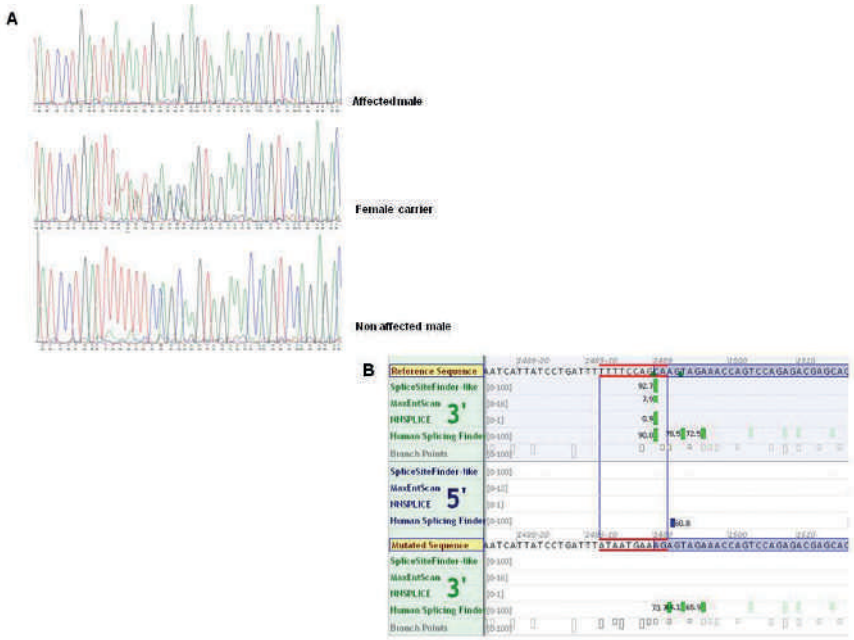

Figure 2 *KIF4A* sequences
(A) shows the sequences of affected males, carrier females and non-affected males.
(B) shows the predicted splice acceptor sites of the reference sequence and the mutated sequence, suggesting that the splice acceptor site of the mutated sequence is severely affected.

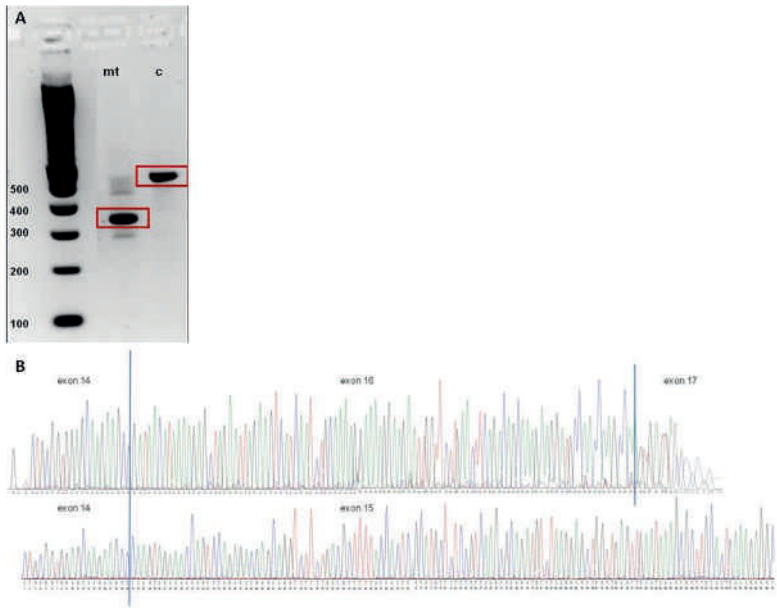

Figure 3 RNA expression studies in cell-lines of patients from family 1 with a mutation in *KIF4A* and control cell-lines, showing effect on splicing

Panels (A) and (B) confirm that the *KIF4* mutation indeed affects the acceptor splice site of exon 15, leading to a skip of exon 15 (186 bp in length), as predicted. RNA was isolated from a cell-line from an affected family member and a healthy control person. Primers for PCR analysis were designed at exon 13/14 (primers CTGCGGTGGAGCAAGAAGCC and AATTTGACCCTCCAGCTCCT, product size 340 bp) and exon 16/17 (CTGCGGTGGAGCAAGAAGCC and AATTTGACCCTCCAGCTCCT, product size 525 bp) bounderies and cDNA was synthesized. (A) Lane 1 shows the band of the patient (mt), which is 185 bp shorter in length as compared to the band in a healthy control (c), likely due to skipping of exon 15. (B) Sequencing of the PCR product of the patient sample showed that the sequence of exon 14 is directly followed by the sequence of exon 16 (upper part) and thus confirmed that exon 15 is skipped. The lower part of the figure shows the normal sequence including exon 15 in a control person.

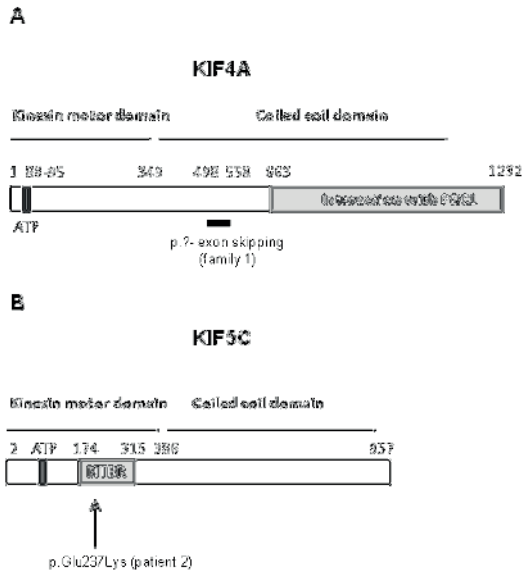

Figure 4 Schematic representations of KIF4A and KIF5C proteins with relative positions of the altered residues
Panel (A) shows the KIF4A protein. PRC1= polycomb-group repressive complex 1.
Panel (B) shows the KIF5C protein. MTBR= microtubule binding region.

Patient 2

Patient 2 was recently described in a large family-based exome sequencing project performed by our group in a series of 100 patients with sporadic ID [26]. Poirier *et al.* also refer to this patient in their paper in which they report another family with a mutation in this gene [19]. In short, patient 2 was born after an uncomplicated pregnancy and delivery with normal growth parameters. She had a severe developmental delay, did not acquire the ability to speak and could only walk with support since the age of 9 -10 years. First seizures manifested at the age of 6 months. Her behavior was characterized by severe automutilation. An MRI-scan of the brain at age 15 years showed signs of cortical malformation mainly affecting the frontal cortex, including a decreased number of gyri, coarse gyri and shallow sulci. (Fig. 5) These abnormalities were also seen to a lesser extent at the temporal cortex and insular cortex. During clinical evaluation at the age of 12 years she had a normal height (-1 SD), but a very dystrophic build and secondary microcephaly (head circumference: 49 cm (< -2.5 SD)). In

addition, she had small hands and feet. She had stereotypic hand movements and a slight hypertonia. There were no evident facial dysmorphisms. Because of the phenotypic similarities to Angelman- and Rett-like syndromes, DNA analysis of *MECP2* (MIM 300005), *FOXG1* (MIM 164874), *CDKL5* (MIM 300203), *UBE3A* (MIM 601623) and 15q11q13 methylation tests were performed, which were all normal. Subsequent 250k SNP array analysis, DNA analysis of *ARX*, and a metabolic screen revealed no abnormalities either.

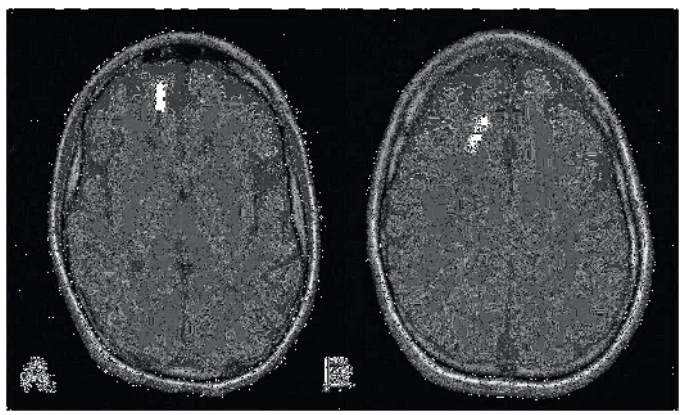

Figure 5 Cerebral MRI scan in patient 2, showing cortical malformation
Panels (A) and (B) show signs of cortical malformation, mainly at the frontal cortex, including a reduction in the number of gyri, which have a coarse aspect, and shallow sulci (indicated by the arrows).

Family-based exome sequencing revealed a highly conserved (PhyloP 6.1) *de novo* c.11465A>C mutation in *KIF5C* (NM 004522.1), predicting a p.(Glu237Lys) substitution. The Grantham score of 56 indicated a moderate physicochemical difference. The mutation affects the motor domain of the KIF5C protein, and may, in contrast to deletions previously reported for this gene [27,28], not lead to haploinsuffiency, but rather suggests a dominant negative effect resulting in abnormal heavy chain dimerization. Figure 4B shows a schematic presentation of the KIF5C protein and the relative position of the altered residue.

Effect of knockdown of *Kif4a* on miniature excitatory (mEPSC) and inhibitory postsynaptic (mIPSC) currents in rat primary hippocampal neurons

To find further supportive evidence that *KIF4A* is involved in the ID phenotype in family 1, we performed functional studies at the level of synaptic function in primary rat hippocampal neurons. This functional assay has previously been successful to show that OPHN1 mediates mGluR-dependent long term depression (LTD) through interaction with the endocytic machinery [29]. Interestingly *Kif4a* knockdown using validated small interference (si)RNAs, resulted in a significant decrease in mEPSC amplitude but an increase in mEPSC frequency compared to control siRNA (Kolmogorov Smirnov (KS) test, $P<0.001$), suggesting that the development of excitatory synapses is hampered in neurons lacking *Kif4a* (Figure 6A-C). Next we measured mIPSCs, a response from quantal release of single $GABA_A$ vesicles. Down-regulation of *Kif4a* decreased mIPSC frequency but not amplitude, indicating that K*if4a* affects presynaptic $GABA_A$ release and /or inhibitory synapse formation without affecting the amount $GABA_A$-receptors (GABAARs) at inhibitory synapses (Fig.6A-C, KS-test, $P<0.001$). We did not observe any changes in the kinetics of mEPSCs or mIPSCs, indicating that the composition and/or function of the glutamate receptors and GABAAR subtype mediating the mEPSCs and mIPSCs respectively were unchanged (Fig.6D, E).

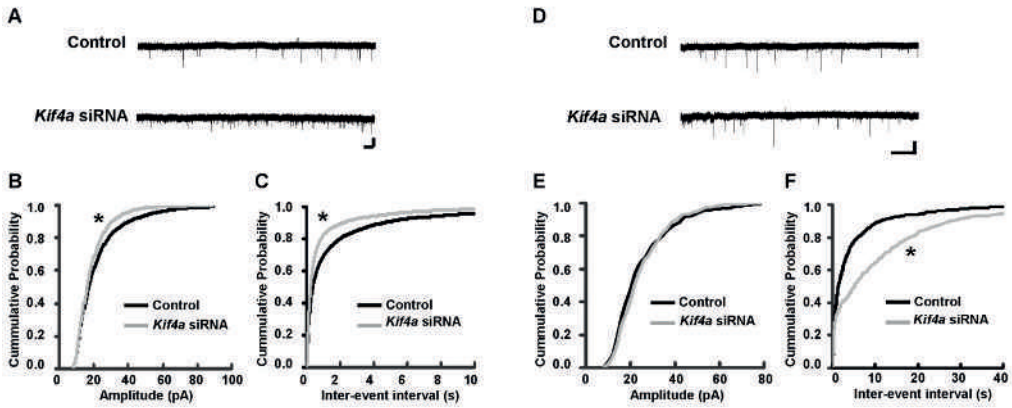

Figure 6 Effect of KIF4A on mEPSC and mIPSC

(A) Representative whole-cell current traces (mEPSC) of a control neuron or a neuron transfected with siRNAs against *Kif4a* at holding potential of −60 mV. Scale bars: 1.2 s and 20 pA. (B, C) Cumulative probability histograms of mEPSC amplitude and inter-event intervals in control (n=39 neurons), *Kif4a* siRNA treated neurons (n=30 neurons). Differences between the conditions for the displayed mEPSC amplitude and inter-event interval cumulative distributions are statistically significant ($P < 0.001$, using Kolmogorov-Smirnov test).

(D) Representative whole-cell current traces (mIPSC) of a control neuron or a neuron transfected with siRNAs against *Kif4a* at holding potential of −60 mV. Scale bars: 16 s and 25 pA. (E, F) Cumulative probability histograms of mIPSC amplitude and inter-event intervals in control (n=7 neurons), *Kif4a* siRNA treated neurons (n=10 neurons). Differences between control and *Kif4a* siRNA are statistically significant for the displayed inter-event interval cumulative distributions but not for the mIPSC amplitude ($P < 0.001$, using Kolmogorov-Smirnov test).

Effect of p. Glu237Lys mutation on KIF5C cellular localization and function.

Since the mutation p.Glu237Lys in KIF5C is predicted to affect the motor domain we first determined whether it affected KIF5c movement along dendrites. To this end we transfected primary rat hippocampal neurons with Yellow Fluorescent Protein (YFP)-tagged wild-type KIF5C (KIF5C-WT) or mutant KIF5C (KIF5C-E237K) construct. KIF5C-WT accumulated in distal regions of the dendrites (Fig.7A, C), whereas KIF5C-E237K showed a significant reduction in distal localization and a relative increased accumulation throughout the cell body (Fig. 7B, C, t-test *P<0.05*). Next to determine the functional consequence of the missense mutation we compared the effect of overexpressing KIF5C-WT versus mutant KIF5C-E237K and control (YFP only) on mEPSCs in hippocampal neurons. Overexpressing KIF5C-WT resulted in an increase

in mEPSC frequency compared to control transfected neurons (Fig.7D-E, KS-test, *P*<0.001). However overexpressing KIF5C-E237K failed to increase mEPSC frequency, but in contrast led to a significant decrease in mEPSC amplitude. Together these data indicate that the missense mutation found in KIF5C leads to a non-functional motor domain.

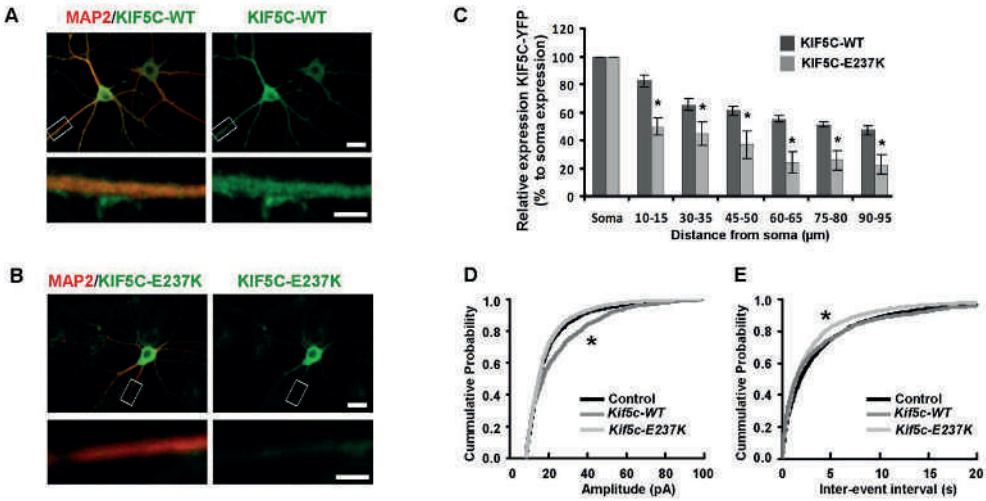

Figure 7 Impact of p.Glu237Lys on KIF5C localization and function
(A, B) Representative images showing the subcellular localization of YFP-tagged KIF5C-WT and KIF5C-E237K. YFP-tagged constructs of KIF5C were expressed in cultured hippocampal neurons and visualized by immunofluorescence staining with an anti-GFP antibody. KIF5C-WT accumulated in the distal regions of the dendrites, in contrast to KIF1C-E237K. The neuronal cell bodies and dendrites were stained with anti-MAP2 antibody. Scale bars upper image: 20 µm, lower image: 4 µm. (C) Quantification of dendritic expression of YFP-tagged KIF5C-WT and KIF5C-E237K. Dendritic signal of KIF5C-WT and KIF5C-E237K was normalized to its signal in the soma (*P* <0.05, using t-test, n=6 neurons). (D, E) Cumulative probability histograms of mEPSC amplitude and inter-event intervals in control (n=30 neurons), KIF5C-WT expressing neurons (n=13 neurons) and KIF5C-E237K expressing neurons (n=27 neurons). Differences between the conditions for the displayed mEPSC amplitude and inter-event interval cumulative distributions are statistically significant (*P* < 0.001, using Kolmogorov-Smirnov test).

Discussion

The role of KIF genes in the origin of ID has so far only received limited attention, although a growing body of work suggests that many ID genes impinge on synaptic function and as such contribute the pathophysiology of the disorder [30]. In particular, the balance between excitatory and inhibitory synaptic input seems to be disturbed in common neurodevelopmental disorders including ID, autism and schizophrenia.

Our data show that both KIF4A and KIF5C are important proteins that regulate synapse development. In particular KIF4A is a critical protein in controlling the tight balance between excitatory and inhibitory inputs during development since knocking down *Kif4a* resulted in a decrease in mIPSCs but an increase in mEPSCs, albeit with a lower amplitude. A disturbed balance between excitatory and inhibitory drive could therefore explain the presence of epilepsy in the patients. Moreover, we showed that the reported missense mutation in *Kif5c* affects its protein function at excitatory synapses.

A synaptic function for KIF4A has so far not been explored, whereas KIF5 was recently reported to be involved in regulating both glutamatergic and GABAergic synaptic transmission in striatal and cortical neurons [31–33]. The specific contribution of KIF5C hereto has however not been determined.

KIF4A belongs to the class of the N5-kinesins and is highly expressed in differentiated young neurons. It consists of a N-terminal motor domain, a central stalk domain and a C-terminal C-domain [34]. Previous studies showed that KIF4A has various functions and plays a role in chromosome condensation and midzone spindle pole formation essential for cytokinesis and chromosome segregation during mitosis, as well as in regulation of activity-dependent neuronal survival and apoptosis, thereby regulating the number of neurons during murine brain development [9,35,36]. After dissociation from the enzymatic protein poly (ADP-ribose) polymerase 1 (PARP1), which prevents apoptosis, KIF4A moves into the neurites. Here, it possibly transports cargoes essential for neuronal development, such as the adhesion molecule L1 which is required for axon formation and synapse development [9,37]. Although KIF4A was shown by several studies to be involved in spindle pole organization, most studies concluded that KIF4A deficient cells show a normal mitotic division. Aneuploidy analysis in cultured blood lymphocytes from one of the patients of family 1 showed no increased level of aneuploid cells, which is in agreement with the observation in most other studies that mitosis is not significantly disturbed [9,35,38].

KIF5C, together with *KIF5A* and *KIF5B*, belongs to the class of N-1 kinesins and is specifically expressed in nervous tissue [1,13,39]. Mice with a homozygous knockout of *KIF5C* are viable and do not show gross abnormalities in the nervous system, except from a smaller brain size and relative loss of motor neurons to sensory neurons. This mild phenotypic presentation is explained by a high similarity between the three KIF5 genes and functional redundancy [13].

The missense mutation in the family reported by Poirier *et al* [19] is associated with a severe phenotype including severe Malformations of Cortical Development (MCD) and microcephaly, which shows remarkable overlap with the phenotype in the present patient 2, who also presented with microcephaly and has signs of cortical malformation on her brain MRI as well. Interestingly, Poirier *et al.* showed that expression of the missense variant that they found in the family with MCD (p.Glu237Val) in *Escheria Coli*, results in a complete inability of the protein to hydrolyze ATP in a microtubule dependent assay. Of note, this missense variant is located at the same position as the here reported variant and affects the microtubule-interacting domain. In addition they found an altered distribution of the protein. These data are in agreement with our results that show that the missense mutation in KIF5C leads to a non-functional motor domain, a significant reduction in distal localization of the protein and a relative increased accumulation throughout the cell body.

In summary, these data support the involvement of members of the kinesin superfamily, *KIF4A* and *KIF5C,* in ID phenotypes. Identification of other patients with mutations in these genes should further confirm the role of *KIF4A* and *KIF5C* in ID phenotypes and may give further insights in the full clinical spectrum. This spectrum likely includes neuronal migration defects as was supported by the aberrant cortical formation in patient 2 and the previously reported family.

At the functional level, we found that both KIF4A and KIF5C may contribute to the pathophysiology of ID by altering the balance between excitatory and inhibitory synaptic efficacy leading to changed neuronal excitability. As such these genes can be added to the growing list of ID genes that influence synaptic functioning [30]. Together with recently reported mutations in similar and other proteins involved in the motor protein complex of the microtubule transport pathway, including *DYNC1H1, KIF2A* and *TUBG1* [19,40], our findings indicate that this pathway may be of great importance to ID, and suggest that other genes encoding proteins in this pathway may well be potential candidates for ID phenotypes.

Materials and Methods

Next generation sequencing (NGS) approaches

Family 1 was included in a larger project involving sequencing of all exons of the X-chromosome in >200 families with X-linked ID. For each family, DNA from one affected male was subjected to targeted enrichment of all X-chromosome specific exons followed by NGS. The enriched and sequenced exons encompassed 99.2% of the 7,759 disease-causing X-chromosomal changes listed in the Human Gene Mutation Database (HGMD, update April 2011). Variants were filtered against dbSNP135, control populations (185 genomes from the 1000 Genomes Project Consortium; http://www.1000genomes.org/data, 200 Danish exomes, the NHLBI Exome Sequencing Project (ESP, freeze 5400)) as well as an in-house database (Kalscheuer *et al.,* personal communication). Variants with a minor allele frequency of ≥ were excluded.

In patient 2 we performed family based whole exome sequencing as previously described by *de Ligt et al* [26].

Confirmation of mutations and segregation analysis were done by Sanger sequencing.

RNA expression studies in cell-lines of patients from family 1 with a mutation in KIF4A

RNA was isolated from a cell-line from an affected family member and a healthy control person. Primers for PCR analysis were designed at exon 13/14 and exon 16/17 bounderies and cDNA was synthesized. Sequencing of the PCR product in an affected family member and the healthy control person was performed to confirm skipping of exon 15 in the patients.

siRNAs, DNA constructs, hippocampal neurons and transfection

The following validated siRNAs were obtained from Sigma Aldrich: *Kif4a*; SASI_Rn02_00290987 5'- CUAAUGACUUCUGUAGCUU-3'; SASI_Rn02_00290988 5'- CAUCUAGAACUGAAACCUA-3'; SASI_Rn02_00290989 5'- CAACCUAGAGGAAACAUUA-3'. *Kif5c*; SASI_Rn02_00231705 5'- GGUUACAAUGGGACAAUUU-3'; SASI_Rn02_00231706; 5'- GCUUCUAGCUUCCACCAGA-3'; SASI_Rn02_00231707 5'- CAGAGAACUCCAGACUCUU-3'. The BLOCK-iT fluorescent oligo (Invitrogen) that is not homologous to any known genes was used as transfection efficiency detector and a negative control. Each siRNA was tested in hippocampal neurons and validated using quantitative PCR. Primary hippocampal neurons were prepared as described previously [29] and transfected with siRNAs at 6 days *in vitro* (DIV).

Three days later, whole-cell recordings were obtained from transfected neurons. In experiments in which we examined the role of KIF5C-WT and KIF5C-E237K on mEPSCs, primary hippocampal neurons were electroporated immediately after dissociation using the Amaxa Nucleofector device (Amaxa GmbH). 3µg total of GFP, KIF5C-WT and KIF5C-E237K plasmids was used per electroporation. Whole-cell recordings were conducted from transfected neurons in every group. The YFP-KIF5c (KIF5c-WT) construct was a gift from Dr. A. Stephenson. The KIF5C mutant (KIF5C-E237K) was generated by introducing a point mutation (E237K) using the Quick Change system (Stratagene).

Measurement of miniature excitatory (mEPSC) and inhibitory postsynaptic currents (mIPSC) in rat primary hippocampal neurons.

Whole-cell voltage-clamp recordings were performed from control neurons or neurons transfected with siRNAs against *Kif4a* or cDNA expressing KIF5C-WT/E237K at holding potential of −60 mV in ACSF containing 2.5 mM CaCl2 and 1.2 mM MgCl2 at 30°C. mEPSCs were recorded in the presence of 1 µM TTX and 0.1 mM picrotoxin. mIPSCs were recorded in the presence of 10 µM CNQX and 100 µM APV. Five to 10 min of recordings were analyzed from each cell using the Mini Analysis Program (Synaptosoft). The amplitude of mEPSCs and mIPSCs is directly related to the postsynaptic strength, whereas the frequency is correlated to the presynaptic release properties and/or the amount of functional synapses.

Immunofluorescence

To detect the localization of KIF5C-WT and KIF5C-E237K transfected primary hippocampal neurons were fixed at 21 DIV in 4% paraformaldehyde with 4% sucrose solution, permeabilized with 0.2% Triton X-100 in PBS, and incubated overnight with following primary antibodies: anti-MAP2 (synaptic system) and anti-GFP (Abcam). As secondary antibodies we used: Alexa-568 and Alexa-488 donkey anti-rabbit or anti-guinea pig (Invitrogen). Immunofluorescence was visualized under a fluorescent microscope (Axio Imager Z1; Zeiss, Basle, Switzerland) equipped with a camera (AxioCam MRm; Zeiss). Images were processed using Axiovision Rel (version 4.6) and analyzed using ImageJ (NIH, Bethesda). For each condition, 3 dendrites per neuron were analyzed (n= 6 neurons/group). Dendritic signal of KIF5C-WT and KIF5C-E237K was normalized to its signal in the soma.

Acknowledgments

We thank the participating patients and their families. We also would like to thank Michél A.A.P Willemsen and Jolanda H. Schieving, from the department of Pediatric neurology of the Radboud University Medical Centre, Nijmegen, The Netherlands, for their expert evaluation of the brain MRI in patient 2. We thank Dr. Anne Stephenson for providing YFP-KIF5C constructs.

Funding

This work was supported by grants from the Consortium ''Stronger on your own feet'' to T.K. and M.H.W., The Netherlands Organization for Health Research and Development (ZonMw grants 916-86-016 to L.E.L.M.V., and 907-00-365 to T.K.), the GENCODYS, an EU FP7 large-scale integrating project grant (241995 to H.v.B. and T.K.) and the MERE-GLU, an EU FP7 Marie Curie Re-integration Grant (PEOPLE-2010-RG, 277091 to N.N.K).

Conflicts of Interest Statement

The authors declare no conflicts of interest.

Web sources

Online Mendelian Inheritance in Man (OMIM), http://www.omim.org/.

References

1. Miki, H., Setou, M., Kaneshiro, K. & Hirokawa, N. All kinesin superfamily protein, KIF, genes in mouse and human. *Proc. Natl. Acad. Sci. U. S. A.* **98,** 7004–11 (2001).
2. Lawrence, C. J. *et al.* A standardized kinesin nomenclature. *J. Cell Biol.* **167,** 19–22 (2004).
3. Mandelkow, E. & Mandelkow, E. M. Kinesin motors and disease. *Trends Cell Biol.* **12,** 585–591 (2002).
4. Hirokawa, N., Niwa, S. & Tanaka, Y. Molecular motors in neurons: transport mechanisms and roles in brain function, development, and disease. *Neuron* **68,** 610–38 (2010).
5. Homma, N. *et al.* Kinesin superfamily protein 2A (KIF2A) functions in suppression of collateral branch extension. *Cell* **114,** 229–239 (2003).
6. Yonekawa, V. *et al.* Defect in synaptic vesicle precursor transport and neuronal cell death in KIF1A motor protein-deficient mice. *J. Cell Biol.* **141,** 431–441 (1998).
7. Marszalek, J. R., Ruiz-Lozano, P., Roberts, E., Chien, K. R. & Goldstein, L. S. B. Situs inversus and embryonic ciliary morphogenesis defects in mouse mutants lacking the KIF3A subunit of kinesin-II. *Proc. Natl. Acad. Sci. U. S. A.* **96,** 5043–5048 (1999).
8. Nonaka, S. *et al.* Randomization of left-right asymmetry due to loss of nodal cilia generating leftward flow of extraembryonic fluid in mice lacking KIF3B motor protein. *Cell* **95,** 829–837 (1998).
9. Midorikawa, R., Takei, Y. & Hirokawa, N. KIF4 Motor Regulates Activity-Dependent Neuronal Survival by Suppressing PARP-1 Enzymatic Activity. *Cell* **125,** 371–383 (2006).
10. Tanaka, Y. *et al.* Targeted disruption of mouse conventional kinesin heavy chain, kif5B, results in abnormal perinuclear clustering of mitochondria. *Cell* **93,** 1147–1158 (1998).
11. Zhao, C. *et al.* Charcot-Marie-Tooth disease type 2A caused by mutation in a microtubule motor KIF1Bbeta. *Cell* **105,** 587–97 (2001).
12. Xia, C. H. *et al.* Abnormal neurofilament transport caused by targeted disruption of neuronal kinesin heavy chain KIF5A. *J. Cell Biol.* **161,** 55–66 (2003).
13. Kanai, Y. *et al.* KIF5C, a Novel Neuronal Kinesin Enriched in Motor Neurons. *J. Neurosci.* **20,** 6374–6384 (2000).
14. Wong, R. W.-C., Setou, M., Teng, J., Takei, Y. & Hirokawa, N. Overexpression of motor protein KIF17 enhances spatial and working memory in transgenic mice. *Proc. Natl. Acad. Sci. U. S. A.* **99,** 14500–14505 (2002).
15. Nakajima, K. *et al.* Molecular Motor KIF5A Is Essential for GABAA Receptor Transport, and KIF5A Deletion Causes Epilepsy. *Neuron* **76,** 945–961 (2012).
16. Erlich, Y. *et al.* Exome sequencing and disease-network analysis of a single family implicate a mutation in KIF1A in hereditary spastic paraparesis Exome sequencing and disease-network analysis of a single family implicate a mutation in KIF1A in hereditary spastic parapares. 658–664 (2011). doi:10.1101/gr.117143.110
17. Hamdan, F. F. *et al.* Excess of de novo deleterious mutations in genes associated with glutamatergic systems in nonsyndromic intellectual disability. *Am. J. Hum. Genet.* **88,** 306–316 (2011).
18. Aulchenko, Y. S. *et al.* Genetic variation in the KIF1B locus influences susceptibility to multiple sclerosis. *Nat. Genet.* **40,** 1402–1403 (2008).
19. Poirier, K. *et al.* Mutations in TUBG1, DYNC1H1, KIF5C and KIF2A cause malformations of cortical development and microcephaly. *Nat. Genet.* **45,** 639–47 (2013).
20. Reid, E. *et al.* A kinesin heavy chain (KIF5A) mutation in hereditary spastic paraplegia (SPG10). *Am. J. Hum. Genet.* **71,** 1189–1194 (2002).
21. Putoux, A. *et al.* KIF7 mutations cause fetal hydrolethalus and acrocallosal syndromes. *Nat. Genet.* **43,** 601–6 (2011).
22. Dafinger, C. *et al.* Mutations in KIF7 link Joubert syndrome with Sonic Hedgehog signaling and microtubule dynamics. *J. Clin. Invest.* **121,** 2662–67 (2011).

23. Najmabadi, H. *et al.* Deep sequencing reveals 50 novel genes for recessive cognitive disorders. *Nature* **478,** 57–63 (2011).
24. Ostergaard, P. *et al.* Mutations in KIF11 cause autosomal-dominant microcephaly variably associated with congenital lymphedema and chorioretinopathy. *Am. J. Hum. Genet.* **90,** 356–362 (2012).
25. Yamada, K. *et al.* Heterozygous mutations of the kinesin KIF21A in congenital fibrosis of the extraocular muscles type 1 (CFEOM1). *Nat. Genet.* **35,** 318–321 (2003).
26. de Ligt, J. *et al.* Diagnostic exome sequencing in persons with severe intellectual disability. *N. Engl. J. Med.* **367,** 1921–9 (2012).
27. Nadif Kasri, N., Nakano-Kobayashi, A. & Van Aelst, L. Rapid synthesis of the X-linked mental retardation protein OPHN1 mediates mGluR-dependent LTD through interaction with the endocytic machinery. *Neuron* **72,** 300–15 (2011).
28. Jaillard, S. *et al.* 2q23.1 microdeletion identified by array comparative genomic hybridisation: an emerging phenotype with Angelman-like features? *J. Med. Genet.* **46,** 847–855 (2009).
29. van Bon, B. W. M. *et al.* The 2q23.1 microdeletion syndrome: clinical and behavioural phenotype. *Eur. J. Hum. Genet.* **18,** 163–170 (2010).
30. Pavlowsky, a, Chelly, J. & Billuart, P. Major synaptic signaling pathways involved in intellectual disability. *Mol. Psychiatry* **17,** 663–663 (2012).
31. Yuen, E. Y., Wei, J., Zhong, P. & Yan, Z. Disrupted GABAAR trafficking and synaptic inhibition in a mouse model of Huntington's disease. *Neurobiol. Dis.* **46,** 497–502 (2012).
32. Twelvetrees, A. E. *et al.* Delivery of GABAARs to Synapses Is Mediated by HAP1-KIF5 and Disrupted by Mutant Huntingtin. *Neuron* **65,** 53–65 (2010).
33. Mandal, M. *et al.* Impaired α-amino-3-hydroxy-5-methyl-4-isoxazolepropionic acid (AMPA) receptor trafficking and function by mutant Huntingtin. *J. Biol. Chem.* **286,** 33719–33728 (2011).
34. Sekine, Y., Kondo, S., Takemura, R., Hirokawa, N. & Biology, C. A Novel Microtubule-based Motor Protein (KIF4) for Organelle Transports, Whose Expression Is Regulated Developmentally. **127,** 187–201 (1994).
35. Zhu, C. & Jiang, W. Cell cycle-dependent translocation of PRC1 on the spindle by Kif4 is essential for midzone formation and cytokinesis. *Pro. Natl. Aca. Sci., USA* **102,** 343–348 (2005).
36. Kurasawa, Y., Earnshaw, W. C., Mochizuki, Y., Dohmae, N. & Todokoro, K. Essential roles of KIF4 and its binding partner PRC1 in organized central spindle midzone formation. *EMBO J.* **23,** 3237–3248 (2004).
37. Peretti, D., Peris, L., Rosso, S., Quiroga, S. & Cáceres, A. Evidence for the involvement of KIF4 in the anterograde transport of L1- containing vesicles. *J. Cell Biol.* **149,** 141–152 (2000).
38. Mazumdar, M., Sundareshan, S. & Misteli, T. Human chromokinesin KIF4A functions in chromosome condensation and segregation. *J. Cell Biol.* **166,** 613–620 (2004).
39. Aizawa, H. *et al.* Kinesin family in murine central nervous system. *J. Cell Biol.* **119,** 1287–1296 (1992).
40. Willemsen, M. H. *et al.* Mutations in DYNC1H1 cause severe intellectual disability with neuronal migration defects. *J. Med. Genet.* **49,** 179–183 (2012).

Chapter 7

General discussion and future prospects

Part of this chapter has been published as a commentary:
Rho GTPases at the synapse: An embarrassment of choice.
Small GTPases. 2016 5:1-8.

How the brain governs cognitive processes is a fundamental question that attracts numerous neuroscientists to dedicate their entire careers for seeking answers. Although considerable progress has been made in the past few decades in neuroscience, we are just beginning to uncover the mysteries of the human brain. The aim of the research described in this thesis is to enrich our knowledge of the cellular and molecular mechanisms underlying learning and memory, and therefore to advance our understanding of how cognition in adulthood is affected by developmental mechanisms in neurodevelopmental disorders, such as ID and ASD. With the main focus on the genes that are involved in Rho GTPase signaling pathways, I have contributed to reveal the roles of several previously uncharacterized genes, most of which are linked to ID, in neuronal development at the synaptic level (**chapters 3-6**). Here, I will reflect on these results and discuss future prospects in a general framework.

1. Rho GAPs and GEFs in the brain

1.1 Transcriptional mapping of novel Rho regulators

Cognitive functions including learning and memory rely on proper performance of the CNS at the cellular and molecular level. Rapid remodeling in the shape and the amount of actin-enriched dendritic spine during development and in response to stimuli has been demonstrated to be critical for normal neuronal function and plasticity. As key regulators of actin cytoskeleton, Rho GTPases and their regulators act as molecular switches in diverse actin-based cellular processes, including modification of spine morphology and synaptic efficacy. So far, more than 80 GEFs and more than 70 GAPs exist in the human genome, [1–3] providing a ratio between the number of Rho GTPases and GEFs/GAPs about 4 to 1. Although lots of efforts have been made to unmask the detailed regulatory role of Rho proteins at different developmental stages in CNS, the field still lacks a complete picture of why and how the brain utilizes “overabundant” molecules involved in Rho GTPase signaling to achieve a precise regulation of synaptic strength during development and cognition. One hypothesis is that excess GEFs and GAPs enable neurons to temporally and spatially restrict their responses to local extracellular cues and further ensure proper connectivity for learning and memory (reviewed in refs. 4, 5). A detailed description of spatial-temporal expression pattern of previously uncharacterized Rho proteins may further help us to appreciate the logic behind the complexity of Rho GTPases and their regulators, and eventually their function in the brain.

In this thesis, I have contributed to generate a transcriptional developmental map of Rho GTPases and their regulators in the hippocampus and the cortex, two core regions govern learning and memory (**chapter 2**). The results revealed, at least in part, the diverse and unique expression patterns of individual genes encoding Rho GTPases and their regulators during hippocampal and cortical development, supporting the hypothesis that the cellular specificity of Rho regulatory proteins determines the functional specificity of Rho GTPase signaling pathways in the brain. For example, I found that *Arhgap12* and *Arhgap15*, two closely related members of the RhoGAP subfamily [6], exhibit complimentary expression patterns. *Arhgap12* was found to be highly expressed in early development whereas the level of *Arhgap15* rapidly increases after birth and reaches a peak level in adulthood. Thus, it is likely that *Arhgap12* and *Arhgap15* govern Rho GTPase signaling pathways and subsequent cellular events at complementary developmental stages. Based on the information provided in this map, I further performed in depth investigations on several interesting Rho regulators including *Arhgap12, Trio and Ocrl1* (**chapters 3-5**). Future experiments identifying gene expression profiles for other uncharacterized Rho regulators will be necessary for completing the transcriptional mapping of Rho regulators and providing an overview of how the brain manipulates these proteins to control synaptic development.

Previous studies have indicated that several transcriptional factors including p53 and Myc can regulate gene expression of some Rho GTPases[7]. However, full characterization of the regulation of developmental expression of Rho regulatory proteins remains elusive. Future experiments will determine the transcriptional mechanisms that control gene expression of Rho proteins during development under physiological and pathophysiological settings. Of note, besides the transcriptional control, levels of Rho GEFs and GAPs can also be fine-tuned at the translational level. For example, microRNAs including miR-21 and miR-138 have been found to regulate Rho GTPase gene expression in non-neuronal cells at the post-transcriptional level [8,9]. Therefore the mRNA levels might not precisely reflect protein levels of Rho regulators. It would be interesting to evaluate how the translational machinery contributes to maintain the homeostasis of Rho regulatory proteins at both whole-cell and single synapse levels for normal neuronal function.

1.2 Synaptic functions of novel Rho regulators

One major aim of this PhD thesis was to uncover the functions of novel Rho GEFs and GAPs during brain development at the synaptic level. Focusing on the Schaffer collateral pathway, the most-studied and best-characterized synapses, I have shown detailed functional analysis of three important Rho regulatory proteins: the RacGAP ARHGAP12 (**chapter 3**), the ID associated RacGEF TRIO (**chapter 4**) and the Lowe syndrome protein OCRL1 (**chapter 5**). Here, based on the results and the previous findings, I propose three possible approaches, in addition to previously summarized regulatory manners (reviewed in ref. 5), for neurons to accurately control synaptic strength via Rho GTPase signaling pathways during development.

a. Using individual multifunctional GEFs/GAPs at synapses

In **chapter 3** of this thesis, I uncovered a dual function for the previously uncharacterized RhoGAP, ARHGAP12, specifically at hippocampal excitatory synapses during development [10] (**Fig. 1A**). ARHGAP12 is able to orchestrate synaptic efficacy by modulating both spine morphology and surface AMPAr levels at the post-synaptic compartment. Overexpression of ARHGAP12 reduced both spine density and volume while knocking down ARHGAP12 resulted in increased spine volume without affecting spine density. Functionally, elevated levels of ARHGAP12 significantly depressed CA3-CA1 synapses, and on the contrary, potentiated excitatory synaptic transmission was observed in ARHGAP12 downregulated neurons. The data further showed that ARHGAP12 is able to actively regulate excitatory AMPAr endocytosis. More importantly, I demonstrated that two distinct pathways are engaged to mediate structural and functional alterations respectively. On one hand, the GAP activity of ARHGAP12 allows it to regulate the activity of its target Rac1 GTPase and subsequently modulate the morphology of dendritic spines. On the other hand, by interacting with the F-BAR protein CIP4, ARHGAP12 is involved in the endocytic machinery and further regulates AMPAr endocytosis. A similar mechanism has been observed in studies of OPHN1, whose mutations have been associated with ID. [11] OPHN1 regulates spine structure through its RhoGAP activity and maintains normal AMPAr recycling via interacting with Homer1b/c. [12,13] Moreover, via interactions with endophilin A2/3, OPHN1 also mediates persistent decreases in surface AMPARs in mGluR-LTD. [14] Together, these findings strongly indicate that neurons can optimize synaptic efficacy by making use of individual multifunctional proteins involved in Rho GTPase signaling at synapses (**Fig. 3A**). It is not hard to imagine that several advantages may come

from this approach. Firstly, using one protein to regulate cellular events that alter synaptic structure and function in the same direction would greatly reinforce and ensure desired synaptic modifications in response to experience and/or development to occur correctly. Secondly, it enables neurons to respond to external cues more rapidly since one signal might already be sufficient to trigger structural and functional modifications simultaneously. Lastly, it provides an optimal energetic setting at synapses in the CNS. It has been shown that the largest component of brain energy is used at synapses and disruptions thereof have been found to present pathological effects (reviewed in ref. 15). Using multifunctional Rho GTPases and their regulators may contribute to turning on an energy-saving mode at synapses and maximize energy supply for normal cognitive processes.

In line with the spatiotemporal specificity of ARHGAP12, namely its unique expression pattern in excitatory neurons of CA1 subregion at early developmental stages, my results suggest that ARHGAP12 functions as a synaptic "brake" during hippocampal development by limiting silent synapses converting to active synapses (**Fig. 1B**). Additionally, I also observed a positive feedback loop between synaptic activity and ARHGAP12 mediated signaling pathway, in the sense that synaptic activity is required for ARHGAP12 repression, and in turn, ARHGAP12 downregulation enhances synaptic efficacy. Overall, these results indicate that by regulating the levels of individual multifunctional molecules involved in Rho GTPase signaling, neurons may adjust to environmental stimuli and developmental changes, and consequently maintain synaptic strength and connectivity in an optimal range.

Notably, *Arhgap12* mRNA was recently identified as a potential target of FMRP, an RNA binding protein that represses translation [16] and loss of function mutations in *FMRP* gene result in Fragile X Syndrome (FXS). A form of protein synthesis-dependent synaptic plasticity, mGluR-LTD, has been demonstrated to be exaggerated in a mouse model of FXS (*Fmr1* KO mice), due to the absence of FMRP mediated repression of "LTD" proteins. Several mechanisms including PICK1-GluA2 interaction, [17,18] OPHN1-endophilin interaction, [14] PKC-dependent phosphorylation of GluA2, and activation of the Rac1-LimK-cofilin signaling pathway [17–20] have been implied in the regulation of mGluR-LTD. Based on these reports and our observation of ARHGAP12 being a repressor of spine morphology and synaptic strength, we speculate that ARHGAP12 could be perfectly situated to act as a coordinator to structurally and functionally weaken synapses during plasticity. Moreover, it could also serve as a potential target to reverse the exaggerated mGluR-LTD phenotype observed in FXS. One of

the current focuses in our group is to seek direct experimental evidence to evaluate this hypothesis. Experiments combining electrophysiological, molecular biological and behavioral approaches in *Arhgap12* knockout animals will provide novel insight of how ARHGAP12 is involved in mGluR-LTD and how neurons command multifunctional GEFs and GAPs to precisely regulate cognitive processes.

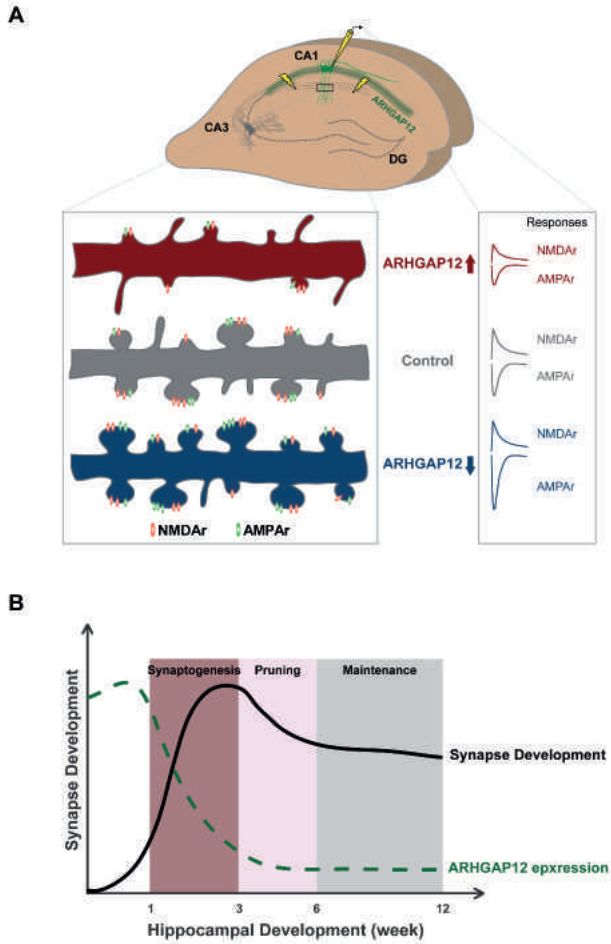

Figure 1 Synaptic function of ARHGAP12 during hippocampal development. (A) ARHGAP12 is almost exclusively expressed in CA1 excitatory neurons. Overexpression of ARHGAP12 significantly reduces both spine density and volume while downregulation leads to increased spine size without affecting the density. Electrophysiologically, elevated ARHGAP12 levels depress both AMPAr- and NMDAr-mediated synaptic transmission whereas reduced ARHGAP12 levels specifically enhance AMPAr-mediated transmission. In addition, knocking down ARHGAP12 promotes silent synapses converting to functional synapses. **(B)** ARHGAP12 acts as a synaptic "brake" during hippocampal development. In rodent, rapid synaptogenesis in the hippocampus occurs between the second and the third postnatal

week followed by a selective pruning in adolescence and maintenance in adulthood. The expression of ARHGAP12 protein in CA1 subregion gradually declines in the first three postnatal weeks and sustains low levels throughout hippocampal development, which releases the "brake" and allows for synaptogenesis.

b. Using homologs displaying opposing effects

Many of the GAPs and GEFs are highly identical in terms of their structure. As it has been proposed, the spatiotemporal expression pattern could explain the functional divergence. A typical example is α-chimaerin, a RhoGAP possessing GAP activity towards Rac1 and to a lesser extend to Cdc42. There are two isoforms of α-chimaerin, α1- and α2- chimaerin, which both contain C1 and RhoGAP domains but differ in that the α2-chimaerin contains an N-terminal SH2 domain that is absent from α1. [21] Interestingly, both isoforms strongly differ in their temporal expression. Whereas α2-chimaerin is strongly expressed early in development, the expression of α1-chimaerin coincides with synaptogenesis, resulting in a high expression in mature neurons. In concordance, both isoforms have been found to have very distinct functions. Alpha2-chimaerin has been found important for axon guidance and neuron migration, [22–24] whereas α1-chimaerin has a specific role in spine pruning in the hippocampus and cerebellum. [25,26]

In addition to the discoveries above, homologs involved in Rho GTPase signaling may also target common cellular processes during development in a counterproductive manner. A striking example occurs along the functional characterization of Trio and its ortholog Kalirin. Initial studies indicated that *Trio* full-knockout mice display embryonic lethality [27]. Moreover, disrupted cerebellum development, such as abnormal neurite growth and granule cell migration, has been observed in conditional knockout mice of *Trio*. [28] Recently, we identified *TRIO* as a responsible gene for mild to borderline ID and further revealed its contribution during neurite outgrowth and basal synaptic transmission (**chapter 4**). [29] Our results showed that reduced Trio levels promote neurite outgrowth and specifically enhance AMPAr-mediated transmission, indicating that the endogenous TRIO restricts these two critical cellular events (**Fig. 2**). Surprisingly, although sharing more than 80% of the sequence, the effect exhibited by TRIO is opposing to that displayed by Kalirin, which stimulates neurites outgrowth and is required for activity-dependent spine enlargement and enhancement of AMPAr-mediated transmission. This scenario is of particular interest since it represents another approach of neurons accurately regulating multiple critical events of neuronal

development. By choosing structural identical homologs displaying opposite synaptic function, neurons may achieve a fine balance that is required for all neuronal events including migration and synaptogenesis and accurately steer brain development in the proper direction (**Fig. 3B**). Of note, a recent study reported that neurons with elevated levels of a specific isoform of TRIO, TRIO-9, displayed increased AMPAr-mediated synaptic transmission. [30] Also, knocking down endogenous TRIO at 1 day in vitro (1 DIV) when Trio is the most profoundly expressed led to a deficit in synaptic transmission, [30] an opposite effect of reducing TRIO levels at a later time point, 4 DIV. These findings imply that variants of GEFs and GAPs might exhibit distinct function and aberrations in their levels occurring at different stages of development may result in diverse, even completely opposing impact at synapses. Future experiments are needed to test this idea.

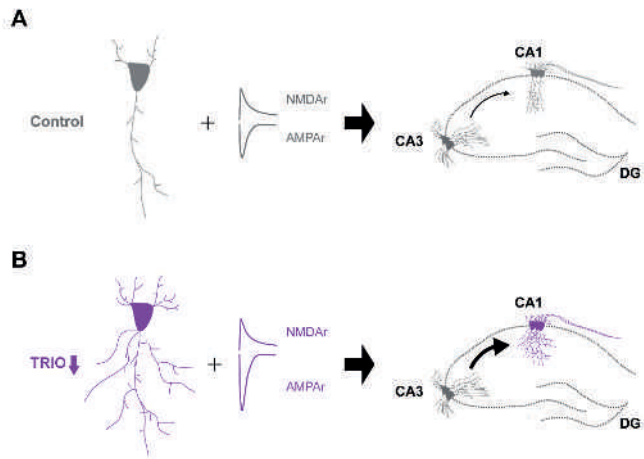

Figure 2 Synaptic function of TRIO in the hippocampus. Reduced expression of TRIO increases dendritic complexity and enhances synaptic transmission at CA3-CA1 synapses.

c. Recruiting multiple GEFs/GAPs to target common cellular events

A recent study reported the contribution of ARHGAP12 in regulating phagocytosis, [31] an important event responsible for eliminating particles in diverse cell types. A common feature of the phagocytic process, regardless of the type of receptor bound or the size of the target particles, is the involvement of actin cytoskeleton remodeling. [32] Interestingly, other studies showed that both phagocytosis and excitatory synaptogenesis require Rac1 activation

downstream of BAI1. [33,34] Schlam et al. have demonstrated that ARHGAP12 acts synergistically with two other GAPs, SH3BP1 and ARHGAP25, to disassemble actin, a critical step underlying phagosome maturation for completing the internalization of large targets. Sustained Rac or Cdc42 activities resulted from silencing one of the three Rho GAPs can compromise phagocytic efficiency. [31] These findings, in RAW 264.7 cell lines, may provide a hint of why and how multiple Rho regulators are required in CNS. Instead of being functionally redundant, multiple Rho regulators, with overlapping functions, might be engaged in the same neuronal event to ensure it takes place flawlessly (**Fig. 3C**). Given that both endogenous ARHGAP12 and TRIO are the most abundant at early developmental stages in the hippocampus and that both are present at synapses and limit synaptic transmission, it stands to reason that ARHGAP12 and TRIO may serve as GEF-GAP partners and restrict synaptic strength collaboratively in order to keep neuronal connectivity optimal. Future experiments are required to evaluate this possibility, clarify respective contributions of ARHGAP12 and TRIO and further identify more pivotal GEFs and/or GAPs partners in controlling normal synaptic function.

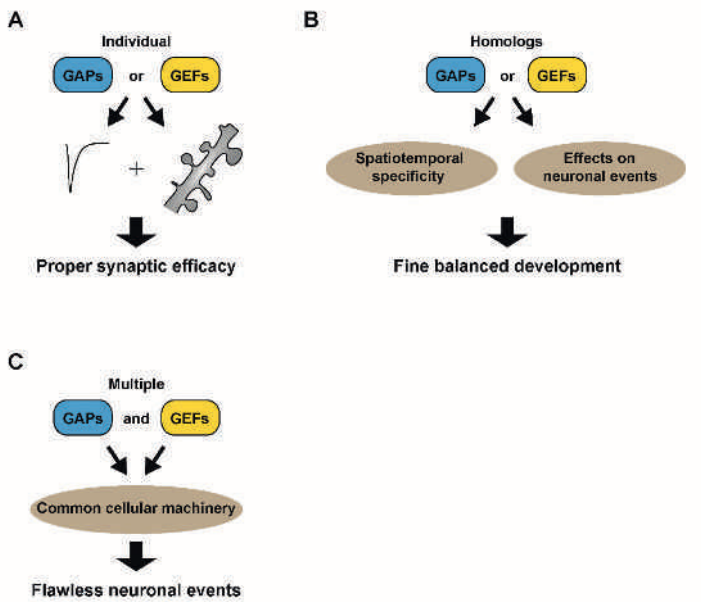

Figure 3 Three approaches utilized by neurons to precisely regulate synaptic efficacy. (A) Using individual multifunctional RhoGTPase regulatory proteins. **(B)** Using homologs displaying opposing effects. **(C)** Recruiting multiple GEFs/GAPs to target common cellular event.

2. AMPAr dysregulation in ID

ID is a prevalent global disorder which is characterized by substantial limitation in both adaptive behavior and intellectual abilities. Apart from environmental factors such as fetal alcohol syndrome, exposure to neurotoxic compounds and extreme malnutrition, genetics is considered to play an important role in the etiology of ID. To date, more than 700 genes have been identified to be associated with ID and the number of ID genes is still increasing [35]. By closely collaborating with geneticists, we combined a top-down approach, namely using genetic techniques and human phenotypes to identify novel ID associated genes, with a bottom-up strategy applying molecular biology, electrophysiology and imaging techniques in cellular models to uncover their functions at the synaptic level and contribute to identify novel therapeutic targets.

With a major focus on the genes involved in Rho GTPase signaling, I have performed functional analysis on four ID associated genes which are presented in this thesis: *TRIO* (**chapter 4**), *OCRL1* (**chapter 5**), *KIF4A* (**chapter 6**) and *KIF5C* (**chapter 6**). Interestingly, in addition to the ability of modulating dendritic spine structure, all four genes appear to directly affect AMPARs, one of the most important receptors mediating fast excitatory transmission in the CNS. For instance, loss of *Trio* impairs AMPAr endocytosis while down-regulation of *Ocrl1* significantly reduces AMPAr endocytosis as well as elevates cellular abundance of AMPARs. Also, in line with previous studies highlighting the role of KIF family members in transporting AMPARs along microtubule tracks in dendrites [36], knocking down *Kif4a* or overexpressing *Kif5c* results in an increased in AMPAr-mediated mEPSCs frequency. Although previous evidence shows that spine geometry is tightly correlated with AMPAr content at synapses, these findings indicate that proteins encoded by ID genes may also target AMPARs directly and contribute to multiple regulatory processes of AMPAr dynamics, such as synthesis, trafficking and degradation, during normal development and cognition. Consistently, studies on other ID proteins support their roles in the direct modulation of AMPARs. For example, RAB39B, whose encoded gene is linked to ID and ASD, has been recently found to interact with protein interacting with C-kinase 1 (PICK1), control surface expression of GluA2 subunit of AMPARs and subsequently synaptic transmission [37]. These findings may raise another interesting question: how are multiple AMPAr modulating proteins organized under physiological conditions? A recent study applying high-content protein analysis identified SorCS1 as a master regulator of synaptic AMPAr trafficking [38]. Linking to major sorting pathways, SorCS1

acts as a hub in controlling receptor surface expression including AMPArs in neurons. This discovery may initiate an interesting concept of studying synapses at a global level. Besides SorCS1, other proteins or machineries might co-exist and function as an intracellular "distribution center" for proteins that possess the ability of direct regulation of AMPArs. Precise and effective sorting and delivery of AMPAr modulating molecules including ARHGAP12, TRIO, OCRL1, KIF4A and KIF5C are required for normal development and cognition. Any misdelivery at improper time and location or delivery of "wrong" products will hamper synaptic transmission and lead to neurological disorders including ID. It would be interesting to test this possibility and identify master molecules of integrating multiple AMPAr regulators. The outcome may provide valuable information of novel therapeutic targets which is efficacious in treating ID.

Although we still have a long way to go before we are able to achieve effective interventions of various neurological disorders, current knowledge may point AMPAr as a potential target for the treatment. Not only are AMPArs critical for basal synaptic transmission and plasticity, but also their activity plays an important role in the maintenance of dendritic spines [39]. Hence, in theory, interventions targeting AMPArs might be beneficial for restoring both structural and functional deficits and, eventually, alleviate or reverse the symptoms in neurodevelopmental disorders including ID [40]. In fact, several AMPAr antagonists have been used in treating epilepsy in spite of the tolerance. It is worth noting that although some positive AMPAr modulators have been shown to improve cognition in health and elderly volunteers [41,42], they have not been advanced into phase II trials due to the low potency or toxicity. It implies that direct regulations of AMPArs might result in dramatic consequences which makes this strategy unsuitable for clinical use. New medications or treatments targeting AMPArs indirectly via AMPAr regulatory molecules such as ARHGAP12 and TRIO may be considered. Furthermore, recent studies have presented encouraging results in treating neurodevelopmental disorders [43,44]. For instance, turning on *SHANK3*, an ASD associated gene, in the adult mice reverses both neuronal structure and function in striatum as well as obsessive grooming behavior [44]. Thus, selectively switching on and off of AMPAr modulators in specific brain regions at certain developmental stages by applying novel genetic and engineering technology may provide promising therapeutic intervention. Future experiments will have to test this possibility.

3. Rho GTPases and sleep disturbances in ID

Although being one of the most burdensome symptoms of ID, sleep disturbances have received surprisingly limited attention in research. In fact, sleep problems have been observed not only in ID, but also in many other neurodevelopmental disorders such as ASD, attention deficit hyperactivity disorders (ADHD) and epilepsy. Sleep disturbances are now included in the diagnostic criteria for several neurodevelopmental disorders. Previous studies have shown that the estimated prevalence of sleep problems in people with ID is as high as 86% [45]. Due to lacking of mechanistic insights, ID patients with sleep disturbances are far from certain to receive effective and personalized treatments. Sustained sleep difficulties, on one hand, negatively influence the behavior of ID patients, on the other hand, significantly increase the parenting burden and family distress. Therefore, there is an urgent need to clarify the underlying mechanisms of sleep disturbances in ID. Based on the frequent correlation between ID and sleep disturbances, two fundamental questions may be asked: 1) Do the processes of sleep and learning/memory share common signaling pathways or neuronal circuitries? 2) Do Rho GTPases and their regulators, whose mutations often lead to ID, play a role in regulating sleep?

Despite that the detailed mechanisms underlying both sleep and learning/memory still remain elusive, we could appreciate and get inspired by previously reported observations. Two major aspects in the field of sleep neurophysiology received the most attention: the biological function of sleep and the regulatory mechanisms of sleep. One dominant hypothesis regarding the function of sleep is the “synaptic homeostasis hypothesis” (SHY) proposed by Cirelli and Tononi [46], which indicates that the fundamental function of sleep is to restore synaptic homeostasis. This hypothesis is supported by direct experimental evidence at the cellular and molecular level. It has been shown that dendritic spine formation and pruning are affected by sleep/wake cycles, in which waking causes a net increase in cortical spines while sleep leads to net spine loss in adult cortex [47]. Also, enhanced synaptic strength has been detected during wakefulness whereas sleep results in an opposing effect [48]. Consistently, 30%-40% reduction of AMPArs as well as removal of synaptic AMPArs have been observed during or after sleep in rats [49,50]. Due to the previous discoveries and the results presented in this thesis, which highlight the importance of Rho GTPase signaling in regulating synaptic structure and function in developing and mature brains, I believe that it is worth to examine whether Rho GTPases and their regulatory proteins could sense the distinct

extracellular cues (e.g. different expression levels of adenosine due to different neuronal activities during sleep and wakefulness), transfer the information and eventually control synaptic homeostasis during sleep/wake states. Interestingly, my preliminary data revealed fluctuations in the protein level of ARHGAP12 at different time during a day (data not shown). It would be interesting to test whether this fluctuations contribute to modifying dendritic spine structure and synaptic transmission during sleep.

Moreover, one influential two-process model of sleep regulation suggests that the interaction of circadian rhythm and sleep pressure (or internal sleep drive) determines the sleep/wake status. OPHN1, a Rho GAP encoded by an ID associated gene *OPHN1*, has be reported to interact with Rev-erbα, a nuclear receptor that represses circadian oscillators in the hippocampus and this interaction is required for normal oscillation. Also, synaptic activity which requires OPHN1 leads to relocation of Rev-erbα into dendritic spines [51]. These discoveries suggest that a communication between biological clocks and neuronal activity which is mediated by Rho proteins exists to maintain both processes balanced. Interestingly, a recent study reported a gene encoding a Rho GAP, *crossveinless-c* (*cv-c*) governs internal sleep drive which is independent on circadian rhythms in Drosophila [52]. *Cv-c* mutants fail to show homeostatic rebound sleep upon sleep deprivation and exhibit impaired memory. It would be interesting to identify whether the impairment of memory is directly caused by mutated *Cv-v* or just a secondary effect of lacking of sleep in general. Together, these discoveries imply that Rho GTPase signaling pathways may play pivotal roles in generating and maintaining normal sleep. Future experiments will identify novel Rho proteins that are involved in regulating sleep as well as neuronal circuitries responsible for sleep regulation, which would help us to comprehend the occurring of sleep disturbances in neurodevelopmental disorders.

Conclusion

Overall, the research reported in the thesis revealed novel functions of several previously uncharacterized Rho GTPase regulators and provides mechanistic insight into how the normal brain regulates cognition and how neurodevelopmental disorders may occur. In addition to the continuous investigation of unraveling the neuronal function of individual GEFs and GAPs, future experiments might also aim for generating an expression profile of Rho regulators at

the single cell, perhaps even at single synapse level. Indeed, novel imaging techniques combined with reporter molecules allow to investigate Rho GTPase signaling at single synapse level. [53] Different cell types in different brain regions may possess their unique identities as reflected by distinct compositions of GEFs and GAPs, which might ultimately determine their responses and contributions in cognitive processes.

References

1. Rossman, K. L., Der, C. J. & Sondek, J. GEF means go: turning on RHO GTPases with guanine nucleotide-exchange factors. *Nat. Rev. Mol. Cell Biol.* **6,** 167–180 (2005).
2. Moon, S. Y. & Zheng, Y. Rho GTPase- activating proteins in cell regulation. *Trends Cell Biol.* **13,** 13–22 (2003).
3. Bos, J. L., Rehmann, H. & Wittinghofer, A. GEFs and GAPs: critical elements in the control of small G proteins. *Cell* **129,** 865–77 (2007).
4. Tolias, K. F., Duman, J. G. & Um, K. Control of synapse development and plasticity by Rho GTPase regulatory proteins. *Prog. Neurobiol.* **94,** 133–148 (2011).
5. Duman, J. G., Mulherkar, S., Tu, Y.-K., Cheng, J. & Tolias, K. F. Mechanisms for spatiotemporal regulation of Rho-GTPase signaling at synapses. *Neurosci. Lett.* **601,** 4–10 (2015).
6. Seoh, M. L., Ng, C. H., Yong, J., Lim, L. & Leung, T. ArhGAP15, a novel human RacGAP protein with GTPase binding property. *FEBS Lett.* **539,** 131–137 (2003).
7. Croft, D. R. & Olson, M. F. Transcriptional regulation of Rho GTPase signaling. *Transcription* **2,** 211–215 (2011).
8. Connolly, E. C., Van Doorslaer, K., Rogler, L. E. & Rogler, C. E. Overexpression of miR-21 promotes an in vitro metastatic phenotype by targeting the tumor suppressor RHOB. *Mol Cancer Res* **8,** 691–700 (2010).
9. Jiang, L. *et al.* Downregulation of the Rho GTPase signaling pathway is involved in the microRNA-138-mediated inhibition of cell migration and invasion in tongue squamous cell carcinoma. *Int. J. Cancer* **127,** 505–512 (2010).
10. Ba, W. *et al.* ARHGAP12 Functions as a Developmental Brake on Excitatory Synapse Function. *Cell Rep.* **14,** 1–14 (2016).
11. Billuart, P. *et al.* Oligophrenin-1 encodes a rhoGAP protein involved in X-linked mental retardation. *Nature* **392,** 923–926 (1998).
12. Nakano-Kobayashi, a., Tai, Y., Nadif Kasri, N. & Van Aelst, L. The X-linked Mental Retardation Protein OPHN1 Interacts with Homer1b/c to Control Spine Endocytic Zone Positioning and Expression of Synaptic Potentiation. *J. Neurosci.* **34,** 8665–8671 (2014).
13. Nadif Kasri, N., Nakano-Kobayashi, A., Malinow, R., Li, B. & Van Aelst, L. The Rho-linked mental retardation protein oligophrenin-1 controls synapse maturation and plasticity by stabilizing AMPA receptors. *Genes Dev.* **23,** 1289–302 (2009).
14. Nadif Kasri, N., Nakano-Kobayashi, A. & Van Aelst, L. Rapid synthesis of the X-linked mental retardation protein OPHN1 mediates mGluR-dependent LTD through interaction with the endocytic machinery. *Neuron* **72,** 300–15 (2011).
15. Harris, J. J., Jolivet, R. & Attwell, D. Synaptic Energy Use and Supply. *Neuron* **75,** 762–777 (2012).
16. Ascano, M. *et al.* FMRP targets distinct mRNA sequence elements to regulate protein expression. *Nature* **492,** 382–6 (2012).
17. Rocca, D. *et al.* The Small GTPase Arf1 Modulates Arp2/3-mediated actin polymerization via PICK1 to regulate synaptic plasticity. *Neuron* **79,** 293–307 (2013).
18. Terashima, A. *et al.* An Essential Role for PICK1 in NMDA Receptor-Dependent Bidirectional Synaptic Plasticity. *Neuron* **57,** 872–882 (2008).
19. Lüscher, C. & Huber, K. M. Group 1 mGluR-dependent synaptic long-term depression: mechanisms and implications for circuitry and disease. *Neuron* **65,** 445–59 (2010).
20. Zhou, Z., Hu, J., Passafaro, M., Xie, W. & Jia, Z. GluA2 (GluR2) regulates metabotropic glutamate receptor-dependent long-term depression through N-cadherin-dependent and cofilin-mediated actin reorganization. *J. Neurosci.* **31,** 819–33 (2011).
21. Hall, C. *et al.* Alpha 2-chimerin, an SH2-containing GTPase-activating protein for the ras-related protein p21rac derived by alternate splicing of the human n-chimerin gene, is selectively expressed in brain regions and testes. *Mol. Cell. Biol.* **13,** 4986–4998 (1993).
22. Iwata, R. *et al.* RacGAP α2-Chimaerin Function in Development Adjusts Cognitive Ability in Adulthood. *Cell Rep.* **8,** 1257–1264 (2014).

23. Beg, A. a., Sommer, J. E., Martin, J. H. & Scheiffele, P. α2-Chimaerin Is an Essential EphA4 Effector in the Assembly of Neuronal Locomotor Circuits. *Neuron* **55,** 768–778 (2007).
24. Ip, J. P. K. *et al.* α2-chimaerin controls neuronal migration and functioning of the cerebral cortex through CRMP-2. *Nat. Neurosci.* **15,** 39–47 (2011).
25. Buttery, P. *et al.* The diacylglycerol-binding protein alpha1-chimaerin regulates dendritic morphology. *Proc. Natl. Acad. Sci. U. S. A.* **103,** 1924–1929 (2006).
26. Van de Ven, T. J., VanDongen, H. M. a & VanDongen, A. M. J. The nonkinase phorbol ester receptor alpha 1-chimerin binds the NMDA receptor NR2A subunit and regulates dendritic spine density. *J. Neurosci.* **25,** 9488–9496 (2005).
27. O'Brien, S. P. *et al.* Skeletal muscle deformity and neuronal disorder in Trio exchange factor-deficient mouse embryos. *Proc. Natl. Acad. Sci. U. S. A.* **97,** 12074–12078 (2000).
28. Peng, Y. J. *et al.* Trio is a key guanine nucleotide exchange factor coordinating regulation of the migration and morphogenesis of granule cells in the developing cerebellum. *J. Biol. Chem.* **285,** 24834–24844 (2010).
29. Ba, W. *et al.* TRIO loss of function is associated with mild intellectual disability and affects dendritic branching and synapse function. *Hum. Mol. Genet.* **25,** 892–902 (2016).
30. Herring, B. E. & Nicoll, R. A. Kalirin and Trio proteins serve critical roles in excitatory synaptic transmission and LTP. *Proc. Natl. Acad. Sci.* **113,** 2264–2269 (2016).
31. Schlam, D. *et al.* Phosphoinositide 3-kinase enables phagocytosis of large particles by terminating actin assembly through Rac/Cdc42 GTPase-activating proteins. *Nat. Commun.* **6,** 8623 (2015).
32. Freeman, S. A. & Grinstein, S. Phagocytosis: Receptors, signal integration, and the cytoskeleton. *Immunol. Rev.* **262,** 193–215 (2014).
33. Duman, J. G. *et al.* The adhesion-GPCR BAI1 regulates synaptogenesis by controlling the recruitment of the Par3/Tiam1 polarity complex to synaptic sites. *J. Neurosci.* **33,** 6964–78 (2013).
34. Park, D. *et al.* BAI1 is an engulfment receptor for apoptotic cells upstream of the ELMO/Dock180/Rac module. *Nature* **450,** 430–434 (2007).
35. Kochinke, K. *et al.* Systematic Phenomics Analysis Deconvolutes Genes Mutated in Intellectual Disability into Biologically Coherent Modules. *Am. J. Hum. Genet.* **98,** 149–164 (2016).
36. Setou, M. *et al.* Glutamate-receptor-interacting protein GRIP1 directly steers kinesin to dendrites. *Nature* **417,** 83–87 (2002).
37. Mignogna, M. L. *et al.* The intellectual disability protein RAB39B selectively regulates GluA2 trafficking to determine synaptic AMPAR composition. *Nat. Commun.* **6,** 6504 (2015).
38. Savas, J. N. *et al.* The Sorting Receptor SorCS1 Regulates Trafficking of Neurexin and AMPA Receptors. *Neuron* **87,** 764–780 (2015).
39. McKinney, R. A., Capogna, M., Dürr, R., Gähwiler, B. H. & Thompson, S. M. Miniature synaptic events maintain dendritic spines via AMPA receptor activation. *Nat. Neurosci.* **2,** 44–49 (1999).
40. Chang, P. K. Y., Verbich, D. & Mckinney, R. A. AMPA receptors as drug targets in neurological disease - advantages, caveats, and future outlook. *Eur. J. Neurosci.* **35,** 1908–1916 (2012).
41. Ingvar, M. *et al.* Enhancement by an Ampakine of Memory Encoding in Humans. *Exp. Neurol.* **146,** 553–559 (1997).
42. Lynch, G., Rex, C. S., Chen, L. Y. & Gall, C. M. The substrates of memory: Defects, treatments, and enhancement. *Eur. J. Pharmacol.* **585,** 2–13 (2008).
43. Silva-santos, S., Woerden, G. M. Van, Bruinsma, C. F. & Mientjes, E. Ube3a reinstatement identifies distinct treatment windows in Angelman syndrome model mice. **125,** 1–8 (2015).
44. Mei, Y. *et al.* Adult restoration of Shank3 expression rescues selective autistic-like phenotypes. *Nature* **530,** 481–4 (2016).
45. Didde, R. & Sigafoos, J. A review of the nature and treatment of sleep disorders in individuals with developmental disabilities. *Res. Dev. Disabil.* **22,** 255–72 (2001).
46. Tononi, G. & Cirelli, C. Sleep and synaptic homeostasis: A hypothesis. *Brain Res. Bull.* **62,** 143–

150 (2003).
47. Maret, S., Faraguna, U., Nelson, A. B., Cirelli, C. & Tononi, G. Sleep and waking modulate spine turnover in the adolescent mouse cortex. *Nat. Neurosci.* **14,** 1418–20 (2011).
48. Liu, Z.-W., Faraguna, U., Cirelli, C., Tononi, G. & Gao, X.-B. Direct Evidence for Wake-Related Increases and Sleep-Related Decreases in Synaptic Strength in Rodent Cortex. *J. Neurosci.* **30,** 8671–8675 (2010).
49. Lanté, F., Toledo-Salas, J.-C., Ondrejcak, T., Rowan, M. J. & Ulrich, D. Removal of synaptic Ca^{2}+-permeable AMPA receptors during sleep. *J. Neurosci.* **31,** 3953–3961 (2011).
50. Vyazovskiy, V. V, Cirelli, C., Pfister-Genskow, M., Faraguna, U. & Tononi, G. Molecular and electrophysiological evidence for net synaptic potentiation in wake and depression in sleep. *Nat. Neurosci.* **11,** 200–8 (2008).
51. Valnegri, P. *et al.* A circadian clock in hippocampus is regulated by interaction between oligophrenin-1 and Rev-erbα. *Nat. Neurosci.* **14,** 1293–301 (2011).
52. Donlea, J. M., Pimentel, D. & Miesenbock, G. Neuronal machinery of sleep homeostasis in Drosophila. *Neuron* **81,** 860–872 (2014).
53. Yasuda, R. Studying signal transduction in single dendritic spines. *Cold Spring Harb. Perspect. Biol.* **4,** 1–16 (2012).

Summary

The aim of this thesis was to provide mechanistic insights into how the brain regulates learning and memory in both health and disease. Specifically, I revealed the neuronal function of several novel genes involved in Rho GTPase signaling, most of which are found mutated in ID patients, at the synaptic level.

Chapter 2 of this thesis presented the spatiotemporal transcriptional pattern of 22 genes encoding Rho GTPases and their regulators during development. Based on the output of this study, following in-depth investigations on three important Rho regulators were performed. **Chapter 3** described the novel synaptic function of a previously unstudied RhoGAP, ARHGAP12. I show that ARHGAP12 is almost exclusively expressed in the CA1 subregion of the hippocampus, a well-studied brain region responsible for spatial learning and navigation. I demonstrate that ARHGAP12 functions as a "structural-functional" coordinator at CA3-CA1 excitatory synapses during development. Specifically, ARHGAP12 negatively controls spine size via its RhoGAP activity and promotes, by interacting with CIP4, postsynaptic AMPAr endocytosis. Knocking down *Arhgap12* leads to precocious maturation of excitatory synapses, as indicated by a reduction in the proportion of silent synapses. In **Chapter 4**, we identified *TRIO*, a gene encoding a RhoGEF, as a responsible gene for mild to borderline ID. TRIO is abundantly expressed during early hippocampal development. Physiologically, TRIO suppresses dendritic formation without affecting the establishment of axon polarity. Consistently, depleting endogenous TRIO significantly enhances synaptic strength of hippocampal CA3-CA1 synapses. In **Chapter 5**, I described the functional characterizations of *Ocrl1*, a gene associated with Lowe Syndrome and type 2 Dent Disease. I show that OCRL1 bidirectionally controls dendritic spine density, miniature excitatory synaptic transmission and LTP. In addition, OCRL1 is involved in the regulation of AMPAr endocytosis and the homeostasis of cellular AMPAr abundance in primary hippocampal neurons. **Chapter 6** described that identification of mutations in KIF4A and KIF5C in patients with ID. Functional analysis reveals emerging roles of KIF4A and KIF5C in maintaining the balance between excitation and inhibition.

In conclusion, the research presented in this thesis highlights the importance of Rho GTPase signaling in maintaining normal development and cognition.

Samenvatting

Het doel van deze thesis was om inzicht te verschaffen in de mechanismen waarmee het brein leren en geheugen reguleert in zowel het gezonde als het zieke brein. Ik beschrijf de neuronale functies van meerdere nieuw-geïdentificeerde genen die betrokken zijn bij Rho GTPase signalering, op het niveau van de synaps. Voor de meeste van deze genen zijn mutaties beschreven in patiënten met verstandelijke beperkingen.

Hoofdstuk 2 van deze thesis beschrijft het spatio-temporele patroon tijdens de ontwikkeling van het brein van de transcriptie van 22 kandidaat-genen die coderen voor Rho GTPases en hun regulatoren. Gebaseerd op de resultaten van deze studie zijn diepgaande vervolgstudies uitgevoerd voor drie belangrijke Rho-regulatoren. **Hoofdstuk 3** beschrijft de synaptische functie van een tot nu toe onbekende RhoGAP, ARHGAP12. Ik toon aan dat ARHGAP12 vrijwel enkel tot expressie komt in het CA1 sub-gebied van de hippocampus, een goed bestudeerde hersengebied met een belangrijke functie in ruimtelijk leren en navigatie. Ik heb aangetoond dat ARHGAP12 functioneert als een “functie/structuur” coördinator in de CA3-CA1 synaps tijdens de ontwikkeling van het brein. Meer specifiek, via het RhoGAP domein reguleert ARHGAP12 de grootte van dendritische spines negatief, en stimuleert het postsynaptische AMPAr endocytose via interactie met CIP4. Knock-down van *Arhgap12* leidt tot premature maturatie van excitatoire synapsen, zoals is af te leiden van de afname van het aandeel van niet actieve synapsen. In **hoofdstuk 4** identificeren we *TRIO*, een gen dat codeert voor een RhoGEF, als een gen dat verantwoordelijk is voor lichte tot milde verstandelijke beperking. TRIO komt hoog tot expressie tijdens de vroege ontwikkeling van de hippocampus. TRIO onderdrukt de formatie van dendrieten, maar heeft geen effect op de vorming van de polariteit van het axon. Als gevolg hiervan versterkt depletie van TRIO CA3-CA1 synapsen in de hippocampus. In **hoofdstuk 5** beschrijf ik de functionele rol van *OCRL1*, een gen dat verband houdt met Lowe Syndroom. Ik toon aan dat OCRL1 spine dichtheid, excitatoire synaptische transmissie en plasticiteit bidirectioneel reguleert. Daarnaast is OCRL1 betrokken bij de regulatie van AMPAr endocytose en de homeostase van de hoeveelheid cellulaire AMPAren in primaire hippocampale culturen. **Hoofdstuk 6** beschrijft de identificatie van mutaties in KIF4A en KIF5C in patienten met verstandelijke beperkingen. Functionele analyse toont de rol van KIF4A en KIF5C in het behouden van de balans tussen excitatie en inhibitie aan.

Het bovenstaande onderzoek benadrukt het belang van Rho GTPase signalering voor normale hersenontwikkeling en cognitie.

List of Publications

1. **Ba W** and Nadif Kasri N.
   RhoGTPases at the synapse: an embarrassment of choice. *Invited commentary*
   Small GTPases. 2016 5:1-8.

2. **Ba W**, Selten MM, van der Raadt J, van Veen H, Li LL, Benevento M, Oudakker AR, Lasabuda RS, Roepman R, van Wezel RJ, Courtney MJ, van Bokhoven H, Nadif Kasri N.
   ARHGAP12 functions as a developmental brake on excitatory synapse function.
   Cell Reports. 2016 16:1355-68.

3. **Ba W**[*], Yan Y[*], Reijnders M.R.F[*], Schuurs-Hoeijmakers JH, Feenstra I, Bongers EM, Bosch DG, De Leeuw N, Pfundt R, Gilissen C, De Vries PF, Veltman JA, Hoischen A, Mefford hc, Eichler EE, Vissers LE, Nadif Kasri N [#], de Vries B.A [#].[*]Co-first author; [#] Co-last author.
   TRIO loss of function is associated with mild intellectual disability and affects dendritic branching and synaptic function.
   Human Molecular Genetics. 2016 25:892-902.

4. Willemsen MH[*], **Ba W**[*], Wissink-Lindhout WM, de Brouwer AP, Haas SA, Bienek M, Hu H, Vissers LE, van Bokhoven H, Kalscheuer V, Nadif Kasri N[#], Kleefstra T[#].[*]Co-first author; [#] Co-last author.
   Involvement of the kinesin family members KIF4A and KIF5C in intellectual disability and synaptic function.
   Journal of Medical Genetics. 2014 51:487-94.

5. **Ba W,** van der Raadt J, Nadif Kasri N.
   Rho GTPase signaling at the synapse: implications for intellectual disability. *Review.*
   Experimental Cell Research. 2013 319:2368-74.

6. Selten MM[*], Meyer F[*], **Ba W**, Valles-Sanchez A, Mass D,Negwer M, Eijsink V, van Vugt R, van Hulten J, van Bakel N, Roosen J, van der Linden R, Schubert D, Verhrij M, Nadif Kasri N [#], Martens G [#].[*]Co-first author; [#] Co-last author.
   Increased GABAB receptor signaling in a rat model for schizophrenia.
   Scientific Reports. In press.

7. Benevento M, Iacono G, Selten M, **Ba W**, Oudakker AR, Frega M, Keller J, Mancini R, Lewerissa E, Kleefstra T, Stunnenberg HG, Zhou H, van Bokhoven H, Nadif Kasri N.
   Histone methylation by the Kleefstra Syndrome protein EHMT1 mediates homeostatic synaptic scaling.
   Neuron. 2016 91:341-55.

8. Olde Loohuis NFM, **Ba W**, Stoerchel PH, Kos A, Jager A, Schratt G, Martens GJ, van Bokhoven H, Nadif Kasri N[#], Aschrafi A[#]. [#] co-last author.

   MicroRNA-137 controls synaptic efficacy and mGluR-dependent LTD through AMPA receptor trafficking.

   Cell Reports. 2015 11:1876-84.

9. Li LL, Melero-Fernandez de Mera RM, Chen J, **Ba W**, Nadif Kasri N, Zhang M, Courtney MJ.

   Unexpected heterodivalent recruitment of NOS1AP to nNOS reveals multiple sites for pharmacological intervention in neuronal disease models.

   Journal of Neuroscience. 2015 35:7349-64.

About the author

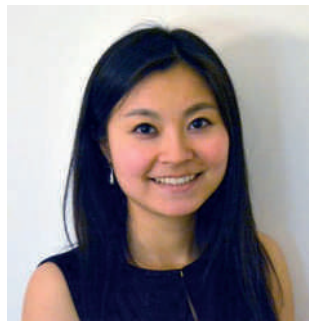

Wei Ba was born on the 30th of June 1984 in Wuhan, China. After completing her bachelor education in Pharmacy, she continued with her master study in Neuropharmacology at Huazhong University of Science and Technology where she became interested in neuroscience. Shortly after receiving her master degree, Wei decided to pursue her scientific career abroad. In 2010, she moved to Genova, Italy. During her stay at the Italian Institute of Technology (IIT) she further developed her skills in molecular biology. In 2011, Wei started her Ph.D. in the group of Dr. Nael Nadif Kasri at the Radboudumc Nijmegen, the Netherlands, where she received extensive training in studying structural and functional synaptic plasticity. In 2016, Wei joined the groups of Prof. Nick Franks and Prof. William Wisden as a postdoctoral researcher at the Imperial College London, UK. She is currently focusing on identifying novel neuronal circuitries modulating sleep.

Photography: Martijn Selten ;)

Acknowledgements

It is finally the time to write down my words of appreciations to everyone who provided help and support all along my journey of completing the Ph.D. in the Netherlands. It is hard not to get emotional when I look back on the past few years, which consist of one of the most important and memorable chapters in my life.

The deepest gratitude, first and foremost, of course goes to my supervisor Dr. Nael Nadif Kasri who gave me the opportunity to pursue my Ph.D. in the Netherlands. I hardly believe that it was six years ago since I joined Nael's group as the first Ph.D. student. From four people initially to over twenty members when I left the lab about half a year ago, it is a great honor to witness the growing of our group. Until now, I still feel blessed and glad to have Nael as my supervisor. "Work hard, play hard", he says often. I therefore took these words and adapted them in my study. The "work hard" part was tough, but now I am enjoying the harvest! As a young and enthusiastic group leader, Nael sets a good example of combining hard working with novel technology and smart ideas to push science forward. Different from many PIs, Nael also encourages us to participate in various international congresses and workshops, by which we could receive the newest information and communicate with pioneers. During all these years, Nael offered great supervision and advices, both in and outside science, whenever I needed. Even now, when I am working in a new lab in a different country, he is still willing to provide help to get me out of trouble. Under his tough outside, what I do see, is a kind and soft heart. No words can truly express my appreciations, but I still want to say, thank you, Nael!

Many thanks to my promoter, Prof. Hans van Bokhoven. I remember that every time we meet in the hallway, Hans always says "Hi Vivien!" with a nice smile on his face. During the discussion about the progress of my projects, he was always critical and inspiring. I am more than grateful for all his support and advices, not only during my Ph.D., but also the entire period of the job hunting as well as grant application.

Also, I would like to thank all my previous students for contributing to my projects. Daisy, I think you were the first student I had during my Ph.D. I was impressed by the beautiful staining of the synaptic markers you could obtain during your internship. Thank you for the contribution in the OCRL1 project as well as helping me experience the Dutch culture! Jori, I was very lucky to have you working on the ARHGAP12 project. As a first year Ph.D. student at

that time, I could not give you enough advice and supervision, but you managed to complete the yeast-two hybrid screening which became an essential part of my ARHGAP12 paper. Also, together with Nael, we worked so hard to meet the deadline of the review which gave us the first publication together. It was nice to work as well as drink coffee in between the experiments with you. Thanks for all the nice work! Inge, you are the sweetest student I ever had! Thanks for sitting behind your computer analyzing thousands of spines for the OCRL1 project. I know that it is huge amount of work but you did a very good job. You organized your data so well that I can still easily trace back what you did two years ago. Thank you for all the help! Rizky, thank you for the nice work on the ARHGAP12, OCRL1 and TRIO projects. I was impressed by how fast you learn new techniques. In the end of your internship, you acquired multiple experimental skills including staining, making organotypic brain slices, gene gun transfecting neurons and analyzing spine morphology. Together, we also set up the protocol of examining AMPAr trafficking on primary neurons which was one of the important parts in the ARHGAP and TRIO papers. I really appreciated what you have contributed to my projects.

Herman! It was great to meet you in my Ph.D. You are doing the coolest job in the world: flying a plane and imaging a brain! Thank you so much for working with me for more than three years. Without your help with two-photon imaging, my life during the Ph.D. would be much more difficult. You are always cheerful and bring lots of fun in the lab. It was very efficient when we sat together in the dark two-photon lab, with loud music and chocolates. Thank you!

I would also like to thank all the colleague in our group. Marco and Steph, together with Martijn, we four started our Ph.D.s in the same year. I shared so many great and important moments with you during the past 5 years. We worked together, drank together and complained together. We supported each other and also annoyed each other haha. We witnessed each other's growth in both science and personal lives. All these moments have become the most precious memory. Thank you all and I wish you all the best in the future! Moritz, you are one of the few people I know whos know almost everything! Although we did not spend years working together, I am very happy to have you and Laura as important friends I met in the Netherlands. Thanks for the support, with nice food and movies! Dirk, it was very nice that you were always cheerful in the lab. Thank you for all the support during my Ph.D. and particularly during my job application. Also, thanks for the spicy sausages! Astrid, thank you for all the help during my Ph.D.! Jon-Ruben, thank you for taking good care of the patch-

clamp rig and helping me organize the animals. Monica, I really enjoyed those days that we did sports together. I wish we could start it earlier. Also, thanks a lot for allowing me to stay at your place when I was waiting for my visa to the UK! Nikkie, Marijn, Aron and Bas, thank you for being around and it was always nice to chat with you.

Special thanks to my Paranimven, Katrin and Teun! I'm honored that you are willing to be my Paranimven. Without your help, it would be very difficult to organize everything from London. Thank you very much for all the help!

To my Chinese friends, Wan Yi, Haiteng, Wan Lin, Huadong, Zewen, Gu Yan and, last but not least, Yanfen, you brought me so much fun during the past few years. I really enjoyed the time that we cooked, traveled and experienced the western culture together. I am happy to see that everyone finds his own path, although it is a pity that we are scatted all around the world. Thanks for all the support and help!

Lieve Petra en Jos, ik ben heel blij jullie als mijn schoonouders te hebben. Hartelijk bedankt voor alle steun en gezelligheid! Lieve Jeroen en Daphne, ik heb geen broers of zussen, maar gelukkig heb ik jullie! Ook jullie bedankt voor alle gezelligheid.

衷心感谢我亲爱的爸妈！是你们的呵护和教导塑造了今天的我。你们无条件的爱一直是我前行的动力和强大的后盾。每当我取得进步，你们总是一起分享我的喜悦，甚至比我更开心；每当我遇到困难，你们总能给我出谋划策，让一切困难变得渺小。感谢你的支持和鼓励，我爱你们！感谢大姨妈，大姨伯，莎姐姐，姐夫，奇奇，贝贝以及所有家人的支持！特别鸣谢张瑛女士， 您精湛的画技给我的论文增色不少，同时也向世界展示了我们中国文化。

Last but not least, special thanks to Martijn, for always being supportive both at work and at home. Your company has made my journey of doing the Ph.D. less difficult and more fun. I have learnt a lot from you, such as your creative and critical way of thinking as well as the rigorous logic. It is amazing that I can always discuss with you about my projects and then get inspired by you. Also because of you, I fell in love with the small but beautiful country, the Netherlands. Thank you for taking good care of me, especially when I'm sick and stressed.

DONDERS
INSTITUTE

ISBN 978-94-6284-095-9

Radboud University Radboudumc